Exploring Immune Checkpoints and Cytokine Signaling to Improve NK Cell Effector Function in Ovarian Cancer

Ralph J.A. Maas

RADBOUD UNIVERSITY PRESS

Radboud Dissertation Series

Exploring Immune Checkpoints and Cytokine Signaling to Improve NK Cell Effector Function in Ovarian Cancer

Ralph Johan Anton Maas

Exploring Immune Checkpoints and Cytokine Signaling to Improve NK Cell Effector Function in Ovarian Cancer
Ralph Maas

Radboud Dissertation Series
ISSN: 2950-2772 (Online); 2950-2780 (Print)

Published by RADBOUD UNIVERSITY PRESS
Postbus 9100, 6500 HA Nijmegen, The Netherlands
www.radbouduniversitypress.nl

Design: Proefschrift AIO | Guus Gijben
Cover: Proefschrift AIO | Guus Gijben
Printing: DPN Rikken/Pumbo

ISBN: 9789465151670
DOI: 10.54195/9789465151670
Free download at: https://doi.org/10.54195/9789465151670

RADBOUD
UNIVERSITY
PRESS

Exploring Immune Checkpoints and Cytokine Signaling to Improve NK Cell Effector Function in Ovarian Cancer

Proefschrift

ter verkrijging van de graad van doctor
aan de Radboud Universiteit Nijmegen
op gezag van de rector magnificus prof. dr. J.M. Sanders
volgens besluit van het college van decanen
in het openbaar te verdedigen op
donderdag 11 december 2025 om 16:30 uur precies

door

Ralph Johan Anton Maas
geboren op 18 april 1992
Te Groesbeek

Promotoren
Prof. dr. H. Dolstra
Prof. dr. J.H. Jansen

Copromotor
Dr. W.A. Hobo

Manuscriptcommissie
Prof. dr. I.J.M. de Vries
Prof. dr. L.A.B. Joosten
Dr. E. Bremer (UMC Groningen)

Table of Contents

Chapter 1

General introduction and outline of this thesis

Introduction

Ovarian Cancer

Ovarian cancer (OC) originates in the ovaries which are located in the pelvis and are responsible for the production of female hormones and eggs for reproduction. OC can be subdivided in different histological subtypes. Of these histological subtypes epithelial ovarium carcinoma (EOC) accounts for the majority (~90%) of OC cases [1]. EOC is further subdivided into serous (75-80%), mucinous (~10%) and clear cell carcinoma (less than 5%). EOC is often diagnosed at a late stage as the disease is typically asymptomatic before appearance of ascites or extra pelvic metastases, and therefore often called the "Silent lady killer" [2, 3]. The FIGO (i.e. International Federation of Gynecology and Obstetrics) system classifies EOC severity based on the extent of the disease. The higher the stage, the more advanced the cancer has developed in patients. Treatment options and prognosis for EOC often depend on the stage of the disease at the time of diagnosis. The stages of EOC ranges from stage I to stage IV. In stage I the cancer is confined to the ovary or ovaries, and in case of intermediate stage II the cancer has spread beyond the ovaries, but is still contained within the pelvis. In stage III the cancer has spread beyond the pelvis to the abdomen and/or lymph nodes, but has not yet reached distant organs while in stage IV the cancer has spread to distant parts of the body such as the liver or lungs.

In Europe, prevalence of OC is high with 17.2 cases per 100.000 inhabitants in 2018 thereby representing ~2.9% of all cancer diagnoses (ECIS, European Cancer Information System). Mortality in Europe was 12.1 cases per 100.000 inhabitants, and accounts for 4.4% of all cancer related deaths in Europe. The 5-year overall survival (OS) is 39.6% (data from 2010 and 2014, excluding Luxembourg, Hungary and Greece due to missing data). For advanced-stage (FIGO stage III and IV) disease survival is much worse with a five-year OS of 28% [4]. This indicates there is much to be gained by improving treatment strategies for this highly lethal disease.

A classic symptom associated with advanced stage EOC is ascites, the condition where fluid collects in the peritoneal cavity. The ascites accumulates in the abdomen as a result of lymphatic obstruction and increased vascular permeability [5]. Importantly, the presence of ascites is associated with reduced survival and poor quality of life [6]. More specifically ascites promotes tumor cell growth, invasion and survival [7-9]. Besides a direct effect on tumor cells, ascites also contains a variety of soluble components that attract immune cells but also negatively influence their

function [10-15]. These soluble factors are secreted by tumor, immune & stromal/ tissue-resident cells [16].

Current first-line treatment for EOC patients encompasses surgical debulking followed by platinum-based chemotherapy or after neoadjuvant chemotherapy (NACT). Despite an excellent remission rate after primary treatment, ~80% of patients develop a recurrence within 3 years [15]. Patients with a recurrence after six months or more following a complete response are categorized as platinum-sensitive and eligible for second-line platinum-based chemotherapy. About 70% patients are considered platinum-sensitive and prolonged survival with platinum-based chemotherapy is possible for some patients. The remaining 30% of patients is platinum-resistant and unlikely to respond to further platinum-based chemotherapy. Second-line therapy options are limited to palliative chemotherapy with carboplatin and paclitaxel, liposomal doxorubicin or gemcitabine. Furthermore, there are few targeted therapies available apart from poly ADP ribose polymerase (PARP) inhibitors for a selection of patients. Eventually, 25% of EOC patients end up platinum resistant (recurrence within 6 months after completion of first-line platinum-based chemotherapy) with few treatment options remaining [17]. Therefore, additional potent treatment strategies are warranted to improve survival. Several studies indicated that EOC is an immunogenic disease. While the presence of regulatory T cells (Tregs) is associated with decreased survival [12-15] the presence of tumor-infiltrating CD8+ T cells is associated with prolonged survival and anti-EOC activity. The role of natural killer (NK) cells is less clear [18-23]. Studies on tumor infiltrating CD56+CD3- NK cells in EOC to date are hindered by lack of robust antibodies that identify all NK cell subsets in tumor tissue, and NK subset markers such as CD57 and CD16 are often used instead [18, 23]. Interestingly, studies have reported that CD103+ NK cells frequently co-infiltrate with CD103+CD8+ T cells in high-grade serous EOC but the precise impact requires further assessment [19]. However, studies on peripheral blood illustrated that low blood CD56+CD3- NK cell counts in EOC patients during chemotherapy are associated with unfavorable prognosis [24]. In this regard, an 11-year follow-up study from 2000 indicated that low peripheral NK cell activity is associated with increased cancer risk in general but highly dependent on tumor type [25]. Therefore, the role of NK cells in EOC patient outcome remains to be elucidated. Nevertheless, preclinical research studies indicate that EOC is sensitive to NK cell attacks [26-28], providing rationale for developing NK cell based immunotherapies for EOC. Furthermore, although the success of immunotherapy with PD1 checkpoint inhibitors has improved prognosis for various cancers, significant survival benefits in EOC have not been demonstrated [29, 30]. Chimeric antigen receptor (CAR) T-cell therapy has shown the potential for immune cell based treatment strategies in B cell malignancies and could be an interesting approach for EOC as well [31-36]. However, due to the lack of a

specific antigens to target like CD19 in the treatment of B cell lymphoma and acute lymphoblastic leukemia, this approach is more challenging for EOC which requires further research to succeed. The interaction between EOC and NK cells and their potential for adoptive NK cell therapy as a novel approach for OC treatment are further investigated in this thesis.

NK cell biology & sources for NK-based immunotherapy

NK cells are large granular cytotoxic lymphocytes and part of the innate immune system. In contrast to CD8+ cytotoxic T cells which rely on clonal expansion upon recognition of specific antigens presented by the major histocompatibility complex (MHC) and co-stimulation, NK cells do not require any prior antigen-dependent activation or expansion and have an innate ability to kill, hence their name. They are activated by lack of self-recognition (MHC class I), through binding of ligands on stressed cells or by antibody-dependent cellular cytotoxicity (ADCC) [37]. Self-tolerance of NK cells is maintained by the sum of inhibitory and activating signals that determine whether the NK cell will be activated. Phenotypically NK cells are classically divided in two main types, $CD56^{dim}CD16^{high}$ cytotoxic NK cells and $CD56^{bright}CD16^{neg}$ cytokine producing NK cells [38]. $CD56^{dim}CD16^{high}$ NK cells are the dominant phenotype found in blood, while $CD56^{bright}CD16^{neg}$ are more abundant in lymphoid tissues [38]. Peripheral blood (PB) derived NK cells can be used as a source for adoptive immunotherapy, but as PB-NK cells are mature and have differentiated their proliferative potential is limited.

Besides naturally occurring NK cells, another source of NK cells that could be utilized for adoptive treatment are immortalized NK cell lines [39]. The most well-known, and the only NK cell line being assessed in the clinic, are NK-92 cells, originally established from a patient with non-Hodgkin's lymphoma [40]. Although NK-92 cells provide a homogenous cell source that could be used for "off-the-shelf" therapeutic use they hold inherent drawbacks such as potential tumorigenicity [40, 41]. Therefore, irradiation of NK-92 is required as a safety measure, but this limits their persistence *in vivo* [41]. Nevertheless, several (pre-)clinical trials have been performed with non-engineered and engineered NK-92 cells with either the higher-affinity CD16a Fc-receptor in combination with tumor-targeting antibodies or CARs [42-45]. These CARs are genetically engineered receptor proteins that bind cancer cell surface-specific antigen proteins such as CD19 for non-Hodgkin lymphoma and EpCAM for certain epithelial solid tumors [46]. CAR consist further of an intracellular activating signaling domains, such as CD28, 41BB and/or CD3ζ, which in combination with its extracellular receptor enables CAR-engineered NK cells to become both activated and bind the cancer cells [47]. Next to the CAR-

dependent activity NK-92 cells exert CAR-independent cytotoxicity against tumor target cells [48].

Another promising source of NK cells with a high potential for expansion are induced pluripotent stem cells (iPSCs). iPSCs are a type of stem cell that can be generated from adult cells, for example skin or blood cells, through reprogramming by introducing transcription factors such as Oct4, Sox2, Klf4, and c-Myc which were used for the first study that described generation of iPSCs [49]. Later studies provided a number of alternative combinations or strategies to generate iPSCs [50, 51]. These iPSCs have unlimited proliferation capability and can be efficiently expanded to generate large numbers of cells *in vitro*. In addition, iPSCs can be differentiate into hematopoietic progenitor cells and subsequently be used to generate large numbers of CD56+CD3- NK cells for infusion to target and destroy cancer cells [52-54]. Additionally, because iPSCs could be generated from a patient's own cells, they are less likely to be rejected by the patient's immune system, which can be a problem with allogeneic sources. The downside is that autologous iPSCs need to be cultured for multiple weeks delaying therapy compared to “off-the-shelf” allogeneic NK cell therapy which can be given as on-demand therapy and more reliably compared to autologous cells that do not always yield sufficient cells for treatment. Similar to NK-92 cells they can be relatively easily genetically engineered with a CAR, but bear the same risk for malignant transformation [55].

Another potentially interesting source to generate NK cells as an “off-the-shelf” product are CD34+ hematopoietic progenitor cells (HPCs) [56-58]. CD34 is expressed on the surface of HPCs which in normal circumstances are responsible for the production of all mature blood cells. We and others have developed culturing protocols to expand and ex vivo generate large numbers of CD34+ hematopoietic progenitor-derived HPC-NK cells from CD34+ umbilical cord blood cells [56-59]. These HPC-NK cells are shown to be more effective EOC cell killers than NK cells found in blood [60]. They also have favorable receptor expression as they are less mature and lack inhibitory checkpoint molecules expressed on more mature PB-NK cells [unpublished data]. This makes HPC-NK cells less likely to be inhibited in the tumor micro-environment and more active against (EOC) target cells while sparing healthy cells [59]. Studies from different groups in various types of hematological cancers, including acute myeloid leukemia (AML) and myelodysplastic syndrome (MDS) have shown that adoptive HPC-NK cell therapy is safe and well tolerated [61, 62]. Similar to iPSCs and NK-92, HPC-NK can be genetically engineered for example with a higher-affinity CD16A [63].

NK cell cytokine support

NK cell-based therapies can be improved through multiple different approaches. For their survival NK cells rely on stimulation by IL-2 and IL-15 [64-68]. IL-2 and IL-15 both induce highly active and proliferating NK cells [59, 69, 70]. Early knockout mouse studies in the 90s have highlighted the importance of IL-15 for NK cell survival [71]. These studies showed that NK cells from IL-2 deficient mice remained functional and maintained their cell numbers relatively well. In contrast, deleting the IL-2Rβ chain which is shared between the IL-2 and IL-15 receptor resulted in significantly reduced NK cell cytotoxic activity and numbers [72, 73]. Additionally, knockout of the IL-2Rγ chain, shared by the receptors for IL-2, IL-4, IL-7, IL-9 and IL-15 resulted in immature NK cells further highlighting the importance of IL-15 signaling in NK cell maturation and function [73, 74]. In accordance, IL-15 and IL-15Rα deficient mice completely lacked NK cells and could not support adoptively transferred NK cells [75, 76]. Besides the direct favorable effect on NK cells, systemic IL-2 treatment in clinical trials was shown to induce high numbers of regulatory T cells, thereby dampening the immune response and NK cell killing efficacy [77, 78]. Both IL-2 and IL-15 have a short half-life of less than one hour [79, 80]. For this reason, a more stable form of IL-15 or alternative methods to administer IL-15 locally were explored. One method would be to genetically engineer NK cells for adoptive transfer to express IL-15, possibly in combination with a CAR [81]. Another method is to structurally alter the IL-15 molecule. N803 is such a modified molecule containing an activating mutation (N72D) that enhances binding to IL-2Rβ and IL-2Rγ, an IL-15Rα sushi domain to allow trans-presentation resulting in a stronger signal, and an IgG1 Fc tail to increase half-life [82, 83].

Although it is important to induce activation and proliferation in vivo, NK cell tumor reactivity and functionality may still be inhibited by the tumor microenvironment, thus hindering NK cell-mediated EOC cell lysis. The immune system has a number of mechanisms in place to prevent it from attacking healthy cells and tissues [84]. Cancer cells can “abuse” these brakes to prevent the immune system from effectively targeting and destroying cancer cells. By identifying and blocking the pathways used by EOC cells to evade NK cell killing the therapeutic effect of (adoptive) NK cell therapy can be enhanced. The inhibitory proteins involved can either be expressed on the cancer cell surface, which would bind the corresponding inhibitory receptor on the NK cells, or they can be secreted or shed by the cancer cell affecting the surrounding immune cells, including NK cells.

NK cell receptors and checkpoint molecules

As eluded to previously, NK cell activation is dependent on the sum of activating and inhibitory receptors. Key inhibitory receptors are called checkpoint inhibitors. These checkpoint molecules play a crucial role in regulating the immune system and prevent the immune system from attacking healthy cells. Cancer cells are known to upregulate the ligands for these checkpoint molecules and thereby inhibit the immune response [85]. This allows cancer cells to evade the immune system and continue to grow and spread. Checkpoint interference has accomplished a breakthrough in cancer treatment with cytotoxic T-lymphocyte-associated protein 4 (CTLA-4) and Programmed cell death protein 1 (PD-1) blockade successfully opening up new treatment strategies for melanoma and lung cancer patients who previously had no treatment options left [29, 30]. Although there are some overlapping checkpoint molecules between T and NK cells, including T cell immunoreceptor with Ig and immunotyrosine-based inhibitory motif (ITIM) domains (TIGIT), the receptor repertoire of NK cells is markedly different than that of T cells.

NK cells have two main categories of receptors, MHC class 1 and non-MHC binding receptors. Killer-cell immunoglobulin-like receptors (KIRs) are the most well-known and comprise a whole family of both activating and inhibitory receptors that bind HLA-A, B, C and G [86]. A recombinant anti-KIR mAB IPH2101 (17F9) with high affinity to the inhibitory KIR2DL1, -2 and -3 receptors (and activating KIR2DS1 and -2 receptors) is lirilumab [87]. Early studies with IPH2101/lirilumab showed that it was promising in mice as a single agent or in combination with rituximab (anti-CD20) in lymphoma [88-92]. In clinical trials it was shown to be safe to administer, but no significant clinical responses were reported and one study even showed reduced IFN-γ production by NK cells after KIR blockade [90]. Follow-up studies with lirilumab confirmed its safety profile [87, 93-95]. One study reported on combination treatment with anti-PD-1 (nivolumab), but showed no clinical improvement with addition of lirilumab or CTLA-4 blocking (ipilimumab) [93]. There are few other anti-KIR antibodies specific to a single KIR subtype making it difficult to measure protein expression with antibody based techniques or block inhibitory KIRs specifically. We did explore KIR blocking, but as it was not the focus of the research published in this thesis this will be further discussed in **Chapter 7**.

A second family of NK cell receptors that binds MHC class 1 (like) molecules is the Natural Killer Group (NKG) 2 receptor family. The NKG2 family is similar to KIR in that it contains both inhibitory and activating receptors. NKG2A has an ITIM and is inhibitory, while NKG2C and NKG2D are activating [96]. Both NKG2A and NKG2C form a heterodimer with CD94, which together bind HLA-E [93]. NKG2D on the

other hand binds stress-inducible MHC class I chain-related gene A and B (MICA/MICB) and ULPB1-6 [97]. Interestingly, NKG2A blockade with anti-NKG2A (monalizumab or IPH2201) is being tested in (pre-)clinical studies [98-101]. NKG2A blockade was shown to be well tolerated and safe, moreover, monalizumab in combination with durvalumab (another anti-PD-1 antibody) showed clinical benefit over durvalumab alone in patients with unresectable non-small-cell lung cancer [98].

The Natural cytotoxicity receptors (NCR) family are a family encompassing mostly activating NK cell receptors that do not bind MHC class 1 nor related proteins. The family comprises of three activating transmembrane receptors, NKp46, NKp44, and NKp30 which help regulate the cytotoxic and cytokine-secreting functions of tissue NK cells. NCRs have been reported to bind a structurally diverse set of ligands including glycosaminoglycans (GAGs), B7-H6, Galectin-3 and NKp44L as reviewed here [102].

Another important family of receptors that do not bind MHC class 1 are DNAX-associated molecule 1 (DNAM-1 or CD226), TIGIT, CD96 (TACTILE) and PVRIG (CD112R) [103]. Nectin-2 (CD112) and poliovirus receptor (PVR or CD155) are the ligands for both DNAM-1 and TIGIT, while CD96 only binds to CD155 and PVRIG only binds CD112 [103-106]. DNAM-1 binding to its ligands triggers NK cell mediated cytotoxicity of target cells. In contrast, TIGIT or PVRIG binding of the same ligands leads to an inhibitory signal. CD96 function has long been poorly understood as CD96 contains both an inhibitory ITIM-like domain in its cytoplasmic portion and a YXXM motif similar to that of activating receptors such as NKG2D [107]. However, a more recent paper using blocking antibodies has demonstrated that CD96 blocking similar to PVRIG and TIGIT can rescue exhausted CD8+ tumor infiltrating lymphocytes (TILs) [108]. The authors demonstrated that mice with cervical cancer and CD96/PD-1 co-blockade enhanced PD-1 blockade alone and resulted in reduced tumor growth and increased CD8+ TIL function. Several other studies have shown that CD96 is negatively correlated with prognosis for cancer patients, although it remains to be investigated whether this is driven by T cells, NK cells or both [109, 110]. Although PVRIG is the most recent addition to this family, some recent papers have already demonstrated that blockade of PVRIG enhances NK cell activity against AML [111]. Another study showed similar results and reported that PVRIG deficient mice were less susceptible to NK cell exhaustion and had reduced tumor growth [112]. Furthermore, PVRIG blockade reversed NK cell exhaustion and inhibited tumor growth. TIGIT, like DNAM-1, is well described and is already being investigated in clinical trials (over 80 trials listed on ClinicalTrials.gov as of December 2023), either alone or in combination with other checkpoints blockers such as anti PD-1 [113]. Most of these clinical trials are still in early phase of

investigation but one trial, CITYSCAPE, already showed TIGIT plus PD-L1 co-blockade resulting in improved progression-free survival compared with PD-L1 blockade alone in PD-L1-positive, recurrent or metastatic non-small-cell lung cancer patients [114].

Finally, there are some receptors that, similar to CD96, remain largely unexplored and their function is not well described. One of these is T-cell immunoglobulin and mucin-containing domain (TIM)-3. For T cells, TIM-3 is a negative regulator of T cell anti-tumor responses as shown by the inability of $TIM3^+$ T cells to produce IFN-γ, TNF-α and IL-2 [115-117]. However, on NK cells TIM-3 is attributed to both inhibitory and activating functions with environment-specific functions [118-121]. Similar to T cells, TIM-3 expression on NK cells is associated with a mature or so called 'exhausted' phenotype [121].

Tumor micro-environment and EOC cell interaction with NK cells

Isolating, culturing and using primary EOC cells to study their interaction with NK cells is a challenging task. Although we and others have cultured our in-house ascites derived EOC cells (**Chapter 3**) the number of cells that can be used for functional testing were generally low as there was no or limited long-term growth of these primary tumor cells. Therefore much of the work presented in this thesis was performed on immortalized cell lines. To this end we used SKOV-3, IGROV-1 and OVCAR-3, which are all epithelial adenocarcinoma cell lines isolated from Caucasian women aged 64, 47 and 60 years, respectively. An advantage of this approach is that these cell lines are widely used for EOC cancer research making our results and findings more easily reproducible and comparable to existing literature. All of these cell lines have high expression of DNAM-1/TIGIT/CD96 ligands NECTIN-2 and PVR and can trigger NK cell degranulation [122].

The soluble factors present in ascites secreted by tumor, immune & stromal/tissue-resident cells are considered to strongly impact immune cell function [123-125]. One such factor, TGF-β1 was shown to be critical for the formation of ascites as TGF-β1 blockade was shown to reduce ascites in a murine model [126]. Ascites is also reported to contain high levels of a variety of other soluble factors including osteoprotegerin (OPG), macrophage inhibiting factor (MIF), regulated on activation, normal T cell expressed and secreted (RANTES), IL-6, IL-8, IL-10 and CCL22 [127, 128]. A recent systematic review combining data of fourteen papers investigating cytokine levels in ascites from EOC patients, found high levels of IL-6 in two out of four studies in which IL-6 levels were assessed and a third when in association with higher TNF-α [129]. Only one out of three studies where IL-10 was

assessed, showed IL-10 levels in ascites to be associated with worse prognosis while the other two did not. One study showed that increased IFN-γ was correlated with a reduced PFS and OS while another study showed that elevated IL-8 and TNF-α associated with worse survival [130, 131].

Although TGF-β1 has been shown to be elevated in ascites from EOC patients, data correlating it to survival is lacking [127, 132-134]. A meta-analysis of genomic profiles of 1525 EOC patients revealed that overexpression of TGF-βRII in EOC debulking specimens correlated with poor prognosis [135]. TGF-β1 is a known driver of polarization towards Tumor Associated Macrophages (TAMs) and can negatively impact NK cell activity [47]. Furthermore, for other types of cancer, TGF-β1 was shown to increase expression levels of inhibitory ligands on cancer cells, such as MHC molecules and immune regulator fatty acid synthase (FASN) [136-138]. Besides impairing NK cell activity TGF-β1 is able to skew NK cells towards a type 1 ILC which are known to exhibit limited antitumoral immune responses [139-142].

Interestingly, NK cell activating cytokines IL-2 and IL-15 are reported to be absent or low in ascites of most patients [143], while IL-12 and IFN-γ are only present in advanced stages (III–IV) EOC patients indicating a hostile environment for NK cell function [127]. This is further invigorated by the presence of soluble ligands for NK cell receptors, another more recently discovered inhibitory mechanism abused by tumor cells to evade immune cell killing [144-147]. Soluble MIC-A and ULBP1/2/3, which can be shed by EOC tumor cells, results in downregulated NKG2D on NK cells [147-149]. Similarly, soluble PVR inhibited DNAM-1 mediated NK activation [146]. Although literature on soluble ligands is relatively scarce, there is ample evidence on cell bound ligands for NK cell receptors. Similar to soluble PVR, tumor cell expression of NECTIN-2 or PVR also leads to down regulation of DNAM-1 on NK cells [150, 151]. B7-H6, a ligand for NKp30, downregulates NKp30 similar to PVR [152]. Chronic exposure to NKG2D ligands results in dysfunctional NK cells and lower NKG2D expression [153].

As described, there is an unmet need for additional therapeutic strategies to improve EOC patient outcome, especially after recurrence. EOC is a relative immunogenic tumor as there appears to be a role for tumor infiltrating lymphocytes in combating EOC. However, the specific role for NK cells in EOC has been largely unexplored with some studies indicating a potential role NK cell based therapies. Identification of dominant pathways inhibiting/activating NK cell function in ascites will be instrumental for the development of new or existing immunotherapeutic (blocking) strategies to maximize NK immunotherapy.

Outline of the thesis:

There is still insufficient understanding of the interaction between the immune system and EOC, a disease with limited treatment strategies. We sought to explore the interaction between EOC and NK cells with the ultimate goal to identify the major soluble and cell bound ligands / cytokines responsible for NK cell inhibition and to block these pathways which might ultimately lead to improved NK cell based treatment strategies.

Chapter 2 of this thesis further explores the role of NK cells in EOC. To this end the frequency and phenotype of NK cells in ascites of EOC patients was assessed and related to clinical outcome. Furthermore, the enhancement of NK cell function was demonstrated in patient-derived NK cells through increased responses when exposed to IL-15 and the super-agonist N803.

In **Chapter 3** the effects of super-agonist N803, with improved properties compared to IL-15, on HPC-NK cell reactivity against EOC and AML are investigated. To demonstrate the supportive and activating effects of N803 on HPC-NK cells, we employed (serial) killing assays and utilized immunodeficient mice bearing OC, revealing heightened killing capacity and reduced tumor growth, respectively.

In **Chapter 4**, high-dimensional single-cell analysis was utilized to investigate NK cells from ascites of high-grade serous EOC patients. This methodology revealed distinct FlowSOM meta-clusters demonstrating an exhausted phenotype, correlating with the (suppressive) soluble factor milieu in the ascites.

Chapter 5 focused on the DNAM-1/TIGIT pathway and showed that TIGIT blockade enhanced functionality of peritoneal NK cells from EOC patients. With an *in vivo* mouse model we showed that DNAM-1 expression on adoptively transferred NK cells was reduced in tumor-bearing mice compared to mice without tumor.

In **Chapter 6** soluble factors, cell composition and inhibitory properties of ascites from high-grade serous EOC patients were explored. This revealed TGF-β1 as an important regulator of NK cell suppression, which could be rescued with TGF-β1 blockade.

Finally, in **Chapter 7** all findings presented in this thesis are summarized and placed in context of the current literature on NK cell immunity against EOC. Furthermore, the future perspectives and research priorities to improve NK cell-based immune-therapies are outlined.

References

1. Matulonis UA, Sood AK, Fallowfield L, Howitt BE, Sehouli J, Karlan BY. *Ovarian cancer.* Nature Reviews Disease Primers. 2016;2(1):16061.

2. Siegel RL, Miller KD, Jemal A. *Cancer Statistics, 2017. CA* Cancer J Clin. 2017;67(1):7-30.

3. Gadducci A, Cosio S, Zola P, Landoni F, Maggino T, Sartori E. *Surveillance procedures for patients treated for epithelial ovarian cancer: a review of the literature.* Int J Gynecol Cancer. 2007;17(1):21-31.

4. Ayhan A, Gultekin M, Taskiran C, Dursun P, Firat P, Bozdag G, et al. *Ascites and epithelial ovarian cancers: a reappraisal with respect to different aspects.* Int J Gynecol Cancer. 2007;17(1):68-75.

5. Sangisetty SL, Miner TJ. *Malignant ascites: A review of prognostic factors, pathophysiology and therapeutic measures.* World J Gastrointest Surg. 2012;4(4):87-95.

6. Ahmed N, Stenvers KL. *Getting to know ovarian cancer ascites: opportunities for targeted therapy-based translational research.* Front Oncol. 2013;3:256.

7. Lane D, Goncharenko-Khaider N, Rancourt C, Piché A. *Ovarian cancer ascites protects from TRAIL-induced cell death through alphavbeta5 integrin-mediated focal adhesion kinase and Akt activation.* Oncogene. 2010;29(24):3519-31.

8. Lane D, Robert V, Grondin R, Rancourt C, Piché A. *Malignant ascites protect against TRAIL-induced apoptosis by activating the PI3K/Akt pathway in human ovarian carcinoma cells.* Int J Cancer. 2007;121(6):1227-37.

9. Puiffe ML, Le Page C, Filali-Mouhim A, Zietarska M, Ouellet V, Tonin PN, et al. *Characterization of ovarian cancer ascites on cell invasion, proliferation, spheroid formation, and gene expression in an in vitro model of epithelial ovarian cancer.* Neoplasia. 2007;9(10):820-9.

10. Belisle JA, Gubbels JA, Raphael CA, Migneault M, Rancourt C, Connor JP, et al. *Peritoneal natural killer cells from epithelial ovarian cancer patients show an altered phenotype and bind to the tumour marker MUC16 (CA125).* Immunology. 2007;122(3):418-29.

11. Santin AD, Hermonat PL, Ravaggi A, Bellone S, Roman JJ, Smith CV, et al. *Phenotypic and functional analysis of tumor-infiltrating lymphocytes compared with tumor-associated lymphocytes from ascitic fluid and peripheral blood lymphocytes in patients with advanced ovarian cancer.* Gynecol Obstet Invest. 2001;51(4):254-61.

12. Lukesova S, Vroblova V, Tosner J, Kopecky J, Sedlakova I, Čermáková E, et al. *Comparative study of various subpopulations of cytotoxic cells in blood and ascites from patients with ovarian carcinoma.* Contemp Oncol (Pozn). 2015;19(4):290-9.

13. Onsrud M, Bosnes V, Grahm I. *cis-Platinum as adjunctive to surgery in early stage ovarian carcinoma: effects on lymphoid cell subpopulations.* Gynecol Oncol. 1986;23(3):323-8.

14. Giuntoli RL, 2nd, Webb TJ, Zoso A, Rogers O, Diaz-Montes TP, Bristow RE, et al. *Ovarian cancer-associated ascites demonstrates altered immune environment: implications for antitumor immunity.* Anticancer Res. 2009;29(8):2875-84.

15. Fumita Y, Tanaka F, Saji F, Nakamuro K. *Immunosuppressive factors in ascites fluids from ovarian cancer patients.* Am J Reprod Immunol (1980). 1984;6(4):175-8.

16. Rickard BP, Conrad C, Sorrin AJ, Ruhi MK, Reader JC, Huang SA, et al. *Malignant Ascites in Ovarian Cancer: Cellular, Acellular, and Biophysical Determinants of Molecular Characteristics and Therapy Response.* Cancers (Basel). 2021;13(17).

17. Tewari KS, Burger RA, Enserro D, Norquist BM, Swisher EM, Brady MF, et al. *Final overall survival of a randomized trial of bevacizumab for primary treatment of ovarian cancer. Journal of Clinical Oncology*. 2019;37(26):2317.

18. Dong HP, Elstrand MB, Holth A, Silins I, Berner A, Trope CG, et al. *NK- and B-cell infiltration correlates with worse outcome in metastatic ovarian carcinoma.* Am J Clin Pathol. 2006;125(3):451-8.

19. Webb JR, Milne K, Watson P, Deleeuw RJ, Nelson BH. *Tumor-infiltrating lymphocytes expressing the tissue resident memory marker CD103 are associated with increased survival in high-grade serous ovarian cancer.* Clin Cancer Res. 2014;20(2):434-44.

20. Gooden M, Lampen M, Jordanova ES, Leffers N, Trimbos JB, van der Burg SH, et al. *HLA-E expression by gynecological cancers restrains tumor-infiltrating CD8$^+$ T lymphocytes.* Proc Natl Acad Sci U S A. 2011;108(26):10656-61.

21. Zhang L, Conejo-Garcia JR, Katsaros D, Gimotty PA, Massobrio M, Regnani G, et al. *Intratumoral T cells, recurrence, and survival in epithelial ovarian cancer.* N Engl J Med. 2003;348(3):203-13.

22. Hwang WT, Adams SF, Tahirovic E, Hagemann IS, Coukos G. *Prognostic significance of tumor-infiltrating T cells in ovarian cancer: a meta-analysis.* Gynecol Oncol. 2012;124(2):192-8.

23. Henriksen JR, Donskov F, Waldstrøm M, Jakobsen A, Hjortkjaer M, Petersen CB, et al. *Favorable prognostic impact of Natural Killer cells and T cells in high-grade serous ovarian carcinoma*. Acta Oncologica. 2020;59(6):652-9.

24. Henriksen JR, Nederby L, Donskov F, Waldstrøm M, Adimi P, Jakobsen A, et al. *Blood natural killer cells during treatment in recurrent ovarian cancer.* Acta Oncologica. 2020;59(11):1365-73.

25. Imai K, Matsuyama S, Miyake S, Suga K, Nakachi K. *Natural cytotoxic activity of peripheral-blood lymphocytes and cancer incidence: an 11-year follow-up study of a general population.* Lancet. 2000;356(9244):1795-9.

26. Geller MA, Knorr DA, Hermanson DA, Pribyl L, Bendzick L, McCullar V, et al. *Intraperitoneal delivery of human natural killer cells for treatment of ovarian cancer in a mouse xenograft model*. Cytotherapy. 2013;15(10):1297-306.

27. Hermanson DL, Bendzick L, Pribyl L, McCullar V, Vogel RI, Miller JS, et al. *Induced Pluripotent Stem Cell-Derived Natural Killer Cells for Treatment of Ovarian Cancer*. Stem Cells. 2016;34(1):93-101.

28. Uppendahl LD, Dahl CM, Miller JS, Felices M, Geller MA. *Natural Killer Cell-Based Immunotherapy in Gynecologic Malignancy: A Review.* Front Immunol. 2017;8:1825.

29. Rotte A. *Combination of CTLA-4 and PD-1 blockers for treatment of cancer.* Journal of Experimental & Clinical Cancer Research. 2019;38(1):255.

30. Dantoing E, Piton N, Salaün M, Thiberville L, Guisier F. *Anti-PD1/PD-L1 Immunotherapy for Non-Small Cell Lung Cancer with Actionable Oncogenic Driver Mutations*. Int J Mol Sci. 2021;22(12).

31. Sterner RC, Sterner RM. *CAR-T cell therapy: current limitations and potential strategies.* Blood Cancer Journal. 2021;11(4):69.

32. Majzner RG, Theruvath JL, Nellan A, Heitzeneder S, Cui Y, Mount CW, et al. *CAR T Cells Targeting B7-H3, a Pan-Cancer Antigen, Demonstrate Potent Preclinical Activity Against Pediatric Solid Tumors and Brain Tumors.* Clin Cancer Res. 2019;25(8):2560-74.

33. Murad JP, Kozlowska AK, Lee HJ, Ramamurthy M, Chang WC, Yazaki P, et al. *Effective Targeting of TAG72(+) Peritoneal Ovarian Tumors via Regional Delivery of CAR-Engineered T Cells.* Front Immunol. 2018;9:2268.

34. Cohen AD, Garfall AL, Stadtmauer EA, Melenhorst JJ, Lacey SF, Lancaster E, et al. *B cell maturation antigen-specific CAR T cells are clinically active in multiple myeloma.* J Clin Invest. 2019;129(6):2210-21.

35. Hege KM, Bergsland EK, Fisher GA, Nemunaitis JJ, Warren RS, McArthur JG, et al. *Safety, tumor trafficking and immunogenicity of chimeric antigen receptor (CAR)-T cells specific for TAG-72 in colorectal cancer*. J Immunother Cancer. 2017;5:22.

36. Neelapu SS, Locke FL, Bartlett NL, Lekakis LJ, Miklos DB, Jacobson CA, et al. *Axicabtagene Ciloleucel CAR T-Cell Therapy in Refractory Large B-Cell Lymphoma*. N Engl J Med. 2017;377(26):2531-44.

37. Shifrin N, Raulet DH, Ardolino M. *NK cell self tolerance, responsiveness and missing self recognition.* Semin Immunol. 2014;26(2):138-44.

38. Poli A, Michel T, Thérésine M, Andrès E, Hentges F, Zimmer J. *CD56bright natural killer (NK) cells: an important NK cell subset*. Immunology. 2009;126(4):458-65.

39. Gong Y, Klein Wolterink RGJ, Wang J, Bos GMJ, Germeraad WTV. *Chimeric antigen receptor natural killer (CAR-NK) cell design and engineering for cancer therapy*. Journal of Hematology & Oncology. 2021;14(1):73.

40. Gong JH, Maki G, Klingemann HG. *Characterization of a human cell line (NK-92) with phenotypical and functional characteristics of activated natural killer cells*. Leukemia. 1994;8(4):652-8.

41. Klingemann HG, Wong E, Maki G. *A cytotoxic NK-cell line (NK-92) for ex vivo purging of leukemia from blood.* Biol Blood Marrow Transplant. 1996;2(2):68-75.

42. Tang X, Yang L, Li Z, Nalin AP, Dai H, Xu T, et al. *First-in-man clinical trial of CAR NK-92 cells: safety test of CD33-CAR NK-92 cells in patients with relapsed and refractory acute myeloid leukemia. American journal of cancer research*. 2018;8(6):1083.

43. Williams BA, Wang XH, Leyton JV, Maghera S, Deif B, Reilly RM, et al. C*D16(+)NK-92 and anti-CD123 monoclonal antibody prolongs survival in primary human acute myeloid leukemia xenografted mice.* Haematologica. 2018;103(10):1720-9.

44. Boyiadzis M, Agha M, Redner RL, Sehgal A, Im A, Hou J-Z, et al. P*hase 1 clinical trial of adoptive immunotherapy using "off-the-shelf" activated natural killer cells in patients with refractory and relapsed acute myeloid leukemia.* Cytotherapy. 2017;19(10):1225-32.

45. Tonn T, Schwabe D, Klingemann HG, Becker S, Esser R, Koehl U, et al. *Treatment of patients with advanced cancer with the natural killer cell line NK-92.* Cytotherapy. 2013;15(12):1563-70.

46. Larson SM, Walthers CM, Ji B, Ghafouri SN, Naparstek J, Trent J, et al. C*D19/CD20 Bispecific Chimeric Antigen Receptor (CAR) in Naive/Memory T Cells for the Treatment of Relapsed or Refractory Non-Hodgkin Lymphoma.* Cancer Discov. 2023;13(3):580-97.

47. Mazza R, Maher J. *Prospects for Development of Induced Pluripotent Stem Cell-Derived CAR-Targeted Immunotherapies.* Archivum Immunologiae et Therapiae Experimentalis. 2022;70.

48. Navarrete-Galvan L, Guglielmo M, Cruz Amaya J, Smith-Gagen J, Lombardi VC, Merica R, et al. *Optimizing NK-92 serial killers: gamma irradiation, CD95/Fas-ligation, and NK or LAK attack limit cytotoxic efficacy.* J Transl Med. 2022;20(1):151.

49. Takahashi K, Yamanaka S. *Induction of Pluripotent Stem Cells from Mouse Embryonic and Adult Fibroblast Cultures by Defined Factors.* Cell. 2006;126(4):663-76.

50. Yu J, Vodyanik MA, Smuga-Otto K, Antosiewicz-Bourget J, Frane JL, Tian S, et al. *Induced Pluripotent Stem Cell Lines Derived from Human Somatic Cells*. Science. 2007;318(5858):1917-20.

51. Wang B, Wu L, Li D, Liu Y, Guo J, Li C, et al. *Induction of Pluripotent Stem Cells from Mouse Embryonic Fibroblasts by Jdp2-Jhdm1b-Mkk6-Glis1-Nanog-Essrb-Sall4.* Cell Reports. 2019;27(12):3473-85.e5.

52. Ni Z, Knorr DA, Clouser CL, Hexum MK, Southern P, Mansky LM, et al. *Human pluripotent stem cells produce natural killer cells that mediate anti-HIV-1 activity by utilizing diverse cellular mechanisms.* J Virol. 2011;85(1):43-50.

53. Woll PS, Grzywacz B, Tian X, Marcus RK, Knorr DA, Verneris MR, et al. *Human embryonic stem cells differentiate into a homogeneous population of natural killer cells with potent in vivo antitumor activity.* Blood. 2009;113(24):6094-101.

54. Woll PS, Martin CH, Miller JS, Kaufman DS. *Human embryonic stem cell-derived NK cells acquire functional receptors and cytolytic activity.* J Immunol. 2005;175(8):5095-103.

55. Li Y, Hermanson DL, Moriarity BS, Kaufman DS. *Human iPSC-Derived Natural Killer Cells Engineered with Chimeric Antigen Receptors Enhance Anti-tumor Activity*. Cell Stem Cell. 2018;23(2):181-92.e5.

56. Cany J, van der Waart AB, Tordoir M, Franssen GM, Hangalapura BN, de Vries J, et al. *Natural killer cells generated from cord blood hematopoietic progenitor cells efficiently target bone marrow-residing human leukemia cells in NOD/SCID/IL2Rg(null) mice.* PLoS One. 2013;8(6):e64384.

57. Spanholtz J, Preijers F, Tordoir M, Trilsbeek C, Paardekooper J, de Witte T, et al. *Clinical-grade generation of active NK cells from cord blood hematopoietic progenitor cells for immunotherapy using a closed-system culture process.* PLoS One. 2011;6(6):e20740.

58. Spanholtz J, Tordoir M, Eissens D, Preijers F, van der Meer A, Joosten I, et al. *High log-scale expansion of functional human natural killer cells from umbilical cord blood CD34-positive cells for adoptive cancer immunotherapy.* PLoS One. 2010;5(2):e9221.

59. Cany J, van der Waart AB, Spanholtz J, Tordoir M, Jansen JH, van der Voort R, et al. *Combined IL-15 and IL-12 drives the generation of CD34(+)-derived natural killer cells with superior maturation and alloreactivity potential following adoptive transfer.* Oncoimmunology. 2015;4(7):e1017701.

60. Hoogstad-van Evert JS, Maas RJ, van der Meer J, Cany J, van der Steen S, Jansen JH, et al. *Peritoneal NK cells are responsive to IL-15 and percentages are correlated with outcome in advanced ovarian cancer patients.* Oncotarget. 2018;9(78):34810-20.

61. Dolstra H, Roeven MWH, Spanholtz J, Hangalapura BN, Tordoir M, Maas F, et al. *Successful Transfer of Umbilical Cord Blood CD34(+) Hematopoietic Stem and Progenitor-derived NK Cells in Older Acute Myeloid Leukemia Patients.* Clin Cancer Res. 2017;23(15):4107-18.

62. Yoon SR, Lee YS, Yang SH, Ahn KH, Lee JH, Lee JH, et al. *Generation of donor natural killer cells from CD34(+) progenitor cells and subsequent infusion after HLA-mismatched allogeneic hematopoietic cell transplantation: a feasibility study.* Bone Marrow Transplant. 2010;45(6):1038-46.

63. van Hauten PMM, Hooijmaijers L, Vidal-Manrique M, van der Waart AB, Hobo W, Wu J, et al. *Engineering of CD34+ progenitor-derived natural killer cells with higher-affinity CD16a for enhanced antibody-dependent cellular cytotoxicity.* Cytotherapy. 2023.

64. Ma A, Koka R, Burkett P. *DIVERSE FUNCTIONS OF IL-2, IL-15, AND IL-7 IN LYMPHOID HOMEOSTASIS.* Annual Review of Immunology. 2006;24(1):657-79.

65. Burton JD, Bamford RN, Peters C, Grant AJ, Kurys G, Goldman CK, et al. *A lymphokine, provisionally designated interleukin T and produced by a human adult T-cell leukemia line, stimulates T-cell proliferation and the induction of lymphokine-activated killer cells*. Proceedings of the National Academy of Sciences. 1994;91(11):4935-9.

66. Carson WE, Giri JG, Lindemann MJ, Linett ML, Ahdieh M, Paxton R, et al. I*nterleukin (IL) 15 is a novel cytokine that activates human natural killer cells via components of the IL-2 receptor.* Journal of Experimental Medicine. 1994;180(4):1395-403.

67. Fehniger TA, Cooper MA, Nuovo GJ, Cella M, Facchetti F, Colonna M, et al. *CD56bright natural killer cells are present in human lymph nodes and are activated by T cell–derived IL-2: a potential new link between adaptive and innate immunity.* Blood. 2003;101(8):3052-7.

68. Trinchieri G. Biology of Natural Killer Cells. In: Dixon FJ, editor. *Advances in Immunology*. 47: Academic Press; 1989. p. 187-376.

69. Waldmann TA. *The biology of interleukin-2 and interleukin-15: implications for cancer therapy and vaccine design.* Nat Rev Immunol. 2006;6(8):595-601.

70. Fehniger TA, Cooper MA, Caligiuri MA. *Interleukin-2 and interleukin-15: immunotherapy for cancer.* Cytokine Growth Factor Rev. 2002;13(2):169-83.

71. Kündig TM, Schorle H, Bachmann MF, Hengartner H, Zinkernagel RM, Horak I. *Immune responses in interleukin-2-deficient mice.* Science. 1993;262(5136):1059-61.

72. Suzuki H, Duncan GS, Takimoto H, Mak TW. *Abnormal development of intestinal intraepithelial lymphocytes and peripheral natural killer cells in mice lacking the IL-2 receptor beta chain*. J Exp Med. 1997;185(3):499-505.

73. Grabstein KH, Eisenman J, Shanebeck K, Rauch C, Srinivasan S, Fung V, et al. *Cloning of a T cell growth factor that interacts with the beta chain of the interleukin-2 receptor.* Science. 1994;264(5161):965-8.

74. DiSanto JP, Müller W, Guy-Grand D, Fischer A, Rajewsky K. *Lymphoid development in mice with a targeted deletion of the interleukin 2 receptor gamma chain.* Proc Natl Acad Sci U S A. 1995;92(2):377-81.

75. Cooper MA, Bush JE, Fehniger TA, VanDeusen JB, Waite RE, Liu Y, et al. *In vivo evidence for a dependence on interleukin 15 for survival of natural killer cells.* Blood. 2002;100(10):3633-8.

76. Kennedy MK, Glaccum M, Brown SN, Butz EA, Viney JL, Embers M, et al. *Reversible defects in natural killer and memory CD8 T cell lineages in interleukin 15-deficient mice.* J Exp Med. 2000;191(5):771-80.

77. Ye C, Brand D, Zheng SG. *Targeting IL-2: an unexpected effect in treating immunological diseases.* Signal Transduction and Targeted Therapy. 2018;3(1):2.

78. Ahmadzadeh M, Rosenberg SA. *IL-2 administration increases CD4+ CD25(hi) Foxp3+ regulatory T cells in cancer patients*. Blood. 2006;107(6):2409-14.

79. Donohue JH, Rosenberg SA. *The fate of interleukin-2 after in vivo administration.* J Immunol. 1983;130(5):2203-8.

80. Chertova E, Bergamaschi C, Chertov O, Sowder R, Bear J, Roser JD, et al. *Characterization and Favorable in Vivo Properties of Heterodimeric Soluble IL-15·IL-15Rα Cytokine Compared to IL-15 Monomer*.* Journal of Biological Chemistry. 2013;288(25):18093-103.

81. Liu E, Tong Y, Dotti G, Shaim H, Savoldo B, Mukherjee M, et al. *Cord blood NK cells engineered to express IL-15 and a CD19-targeted CAR show long-term persistence and potent antitumor activity.* Leukemia. 2018;32(2):520-31.

82. Zhu X, Marcus WD, Xu W, Lee HI, Han K, Egan JO, et al. *Novel human interleukin-15 agonists*. J Immunol. 2009;183(6):3598-607.

83. Han KP, Zhu X, Liu B, Jeng E, Kong L, Yovandich JL, et al. *IL-15:IL-15 receptor alpha superagonist complex: high-level co-expression in recombinant mammalian cells, purification and characterization.* Cytokine. 2011;56(3):804-10.

84. Rose NR. *Mechanisms of Autoimmunity.* Semin Liver Dis. 2002;22(04):387-94.

85. Pardoll DM. *The blockade of immune checkpoints in cancer immunotherapy*. Nat Rev Cancer. 2012;12(4):252-64.

86. Campbell KS, Purdy AK. S*tructure/function of human killer cell immunoglobulin-like receptors: lessons from polymorphisms, evolution, crystal structures and mutations*. Immunology. 2011;132(3):315-25.

87. Vey N, Karlin L, Sadot-Lebouvier S, Broussais F, Berton-Rigaud D, Rey J, et al. *A phase 1 study of lirilumab (antibody against killer immunoglobulin-like receptor antibody KIR2D; IPH2102) in patients with solid tumors and hematologic malignancies.* Oncotarget. 2018;9(25):17675-88.

88. Korde N, Carlsten M, Lee MJ, Minter A, Tan E, Kwok M, et al. *A phase II trial of pan-KIR2D blockade with IPH2101 in smoldering multiple myeloma.* Haematologica. 2014;99(6):e81-3.

89. Vey N, Bourhis J-H, Boissel N, Bordessoule D, Prebet T, Charbonnier A, et al. *A phase 1 trial of the anti-inhibitory KIR mAb IPH2101 for AML in complete remission.* Blood. 2012;120(22):4317-23.

90. Carlsten M, Korde N, Kotecha R, Reger R, Bor S, Kazandjian D, et al. *Checkpoint Inhibition of KIR2D with the Monoclonal Antibody IPH2101 Induces Contraction and Hyporesponsiveness of NK Cells in Patients with Myeloma.* Clin Cancer Res. 2016;22(21):5211-22.

91. Benson DM, Jr., Hofmeister CC, Padmanabhan S, Suvannasankha A, Jagannath S, Abonour R, et al. *A phase 1 trial of the anti-KIR antibody IPH2101 in patients with relapsed/refractory multiple myeloma.* Blood. 2012;120(22):4324-33.

92. Kohrt HE, Thielens A, Marabelle A, Sagiv-Barfi I, Sola C, Chanuc F, et al. *Anti-KIR antibody enhancement of anti-lymphoma activity of natural killer cells as monotherapy and in combination with anti-CD20 antibodies*. Blood. 2014;123(5):678-86.

93. Armand P, Lesokhin A, Borrello I, Timmerman J, Gutierrez M, Zhu L, et al. *A phase 1b study of dual PD-1 and CTLA-4 or KIR blockade in patients with relapsed/refractory lymphoid malignancies.* Leukemia. 2021;35(3):777-86.

94. Yalniz FF, Daver N, Rezvani K, Kornblau S, Ohanian M, Borthakur G, et al. *A Pilot Trial of Lirilumab With or Without Azacitidine for Patients With Myelodysplastic Syndrome*. Clin Lymphoma Myeloma Leuk. 2018;18(10):658-63.e2.

95. Hanna GJ, O'Neill A, Shin KY, Wong K, Jo VY, Quinn CT, et al. *Neoadjuvant and Adjuvant Nivolumab and Lirilumab in Patients with Recurrent, Resectable Squamous Cell Carcinoma of the Head and Neck.* Clin Cancer Res. 2022;28(3):468-78.

96. Borrego F, Masilamani M, Marusina AI, Tang X, Coligan JE. *The CD94/NKG2 family of receptors*. Immunologic Research. 2006;35(3):263-77.

97. Sutherland CL, Rabinovich B, Chalupny NJ, Brawand P, Miller R, Cosman D. *ULBPs, human ligands of the NKG2D receptor, stimulate tumor immunity with enhancement by IL-15.* Blood. 2006;108(4):1313-9.

98. Herbst RS, Majem M, Barlesi F, Carcereny E, Chu Q, Monnet I, et al. *COAST: An Open-Label, Phase II, Multidrug Platform Study of Durvalumab Alone or in Combination With Oleclumab or Monalizumab in Patients With Unresectable, Stage III Non-Small-Cell Lung Cancer*. J Clin Oncol. 2022;40(29):3383-93.

99. Galot R, Le Tourneau C, Saada-Bouzid E, Daste A, Even C, Debruyne P, et al. *A phase II study of monalizumab in patients with recurrent/metastatic squamous cell carcinoma of the head and neck: The I1 cohort of the EORTC-HNCG-1559 UPSTREAM trial.* Eur J Cancer. 2021;158:17-26.

100. Borst L, van der Burg SH, van Hall T. *The NKG2A–HLA-E Axis as a Novel Checkpoint in the Tumor Microenvironment*. Clinical Cancer Research. 2020;26(21):5549-56.

101. Tinker AV, Hirte HW, Provencher D, Butler M, Ritter H, Tu D, et al. *Dose-Ranging and Cohort-Expansion Study of Monalizumab (IPH2201) in Patients with Advanced Gynecologic Malignancies: A Trial of the Canadian Cancer Trials Group (CCTG): IND221.* Clin Cancer Res. 2019;25(20):6052-60.

102. Barrow AD, Martin CJ, Colonna M. *The Natural Cytotoxicity Receptors in Health and Disease.* Frontiers in Immunology. 2019;10.

103. Sanchez-Correa B, Valhondo I, Hassouneh F, Lopez-Sejas N, Pera A, Bergua JM, et al. *DNAM-1 and the TIGIT/PVRIG/TACTILE Axis: Novel Immune Checkpoints for Natural Killer Cell-Based Cancer Immunotherapy.* Cancers (Basel). 2019;11(6).

104. Fuchs A, Colonna M. *The role of NK cell recognition of nectin and nectin-like proteins in tumor immunosurveillance*. Semin Cancer Biol. 2006;16(5):359-66.

105. Chauvin J-M, Zarour HM. *TIGIT in cancer immunotherapy*. Journal for ImmunoTherapy of Cancer. 2020;8(2):e000957.

106. Jin H-S, Park Y. *Hitting the complexity of the TIGIT-CD96-CD112R-CD226 axis for next-generation cancer immunotherapy*. BMB reports. 2020;54.

107. Chambers CA. *The expanding world of co-stimulation: the two-signal model revisited*. Trends in Immunology. 2001;22(4):217-23.

108. Wang Y, Wang C, Qiu J, Qu X, Peng J, Lu C, et al. *Targeting CD96 overcomes PD-1 blockade resistance by enhancing CD8+ TIL function in cervical cancer.* Journal for ImmunoTherapy of Cancer. 2022;10(3):e003667.

109. Sun H, Huang Q, Huang M, Wen H, Lin R, Zheng M, et al. *Human CD96 Correlates to Natural Killer Cell Exhaustion and Predicts the Prognosis of Human Hepatocellular Carcinoma.* Hepatology. 2019;70(1):168-83.

110. Liu F, Huang J, He F, Ma X, Fan F, Meng M, et al. *CD96, a new immune checkpoint, correlates with immune profile and clinical outcome of glioma.* Scientific Reports. 2020;10(1):10768.

111. Li J, Whelan S, Kotturi MF, Meyran D, D'Souza C, Hansen K, et al. *PVRIG is a novel natural killer cell immune checkpoint receptor in acute myeloid leukemia*. Haematologica. 2021;106(12):3115-24.

112. Li Y, Zhang Y, Cao G, Zheng X, Sun C, Wei H, et al. *Blockade of checkpoint receptor PVRIG unleashes anti-tumor immunity of NK cells in murine and human solid tumors*. Journal of Hematology & Oncology. 2021;14(1):100.

113. Pawłowska A, Skiba W, Suszczyk D, Kuryło W, Jakubowicz-Gil J, Paduch R, et al. *The Dual Blockade of the TIGIT and PD-1/PD-L1 Pathway as a New Hope for Ovarian Cancer Patients.* Cancers (Basel). 2022;14(23).

114. Cho BC, Abreu DR, Hussein M, Cobo M, Patel AJ, Secen N, et al. *Tiragolumab plus atezolizumab versus placebo plus atezolizumab as a first-line treatment for PD-L1-selected non-small-cell lung cancer (CITYSCAPE): primary and follow-up analyses of a randomised, double-blind, phase 2 study.* The Lancet Oncology. 2022;23(6):781-92.

115. Cai C, Xu YF, Wu ZJ, Dong Q, Li MY, Olson JC, et al. *Tim-3 expression represents dysfunctional tumor infiltrating T cells in renal cell carcinoma.* World J Urol. 2016;34(4):561-7.

116. Liu Z, Han H, He X, Li S, Wu C, Yu C, et al. *Expression of the galectin-9-Tim-3 pathway in glioma tissues is associated with the clinical manifestations of glioma*. Oncol Lett. 2016;11(3):1829-34.

117. Liu F, Liu Y, Chen Z. *Tim-3 expression and its role in hepatocellular carcinoma.* J Hematol Oncol. 2018;11(1):126.

118. Dao TN, Utturkar S, Atallah Lanman N, Matosevic S. *TIM-3 Expression Is Downregulated on Human NK Cells in Response to Cancer Targets in Synergy with Activation*. Cancers (Basel). 2020;12(9).

119. Ndhlovu LC, Lopez-Vergès S, Barbour JD, Jones RB, Jha AR, Long BR, et al. *Tim-3 marks human natural killer cell maturation and suppresses cell-mediated cytotoxicity.* Blood. 2012;119(16):3734-43.

120. Gleason MK, Lenvik TR, McCullar V, Felices M, O'Brien MS, Cooley SA, et al. *Tim-3 is an inducible human natural killer cell receptor that enhances interferon gamma production in response to galectin-9.* Blood. 2012;119(13):3064-72.

121. da Silva IP, Gallois A, Jimenez-Baranda S, Khan S, Anderson AC, Kuchroo VK, et al. *Reversal of NK-cell exhaustion in advanced melanoma by Tim-3 blockade*. Cancer Immunol Res. 2014;2(5):410-22.

122. Maas RJ, Hoogstad-van Evert JS, Van der Meer JM, Mekers V, Rezaeifard S, Korman AJ, et al. *TIGIT blockade enhances functionality of peritoneal NK cells with altered expression of DNAM-1/TIGIT/CD96 checkpoint molecules in ovarian cancer*. Oncoimmunology. 2020;9(1):1843247.

123. Gong Y, Yang J, Wang Y, Xue L, Wang J. *Metabolic factors contribute to T-cell inhibition in the ovarian cancer ascites.* Int J Cancer. 2020;147(7):1768-77.

124. Song M, Sandoval TA, Chae CS, Chopra S, Tan C, Rutkowski MR, et al. *IRE1α-XBP1 controls T cell function in ovarian cancer by regulating mitochondrial activity.* Nature. 2018;562(7727):423-8.

125. Simpson-Abelson MR, Loyall JL, Lehman HK, Barnas JL, Minderman H, O'Loughlin KL, et al. *Human ovarian tumor ascites fluids rapidly and reversibly inhibit T cell receptor-induced NF-κB and NFAT signaling in tumor-associated T cells.* Cancer Immun. 2013;13:14.

126. Liao S, Liu J, Lin P, Shi T, Jain RK, Xu L. *TGF-beta blockade controls ascites by preventing abnormalization of lymphatic vessels in orthotopic human ovarian carcinoma models.* Clin Cancer Res. 2011;17(6):1415-24.

127. Yigit R, Figdor CG, Zusterzeel PL, Pots JM, Torensma R, Massuger LF. *Cytokine analysis as a tool to understand tumour-host interaction in ovarian cancer.* Eur J Cancer. 2011;47(12):1883-9.

128. Matte I, Lane D, Laplante C, Rancourt C, Piché A. *Profiling of cytokines in human epithelial ovarian cancer ascites*. Am J Cancer Res. 2012;2(5):566-80.

129. Fahmi MN, Pradjatmo H, Astuti I, Nindrea RD. *Cytokines as Prognostic Biomarkers of Epithelial Ovarian Cancer (EOC): A Systematic Review and Meta-Analysis*. Asian Pac J Cancer Prev. 2021;22(2):315-23.

130. Chen YL, Cheng WF, Chang MC, Lin HW, Huang CT, Chien CL, et al. *Interferon-gamma in ascites could be a predictive biomarker of outcome in ovarian carcinoma*. Gynecol Oncol. 2013;131(1):63-8.

131. Kolomeyevskaya N, Eng KH, Khan AN, Grzankowski KS, Singel KL, Moysich K, et al. *Cytokine profiling of ascites at primary surgery identifies an interaction of tumor necrosis factor-α and interleukin-6 in predicting reduced progression-free survival in epithelial ovarian cancer*. Gynecol Oncol. 2015;138(2):352-7.

132. Yang L, Zhang X, Ma Y, Zhao X, Li B, Wang H. *Ascites promotes cell migration through the repression of miR-125b in ovarian cancer.* Oncotarget. 2017;8(31):51008-15.

133. Santin AD, Bellone S, Ravaggi A, Roman J, Smith CV, Pecorelli S, et al. *Increased levels of interleukin-10 and transforming growth factor-beta in the plasma and ascitic fluid of patients with advanced ovarian cancer.* Bjog. 2001;108(8):804-8.

134. da Silva RF, Yoshida A, Cardozo DM, Jales RM, Paust S, Derchain S, et al. *Natural Killer Cells Response to IL-2 Stimulation Is Distinct between Ascites with the Presence or Absence of Malignant Cells in Ovarian Cancer Patients*. Int J Mol Sci. 2017;18(5).

135. Riester M, Wei W, Waldron L, Culhane AC, Trippa L, Oliva E, et al. *Risk prediction for late-stage ovarian cancer by meta-analysis of 1525 patient samples.* J Natl Cancer Inst. 2014;106(5).

136. Guan Z, Song B, Liu F, Sun D, Wang K, Qu H. *TGF-β induces HLA-G expression through inhibiting miR-152 in gastric cancer cells*. J Biomed Sci. 2015;22:107.

137. Shen M, Tsai Y, Zhu R, Keng PC, Chen Y, Chen Y, et al. *FASN-TGF-β1-PD-L1 axis contributes to the development of resistance to NK cell cytotoxicity of cisplatin-resistant lung cancer cells.* Biochim Biophys Acta Mol Cell Biol Lipids. 2018;1863(3):313-22.

138. AlHossiny M, Luo L, Frazier WR, Steiner N, Gusev Y, Kallakury B, et al. *Ly6E/K Signaling to TGFβ Promotes Breast Cancer Progression, Immune Escape, and Drug Resistance.* Cancer Research. 2016;76(11):3376-86.

139. Vienne M, Etiennot M, Escalière B, Galluso J, Spinelli L, Guia S, et al. *Type 1 Innate Lymphoid Cells Limit the Antitumoral Immune Response*. Frontiers in Immunology. 2021;12.

140. Gao Y, Souza-Fonseca-Guimaraes F, Bald T, Ng SS, Young A, Ngiow SF, et al. T*umor immunoevasion by the conversion of effector NK cells into type 1 innate lymphoid cells.* Nat Immunol. 2017;18(9):1004-15.

141. Cortez VS, Ulland TK, Cervantes-Barragan L, Bando JK, Robinette ML, Wang Q, et al. *SMAD4 impedes the conversion of NK cells into ILC1-like cells by curtailing non-canonical TGF-β signaling*. Nat Immunol. 2017;18(9):995-1003.

142. Fionda C, Stabile H, Cerboni C, Soriani A, Gismondi A, Cippitelli M, et al. *Hitting More Birds with a Stone: Impact of TGF-β on ILC Activity in Cancer.* J Clin Med. 2020;9(1).

143. Tonetti CR, de Souza-Araújo CN, Yoshida A, da Silva RF, Alves PC, Mazzola TN, et al. *Ovarian Cancer-Associated Ascites Have High Proportions of Cytokine-Responsive CD56bright NK Cells.* Cells [Internet]. 2021; 10(7).

144. Chitadze G, Bhat J, Lettau M, Janssen O, Kabelitz D. *Generation of soluble NKG2D ligands: proteolytic cleavage, exosome secretion and functional implications*. Scand J Immunol. 2013;78(2):120-9.

145. Reiners KS, Topolar D, Henke A, Simhadri VR, Kessler J, Sauer M, et al. *Soluble ligands for NK cell receptors promote evasion of chronic lymphocytic leukemia cells from NK cell anti-tumor activity.* Blood. 2013;121(18):3658-65.

146. Okumura G, Iguchi-Manaka A, Murata R, Yamashita-Kanemaru Y, Shibuya A, Shibuya K. *Tumor-derived soluble CD155 inhibits DNAM-1-mediated antitumor activity of natural killer cells*. J Exp Med. 2020;217(4):1.

147. Xing S, Ferrari de Andrade L. *NKG2D and MICA/B shedding: a 'tag game' between NK cells and malignant cells.* Clin Transl Immunology. 2020;9(12):e1230.

148. Hilpert J, Grosse-Hovest L, Grünebach F, Buechele C, Nuebling T, Raum T, et al. *Comprehensive analysis of NKG2D ligand expression and release in leukemia: implications for NKG2D-mediated NK cell responses.* J Immunol. 2012;189(3):1360-71.

149. Groh V, Wu J, Yee C, Spies T. *Tumour-derived soluble MIC ligands impair expression of NKG2D and T-cell activation*. Nature. 2002;419(6908):734-8.

150. Carlsten M, Norell H, Bryceson YT, Poschke I, Schedvins K, Ljunggren HG, et al. *Primary human tumor cells expressing CD155 impair tumor targeting by down-regulating DNAM-1 on NK cells.* J Immunol. 2009;183(8):4921-30.

151. Sanchez-Correa B, Gayoso I, Bergua JM, Casado JG, Morgado S, Solana R, et al. *Decreased expression of DNAM-1 on NK cells from acute myeloid leukemia patients*. Immunol Cell Biol. 2012;90(1):109-15.

152. Pesce S, Tabellini G, Cantoni C, Patrizi O, Coltrini D, Rampinelli F, et al. *B7-H6-mediated downregulation of NKp30 in NK cells contributes to ovarian carcinoma immune escape.* Oncoim munology. 2015;4(4):e1001224.

153. Coudert JD, Zimmer J, Tomasello E, Cebecauer M, Colonna M, Vivier E, et al. *Altered NKG2D function in NK cells induced by chronic exposure to NKG2D ligand-expressing tumor cells.* Blood. 2005;106(5):1711-7.

Chapter 2

Peritoneal NK cells are responsive to IL-15 and percentages are correlated with outcome in advanced ovarian cancer patients

Janneke S. Hoogstad-van Evert, Ralph J.A. Maas*, Jolien M.R. van der Meer*, Jeannette Cany, Sophieke van der Steen, Joop H. Jansen, Jeffrey S. Miller, Ruud Bekkers, Willemijn Hobo, Leon Massuger,[#] and Harry Dolstra[#]

*[#]these authors contributed equally

Oncotarget. 2018 Oct 5; 9(78): 34810–348

Abstract

The demonstration that ovarian carcinoma (OC) is an immunogenic disease, opens opportunities to explore immunotherapeutic interventions to improve clinical outcome. In this regard, NK cell based immunotherapy could be promising as it has been demonstrated that OC cells are susceptible to killing by cytokine-stimulated NK cells. Here, we evaluated whether percentage, phenotype, function and IL-15 responsiveness of ascites-derived natural killer (NK) cells is related to progression-free survival (PFS) and overall survival (OS) of advanced stage OC patients. Generally, a lower percentage of NK cells within the lymphocyte fraction was seen in OC ascites (mean 17.4 ± 2.7%) versus benign peritoneal fluids (48.1 ± 6.8%; $p < 0.0001$). Importantly, a higher CD56+ NK cell percentage in ascites was associated with a better PFS ($p = 0.01$) and OS ($p = 0.002$) in OC patients. Furthermore, the functionality of ascites-derived NK cells in terms of CD107a/IFN-γ activity was comparable to that of healthy donor peripheral blood NK cells, and stimulation with monomeric IL-15 or IL-15 superagonist ALT-803 potently improved their reactivity towards tumor cells. By showing that a higher NK cell percentage is related to better outcome in OC patients and NK cell functionality can be boosted by IL-15 receptor stimulation, a part of NK cell immunity in OC is further deciphered to exploit NK cell based immunotherapy.

Introduction

Because ovarian carcinoma (OC) is generally asymptomatic until ascites or metastases beyond the ovaries have developed, patients are often diagnosed in advanced stage. Moreover, the presence and progression of ascites is associated with dismal prognosis and poor quality of life [1]. Current therapy consists of debulking surgery combined with platinum/taxane chemotherapy, but the majority of patients develop a recurrence within 3 years. Especially, for women with advanced stage disease the prognosis is dismal, and despite therapeutic advances the 5-year survival is only 28% [2].

Since many studies demonstrated that OC is an immunogenic disease, further research is needed to explore the opportunities of immunotherapeutic interventions to improve clinical outcome. In this regard, OC ascites is an attractive source to study immune cell function in patients because tumor cells and immune cells are both present. Furthermore, ascites contains a variety of immunosuppressive cellular and soluble components that influence the function of tumor-targeting lymphocytes [3–8]. Several studies showed that presence of tumor-infiltrating lymphocytes positively correlated with survival in cancer patients [9–16]. While the importance of CD8+ T cell infiltration has been clearly demonstrated, the role of infiltrating innate natural killer (NK) cells remains unclear. Interestingly, it was reported that CD103+ tumor-infiltrating NK cells often co-infiltrate with CD8+CD103+ T cells, yet the contribution of NK cells to improving outcome is difficult to assess [11]. Therefore, more research is required to decipher the role of NK cell immunity in OC patients.

NK cells are activated against neoplastic cells through a balance of activating and inhibitory receptors [17, 18]. Epidemiological research has shown that low NK cell activity is associated with increased cancer risk in humans [19]. For OC patients, decreased functionality of ascites-derived NK cells has been observed [20], which could be partially attributed to the low expression of various activating NK cell receptors including CD16, DNAM-1 and NKp30 [8, 21, 22]. Similarly, ascites-derived T cells are rather inactive, though proliferation and functionality can be partially restored by cytokine stimulation [23]. NK cells from ascites also exhibit low cytotoxic efficacy, which could be reinvigorated by IL-2 or IL-15 [24]. In this regard, Felices et al. recently reported that the, ALT-803, a fusion protein complex of IL-15 variant (N72D) bound to sushi domain of IL-15Rα fused to IgG1 Fc, potently enhanced the function of ascites-derived NK cells and healthy donor peripheral blood NK cells exposed to ascites fluid [25]. Most importantly, many studies demonstrated that OC cells are susceptible to killing by cytokine-stimulated NK cells [26–41].

In this study, we characterized NK cell percentage, phenotype and functionality in ascites of advanced OC patients in relation to clinical outcome, and investigated their responsiveness to IL-15 receptor mediated stimulation. We observed that a higher CD56+ NK cell proportion within the ascites lymphocyte fraction was associated with better progression free survival (PFS; $p = 0.01$) and overall survival (OS; $p = 0.002$) in OC patients. Furthermore, we demonstrated that the cytolytic function of ascites-derived NK cells can be effectively reinvigorated with either monomeric IL-15 or the IL-15 superagonist fusion complex, ALT-803. These findings indicate that boosting NK cell expansion and functionality by immunotherapeutic strategies could improve survival in OC patients.

Materials and methods

Ascites fluid samples were prospectively collected at diagnosis or first surgery of patients with stage IIIc or IV high-grade serous papillary OC between January 2009 and January 2013 at the Radboud University Medical Center (RUMC). Study approval was given by the Regional Committee for Medical Research Ethics (CMO 2013-516) and performed according to the Code for Proper Secondary Use of Human Tissue (Dutch Federation of Biomedical Scientific Societies, www.federa.org). Ascites was filtered using a 100 μm filter, washed and MNCs were isolated by Ficoll-Hypaque density gradient centrifugation. Subsequently, obtained cells were cryopreserved and stored in liquid nitrogen until use. From this biobank we randomly selected ascitic cell samples from 20°C patients. For the benign control group, samples were collected at benign gynecological surgeries. Main indication for diagnostic laparoscopy was abdominal pain, samples were included only if pathological findings were absent. Detection of cysts, endometriosis and adhesions at laparoscopy were exclusion criteria. These benign samples were processed and analyzed on the day of surgery. Medical records were retrospectively reviewed and relevant clinical and pathology data were extracted. Time of diagnosis was considered to be the date of the primary surgical procedure. Time from diagnosis to death was calculated for OS. PFS was calculated as time of last chemotherapy till diagnosis of biochemical or radiologic recurrence. Median survival was expressed in months.

Patients were divided in groups for Figure Figure1C1C and Figure Figure22 based on median overall survival, poor survival are the patients with an overall survival of less than the median (19 months), good survival are the patients with an overall survival of more than 19 months.

For Figure 1E and 1G patients were divided based on median NK cell frequency, for Figure 1F and 1H groups are divided by median CD3 cell frequency.

Flow cytometry

MNCs were stained with labeled antibodies, CD3 ECD (Biolegend), CD45 Krome Orange (R&D systems), CD56 PE-Cy5 (Biolegend), CD16 APC-Cy7 (Biologend), CD326 PerCPCy5.5 (Biolegend). Phenotypic analysis was performed using DNAM-1 FITC (Becton Dickinson), 2B4 FITC (Biolegend), NKG2A APC (Beckman Coulter), NKG2D APC (Biolegend), NKp30 PE (Biolegend) and NKp46 PE(Biolegend), isotype controls for IgG1 and IgG2a, (all Biolegend). Dead cells were stained with 1:1000 diluted sytox blue (Life Technologies; Invitrogen). Flow cytometry analysis was performed on a Gallios flow cytometer from Beckman Coulter. Analysis was done in Kaluza 1.5 (Beckman Coulter). Gating strategy is shown in Supplementary Figure 1.

K562 and SKOV-3 cell lines

OC cell line SKOV-3 was cultured in Roswell Park Memorial Institute medium (RPMI 1640; Gibco) medium supplemented with 10% Fetal Calf Serum (FCS; Integro). The chronic myeloid leukemia cell line K562 was cultured in Iscove's Modified Dulbecco's Medium (IMDM) with 10% FCS.

Functional assay (CD107a and IFN-γ)

After thawing ascites MNCs or PBMCs were cultured overnight with 1 nM IL-15 (Immunotools), 1 nM ALT-803 (Altor Bioscience) or without cytokine support in IMDM with 10% FCS and 1% penicillin/streptomycin (p/s). Subsequently, 1 × 106 cells were co-cultured with 0.5 × 106 K562 cells, 0.5 × 106 SKOV-3 cells or without target cells for 4 hours in IMDM with 10% FCS and 1% p/s and anti-CD107a PE-Cy7 (Biolegend) in a 24-well plate. After 1 h of co-culture, brefeldin A (BD) was added. Finally, cells in each well were gently resuspended and stained with labeled antibodies, CD56 BV510 (Biolegend), CD45 AF700 (Invitrogen), CD3 ECD (Beckman Coulter), CD69 BV421 (Biolegend) or isotype IgG1BV421 (BD biosciences), and TRAIL APC or isotype IgG1 APC (both Biolegend). Dead cells were stained with 1:1000 in PBS diluted eFluor780. Next, cells were fixed, permeabilized and stained with anti-IFN-γ or isotype IgG1 FITC (BD biosciences) and anti-perforin or isotype IgG2b PE (Biolegend). Flow cytometry acquisition was performed on a Gallios flow cytometer from Beckman Coulter. Analysis was done in Kaluza 1.5 (Beckman Coulter).

Statistical analysis

Statistical analysis was performed in Graphpad Prism software package version 5.03. Flow cytometry data was expressed as percentage positive cells. Data were analyzed using two-way ANOVA for group comparison or one-way ANOVA with Bonferroni post-hoc correction if more than two groups were compared. Unpaired T-tests were performed for comparison of two single groups, as indicated. Differences were considered significant when the p value was < 0.05. Survival curves were analyzed by Log rank (Mantel-Cox) test.

Results

Patient cohort characteristics

For this study, we selected ascites fluid samples collected at diagnosis or first surgery of patients with stage IIIc or IV high-grade serous papillary OC. The mean age of the selected OC patient cohort (n = 20) was 64 ± 8.8 years and 48 ± 8.1 years for the benign gynecological disorder control group (n = 10). The median OS and PFS of the OC patient cohort at time of analysis was 19 months and 6 months, respectively. Based on the median OS, the patient cohort was divided in two groups: i.e. poor survival group (n = 10) with an OS of less than 19 months and good survival group (n = 10) with an OS of more than 19 months (Table (Table1).1). The OS and PFS in the good survival group were 32.9 ± 11.2 and 19.7 ± 16.4 months, respectively. Whereas the OS and PFS in the poor survival group was only 10.3 ± 4.4 and 3.2 ± 2.3 months, respectively. Further characteristics of the two OC patient groups are shown in Table Table1.1. Patients in the good survival group were younger and were less often postmenopausal. In both groups, half of the OC patients were treated with primary surgery, and half with neo-adjuvant chemotherapy. CA-125 levels were higher in the good survival group.

Table 1: ***Patient characteristics***

	Characteristics	Good survival (n = 10)	Poor survival (n = 10)
Baseline	Age mean (SD)	57.2 (8.4)	69.0 (11.4)
	CA-125 mean (95% CI)	1532 (641–2423)	1268 (199–2337)
	Postmenopausal	70%	90%
Treatment	Neoadjuvant Chemotherapy	50%	60%
	Primary surgery	50%	40%
Debulking	Complete Debulking	20%	20%
	(Sub-) Optimal Debulking	80%	70%
	No Debulking	0%	10%
Survival	PFS mean (SD)	19.7 (16.4)	3.2 (2.3)
	OS mean (SD)	32.9 (11.2)	10.3 (4.4)

High peritoneal NK cell proportion within the lymphocyte fraction is associated with better survival of OC patients

First, we assessed the percentages of NK, NKT and T cells within the lymphocyte fraction in cryopreserved ascites samples of the selected OC patients by flow cytometry and compared those with peritoneal fluid of 10 patients with a benign gynecological disorder. Within the total cell fraction OC ascites contained 38.8 ± 24.8% lymphocytes, 40.5 ± 24.7% CD45+ non-lymphocytes and 16.4 ± 23.5% CD45- non-hematopoietic tumor cells, and the benign samples contained 58.7 ± 40.4% lymphocytes and 36.5 ± 34.1% non-lymphocytes within CD45+ leucocytes (Figure 1A). Within the lymphocytes a significantly lower CD3-CD56+ NK cell percentage was seen in OC patient ascites (mean 17.1 ± 2.7%) compared to benign peritoneal fluid (48.1 ± 6.8%, $p < 0.0001$; Figure Figure1B).1B). Furthermore, lower CD3+ T cell and CD3+CD56+ NKT cell percentages were observed within the lymphocyte population in OC patient ascites. The population of non T-, non-NKT, non-NK cells in the lymphocyte gate, presumably B cells, was more prominent in the malignant samples (Figure 1B). Notably, the group of OC patients with poor survival had 14.5 ± 3.6% NK cells versus 23.6 ± 4.0% in the patients with good survival (Figure 1C). In addition, we observed a significant shift in the $CD56^{dim/bright}$ ratio in OC patients in comparison to peritoneal fluid of patients with a benign gynecological disorder (Figure 1D). Generally, in healthy donor blood around 90% cytotoxic $CD56^{dim}$ and 10% regulatory $CD56^{bright}$ cells are present [42]. In contrast, in the benign ascites samples we found 32.4 ± 3.7% $CD56^{dim}$ cells and 67.5 ± 3.7% $CD56^{bright}$ cells, respectively. In OC patient ascites, however, the ratio was more in

favor of the cytotoxic $CD56^{dim}$ population with 54.7 ± 4.0% $CD56^{dim}$ and 45.4 ± 4.0% $CD56^{bright}$ cells, compared to the benign peritoneal fluids (Figure 1D).

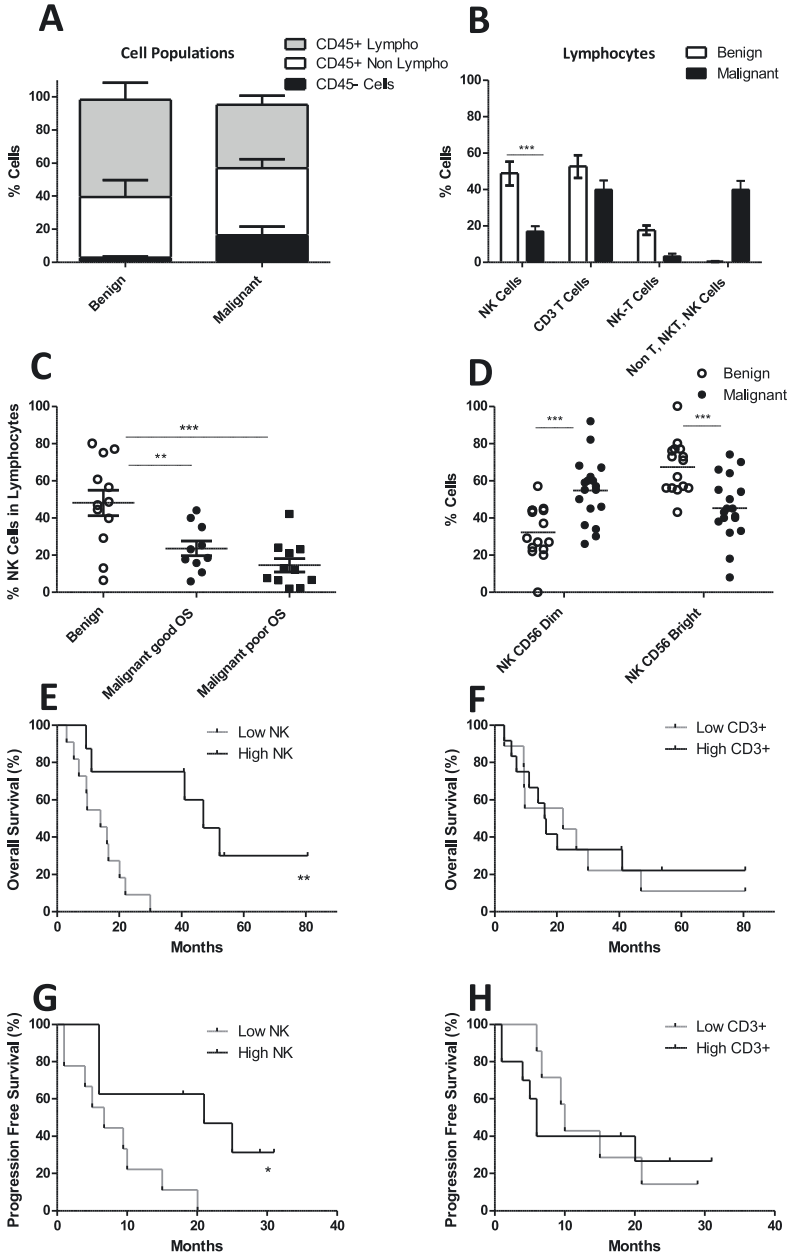

Figure 1: ***NK, NKT and T cell percentage in benign ascites and ascites from ovarian cancer patients***
*(A) Fraction of CD45+ lymphocytes (white), CD45+ non-lymphocytes (grey) and CD45- cells (black) cell populations within peritoneal fluid of benign compared to malignant ovarian cancer patients, based on flow cytometric analysis of CD45 expression and forward/side scatter. (B) Percentage of NK cells, T cells, NKT cells and other lymphocytes within benign and malignant ascites. The percentage NK cells within the lymphocyte population is significantly different, two tailed T-test $p < 0.0001$. (C) Within the lymphocyte population the percentage of NK cells is depicted. The group of malignant ovarian carcinoma ascites patients is divided into good and poor survival based on the median survival of the analyzed patient cohort (n = 20). (D) The NK cell population is subdivided based on CD56 bright and CD56 dim cells. (E) Overall survival curve of OC patients groups with low and high CD56+ NK cell percentages in ascites. (F) Overall survival curve of OC patients groups with low and high CD3+ T cell percentages in ascites. (G–H) Progression free survival curves for low and high CD56+ NK cell and CD3+ T cell percentages in ascites. Error bars represent mean + SEM. When 2 groups were compared the Student T-test was used whereas a one-way ANOVA with Bonferroni correction was performed when comparing 3 groups. ***p = 0.001.*

Next, we divided the OC patients in two groups based on the median ascites NK cell percentage within the lymphocyte fraction into high (mean 31.4 ± 9.4%) and low (mean 8.9 ± 4.6%) percentage groups. We observed that both OS ($p = 0.002$, hazard ratio = 5.7) and PFS ($p = 0.01$, hazard ratio = 4.7) were significantly better in OC patients with a high peritoneal NK cell percentage versus patients with a low NK cell percentage in the lymphocyte fraction (Figure 1E and 1G). Notably, this relationship was not observed for CD3+ T cell percentages in ascites (Figure 1F and 1H). Interestingly, in the high NK group three patients are still alive after a follow-up of ≥50 months. Altogether, these data indicate that the CD56+ NK cell percentage within the lymphocyte fraction in ascites fluid of OC patients is positively correlated with clinical outcome.

Ascites-derived NK cells of poor survival ovarian carcinoma patients exhibit low expression levels of activating receptors

Next to the percentage of NK cells in ascites, we studied whether survival of OC patients was associated with differential expression of NK cell activating receptors. Hereto, we performed flow cytometry analysis on the ascites-derived NK cells of the selected patient cohort and benign ascites controls (Figure (Figure2).2). While 2B4 had equally high positivity on both benign and malignant peritoneal fluid NK cells, NKG2D was low to undetectable on these NK cells. Remarkably, NKp30 was almost absent on NK cells in malignant samples (mean 3%), whereas it was significantly higher on NK cells from benign samples (mean 79%). NKG2A can suppress activation, and shows no significant differences between benign and malignant samples. Moreover, NKp46 and DNAM-1 were significantly lower expressed on NK cells in malignant samples, especially in patients with a poor OS. Together, these data indicate that ascites NK cells of OC patients with poor survival have significantly lower expression of activation receptors on their surface.

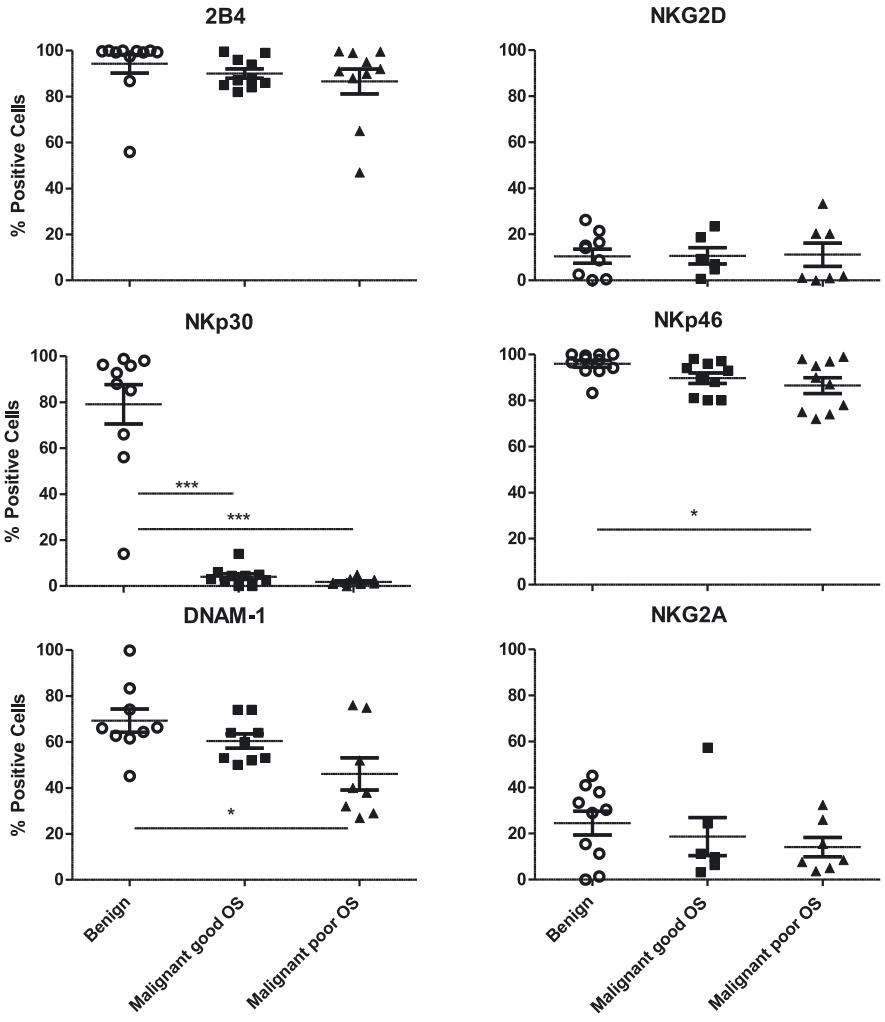

Figure 2: ***Expression of activating receptors on CD45+CD3-CD56+ NK cells***

*Percentage positive 2B4, NKG2D, NKp46, NKp30, DNAM-1 and NKG2A NK cells of CD56+ NK cells in benign and malignant peritoneal fluid. The group of malignant ovarian carcinoma ascites patients is divided into lower than median overall survival and higher than median overall survival. Error bars represent mean + SEM. One way ANOVA with Bonferroni correction was performed when comparing the groups. *= $p < 0.05$, ***= $p < 0.001$.*

Ascites-derived NK cells possess equal cytotoxic function as peripheral blood NK cells from healthy donors

Next, we addressed the functional activity of peritoneal fluid NK cells of OC patients in comparison to peripheral blood (PB)-NK cells from healthy donors. Here, we cultured MNCs from ascites of OC patients or PB of healthy controls overnight in the presence of IL-15, whereupon total cells were challenged for 4 hours with either K562 (control), SKOV-3 OC or without tumor cells and subsequently analyzed by flow cytometry. We examined expression of the activation markers CD69 and TRAIL, the degranulation of NK cells using CD107a, and intracellular IFN-γ positivity. Both ascites and control NK cells showed high CD69 expression, while TRAIL levels decreased upon tumor challenge (Figure 3A and 3B). Furthermore, ascites-derived NK cells were capable of exerting a CD107a degranulation and IFN-γ response against K562 cells (Figure 3C and 3D). However, reactivity of ascites-derived NK cells greatly varied between different OC patients, therefore no significant differences were observed as compared to healthy donor NK cells. Notably, for both OC ascites and healthy donor NK cells the response against SKOV-3 OC cells was poor. Together, these data demonstrate that OC ascites-derived NK cells have equivalent degranulation and IFN-γ secretion capacity as healthy donor PB-NK cells, yet responsiveness against SKOV-3 OC cells is limited.

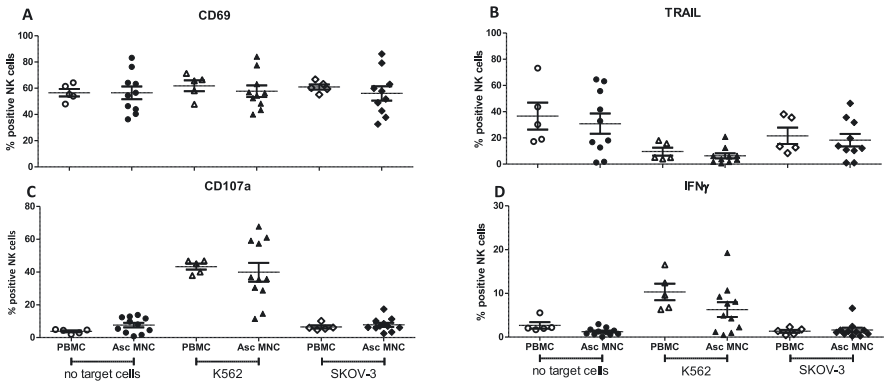

Figure 3: ***Degranulation assay comparing NK cells in healthy donor (HD) peripheral blood mononuclear cells (PBMCs) with ascites mononuclear cells (MNCs)***

Percentage CD56+ NK cells positive for (A) CD69, (B) TRAIL, (C) CD107a, (D) IFN-γ, after 4 h stimulation with no target cells, K562 or SKOV-3 tumor cells. Error bars represent mean + SEM. Open symbols depict HD PBMCs, closed symbols depict ascites MNCs. One way ANOVA with Bonferroni correction was performed when comparing the groups.

Functionality of ascites NK cells can be effectively boosted by IL-15 or ALT-803 stimulation

To improve peritoneal NK cell reactivity against OC, we investigated whether boosting with monomeric recombinant human IL-15 or the human IL-15 superagonist fusion complex, ALT-803. Interestingly, IL-15 receptor-mediated stimulation already enhanced CD107a expression and IFN-γ secretion capacity of the NK cells in the absence of tumor challenge (Figure 4A and 4D). Most importantly, ascites-derived NK responsiveness against K562 and especially SKOV-3 OC cells could be potently augmented by IL-15 or ALT-803 stimulation ($p < 0.001$ for CD107a and $p < 0.01$ for IFN-γ; Figure 4B, 4C, 4E and 4F). These data demonstrate that the function activation of NK cells in ascites can be efficiently rescued with IL-15 or ALT-803.

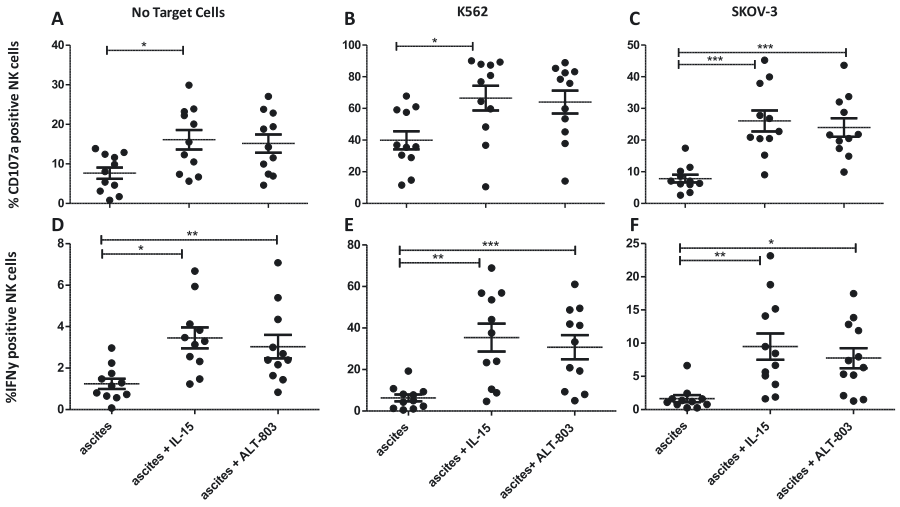

Figure 4: ***Degranulation assay comparing ascites CD56+ NK cells with and without monomeric IL-15 or ALT-803 stimulation***

*(A–C) Percentage CD56+ NK cells positive for CD107a after 4 h co-culture with no stimulation (A), K562 cells (B) or SKOV-3 cells (C). (D–F) Percentage CD56+ NK cells positive for IFN-γ after 4 h co-culture with no stimulation (D), K562 cells (E) or SKOV-3 cells (F). Error bars represent mean + SEM. One way ANOVA with Bonferroni correction was performed when comparing the groups. * = $p < 0.05$, ** = $p < 0.01$, *** = $p < 0.001$.*

Discussion

NK cells are activated against cancer cells via activating and inhibitory receptors, and the balance in these signals determines the magnitude of their activity. [17, 18] Epidemiological research has shown that low NK cell activity is associated with increased cancer risk in humans [19]. Moreover, NK cells have been identified to play a role in tumor surveillance due to enhanced surface expression of ligands for activating receptors on tumor cells by the DNA damage response [43]. Together these studies underscore the contribution of NK cell function in anti-cancer immunity. However, there is limited data on the contribution of NK cell immunity on the clinical outcome of women with ovarian carcinoma. In the present study, we found that the percentage of CD56+ NK cells within the lymphocyte fraction in ascites fluid is related to OS and PFS, and that ascites-derived NK cells have lower expression of activation markers than benign peritoneal fluid NK cells. Although, ascites-resident NK cells have poor reactivity against SKOV-3 OC cells (similarly as PB-NK cells) they can be effectively boosted by IL-15 receptor mediated stimulation.

In our current study, OC patients were randomly selected from our ascites biobank. Nevertheless, as large amounts of ascites MNCs was required for these studies, we thereby selected automatically a group of patients with a relatively poor prognosis. A remarkably high percentage of these patients did not undergo complete debulking surgery, however since rates of complete debulking were comparable in both the poor and good OS groups, we believe that the impact of incomplete debulking on our NK cell correlative results is limited. Notably, the OS of our patient cohort is comparable to a large national cohort [44]. Although there were age differences between the benign control and the OC groups we do not expect impact on our findings, as it has been reported for PB that NK cell percentages are very stable and do not change with age [45].

Notably, a higher NK cell percentage within the lymphocyte fraction was found in peritoneal fluid of benign control subjects than in ascites of OC patients. Often peritoneal fluid of healthy individuals is used in endometriosis research, and also in this disease a significantly lower percentage of NK cells in peritoneal fluid has been reported [46]. In OC the only relation between clinical outcome and NK cells in ascites was described by Dong et al., and they reported CD16 positive cells to be associated with poorer outcome of OC patients. Unfortunately, CD56 expression was not evaluated in their report [12]. Our paper is the first report to show a relationship between the CD56+ NK cell proportion within the ascites lymphocyte fraction and clinical outcome parameters. While the importance of CD8+ T cell infiltration within OC tumors has been clearly demonstrated, and also CD3+ T cells in ascites have been

found to correlate with better outcome [47, 48], a relation between CD3+ T cell percentage and survival was not observed in our cohort. Besides percentages, absolute numbers of infiltrating lymphocytes is an important parameter for correlation with clinical outcome. However, as volume and cellular density in ascites differed greatly between OC patients, we believe that the percentage within the lymphocyte population was the most objective way to compare cell populations. For future research, it would be interesting to investigate how ascites NK cells differ from blood NK cell numbers, phenotype and function in the same OC patient.

It has been previously reported that OC ascites NK cells have been described to exhibit lower expression of the activating markers NKp30, NKp46, NKG2D and DNAM-1 compared to healthy donor PB-NK cells [8, 49]. In our study, we observed the same significantly lower expression of NKp30, NKp46 and DNAM-1 on OC ascites-derived NK cells compared to NK cells from benign peritoneal fluid. However, the relationship between NKG2D and prognosis was not found in our dataset. Interestingly, we observed a significant lower NK cell expression of NKp30 in poor prognosis versus good prognosis ascites samples, suggesting that NKp30 expression changes in the poor prognosis OC environment. The same has been reported in acute myeloid leukemia, where NKp30 is proposed as a prognostic biomarker based on its low expression on NK cells in poor prognosis patients [50]. Further validation in a larger patient cohort is required to establish prognostic biomarkers in OC patients.

In our functional studies, ascites-derived NK cells demonstrated equal degranulation and cytokine secretion potential as healthy donor PB-NK cells. This corresponds with findings by Felices et al. who showed comparable levels of CD107a after stimulation in the presence or absence of tumor cells [25]. In contrast, other reports demonstrated that ascites-derived NK cells were dysfunctional, with decreased CD16 expression and low cytotoxic capacity [6, 51, 52]. Here, we showed that ascites-derived NK cells were highly capable of recognizing K562 tumor cells, but exhibited poor SKOV-3 OC cell reactivity. Most importantly, we demonstrated that stimulation with IL-15 or ALT-803 could reinvigorate NK cell degranulation and IFN-γ production, especially against SKOV-3 OC cells. Although our ex vivo studies did not show any difference between IL-15 and ALT-803, ALT-803 is likely more potent in long-term assays and in vivo because of its longer half-life [53, 54].

Concluding, this report shows a significant association between the percentage and phenotype of NK cells within the lymphocyte fraction in peritoneal fluid and survival of OC patients. Moreover, we demonstrated that peritoneal NK cell reactivity against OC tumor cells can be efficiently boosted by IL-15 receptor-mediated stimulation.

The relationship between availability of NK cells in the abdominal cavity and the potentiating effect of IL-15 indicates that intraperitoneal NK cell adoptive transfer combined with IL-15 administration could be an interesting new therapy for OC patients to improve outcome. Currently, a phase 1 clinical trial testing intraperitoneal ALT-803 therapy in OC patients is enrolling patients in the US (NCT0354909) and a phase 1 clinical trial on intraperitoneal NK cell therapy exploiting CD34+ progenitor-derived NK cells is open in the Netherlands (NCT03539406). By demonstrating that high NK cell percentages are associated with better outcome in OC patients and peritoneal NK cell functionality can be boosted by IL-15 receptor stimulation, a part of NK cell immunity in OC is further deciphered to exploit NK cell based immunotherapy in these poor prognosis patients.

References

1. Ahmed N, Stenvers KL. *Getting to know ovarian cancer ascites: opportunities for targeted therapy-based translational research.* Front Oncol. 2013;3:256.

2. Siegel RL, Miller KD, Jemal A. *Cancer Statistics, 2017. CA* Cancer J Clin. 2017;67:7–30.

3. Fumita Y, Tanaka F, Saji F, Nakamuro K. *Immunosuppressive factors in ascites fluids from ovarian cancer patients.* Am J Reprod Immunol. 1984;6:175–178.

4. Giuntoli RL, 2nd, Webb TJ, Zoso A, Rogers O, Diaz-Montes TP, Bristow RE, Oelke M. *Ovarian cancer-associated ascites demonstrates altered immune environment: implications for antitumor immunity.* Anticancer Res. 2009;29:2875–2884.

5. Onsrud M, Bosnes V, Grahm I. *cis-Platinum as adjunctive to surgery in early stage ovarian carcinoma: effects on lymphoid cell subpopulations*. Gynecol Oncol. 1986;23:323–328.

6. Lukesova S, Vroblova V, Tosner J, Kopecky J, Sedlakova I, Cermakova E, Vokurkova D, Kopecky O. *Comparative study of various subpopulations of cytotoxic cells in blood and ascites from patients with ovarian carcinoma.* Contemp Oncol (Pozn) 2015;19:290–299.

7. Santin AD, Hermonat PL, Ravaggi A, Bellone S, Roman JJ, Smith CV, Pecorelli S, Radominska-Pandya A, Cannon MJ, Parham GP. *Phenotypic and functional analysis of tumor-infiltrating lymphocytes compared with tumor-associated lymphocytes from ascitic fluid and peripheral blood lymphocytes in patients with advanced ovarian cancer.* Gynecol Obstet Invest. 2001;51:254–261.

8. Belisle JA, Gubbels JA, Raphael CA, Migneault M, Rancourt C, Connor JP, Patankar MS. *Peritoneal natural killer cells from epithelial ovarian cancer patients show an altered phenotype and bind to the tumour marker MUC16 (CA125) Immunology.* 2007;122:418–429.

9. Coca S, Perez-Piqueras J, Martinez D, Colmenarejo A, Saez MA, Vallejo C, Martos JA, Moreno M. *The prognostic significance of intratumoral natural killer cells in patients with colorectal carcinoma.* Cancer. 1997;79:2320–2328.

10. Gooden M, Lampen M, Jordanova ES, Leffers N, Trimbos JB, van der Burg SH, Nijman H, van Hall T. *HLA-E expression by gynecological cancers restrains tumor-infiltrating CD8(+) T lymphocytes.* Proc Natl Acad Sci U S A. 2011;108:10656–10661.

11. Webb JR, Milne K, Watson P, Deleeuw RJ, Nelson BH. *Tumor-infiltrating lymphocytes expressing the tissue resident memory marker CD103 are associated with increased survival in high-grade serous ovarian cancer.* Clin Cancer Res. 2014;20:434–444.

12. Dong HP, Elstrand MB, Holth A, Silins I, Berner A, Trope CG, Davidson B, Risberg B. *NK- and B-cell infiltration correlates with worse outcome in metastatic ovarian carcinoma.* Am J Clin Pathol. 2006;125:451–458.

13. Ishigami S, Natsugoe S, Tokuda K, Nakajo A, Che X, Iwashige H, Aridome K, Hokita S, Aikou T. *Prognostic value of intratumoral natural killer cells in gastric carcinoma.* Cancer. 2000;88:577–583.

14. Tian W, Wang L, Yuan L, Duan W, Zhao W, Wang S, Zhang Q. *A prognostic risk model for patients with triple negative breast cancer based on stromal natural killer cells, tumor-associated macrophages and growth-arrest specific protein 6.* Cancer Sci. 2016;107:882–889.

15. Turkseven MR, Oygur T. *Evaluation of natural killer cell defense in oral squamous cell carcinoma.* Oral Oncol. 2010;46:e34–37.

16. Sconocchia G, Eppenberger S, Spagnoli GC, Tornillo L, Droeser R, Caratelli S, Ferrelli F, Coppola A, Arriga R, Lauro D, Iezzi G, Terracciano L, Ferrone S. *NK cells and T cells cooperate during the clinical course of colorectal cancer.* Oncoimmunology. 2014;3:e952197.

17. Vivier E, Tomasello E, Baratin M, Walzer T, Ugolini S. *Functions of natural killer cells.* Nat Immunol. 2008;9:503–510.

18. Andre P, Castriconi R, Espeli M, Anfossi N, Juarez T, Hue S, Conway H, Romagne F, Dondero A, Nanni M, Caillat-Zucman S, Raulet DH, Bottino C, et al. *Comparative analysis of human NK cell activation induced by NKG2D and natural cytotoxicity receptors.* Eur J Immunol. 2004;34:961–971.

19. Imai K, Matsuyama S, Miyake S, Suga K, Nakachi K. *Natural cytotoxic activity of peripheral-blood lymphocytes and cancer incidence: an 11-year follow-up study of a general population.* Lancet. 2000;356:1795–1799.

20. Morvan MG, Lanier LL. *NK cells and cancer: you can teach innate cells new tricks.* Nat Rev Cancer. 2016;16:7–19.

21. Pesce S, Tabellini G, Cantoni C, Patrizi O, Coltrini D, Rampinelli F, Matta J, Vivier E, Moretta A, Parolini S, Marcenaro E. *B7-H6-mediated downregulation of NKp30 in NK cells contributes to ovarian carcinoma immune escape.* Oncoimmunology. 2015;4:e1001224.

22. Berek JS, Bast RC, Jr, Lichtenstein A, Hacker NF, Spina CA, Lagasse LD, Knapp RC, Zighelboim J. *Lymphocyte cytotoxicity in the peritoneal cavity and blood of patients with ovarian cancer.* Obstet Gynecol. 1984;64:708–714.

23. Tran E, Nielsen JS, Wick DA, Ng AV, Johnson LD, Nesslinger NJ, McMurtrie E, Webb JR, Nelson BH. *Polyfunctional T-cell responses are disrupted by the ovarian cancer ascites environment and only partially restored by clinically relevant cytokines*. PLoS One. 2010;5:e15625.

24. da Silva RF, Yoshida A, Cardozo DM, Jales RM, Paust S, Derchain S, Guimaraes F. *Natural Killer Cells Response to IL-2 Stimulation Is Distinct between Ascites with the Presence or Absence of Malignant Cells in Ovarian Cancer Patients.* Int J Mol Sci. 2017;18:856.

25. Felices M, Chu S, Kodal B, Bendzick L, Ryan C, Lenvik AJ, Boylan KLM, Wong HC, Skubitz APN, Miller JS, Geller MA. *IL-15 super-agonist (ALT-803) enhances natural killer (NK) cell function against ovarian cancer.* Gynecol Oncol. 2017;145:453–461.

26. Kloss S, Chambron N, Gardlowski T, Weil S, Koch J, Esser R, Pogge von Strandmann E, Morgan MA, Arseniev L, Seitz O, Kohl U. *Cetuximab Reconstitutes Pro-Inflammatory Cytokine Secretions and Tumor-Infiltrating Capabilities of sMICA-Inhibited NK Cells in HNSCC Tumor Spheroids.* Front Immunol. 2015;6:543.

27. Cany J, van der Waart AB, Spanholtz J, Tordoir M, Jansen JH, van der Voort R, Schaap NM, Dolstra H. *Combined IL-15 and IL-12 drives the generation of CD34-derived natural killer cells with superior maturation and alloreactivity potential following adoptive transfer.* Oncoimmunology. 2015;4:e1017701.

28. Cany J, van der Waart AB, Tordoir M, Franssen GM, Hangalapura BN, de Vries J, Boerman O, Schaap N, van der Voort R, Spanholtz J, Dolstra H. *Natural killer cells generated from cord blood hematopoietic progenitor cells efficiently target bone marrow-residing human leukemia cells in NOD/SCID/IL2Rg(null) mice.* PLoS One. 2013;8:e64384.

29. Roeven MW, Thordardottir S, Kohela A, Maas F, Preijers F, Jansen JH, Blijlevens NM, Cany J, Schaap N, Dolstra H. *The Aryl Hydrocarbon Receptor Antagonist StemRegenin1 Improves In Vitro Generation of Highly Functional Natural Killer Cells from CD34(+) Hematopoietic Stem and Progenitor Cells.* Stem Cells Dev. 2015;24:2886–2898.

30. TM, Dolstra H. *High log-scale expansion of functional human natural killer cells from umbilical cord blood CD34-positive cells for adoptive cancer immunotherapy*. PLoS One. 2010;5:e9221.

31. Geller MA, Knorr DA, Hermanson DA, Pribyl L, Bendzick L, McCullar V, Miller JS, Kaufman DS. *Intraperitoneal delivery of human natural killer cells for treatment of ovarian cancer in a mouse xenograft model.* Cytotherapy. 2013;15:1297–1306.

32. Geller MA, Miller JS. *Use of allogeneic NK cells for cancer immunotherapy. Immunotherapy*. 2011;3:1445–1459.

33. Hermanson DL, Bendzick L, Pribyl L, McCullar V, Vogel RI, Miller JS, Geller MA, Kaufman DS. *Induced Pluripotent Stem Cell-Derived Natural Killer Cells for Treatment of Ovarian Cancer.* Stem Cells. 2016;34:93–101.

34. Bachanova V, Cooley S, Defor TE, Verneris MR, Zhang B, McKenna DH, Curtsinger J, Panoskaltsis-Mortari A, Lewis D, Hippen K, McGlave P, Weisdorf DJ, Blazar BR, et al. *Clearance of acute myeloid leukemia by haploidentical natural killer cells is improved using IL-2 diphtheria toxin fusion protein.* Blood. 2014;123:3855–3863.

35. Giannattasio A, Weil S, Kloess S, Ansari N, Stelzer EH, Cerwenka A, Steinle A, Koehl U, Koch J. *Cytotoxicity and infiltration of human NK cells in In Vivo-like tumor spheroids*. BMC Cancer. 2015;15:351.

36. Bhat R, Watzl C. S*erial killing of tumor cells by human natural killer cells—enhancement by therapeutic antibodies.* PLoS One. 2007;2:e326.

37. Ames E, Canter RJ, Grossenbacher SK, Mac S, Chen M, Smith RC, Hagino T, Perez-Cunningham J, Sckisel GD, Urayama S, Monjazeb AM, Fragoso RC, Sayers TJ, et al. *NK Cells Preferentially Target Tumor Cells with a Cancer Stem Cell Phenotype*. J Immunol. 2015;195:4010–4019.

38. Kozlowska AK, Kaur K, Topchyan P, Jewett A. *Novel strategies to target cancer stem cells by NK cells; studies in humanized mice.* Front Biosci (Landmark Ed) 2017;22:370–384.

39. Koh J, Lee SB, Park H, Lee HJ, Cho NH, Kim J. *Susceptibility of CD24(+) ovarian cancer cells to anti-cancer drugs and natural killer cells. Biochem Biophys* Res Commun. 2012;427:373–378.

40. Choi PJ, Mitchison TJ. *Imaging burst kinetics and spatial coordination during serial killing by single natural killer cells.* Proc Natl Acad Sci USA. 2013;110:6488–6493.

41. Rosario M, Liu B, Kong L, Collins LI, Schneider SE, Chen X, Han K, Jeng EK, Rhode PR, Leong JW, Schappe T, Jewell BA, Keppel CR, et al. *The IL-15-Based ALT-803 Complex Enhances FcgammaRIIIa-Triggered NK Cell Responses and In Vivo Clearance of B Cell Lymphomas*. Clin Cancer Res. 2016;22:596–608.

42. Vivier E, Nunes JA, Vely F. *Natural killer cell signaling pathways.* Science. 2004;306:1517–1519.

43. Vivier E, Raulet DH, Moretta A, Caligiuri MA, Zitvogel L, Lanier LL, Yokoyama WM, Ugolini S. *Innate or adaptive immunity. The example of natural killer cells*. Science. 2011;331:44–49.

44. Timmermans M, Sonke GS, Van de Vijver KK, van der Aa MA, Kruitwagen R. *No improvement in long-term survival for epithelial ovarian cancer patients: A population-based study between 1989 and 2014 in the Netherlands*. Eur J Cancer. 2017;88:31–37.

45. Almeida-Oliveira A, Smith-Carvalho M, Porto LC, Cardoso-Oliveira J, Ribeiro Ados S, Falcao RR, Abdelhay E, Bouzas LF, Thuler LC, Ornellas MH, Diamond HR. *Age-related changes in natural killer cell receptors from childhood through old age.* Hum Immunol. 2011;72:319–329.

46. Kang YJ, Jeung IC, Park A, Park YJ, Jung H, Kim TD, Lee HG, Choi I, Yoon SR. *An increased level of IL-6 suppresses NK cell activity in peritoneal fluid of patients with endometriosis via regulation of SHP-2 expression*. Hum Reprod. 2014;29:2176–2189.

47. Lieber S, Reinartz S, Raifer H, Finkernagel F, Dreyer T, Bronger H, Jansen JM, Wagner U, Worzfeld T, Muller R, Huber M. *Prognosis of ovarian cancer is associated with effector memory CD8(+) T cell accumulation in ascites, CXCL9 levels and activation-triggered signal transduction in T cells.* Oncoimmunology. 2018;7:e1424672.

48. Worzfeld T, Pogge von Strandmann E, Huber M, Adhikary T, Wagner U, Reinartz S, Muller R. *The Unique Molecular and Cellular Microenvironment of Ovarian Cancer.* Front Oncol. 2017;7:24.

49. Nham T, Poznanski SM, Fan IY, Shenouda MM, Chew MV, Lee AJ, Vahedi F, Karimi Y, Butcher M, Lee DA, Hirte H, Ashkar AA. *Ex vivo-expanded NK cells from blood and ascites of ovarian cancer patients are cytotoxic against autologous primary ovarian cancer cells.* Cancer Immunol Immunother. 2018;67:575–587.

50. Chretien AS, Fauriat C, Orlanducci F, Rey J, Borg GB, Gautherot E, Granjeaud S, Demerle C, Hamel JF, Cerwenka A, von Strandmann EP, Ifrah N, Lacombe C, et al. *NKp30 expression is a prognostic immune biomarker for stratification of patients with intermediate-risk acute myeloid leukemia.* Oncotarget. 2017;8:49548–63.

51. Lai P, Rabinowich H, Crowley-Nowick PA, Bell MC, Mantovani G, Whiteside TL. *Alterations in expression and function of signal-transducing proteins in tumor-associated T and natural killer cells in patients with ovarian carcinoma.* Clin Cancer Res. 1996;2:161–173.

52. Ioannides CG, Platsoucas CD, Rashed S, Wharton JT, Edwards CL, Freedman RS. *Tumor cytolysis by lymphocytes infiltrating ovarian malignant ascites.* Cancer Res. 1991;51:4257–4265.

53. Rhode PR, Egan JO, Xu W, Hong H, Webb GM, Chen X, Liu B, Zhu X, Wen J, You L, Kong L, Edwards AC, Han K, et al. *Comparison of the Superagonist Complex, ALT-803, to IL15 as Cancer Immunotherapeutics in Animal Models.* Cancer Immunol Res. 2016;4:49–60.

54. Han KP, Zhu X, Liu B, Jeng E, Kong L, Yovandich JL, Vyas VV, Marcus WD, Chavaillaz PA, Romero CA, Rhode PR, Wong HC. *IL-15: IL-15 receptor alpha superagonist complex: high-level co-expression in recombinant mammalian cells, purification and characterization.* Cytokine. 2011;56:804–810.

Supplemental data

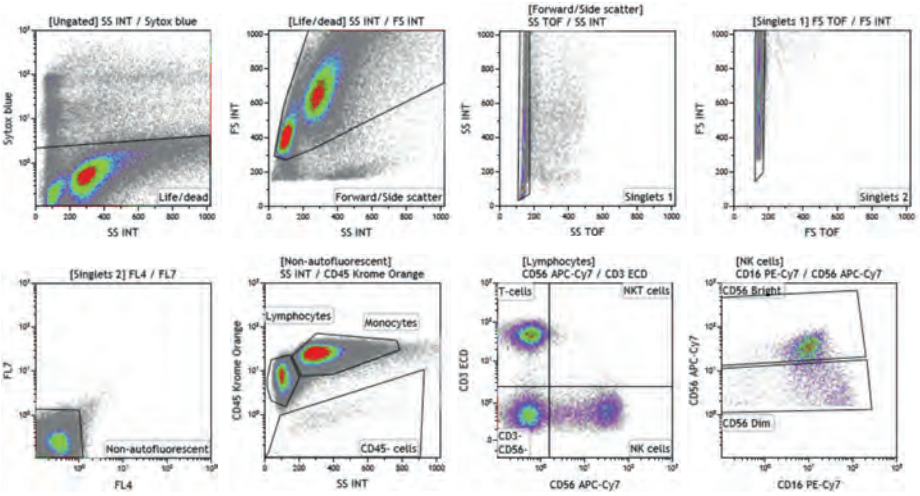

Supplementary Figure 1: ***Gating strategy for CD56+ NK cells and CD56 dim versus CD56 bright in ascites.***

In (A) and (B) life cells are gated, in (C and D) the single cells are selected and in (E) auto fluorescent cells are excluded from further analysis. In (F) the lymphocytes are gated. In (G) the CD56 positive cells are seen, with two populations. In (H) the NK CD56 bright and the NK CD56 dim are gated.

Chapter 3

IL-15 superagonist N-803 improves IFNγ production and killing of leukemia and ovarian cancer cells by CD34+ progenitor-derived NK cells

Jolien M.R. van der Meer, Ralph J.A. Maas *, Karolin Guldevall*, Kim Klarenaar, Paul K.J.D. De Jonge, Janneke S. Hoogstad-van Evert, Anniek B. van der Waart, Jeanette Cany, Jeffrey T. Safrit, John H. Lee, Esther Wagena, Peter Friedl, Björn Önfelt, Leon F. Massuger, Nicolaas P.M. Schaap, Joop H. Jansen, Willemijn Hobo, Harry Dolstra

*these authors contributed equally

Cancer Immunol Immunother. 2021;70(5):1305-1321.

Abstract

Allogeneic natural killer (NK) cell transfer is a potential immunotherapy to eliminate and control cancer. A promising source are CD34 + hematopoietic progenitor cells (HPCs), since large numbers of cytotoxic NK cells can be generated. Effective boosting of NK cell function can be achieved by interleukin (IL)-15. However, its in vivo half-life is short and potent trans-presentation by IL-15 receptor α (IL-15Rα) is absent. Therefore, ImmunityBio developed IL-15 superagonist N-803, which combines IL-15 with an activating mutation, an IL-15Rα sushi domain for trans-presentation, and IgG1-Fc for increased half-life. Here, we investigated whether and how N-803 improves HPC-NK cell functionality in leukemia and ovarian cancer (OC) models in vitro and in vivo in OC-bearing immunodeficient mice. We used flow cytometry-based assays, enzyme-linked immunosorbent assay, microscopy-based serial killing assays, and bioluminescence imaging, for in vitro and in vivo experiments. N-803 increased HPC-NK cell proliferation and interferon (IFN)γ production. On leukemia cells, co-culture with HPC-NK cells and N-803 increased ICAM-1 expression. Furthermore, N-803 improved HPC-NK cell-mediated (serial) leukemia killing. Treating OC spheroids with HPC-NK cells and N-803 increased IFNγ-induced CXCL10 secretion, and target killing after prolonged exposure. In immunodeficient mice bearing human OC, N-803 supported HPC-NK cell persistence in combination with total human immunoglobulins to prevent Fc-mediated HPC-NK cell depletion. Moreover, this combination treatment decreased tumor growth. In conclusion, N-803 is a promising IL-15-based compound that boosts HPC-NK cell expansion and functionality in vitro and in vivo. Adding N-803 to HPC-NK cell therapy could improve cancer immunotherapy.

IntroductionNatural killer (NK) cell therapy is an attractive strategy for cancer treatment as it selectively targets tumor cells without harming healthy tissues [1-3]. Moreover, numerous malignancies including hematopoietic and epithelial tumors are susceptible to NK cell-mediated immunity [4-8]. Since autologous NK cell infusion yields limited clinical responses [3], current approaches mostly involve allogeneic NK cell infusion in combination with cytokine support leading to improved responses [1,2].

A promising source for allogeneic NK cell therapy are CD34+ hematopoietic progenitor cell (HPC)-derived NK cells, since large numbers of cytotoxic NK cells can be generated from various sources, including umbilical cord blood (UCB). First, CD34+ HPCs are expanded and subsequently differentiated into $CD56^+$ HPC-NK cells, leading to more than thousand-fold expansion and high NK cell purity [9-11]. HPC-NK cells are highly functional, since they have high activating receptor expression, degranulation capacity, interferon (IFN)γ production, and tumor cell

killing capacity [9-13]. Furthermore, we have shown that HPC-NK cells mediate anti-tumor responses in leukemia and ovarian cancer (OC) models in mice, leading to prolonged survival [11,12,14]. To further maximize the anti-tumor effects of HPC-NK cell therapy, combination treatments can be explored to maintain NK cell proliferation and activation and/or to augment NK cell-mediated killing of tumor cells.

Interleukin (IL)-2 is traditionally used to boost proliferation of adoptively transferred NK cells *in vivo* [1,2,15-17]. However, IL-2 has been shown to also expand regulatory T cells (Tregs), that may reduce NK cell functionality [18,19]. Alternatively, IL-15 is crucial for NK cell survival, proliferation, and effector function [20,21], but does not induce Treg expansion [22,23]. Unfortunately, the *in vivo* half-life of recombinant IL-15 is short (≈40 minutes) [24]. Moreover, IL-15 is most potent when trans-presented by cells expressing the IL-15 receptor α (IL-15Rα) [25]. Hence, a novel IL-15 superagonist called N-803 (formerly known as ALT-803) has been developed, consisting of IL-15 with an activating mutation (N72D) that enhances binding to CD122 and CD122/CD132 activation, an IL-15Rα sushi domain to mimic typical trans-presentation, and an IgG1 Fc tail to increase half-life. N-803 has a more than 25-fold increased biological activity based on proliferation of 32Dβ cells [26] and more than 35-fold increased half-life (25h) compared to IL-15 [24]. First reported clinical trials of N-803 in cancer patients revealed that it is well tolerated and stimulates NK cell activation and expansion [27,28] and CD8+ T cells, but not Tregs [27]. *In vitro*, N-803 enhances functionality and tumor killing potential of peripheral blood (PB)-NK cells [29,30] and ascites-derived NK cells [30,31]. *In vivo*, PB-NK cell infusion in combination with N-803 administration results in significantly decreased tumor growth in NOD/SCID/IL2Rγnull (NSG) mice bearing human OC [30].

Our study goal was to investigate whether and how N-803 enhances HPC-NK cell functionality in leukemia and OC models, and whether N-803 supports HPC-NK cell persistence and anti-tumor effects in OC-bearing NSG mice. We found that N-803 can increase IFNγ production of HPC-NK cells and augment HPC-NK cell-mediated killing of OC and leukemia cells *in vitro*. Moreover, N-803 supports HPC-NK cell persistence and limits tumor growth in NSG mice bearing human OC.

Materials and Methods

HPC-NK cell culture

UCB collection at delivery was approved (see Declarations). HPC-NK cells were generated as described [11] with the following minor modifications. Cells were cultured for 5-7 weeks in 6-well tissue culture plates (Corning, 3506), using NK MACS Basal medium and supplement (NK MACS, Miltenyi Biotec, 130-114-429) complemented with 10% human serum (HS, Sanquin) during expansion (day 0-14) and 2-10% HS during differentiation (from day 14). HPC-NK cells (>70% CD56+) were used directly or cryopreserved. Cryopreserved HPC-NK cells were thawed and used after 5-7 days of culture in NK MACS containing 10% HS, 50 ng/ml recombinant human (rh)IL-15 (Immunotools, 11340155) and 0.2 ng/ml rhIL-12 (Miltenyi Biotec, 130-096-704). For experiments, HPC-NK cells were resuspended in Iscove's Modified Dulbecco's Medium (IMDM, Gibco,21980-032) supplemented with 10% fetal calf serum (FCS, Integro, 5-45900 or Corning, 35-079-CV) (IMDM10), except assays with primary AML samples (10% HS), proliferation assays, and some serial killing experiments in microwells (NK MACS medium + 10% HS or FCS, respectively).

PB-NK cell isolation

To obtain PB-NK cells, peripheral blood mononuclear cells were isolated from healthy donor buffy coats (Sanquin Blood Supply Foundation) by density gradient Ficoll-paque^{TM} PLUS (Sigma-Aldrich, 17-1440-03) centrifugation. Next, PB-NK cells were isolated using a magnetic bead-based NK cell enrichment kit (StemCell Technologies, 19055) resulting in ≥90% purity. PB-NK cells were resuspended in IMDM10 for experiments.

Tumor cell culture

OC cell lines SKOV-3, IGROV-1 and OVCAR-3 (RRID:CVCL_0532, RRID:CVCL_1304 and RRID:CVCL_0465, respectively) were cultured in Roswell Park Memorial Institute 1640 medium (RPMI, Gibco, 21875-034) supplemented with 10% FCS for SKOV-3 and IGROV-1 or 20% FCS and 1 µg/ml insulin (Merck, i0516) for OVCAR-3. SKOV-3 was transduced with luciferase (luc) and green fluorescent protein (GFP) (SKOV-3-luc-GFP) and cloned as described [11], and used for killing assays. Leukemia cell lines K562 and THP-1 (RRID:CVCL_0004 and RRID:CVCL_0006, respectively) were cultured in IMDM10. All cell lines were cultured for maximally three months and were mycoplasma free. SKOV-3, K562 and THP-1 were purchased from ATCC, IGROV-1 and OVCAR-3 were provided by Prof.

Dr. OC Boerman, Department of Nuclear Medicine, Radboudumc, Nijmegen, the Netherlands.

Tumor spheroid generation

Spheroids were generated from SKOV-3 and SKOV-3-luc-GFP as described in Hoogstad-van Evert *et al*. [11] with the following adaptations. Culture medium was not supplemented with bovine serum albumin but with 10% FCS and 1% penicillin/ streptomycin (MP Biomedicals, 1670049) and agarose medium with 2% penicillin/ streptomycin. Tumor spheroids were used 3-5 days after initial seeding.

Flow cytometry (FCM)-based assays

FCM samples were measured on one of the following flow cytometers: FC500, Gallios, CytoFLEX (all Beckman Coulter).

NK cell proliferation

NK cells were labeled with eFluor450 (eBioScience, 65-0842-85) and cultured in NK MACS/10% HS with/without rhIL-15 or N-803 (ImmunityBio). Cytokines were refreshed on day 3 and FCM analysis was performed on day 3 and 6. Dead cells were excluded using Fixable Viability Dye eFluor780 (eBiosciences, 65-0865-18). The proliferation gate was set on 1% in the no cytokine condition on day 3. NK cell numbers were based on CD56 gating (CD56-PE-Cy7, Beckman Coulter, A21692) and measuring for a fixed time.

Intercellular adhesion molecule 1 (ICAM-1) expression

Tumor cell lines and NK cells were plated at an effector-to-target (E:T) ratio of 0.6:1, with 0 or 1 nM N-803. After overnight-24h co-incubation, cells were stained with antibodies CD56-PE-Cy7 (BioLegend, 318318), ICAM-1-FITC (Biolegend, 353108) (and CD15-PE (IQ Products, IQP-129R) for THP-1). Primary AML samples were labelled with 0.25 μM carboxyfluorescein diacetate succinimidyl ester (CFSE, Invitrogen, C1157), co-cultured with NK cells (E:T ratio 0.1:1 or 0.3:1) for 48h and stained with CD33 BV605 (BD Biosciences, 740400) and ICAM-1 PE-Vio770 (Miltenyi Biotec, 130-104-031). Primary AML samples contained >90% blasts based on CD33 expression. Obtaining primary AML cells and patient data at diagnosis was approved (see Declarations).

IFNγ and perforin content

For IFNγ content, HPC-NK cells were stimulated for 4h with K562, THP-1 or SKOV-3 at an E:T ratio of 1.5:1, in the absence or presence of 1 nM N-803, 1 nM

rhIL-15, or 1000 U/ml rhIL-2 (Chiron, NDC 53905-991-01) and in the presence of brefeldin A (added after 1h, BD Biosciences, 555029). For perforin production, PB-NK cells and HPC-NK cells were primed overnight with or without 1 nM N-803.

After stimulation, surface staining was performed of CD56-BV510 (Biolegend, 318340), and intracellular staining of perforin-PE (Biolegend, 308106) and IFNγ-FITC (BD Biosciences, 554700). Dead cells were excluded using Fixable Viability Dye eFluor780. IFNγ analysis was performed by gating on $CD56^+$ $perforin^+$ NK cells, using unstimulated cells as control. Perforin analysis was performed by gating on $CD56^+$ NK cells.

Killing assay

Targets were plated at 30,000 cells/well in 96-well plates (round-bottom for leukemia cells, flat-bottom for OC cells). Targets or HPC-NK/PB-NK cells were labeled with 0.25-1 μM CFSE, and co-cultured at different E:T ratios with or without 1 nM N-803. Notably, SKOV-3-luc-GFP was not labeled with CFSE. OC cells were plated 3h in advance to allow for adherence. After overnight (cell line) or 48h (primary cells) co-culture, supernatants were harvested and stored at -20^{o}C for enzyme-linked immunosorbent assay (ELISA). Next, leukemia cells and/or NK cells were collected. OC cells were trypsinized using trypLE (Gibco, 12605028) and collected. Subsequently, viability marker 7-Aminoactinomycin D (7-AAD, Sigma, A9400) was added and targets were analyzed. Percentage of target killing by NK cells was calculated as follows: (1 – (number of viable targets after co-culture with NK cells) / (number of viable targets cultured without NK cells)) x 100%.

Spheroid killing assay

For spheroid killing assays, SKOV-3-luc-GFP cells were used. For overnight assays, different HPC-NK cell numbers were added with or without 1 nM N-803. After co-culture, supernatant was collected for ELISA. For 7-day assays, 13.000 HPC-NK cells and 0, 0.1 or 1.0 nM N-803 or rhIL-15 was used and after 7 days HPC-NK cells were counted based on CD56 positivity and 7-AAD negativity. Spheroids were washed, disrupted using trypLE and targets were counted based on GFP positivity and 7-AAD negativity.

Infiltration assay

SKOV-3-luc-GFP or SKOV-3 spheroids were co-cultured with 200.000 HPC-NK cells with or without 1 nM N-803. In SKOV-3 experiments, HPC-NK cells were labeled with 1 μM CFSE before or CD56-PE-Cy7 after co-culture. After 3h co-culture, infiltrated and non-infiltrated NK cells were separated as described [32].

First, supernatant was collected containing non-infiltrated NK cells. Next, spheroids were washed, disrupted using trypLE, and infiltrated NK cells were collected. 7-AAD negative and CD56 or CFSE positive NK cells were counted.

ELISA

Supernatants were thawed to evaluate IFNγ, granzyme B and C-X-C motif chemokine 10 (CXCL10) secretion by ELISA according to manufacturer's instructions (IFNγ, Endogen, M700A, granzyme B, MABTECH, 3485-IH-6, and CXCL10, R&D Systems, DY266-05).

NK cell serial killing experiments in microwells

Experiments were executed with small adaptations from Guldevall *et al.* [33]. HPC-NK cells were stained with 1 µM CFSE (BD Biosciences, 565082) or 2.5 µM CellTrace Yellow (Invitrogen, C34567). Targets were labeled with 1-2 µM Far Red (Invitrogen, C34564) and dead cells were detected by 1 µM sytox blue (Invitrogen, S11348) or 50 nM sytox green (Invitrogen, S7020). After a pre-screening with targets only in microwells (50x50x300 μm^3), HPC-NK cells were stochastically seeded with or without 1 nM N-803, 1 nM rhIL-15 or 1000 U/ml rhIL-2. Screening lasted for 12h, using an inverted confocal microscope equipped with x10 objective (Zeiss, LSM 880) at 37°C, 5% CO_2, with an image captured every 6h. Wells with or without N-803 were imaged in parallel by separating compartments of the chip using a polydimethylsiloxane gasket. Image analysis was performed with a MatLab script developed in-house. E:T ratios of 1:5 to 1:10 were analyzed. Only wells with 1 NK cell were analyzed.

Organotypic 3D collagen matrix assay

Organotypic 3D collagen matrix assays were performed as described [34]. In brief, 7,500 SKOV-3-luc-GFP cells were plated on a flat-bottom 96-well imaging plate (Greiner CELLSTAR®, 655090). After overnight adherence, 7,500 HPC-NK cells were added in a collagen solution (75 µl/well PureCol1, Advanced Biomatrix, 5005, 3 mg/ml) containing no or 1 nM N-803. After polymerization, no or 1 nM N-803 was added and cells were imaged by time-lapse bright field microscopy with x20 objective (BD, Pathway 855) at 37°C, 5% CO_2. Images were captured every 70 seconds for ~24h and subsequently, manual analysis of single cells was performed. Only serial killers were analyzed, defined as NK cells killing two or more targets. Inclusion criteria for cytotoxic events were (i) contact occurred between a single NK cell to a single target, (ii) the target was visible from the start of the movie.

Mouse experiments

Animal experiments were performed according to approved protocols (see Declarations). For experiment 1, 24 female NSG mice (Jackson Laboratories) of 6-20 weeks old were injected intraperitoneally (i.p.) with 0.2 million SKOV-3-luc-GFP cells (day -4) and divided into four treatment groups based on block randomization after Bioluminescence imaging (BLI) 3 days later (day -1). On day 0, mice were infused i.p. with HPC-NK cells (12 million/mouse). From day 0-15, mice (average weight was 25g) received i.p. injections of 50 or 200 µg/kg N-803 twice weekly, or 2.5 µg rhIL-15 (~7x more molecules compared to 50 µg/kg N-803) or phosphate buffered saline (PBS) every two days. Mice were sacrificed at day 15 or 16. Then, a peritoneal wash was performed and NK cells were labeled with mCD45-AF700 (Biolegend, 103128), hCD45-KO (Beckman Coulter, B36294) and hCD56-PE-Cy7 (Biolegend, 318318) and counted by flow cytometry.

Experiment 2 had a similar design with the following adaptations: 30 NSG mice were divided into five treatment groups and on day -5, two groups were irradiated with 2.25 Gy. From day -1 onwards, one group received i.p. nanogam (total human immunoglobulins, Sanquin Bloodbank) injections (50 mg) weekly one day before N-803 injection. From days 0-15, mice received i.p. injections of 50 µg/kg N-803 twice weekly or 2.5 µg rhIL-15 every two days. Prior to HPC-NK cell injection, CD16 expression was determined using viability dye eFluor780, CD56-BV510 (Biolegend, 318340) and CD16-BV421 (Biolegend, 302038). Mice were sacrificed at day 14 or 15.

Experiment 3 had a comparable design with the following differences: from day -1 onwards, all (21, divided into three treatment groups) mice received nanogam. On day 0 and 4, mice were infused with i.p. HPC-NK cells (8-9 million/mouse/infusion) or PBS. Mice receiving HPC-NK cells also received i.p. injections of 2.5 µg rhIL-15 every two days or 50 µg/kg N-803 twice weekly from day 0-24. BLI was performed weekly until signal saturation, following i.p. injection with 150 mg/kg D-luciferin (PerkinElmer, 122799) and isoflurane anesthesia. Ten minutes after injection, BLI images were collected in an *In Vivo* Imaging System using Living Image software.
A Region Of Interest was drawn around the torsos of the mice, and the integrated flux of photons (photons/second/cm^2/steradian) was analyzed.

Statistical analysis

Statistical analysis was performed using Graphpad Prism software version 5.03. Fold changes, lag phase to apoptosis and NK cell numbers in mice were first log transformed. Two-sided student t-tests and one-way and two-way ANOVAs were used

as indicated in the figure legends. Significance was defined as $p<0.05$ (*), $p<0.01$ (**) and $p<0.001$ (***).

Results

N-803 enhances HPC-NK cell proliferation, IFNγ production, and leukemia killing

Previously, we showed that N-803 outperforms rhIL-15 in inducing HPC-NK cell proliferation at 0.1 nM [35]. To confirm the optimal N-803 concentration, we performed proliferation assays with different concentrations of rhIL-15 or N-803 for 6 days. Indeed, N-803 induced HPC-NK cell proliferation in a dose-dependent manner (Fig. 1A-B). In comparison with rhIL-15, N-803 was superior in boosting NK cell proliferation at 0.1 nM (33% to 64%) and proliferation was similar at 1.0 nM (90% to 92%). All further experiments were performed using 1.0 nM N-803, which induced the most proliferation.

Next, we stimulated HPC-NK cells with leukemia cell lines K562 or THP-1 for 4h with or without N-803 and analyzed IFNγ production. N-803 increased IFNγ production in the presence of K562 or THP-1 (Fig. 1C). RhIL-15 and rhIL-2 showed comparable effects as N-803 (Supplementary Fig. 1A). To investigate whether IFNγ secretion was augmented, we co-cultured HPC-NK cells with K562 or THP-1 overnight with/without N-803, harvested supernatants and performed ELISA. Accordingly, HPC-NK cell-mediated IFNγ secretion was enhanced by N-803 (Fig. 1D).

Since IFNγ promotes ICAM-1 expression on leukemia cells [36], HPC-NK cells were co-cultured overnight with K562 or THP-1 with or without N-803, whereupon ICAM-1 expression was analyzed. HPC-NK cell co-culture significantly upregulated ICAM-1 on K562 and THP-1, while N-803 treatment did not (Fig. 1E). Importantly, N-803 combined with HPC-NK cells further boosted ICAM-1 expression on THP-1.

As increased ICAM-1 expression stimulates NK cell-mediated killing due to strengthened interactions of NK cells and targets [36], we next investigated NK cell-mediated tumor killing. Leukemia killing was measured after overnight co-culture with HPC-NK cells and with or without N-803. Correlating with ICAM-1 expression, N-803 did not increase HPC-NK cell-mediated K562 killing, but significantly augmented HPC-NK cell-mediated THP-1 killing (Fig. 1F-G). To compare the killing capacity of HPC-NK cells and PB-NK cells, we co-cultured HPC-NK cells or PB-NK cells with K562 or THP-1 with or without N-803. For MHC-I negative K562, N-803 did not improve HPC-NK cell-mediated killing at all, while it did seem to improve

PB-NK cell mediated killing at the second highest NK cell dose (Supplementary Fig. 1B). With regard to MHC-I positive THP-1, N-803 increased HPC-NK and PB-NK cell-mediated killing at all NK cell doses (Supplementary Fig. 1C). For both K562 and THP-1, HPC-NK cells were better killers than PB-NK cells at all NK cell doses, except the highest NK cell dose for K562 at which killing was maximal for both NK cell sources. Next, we evaluated the perforin content and granzyme B release of HPC-NK cells and PB-NK cells after priming with N-803 by intracellular staining and ELISA, respectively. We found that both HPC-NK cells and PB-NK cells upregulate perforin and granzyme B levels upon N-803 priming (Supplementary Fig. 1D-E). The higher killing capacity of HPC-NK cells did not correspond to perforin content, but did correlate with a higher granzyme B release versus PB-NK cells.

Table 1: ***Primary AML patient sample characteristics***

AML#	Origin	FAB classification	% blasts
1	Bone Marrow	M0	93
2	Bone Marrow	M2	91
3	Bone Marrow	M2	98
4	Bone Marrow	M1	99
5	Bone Marrow	M2	98

FAB: French-American-British

To confirm our findings, we co-cultured HPC-NK cells with primary AML samples from patients (Table 1) for 48h with/without N-803 and investigated IFNγ production, ICAM-1 expression, and killing.

N-803 significantly enhanced IFNγ production at an E:T ratio of 1:1 and 3:1 (Fig. 1H), upregulated ICAM-1 expression in the presence of HPC-NK cells (Fig. 1I) and most importantly increased primary AML killing by HPC-NK cells (Fig. 1J). Collectively, these data show that N-803 boosts IFNγ production by HPC-NK cells, promotes ICAM-1 expression on leukemia cells and improves HPC-NK cell-mediated leukemia killing.

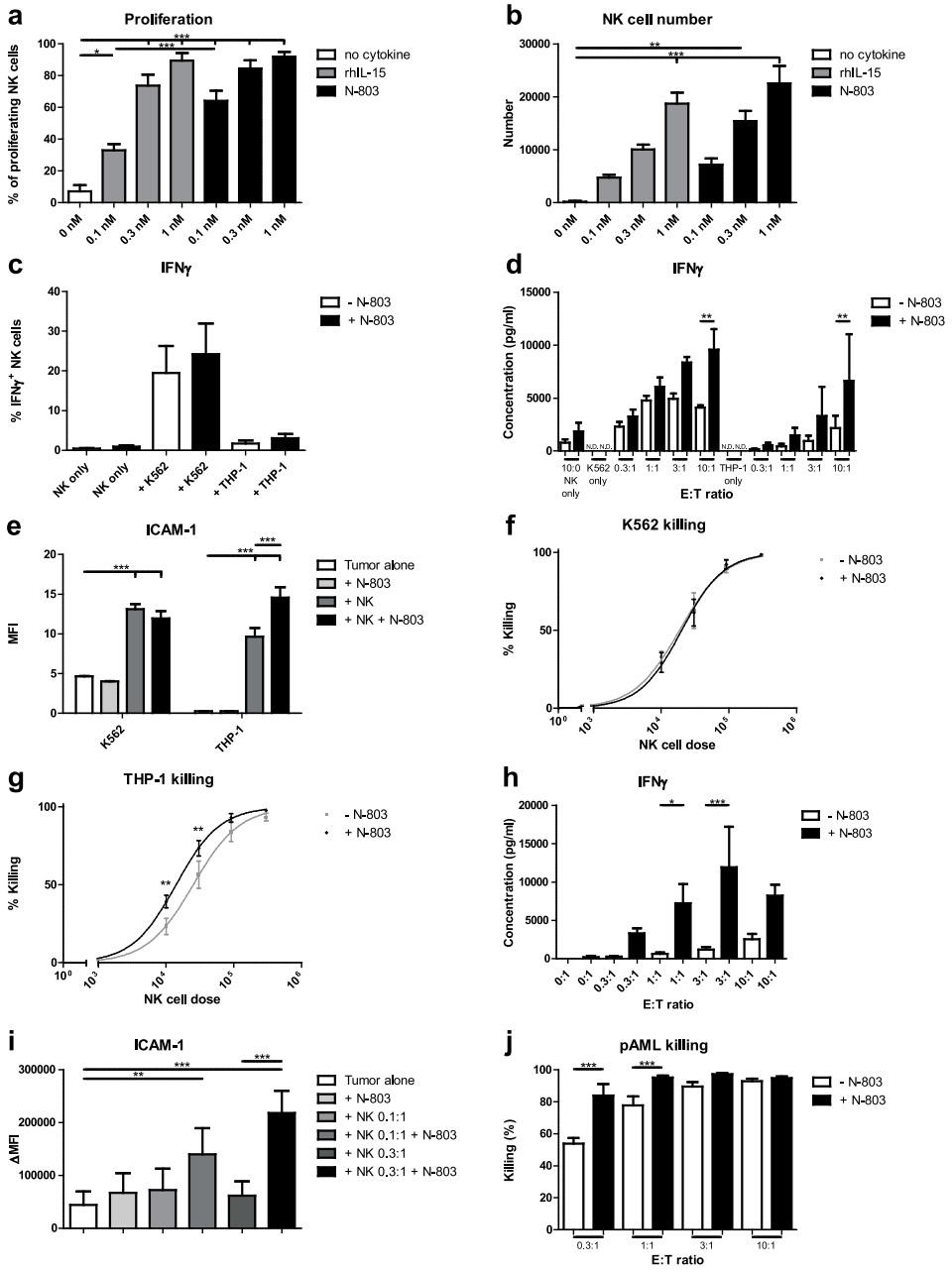
a
Proliferation
% of proliferating NK cells
no cytokine
rhIL-15
N-803
0 nM
0.1 nM
0.3 nM
1 nM
0.1 nM
0.3 nM
1 nM
b
NK cell number
Number
no cytokine
rhIL-15
N-803
c
IFNγ
% IFNγ+ NK cells
- N-803
+ N-803
NK only
NK only
+ K562
+ K562
+ THP-1
+ THP-1
d
IFNγ
Concentration (pg/ml)
- N-803
+ N-803
N.D.
N.D.
N.D.
N.D.
10:0 NK only
K562 only
0.3:1
1:1
3:1
10:1
THP-1 only
0.3:1
1:1
3:1
10:1
E:T ratio
e
ICAM-1
MFI
Tumor alone
+ N-803
+ NK
+ NK + N-803
K562
THP-1
f
K562 killing
% Killing
- N-803
+ N-803
NK cell dose
g
THP-1 killing
% Killing
- N-803
+ N-803
NK cell dose
h
IFNγ
Concentration (pg/ml)
- N-803
+ N-803
0:1
0.1:1
0.3:1
1:1
1:1
3:1
3:1
10:1
10:1
E:T ratio
i
ICAM-1
ΔMFI
Tumor alone
+ N-803
+ NK 0.1:1
+ NK 0.1:1 + N-803
+ NK 0.3:1
+ NK 0.3:1 + N-803
j
pAML killing
Killing (%)
- N-803
+ N-803
0.3:1
1:1
3:1
10:1
E:T ratio

Figure 1: ***N-803 enhances HPC-NK cell proliferation, IFNγ production, and leukemia killing*** *A-B. (A) Percentage of proliferating HPC-NK cells based on proliferation dye eFluor450 staining (n=3-4) (B) number of HPC-NK cells based on CD56 antibody staining (n=4-5) 6 days after incubation with no cytokine (white), rhIL-15 (grey) or N-803 (black). (C) Percentage of IFNγ$^+$ HPC-NK cells 4h after incubation with K562 or THP-1, with (black) or without (white) 1 nM N-803 combined for NK only (n=6), K562 (n=6) or THP-1 (n=4). (D) IFNγ concentration (pg/ml) after overnight co-culture of HPC-NK cells and K562 (n=3) or THP-1 (n=4) with or without 1 nM N-803 (without, white; with N-803, black, N.D.=not detectable). (E) Geometric Mean Fluorescence Intensity (MFI) of ICAM-1 expression after overnight culture of K562 (n=3) or THP-1 (n=4, white), and addition of N-803 (light grey), HPC-NK cells (dark grey) or both (black). F-G. Percentage of (F) K562 (n=3) or (G) THP-1 (n=4) killing after overnight co-culture with HPC-NK cells and 0 (grey) or 1 nM N-803 (black). (H) IFNγ concentration (pg/ml) after 48h co-culture of HPC-NK cells and primary AML (pAML) cells (n=5) with 1 nM N-803 (black) or without cytokine (white). (I) MFI of ICAM-1 expression after 48h culture of pAML cells (n=4, white), addition of N-803 (lightest grey), HPC-NK cells or both (different shades of grey/black). (J) Percentage of primary AML (pAML) cell killing (n=5) after 48h co-culture with HPC-NK cells and 0 (white) or 1 nM N-803 (black). Graphs show mean ± SEM for A-G, I-J. One-way ANOVA with Bonferroni correction was used (repeated measures for F-G, I-J) to test for statistical significance.*

N-803 enhances serial killing properties of HPC-NK cells against leukemia

To examine whether N-803 improves serial killing properties of HPC-NK cells against leukemia, we performed 12h experiments using microwells for live cell imaging with single cell resolution [33]. Here, 22 or 31% of HPC-NK cells serially killed (≥2 targets with at least 5 targets present at t=0h) K562 and THP-1, respectively (Fig. 2A-B). N-803 seemed to enhance these percentages, most distinct for THP-1 (37%, p=0.07). Most killing HPC-NK cells killed 1 target, followed by 2, 3, 4 and 5 or more targets (Fig. 2C-D). N-803 seemed to increase the number of targets killed by HPC-NK cell serial killers, most pronounced for THP-1. Spontaneous target death was detected in the minority of wells without HPC-NK cells (15% for K562, 45% for THP-1, Fig. 2E-F) and was not affected by N-803. Notably, the majority of targets was killed by serial killer HPC-NK cells (66%, Fig. 2G-H). N-803 augmented this percentage to 69% for K562 and 78% for THP-1. RhIL-2 and rhIL-15 displayed similar results as N-803 (Supplementary Fig. 2). Together, these data demonstrate that N-803 improves serial killing properties of HPC-NK cells against leukemia.

N-803 does not promote short-term HPC-NK cell-mediated killing of OC cell monolayers

To investigate whether N-803 also enhances the HPC-NK cell functionality towards OC cells, we stimulated HPC-NK cells with OC cell line SKOV-3 with/without N-803 for 4h and evaluated IFNγ production. Similar to leukemia, IFNγ production significantly increased by N-803, for HPC-NK cells with and without SKOV-3 (Fig. 3A-B): median 1.5-fold for HPC-NK cells+SKOV-3, $p<0.01$. Accordingly, IFNγ

secretion determined by ELISA was slightly increased by N-803 (Fig. 3C-D). However, no ICAM-1 upregulation was observed on SKOV-3 after addition of HPC-NK cells and N-803, compared to addition of HPC-NK cells alone (Fig. 3E). Likewise, N-803 did not improve HPC-NK cell-mediated SKOV-3 killing (Fig. 3F). OC cell lines IGROV-1 and OVCAR-3 showed similar killing results as SKOV-3 (Supplementary Fig. 3); rhIL-15 displayed comparable overnight IFNγ production and SKOV-3 killing as N-803 (data not shown).

Although N-803 did not improve overnight HPC-NK cell-mediated SKOV-3 killing, we next studied whether interaction abilities and serial killing properties of HPC-NK cells against OC were affected by N-803 in an organotypic 3D collagen matrix assay, mimicking interstitial tissue. Lag phase to SKOV-3 apoptosis (time from first contact to kill) due to serial killing by HPC-NK cells was mostly short with a median of 19 minutes for the first kill and similar times for the second kill (Fig. 3G). N-803 did not change these times for the first or second kill. Altogether, these data indicate that despite slightly enhanced IFNγ production, N-803 could not increase ICAM-1 expression and short-term HPC-NK cell-mediated (serial) killing of OC cells.

N-803 increases CXCL10 production and improves long-term HPC-NK cell-mediated killing in OC spheroids

Next, we addressed the effects of N-803 in SKOV-3(-luc-GFP) spheroids to mimic three-dimensional growth of OC *in vivo*. HPC-NK cells were co-cultured with spheroids overnight and ELISA of supernatants was performed to determine IFNγ and CXCL10 secretion. Overall, N-803 enhanced IFNγ secretion of HPC-NK cells co-cultured with spheroids (Fig. 4A-B). Furthermore, CXCL10 production was significantly boosted by spheroids co-cultured with HPC-NK cells and N-803 (Fig. 4C-D). Since CXCL10 attracts C-X-C chemokine receptor 3 (CXCR3)+ HPC-NK cells [14], we performed 3h infiltration assays with spheroids and HPC-NK cells, in which no effect of N-803 on infiltration was observed (Fig. 4E). Moreover, N-803 did not improve HPC-NK cell-mediated spheroid killing within 24h (Fig. 4F). All short-term assays with rhIL-15 or rhIL-2 showed comparable results as N-803 (data not shown). Importantly, a long-term killing assay showed that N-803 significantly enhanced HPC-NK cell expansion and HPC-NK cell-mediated spheroid killing (Fig. 4G-H). A dose-dependent killing effect of N-803 was found and rhIL-15 displayed similar effects as N-803 (Supplementary Fig. 4). Collectively, these experiments demonstrate that N-803 increases IFNγ and CXCL10 secretion in co-cultures of OC spheroids and HPC-NK cells. Furthermore, N-803 induces HPC-NK cell expansion and boosts OC spheroid destruction during long-term co-cultures.

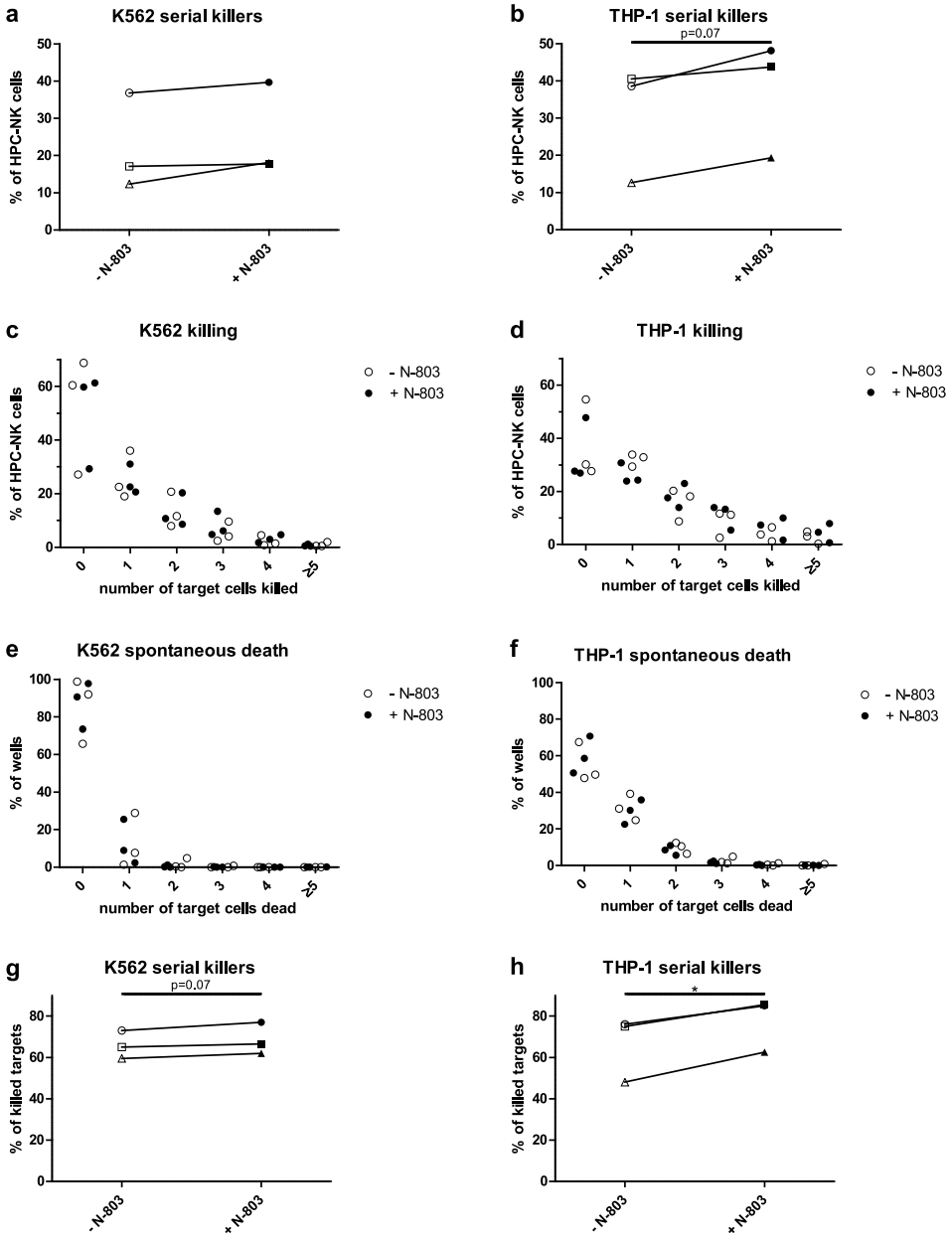
a
K562 serial killers
% of HPC-NK cells
- N-803
+ N-803
b
THP-1 serial killers
p=0.07
c
K562 killing
number of target cells killed
d
THP-1 killing
e
K562 spontaneous death
% of wells
number of target cells dead
f
THP-1 spontaneous death
g
K562 serial killers
% of killed targets
h
THP-1 serial killers
*

Figure 2: ***N-803 enhances serial killing properties of HPC-NK cells against leukemia***

A-B. Percentage of serial killers after 12h co-culture of HPC-NK cells and (A) K562 (n=3) or (B) THP-1 (n=3) with 0 or 1 nM N-803. At least 125 NK cells were analyzed. C-D. Percentage of wells showing the number of (C) K562 (n=3) or (D) THP-1 (n=3) cells killed in the presence of individual HPC-NK cells after 12h co-culture with 0 (white) or 1 nM N-803 (black). At least 125 NK cells were analyzed. E-F. Percentage of wells showing spontaneous (E) K562 (n=3) or (F) THP-1 (n=3) cell death after 12h culture without HPC-NK cells and with 0 (white) or 1 nM N-803 (black). At least 173 targets were analyzed. G-H. Percentage of killed (G) K562 (n=3) or (H) THP-1 (n=3) cells killed by serial killers after 12h co-culture with HPC-NK cells and no cytokine or 1 nM N-803. At least 126 killed targets were analyzed. Graphs show mean ± SEM. Paired t-tests were used for A-B, G-H and repeated measures one-way ANOVA with Bonferroni correction was used for C-F to test for statistical significance.

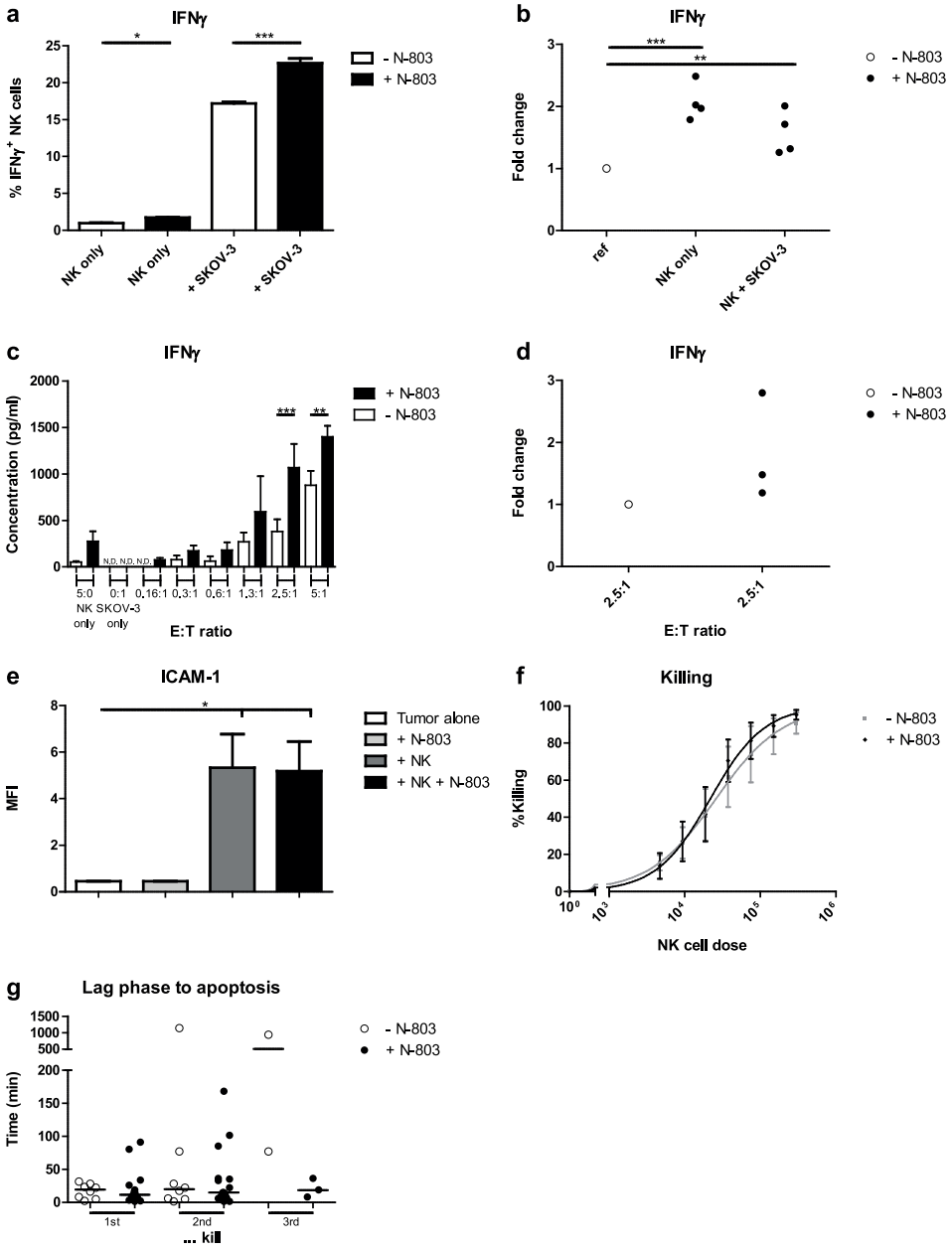
a
IFNγ
% IFNγ+ NK cells
- N-803
+ N-803
NK only
NK only
+ SKOV-3
+ SKOV-3
b
IFNγ
Fold change
- N-803
+ N-803
ref
NK only
NK + SKOV-3
c
IFNγ
Concentration (pg/ml)
+ N-803
- N-803
N.D. N.D. N.D.
5:0 NK only
0:1 SKOV-3 only
0.16:1
0.3:1
0.6:1
1.3:1
2.5:1
5:1
E:T ratio
d
IFNγ
Fold change
- N-803
+ N-803
2.5:1
2.5:1
E:T ratio
e
ICAM-1
MFI
Tumor alone
+ N-803
+ NK
+ NK + N-803
f
Killing
%Killing
- N-803
+ N-803
NK cell dose
g
Lag phase to apoptosis
Time (min)
- N-803
+ N-803
1st
2nd
3rd
... kill

Figure 3: ***N-803 does not promote short-term HPC-NK cell-mediated killing of OC cell monolayers***
A-B. (A) Percentage of IFNγ$^+$ HPC-NK cells or (B) fold change of the percentage after 4h incubation with OC cell line SKOV-3, and 0 (white) or 1 nM N-803 (black) (A) in a representative HPC-NK cell donor containing duplos/triplos or (B) combined (n=4) and compared to the same cells without cytokine (ref). C-D. (C) IFNγ concentration (pg/ml) or (D) fold change of IFNγ concentration after overnight co-culture of HPC-NK cells and SKOV-3 with 0 (white) or 1 nM N-803 (black) (C) in a representative HPC-NK cell donor containing triplos (N.D.=not detectable) or (D) combined compared to without cytokine (n=3). (E) MFI of ICAM-1 expression after overnight culture of SKOV-3 (white), addition of N-803 (light grey), HPC-NK cells (dark grey) or both (black) (n=3). (F) Percentage of SKOV-3 killing after overnight co-culture with HPC-NK cells and 0 (grey) or 1 nM N-803 (black) (n=4). (G) Lag phase to apoptosis of SKOV-3 for the 1st, 2nd and 3rd kill by serial killer HPC-NK cells with 0 (white) or 1 nM N-803 (black) (n=1). Graphs show mean ± SD for A, C/SEM for E-F, and median for G. One-way ANOVA with Bonferroni correction was used (after log transformation for B, D, G, repeated measures for B, D-F) to test for statistical significance.

HPC-NK cells combined with N-803 and nanogam show anti-tumor effects in mice bearing human OC

To determine whether N-803 promotes HPC-NK cell persistence and anti-tumor effects in a human OC mouse model, we used NSG mice bearing peritoneal SKOV-3-luc-GFP tumor nodules [11]. In experiment 1, mice were treated i.p. with HPC-NK cells in combination with PBS, rhIL-15, or N-803 for two weeks and afterwards peritoneal washes were performed. As expected, HPC-NK cells were present in the rhIL-15 group but surprisingly HPC-NK cells were nearly absent in the N-803 groups (Fig. 5A). We hypothesized that the Fc part of N-803 binds to Fc receptors, resulting in Fc-mediated HPC-NK cell depletion, in NSG mice lacking immunoglobulins. Hence, in experiment 2 we used irradiation or nanogam (*i.e.* total human immunoglobulins) to kill or inactivate immune cells containing Fc receptors present in NSG mice, or to block Fc receptors, respectively to prevent Fc-mediated HPC-NK cell depletion in the presence of N-803. To determine if there was risk for Fc-mediated fratricide, CD16 expression was determined prior to HPC-NK cell injection, which showed 20% CD16$^+$ HPC-NK cells (Supplementary Fig. 5). Irradiation could not prevent N-803-mediated depletion but nanogam could, resulting in HPC-NK cell persistence and similar NK cell numbers as rhIL-15 treatment (Fig. 5B).

Finally, we evaluated tumor growth (experiment 3) in mice treated with two i.p. HPC-NK cell injections in combination with N-803 or rhIL-15, and nanogam compared to a group only receiving nanogam. This experiment showed that both combination treatments significantly reduced tumor growth, compared to the control group (Fig. 5C-D). To conclude, we demonstrate that nanogam restores HPC-NK cell persistence in OC bearing NSG mice receiving N-803. Importantly, HPC-NK cell, N-803 and nanogam combination treatment has an anti-OC effect *in vivo*.

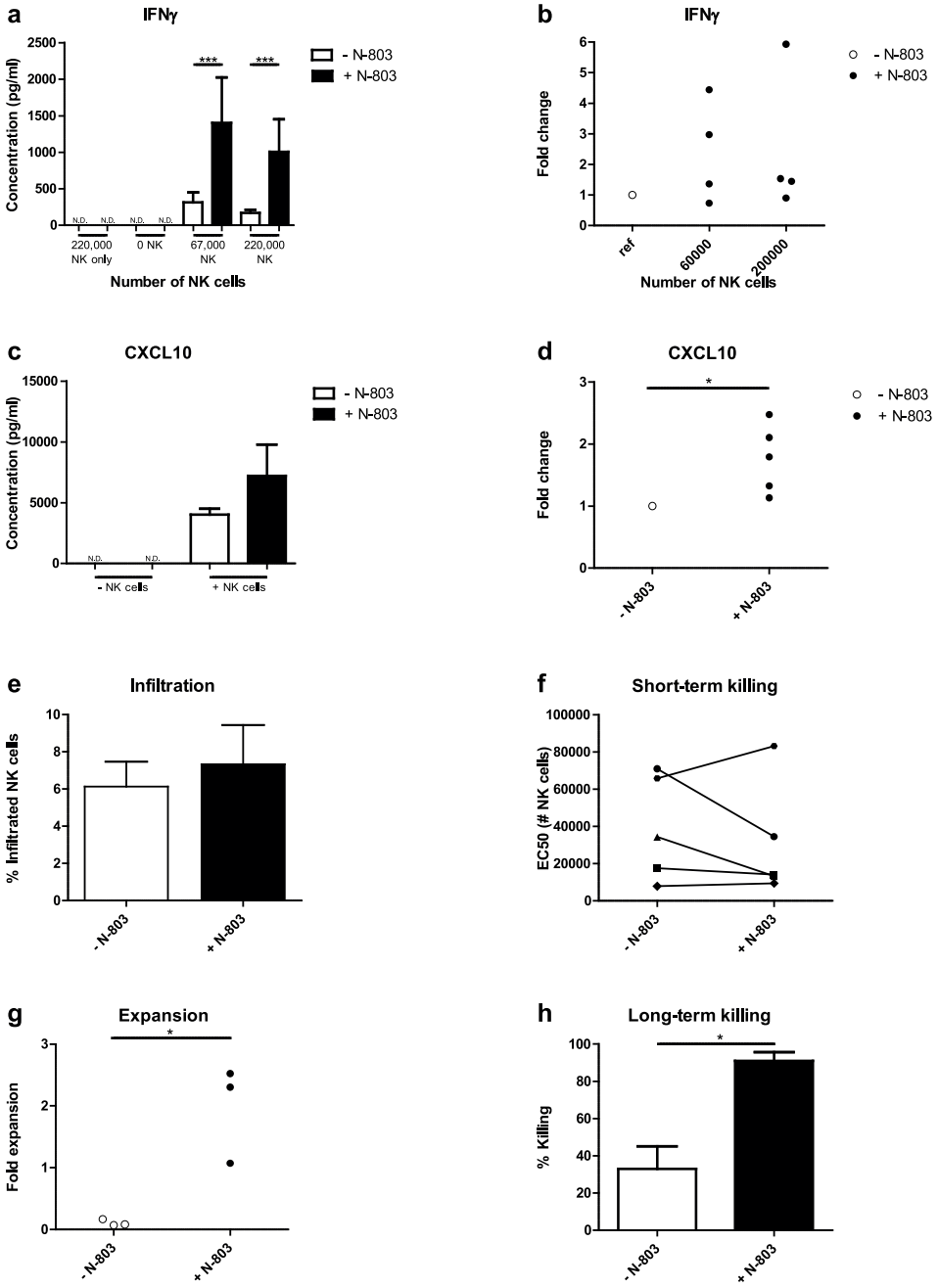
a
IFNγ
Concentration (pg/ml)
2500
2000
1500
1000
500
0
***
***
- N-803
+ N-803
N.D.
N.D.
N.D.
N.D.
220,000 NK only
0 NK
67,000 NK
220,000 NK
Number of NK cells
b
IFNγ
Fold change
6
5
4
3
2
1
0
- N-803
+ N-803
ref
60000
200000
Number of NK cells
c
CXCL10
Concentration (pg/ml)
15000
10000
5000
0
- N-803
+ N-803
N.D.
N.D.
- NK cells
+ NK cells
d
CXCL10
Fold change
3
2
1
0
*
- N-803
+ N-803
- N-803
+ N-803
e
Infiltration
% Infiltrated NK cells
10
8
6
4
2
0
- N-803
+ N-803
f
Short-term killing
EC50 (# NK cells)
100000
80000
60000
40000
20000
0
- N-803
+ N-803
g
Expansion
Fold expansion
3
2
1
0
*
- N-803
+ N-803
h
Long-term killing
% Killing
100
80
60
40
20
0
*
- N-803
+ N-803

Figure 4: ***N-803 increases CXCL10 production and improves long-term HPC-NK cell-mediated killing in OC spheroids***

A-B. (A) IFNγ concentration (pg/ml) or (B) fold change of IFNγ concentration after overnight co-culture of HPC-NK cells and spheroids of OC cell line SKOV-3 with 0 (white) or 1 nM N-803 (black) (A) in a representative HPC-NK cell donor containing fiveplos/sixplos (N.D.=not detectable) or (B) combined (n=4) and compared to the same number of NK cells without cytokine (ref, 55,600-67,000 and 170,000-220,000 HPC-NK cells). C-D. (C) CXCL10 concentration (pg/ml) or (D) fold change of CXCL10 concentration after overnight co-culture of HPC-NK cells and SKOV-3 spheroids with 0 (white) or 1 nM N-803 (black) (C) in a representative HPC-NK cell donor containing triplos (0-67,000 HPC-NK cells, N.D.=not detectable) or (D) combined (n=5) compared to no cytokine (6,700-67,000 HPC-NK cells). (E) Percentage of infiltrated HPC-NK cells into SKOV-3 spheroids after 3h co-incubation with 0 or 1 nM N-803 (n=8). (F) EC50 = HPC-NK cell dose needed to kill 50% of SKOV-3 in a spheroid with or without N-803 (n=5). (G) Fold expansion of HPC-NK cells in the presence of a SKOV-3 spheroid after 1 week co-incubation with 0 or 1 nM N-803 (n=3). (H) Percentage of SKOV-3 spheroid killing after 1 week co-culture with HPC-NK cells and 0 or 1 nM N-803 (n=4). Graphs show mean ± SD for A, C/SEM for E, H. T-tests were used for C-H (paired for E-H, unpaired for C, one-sample for D, after log transformation for D and G) and a repeated measures one-way ANOVA with Bonferroni correction for A and B (after log transformation for B) to test for statistical significance.

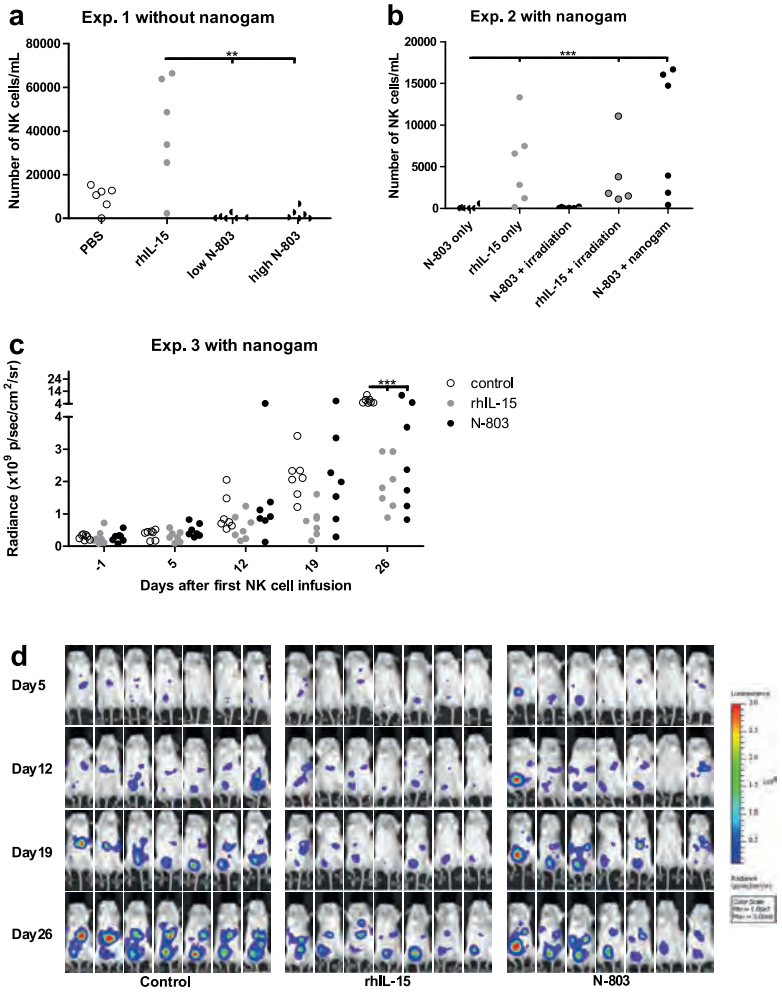

Figure 5: ***HPC-NK cells combined with N-803 and nanogam show anti-tumor effects in mice bearing human OC***

(A) Experiment 1: number of HPC-NK cells per ml in the peritoneal wash of SKOV-3 bearing NSG mice (0.2 million tumor cells injected 4 days before HPC-NK cell treatment) 15/16 days after treatment with HPC-NK cells in combination with phosphate-buffered saline (PBS), 2.5 µg rhIL-15, or 50 or 200 µg/kg N-803 (6 mice per group). (B) Experiment 2: number of HPC-NK cells per ml in the peritoneal wash of SKOV-3 bearing NSG mice (0.2 million tumor cells injected 4 days before HPC-NK cell treatment) 14/15 days after treatment with HPC-NK cells in combination with 50 µg/kg N-803, 2.5 µg rhIL-15, 50 µg/kg N-803 + nanogam, 50 µg/kg N-803 + 2.25 Gy irradiation, or 2.5 µg rhIL-15 + 2.25 Gy irradiation (6 mice per group). (C) Experiment 3: radiance (photons/second/cm^2/steradian) of tumors in SKOV-3 bearing NSG mice (0.2 million tumor cells injected 4 days before the first HPC-NK cell infusion) treated with nanogam + PBS (white, control), nanogam + 2 HPC-NK cell infusions + 2.5 µg rhIL-15 (grey) or nanogam + 2 HPC-NK cell infusions + 50 µg/kg N-803 (black) over time (7 mice per group). (D) BLI images from (C) acquired over time. One-way ANOVA with Bonferroni correction was used for A-B (after log transformation for A and B), and a repeated-measures two-way ANOVA with Bonferroni correction for C to test for statistical significance.

Discussion

Allogeneic NK cell therapy is a promising approach for cancer treatment and HPC-NK cells mediate anti-tumor responses in leukemia and OC models [11,12,14]. However, tumor eradication is not complete in xenograft NSG models, indicating room for improvement. Optimizing HPC-NK cell anti-tumor efficacy can be achieved by cytokine co-administration. This study investigated whether and how IL-15 superagonist N-803 improves HPC-NK cell functionality in leukemia and OC models, and whether N-803 supports *in vivo* HPC-NK cell persistence and anti-OC effects.

First, we confirmed that N-803 dose dependently induces HPC-NK cell proliferation. Compared to rhIL-15, N-803 leads to higher proliferation at 0.1 nM but not 1.0 nM, caused by reaching maximum proliferation, which is in line with previous reports [30,35]. Next, we demonstrated that N-803 improves IFNγ production of HPC-NK cells. This effect has been demonstrated in numerous NK cell studies [29,30,37-42]. In addition, N-803 increases ICAM-1 expression on leukemia cells after HPC-NK cell co-culture and improves (serial) leukemia killing. Since HPC-NK cells have high lymphocyte function associated antigen 1 (LFA-1) expression [11,12,35], the receptor for ICAM-1, the interaction strength between HPC-NK cells and targets is dependent on ICAM-1 expression. Increased ICAM-1 expression leads to stronger interactions, resulting in targets being more sensitive to killing [12,36]. Interestingly, these effects were found with primary AML and THP-1, but not K562, which may be attributed to unaffected ICAM-1 expression on K562 by N-803. Furthermore, K562 is MHC-I negative, making it very sensitive to NK cell-mediated killing. Since HPC-NK cells are highly potent killers compared to PB-NK cells, this leaves a narrow window for improvement. However, for less susceptible MHC-I positive THP-1 cells HPC-NK and PB-NK cell-mediated killing could be improved by N-803. Importantly, we showed for the first time that N-803 promotes HPC-NK cell serial killing properties and that some HPC-NK cells kill 5 or more leukemia cells within 12h. This is in line with studies using PB-NK or NK-92 cells, in which up to 6 [43], 7 [44], 8 [33], or 14 [45] serial kills were reported within 6-16h. Our findings further revealed that a minority of HPC-NK cells is a serial killer, responsible for the majority of killing. This is in accordance with previous studies [33,44].

Moreover, we assessed HPC-NK cell serial killing properties against OC cells. As expected based on OC monolayer killing experiments, N-803 did not improve serial killing against OC. Nevertheless, serial killer HPC-NK cells generally kill quickly (median 19 minutes for the first kill) after initial contact. This median lag phase is similar as in Vanherberghen's study [44], where the mean lag phase (time to lytic hit + time to death) was 17.5 minutes for serial killers. In our OC model, serial killer HPC-NK cells kill up to 3 targets, which is lower than our leukemia model and other

studies [33,43-45]. Potential explanations for those differences are that we used a low target density and a high E:T ratio in the OC model, while in our leukemia model and other studies higher target densities and/or lower E:T ratios were used. For low target cell densities, we and others[43,45] observed that NK cells often stay in contact with apoptotic cells, limiting the number of serial kills. Lower E:T ratios allow for better serial killing detection, because every NK cell can kill more targets. Furthermore, intrinsic differences between used targets impact sensitivity to (serial) killing by NK cells[33,45]. For instance, SKOV-3 used in our OC model is more difficult to kill than K562 used in our leukemia model and other studies (Fig. 1 and 3).

In OC spheroids, N-803 significantly increases IFNγ and CXCL10 secretion during overnight co-culture with HPC-NK cells. Because HPC-NK cells have high CXCR3 expression [11-14,35], increased CXCL10 secretion could improve NK cell infiltration. Since the relatively high amount of HPC-NK cells, needed for infiltration assays, destroys OC spheroids after overnight incubation, we measured infiltration after 3h. In this model, no effect of N-803 on HPC-NK cell infiltration was observed, though 3h co-incubation is likely too short to increase IFNγ and CXCL10 secretion and impact HPC NK cell infiltration. Importantly, in long-term assays, using less HPC-NK cells, N-803 improves HPC-NK cell expansion, and therefore OC spheroid killing at the longer term.

Finally, we showed that *in vivo* N-803 supports peritoneal HPC-NK cell persistence in the presence of human immunoglobulins (nanogam) in NSG mice bearing human OC and this combination treatment has an anti-OC effect. Similar findings were reported by Felices *et al*. [30], demonstrating improved OC tumor control in NSG mice treated with PB-NK cells in combination with N-803 compared to no treatment or NK cells alone. Since HPC-NK cells hardly persist without cytokine support, and clinical trials will be conducted with cytokine support, we chose to compare HPC-NK cells plus N-803 (or rhIL-15) treatment to no treatment. Notably, pre-treatment of NSG mice with human immunoglobulin (nanogam) was required to prevent Fc-mediated HPC-NK cell depletion by N-803 treatment. In patients, pre-treatment with nanogam will not be necessary, since they have immunoglobulins. In Felices' study sublethal irradiation (2.25 Gy) was sufficient to prevent Fc-mediated depletion of PB-NK cells, while in our study sublethal irradiation (2.25 Gy) did not rescue Fc-mediated depletion of HPC-NK cells. One of the differences in the design of these two studies is the timing of irradiation: we irradiated the mice one day before tumor injection, while they irradiated the mice one day before NK cell injection. It might be that in our study immune cells containing Fc receptors in the NSG mice recovered or repopulated before the first N-803 injection, which could have led to Fc-mediated depletion. Alternatively, it could be that HPC-NK cells are more sensitive to Fc-mediated NK cell depletion than PB-NK cells due to differences in activation status.

Around 20% of the HPC-NK cells had CD16 expression before NK cell injection (Supplementary Fig 5), indicating that Fc-mediated fratricide might have been possible. Moreover, we know from our previous publications that CD16 expression is upregulated in NSG mice *in vivo* [12,14], increasing the risk for Fc-mediated fratricide. Fortunately, Fc-mediated depletion of HPC-NK cells could be prevented by nanogam injection in NSG mice.

Comparing N-803 with rhIL-15 shows that *in vivo* OC growth was similar. However, it is important to note that the amount of molecules per dose was ~7x lower for N-803 than rhIL-15 and rhIL-15 was given more frequently. Assuming all N-803 or rhIL-15 was consumed before the next dose administration, this suggests that N-803 may indeed have a higher biological activity compared to rhIL-15. *In vivo* experiments with leukemia-bearing NSG mice, NK cells and N-803 have previously been carried out [35,39]. Wagner *et al*. showed K562 leukemia control by N-803-primed PB-NK cells [39] and Cany *et al*. demonstrated intra-femoral THP-1 leukemia control by HPC-NK cells, N-803, and decitabine [35]. Since we found HPC-NK cell depletion in our i.p. OC model, repeating Cany's leukemia study with nanogam might improve treatment results in mice.

Collectively, our results imply that N-803 is an attractive compound to promote HPC-NK cell expansion and functionality for NK cell therapy. Currently, two phase 1 clinical trials with N-803 are recruiting patients in the US in various cancer types (NCT03054909 and NCT02890758). In addition, N-803 has been shown to enhance antibody-dependent cellular cytotoxicity *in vitro* [38,41] and checkpoint blockade therapy in cancer-bearing mice [40]. For future studies, it would be interesting to compare N-803 to the standard IL-2 co-administration with NK cell adoptive transfer for anti-tumor efficacy, to evaluate whether IL-2 can be replaced by N-803 to prevent Treg-expansion in cancer patients.

In conclusion, N-803 boosts HPC-NK cell proliferation and IFNγ production *in vitro*. Furthermore, N-803 improves (serial) leukemia killing and long-term OC spheroid destruction by HPC-NK cells. *In vivo*, N-803 in combination with human immunoglobulin supports HPC-NK cell persistence in NSG mice and this combination treatment mediates an anti-OC effect. In conclusion, N-803 is a promising IL-15-based compound to improve NK cell-based cancer immunotherapy.

References

1. Miller JS, Soignier Y, Panoskaltsis-Mortari A, McNearney SA, Yun GH, Fautsch SK, McKenna D, Le C, Defor TE, Burns LJ, Orchard PJ, Blazar BR, Wagner JE, Slungaard A, Weisdorf DJ, Okazaki IJ, McGlave PB. *Successful adoptive transfer and in vivo expansion of human haploidentical NK cells in patients with cancer.* Blood. 2005;105(8):3051–3057.

2. Curti A, Ruggeri L, D'Addio A, Bontadini A, Dan E, Motta MR, Trabanelli S, Giudice V, Urbani E, Martinelli G, Paolini S, Fruet F, Isidori A, Parisi S, Bandini G, Baccarani M, Velardi A, Lemoli RM. *Successful transfer of alloreactive haploidentical KIR ligand-mismatched natural killer cells after infusion in elderly high risk acute myeloid leukemia patients*. Blood. 2011;118(12):3273–3279.

3. Burns LJ, Weisdorf DJ, DeFor TE, Vesole DH, Repka TL, Blazar BR, Burger SR, Panoskaltsis-Mortari A, Keever-Taylor CA, Zhang MJ, Miller JS. *IL-2-based immunotherapy after autologous transplantation for lymphoma and breast cancer induces immune activation and cytokine release: a phase I/II trial.* Bone Marrow Trans. 2003;32(2):177–186.

4. Norell H, Carlsten M, Ohlum T, Malmberg KJ, Masucci G, Schedvins K, Altermann W, Handke D, Atkins D, Seliger B, Kiessling R. *Frequent loss of HLA-A2 expression in metastasizing ovarian carcinomas associated with genomic haplotype loss and HLA-A2-restricted HER-2/neu-specific immunity*. Can Res. 2006;66(12):6387–6394.

5. Vago L, Perna SK, Zanussi M, Mazzi B, Barlassina C, Stanghellini MT, Perrelli NF, Cosentino C, Torri F, Angius A, Forno B, Casucci M, Bernardi M, Peccatori J, Corti C, Bondanza A, Ferrari M, Rossini S, Roncarolo MG, Bordignon C, Bonini C, Ciceri F, Fleischhauer K. *Loss of mismatched HLA in leukemia after stem-cell transplantation.* The New England journal of medicine. 2009;361(5):478–488.

6. Vitale M, Pelusi G, Taroni B, Gobbi G, Micheloni C, Rezzani R, Donato F, Wang X, Ferrone S. *HLA class I antigen down-regulation in primary ovary carcinoma lesions: association with disease stage.* Clin Cancer Res Off J Am Assoc Cancer Res. 2005;11(1):67–72.

7. Li K, Mandai M, Hamanishi J, Matsumura N, Suzuki A, Yagi H, Yamaguchi K, Baba T, Fujii S, Konishi I. *Clinical significance of the NKG2D ligands, MICA/B and ULBP2 in ovarian cancer: high expression of ULBP2 is an indicator of poor prognosis*. Cancer Immunol Immunothera. 2009;58(5):641–652.

8. Mastaglio S, Wong E, Perera T, Ripley J, Blombery P, Smyth MJ, Koldej R, Ritchie D. *Natural killer receptor ligand expression on acute myeloid leukemia impacts survival and relapse after chemotherapy.* Blood Adv. 2018;2(4):335–346.

9. Spanholtz J, Tordoir M, Eissens D, Preijers F, van der Meer A, Joosten I, Schaap N, de Witte TM, Dolstra H. *High log-scale expansion of functional human natural killer cells from umbilical cord blood CD34-positive cells for adoptive cancer immunotherapy.* PLoS ONE. 2010;5(2):e9221.

10. Spanholtz J, Preijers F, Tordoir M, Trilsbeek C, Paardekooper J, de Witte T, Schaap N, Dolstra H. *Clinical-grade generation of active NK cells from cord blood hematopoietic progenitor cells for immunotherapy using a closed-system culture process*. PLoS ONE. 2011;6(6):e20740.

11. Hoogstad-van Evert JS, Cany J, van den Brand D, Oudenampsen M, Brock R, Torensma R, Bekkers RL, Jansen JH, Massuger LF, Dolstra H. Umbilical cord blood *CD34(+) progenitor-derived NK cells efficiently kill ovarian cancer spheroids and intraperitoneal tumors in NOD/SCID/IL2Rg(null) mice*. Oncoimmunology. 2017;6(8):e1320630.

12. Cany J, van der Waart AB, Spanholtz J, Tordoir M, Jansen JH, van der Voort R, Schaap NM, Dolstra H. *Combined IL-15 and IL-12 drives the generation of CD34+-derived natural killer cells with superior maturation and alloreactivity potential following adoptive transfer*. Oncoimmunology. 2015;4(7):e1017701.

13. Roeven MW, Thordardottir S, Kohela A, Maas F, Preijers F, Jansen JH, Blijlevens NM, Cany J, Schaap N, Dolstra H. *The Aryl hydrocarbon receptor antagonist stemregenin1 improves in vitro generation of highly functional natural killer cells from CD34(+) hematopoietic stem and progenitor cells*. Stem Cells Dev. 2015;24(24):2886–2898.

14. O, Schaap N, van der Voort R, Spanholtz J, Dolstra H. *Natural killer cells generated from cord blood hematopoietic progenitor cells efficiently target bone marrow-residing human leukemia cells in NOD/SCID/IL2Rg(null) mice.* PLoS ONE. 2013;8(6):e64384.

15. Rubnitz JE, Inaba H, Ribeiro RC, Pounds S, Rooney B, Bell T, Pui CH, Leung W. *NKAML: a pilot study to determine the safety and feasibility of haploidentical natural killer cell transplantation in childhood acute myeloid leukemia.* J Clin Oncol Off Am Soc Oncol. 2010;28(6):955–959.

16. Curti A, Ruggeri L, Parisi S, Bontadini A, Dan E, Motta MR, Rizzi S, Trabanelli S, Ocadlikova D, Lecciso M, Giudice V, Fruet F, Urbani E, Papayannidis C, Martinelli G, Bandini G, Bonifazi F, Lewis RE, Cavo M, Velardi A, Lemoli RM. *Larger size of donor alloreactive NK cell repertoire correlates with better response to NK cell immunotherapy in elderly acute myeloid leukemia patients*. Clin Cancer Res Off J Am Assoc Cancer Res. 2016;22(8):1914–1921.

17. Hoogstad-van Evert J, Bekkers R, Ottevanger N, Schaap N, Hobo W, Jansen JH, Massuger L, Dolstra H. *Intraperitoneal infusion of ex vivo-cultured allogeneic NK cells in recurrent ovarian carcinoma patients (a phase I study).* Medicine. 2019;98(5):e14290.

18. Ahmadzadeh M, Rosenberg SA. *IL-2 administration increases CD4+ CD25(hi) Foxp3+ regulatory T cells in cancer patients.* Blood. 2006;107(6):2409–2414.

19. Wei S, Kryczek I, Edwards RP, Zou L, Szeliga W, Banerjee M, Cost M, Cheng P, Chang A, Redman B, Herberman RB, Zou W. *Interleukin-2 administration alters the CD4+FOXP3+ T-cell pool and tumor trafficking in patients with ovarian carcinoma*. Can Res. 2007;67(15):7487–7494.

20. Carson WE, Fehniger TA, Haldar S, Eckhert K, Lindemann MJ, Lai CF, Croce CM, Baumann H, Caligiuri MA. *A potential role for interleukin-15 in the regulation of human natural killer cell survival*. J Clin Investig. 1997;99(5):937–943.

21. Cooper MA, Bush JE, Fehniger TA, VanDeusen JB, Waite RE, Liu Y, Aguila HL, Caligiuri MA. *In vivo evidence for a dependence on interleukin 15 for survival of natural killer cells*. Blood. 2002;100(10):3633–3638.

22. Fontenot JD, Rasmussen JP, Gavin MA, Rudensky AY. *A function for interleukin 2 in Foxp3-expressing regulatory T cells.* Nat Immunol. 2005;6(11):1142–1151.

23. Waldmann TA. *The biology of interleukin-2 and interleukin-15: implications for cancer therapy and vaccine design*. Nat Rev Immunol. 2006;6(8):595–601.

24. Han KP, Zhu X, Liu B, Jeng E, Kong L, Yovandich JL, Vyas VV, Marcus WD, Chavaillaz PA, Romero CA, Rhode PR, Wong HC. *IL-15:IL-15 receptor alpha superagonist complex: high-level co-expression in recombinant mammalian cells, purification and characterization.* Cytokine. 2011;56(3):804–810.

25. Dubois S, Mariner J, Waldmann TA, Tagaya Y. *IL-15Ralpha recycles and presents IL-15 In trans to neighboring cells*. Immunity. 2002;17(5):537–547.

26. Zhu X, Marcus WD, Xu W, Lee HI, Han K, Egan JO, Yovandich JL, Rhode PR, Wong HC. *Novel human interleukin-15 agonists*. J immunol. 2009;183(6):3598–3607.

27. Romee R, Cooley S, Berrien-Elliott MM, Westervelt P, Verneris MR, Wagner JE, Weisdorf DJ, Blazar BR, Ustun C, DeFor TE, Vivek S, Peck L, DiPersio JF, Cashen AF, Kyllo R, Musiek A, Schaffer A, Anadkat MJ, Rosman I, Miller D, Egan JO, Jeng EK, Rock A, Wong HC, Fehniger TA, Miller JS. *First-in-human Phase 1 clinical study of the IL-15 superagonist complex ALT-803 to treat relapse after transplantation*. Blood. 2018

28. Margolin K, Morishima C, Velcheti V, Miller JS, Lee SM, Silk AW, Holtan SG, Lacroix AM, Fling SP, Kaiser JC, Egan JO, Jones M, Rhode PR, Rock AD, Cheever MA, Wong HC, Ernstoff MS. *Phase I Trial of ALT-803, A Novel Recombinant IL15 Complex, in Patients with Advanced Solid Tumors.* Clin Cancer Res Off J Am Assoc Res. 2018;24(22):5552–5561.

29. Rosario M, Liu B, Kong L, Collins LI, Schneider SE, Chen X, Han K, Jeng EK, Rhode PR, Leong JW, Schappe T, Jewell BA, Keppel CR, Shah K, Hess B, Romee R, Piwnica-Worms DR, Cashen AF, Bartlett NL, Wong HC, Fehniger TA. *The IL-15-based ALT-803 complex enhances fcgammariiia-triggered NK cell responses and in vivo clearance of B Cell lymphomas.* Clin Cancer Res Off J Am Assoc Res. 2016;22(3):596–608.

30. Felices M, Chu S, Kodal B, Bendzick L, Ryan C, Lenvik AJ, Boylan KL, Wong HC, Skubitz AP, Miller JS, Geller MA. *IL-15 super-agonist (ALT-803) enhances natural killer (NK) cell function against ovarian cancer.* Gynecol Oncol. 2017

31. Hoogstad-van Evert JS, Maas RJ, van der Meer J, Cany J, van der Steen S, Jansen JH, Miller JS, Bekkers R, Hobo W, Massuger L, Dolstra H. *Peritoneal NK cells are responsive to IL-15 and percentages are correlated with outcome in advanced ovarian cancer patients.* Oncotarget. 2018;9 (78):34810–34820.

32. Giannattasio A, Weil S, Kloess S, Ansari N, Stelzer EH, Cerwenka A, Steinle A, Koehl U, Koch J. *Cytotoxicity and infiltration of human NK cells in in vivo-like tumor spheroids.* BMC cancer. 2015;15:351.

33. Guldevall K, Brandt L, Forslund E, Olofsson K, Frisk TW, Olofsson PE, Gustafsson K, Manneberg O, Vanherberghen B, Brismar H, Karre K, Uhlin M, Onfelt B. *Microchip screening platform for single cell assessment of NK cell cytotoxicity*. Front Immunol. 2016;7:119.

34. Weigelin B, Friedl P.*A three-dimensional organotypic assay to measure target cell killing by cytotoxic T lymphocytes*. Biochem Pharmacol. 2010;80(12):2087–2091.

35. Cany J, Roeven MWH, Hoogstad-van Evert JS, Hobo W, Maas F, Franco Fernandez R, Blijlevens NMA, van der Velden WJ, Huls G, Jansen JH, Schaap NPM, Dolstra H. *Decitabine enhances targeting of AML cells by CD34(+) progenitor-derived NK cells in NOD/SCID/IL2Rg(null) mice.* Blood. 2018;131(2):202–214.

36. Wang R, Jaw JJ, Stutzman NC, Zou Z, Sun PD. *Natural killer cell-produced IFN-gamma and TNF-alpha induce target cell cytolysis through up-regulation of ICAM-1*. J Leukoc Biol. 2012;91(2):299–309.

37. Basher F, Jeng EK, Wong H, Wu J. *Cooperative therapeutic anti-tumor effect of IL-15 agonist ALT-803 and co-targeting soluble NKG2D ligand sMIC.* Oncotarget. 2016;7(1):814–830.

38. Fantini M, David JM, Wong HC, Annunziata CM, Arlen PM, Tsang KY. *An IL-15 superagonist, ALT-803, enhances antibody-dependent cell-mediated cytotoxicity elicited by the monoclonal antibody NEO-201 against human carcinoma cells.* Cancer Biothera Radiopharma. 2019

39. Wagner JA, Rosario M, Romee R, Berrien-Elliott MM, Schneider SE, Leong JW, Sullivan RP, Jewell BA, Becker-Hapak M, Schappe T, Abdel-Latif S, Ireland AR, Jaishankar D, King JA, Vij R, Clement D, Goodridge J, Malmberg KJ, Wong HC, Fehniger TA. *CD56bright NK cells exhibit potent antitumor responses following IL-15 priming*. J Clin Investig. 2017

40. Knudson KM, Hicks KC, Alter S, Schlom J, Gameiro SR. *Mechanisms involved in IL-15 superagonist enhancement of anti-PD-L1 therapy*. J Immunother Cancer. 2019;7(1):82.

41. Pinette A, McMichael E, Courtney NB, Duggan M, Benner BN, Choueiry F, Yu L, Abood D, Mace TA, Carson WE., 3rd *An IL-15-based superagonist ALT-803 enhances the NK cell response to cetuximab-treated squamous cell carcinoma of the head and neck*. Cancer Immunol Immunother. 2019;68(8):1379–1389.

42. Rhode PR, Egan JO, Xu W, Hong H, Webb GM, Chen X, Liu B, Zhu X, Wen J, You L, Kong L, Edwards AC, Han K, Shi S, Alter S, Sacha JB, Jeng EK, Cai W, Wong HC. *Comparison of the superagonist complex, ALT-803, to IL15 as cancer immunotherapeutics in animal models.* Cancer Immunol Res. 2016;4(1):49–60.

43. Bhat R, Watzl C. *Serial killing of tumor cells by human natural killer cells–enhancement by therapeutic antibodies*. PLoS ONE. 2007;2(3):e326.

44. Vanherberghen B, Olofsson PE, Forslund E, Sternberg-Simon M, Khorshidi MA, Pacouret S, Guldevall K, Enqvist M, Malmberg KJ, Mehr R, Onfelt B. *Classification of human natural killer cells based on migration behavior and cytotoxic response*. Blood. 2013;121(8):1326–1334.

45. Choi PJ, Mitchison TJ. I*maging burst kinetics and spatial coordination during serial killing by single natural killer cells*. Proc Natl Acad Sci USA. 2013;110(16):6488–6493.

Supplemental Data

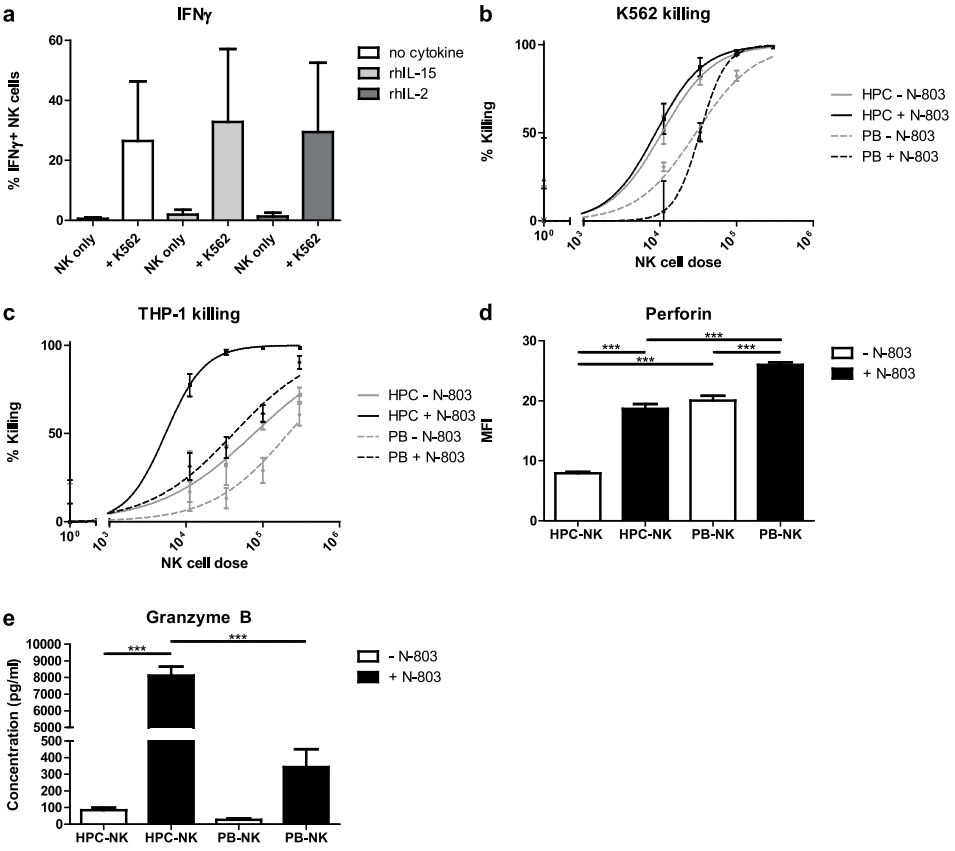

Supplementary Figure 1: ***rhIL-15 and rhIL-2 increase IFNγ production in the presence of K562 and HPC-NK cells are better killers compared to PB-NK cells which correlates with a higher granzyme B release.***

A. Percentage of IFNγ+ HPC-NK cells 4h after incubation with leukemia cell line K562 and no cytokine (white), 1 nM rhIL-15 (light grey) or 1000 U/ml rhIL-2 (dark grey) (n=2). B-C. Percentage of (B) K562 or (C) THP-1 killing after overnight co-culture with HPC-NK cells continuous line) or PB-NK cells (dashed line) and 0 (grey) or 1 nM N-803 (black) (n=1, triplos). D. MFI of perforin expression in HPC-NK cells or PB-NK cells after overnight priming with or without 1 nM N-803. E. Granzyme B concentration (pg/ml) after overnight priming of HPC-NK cells and PB-NK cells with or without 1 nM N-803. Graph shows mean ± SEM for A/SD for B-E. One-way ANOVA with Bonferroni correction was used for A, D-E (repeated measures for A) to test for statistical significance.

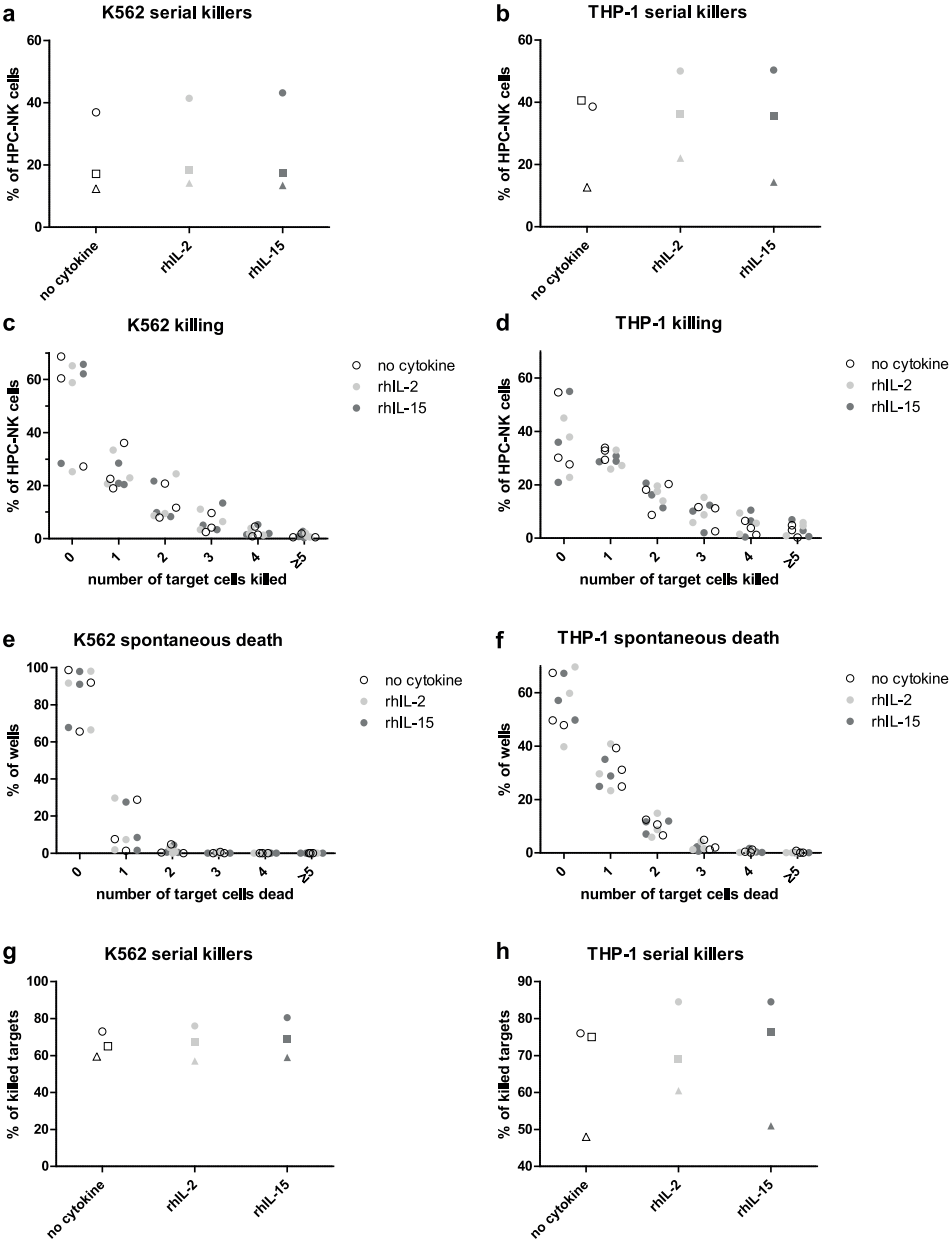
a
K562 serial killers
% of HPC-NK cells
no cytokine
rhIL-2
rhIL-15
b
THP-1 serial killers
% of HPC-NK cells
no cytokine
rhIL-2
rhIL-15
c
K562 killing
% of HPC-NK cells
number of target cells killed
no cytokine
rhIL-2
rhIL-15
d
THP-1 killing
% of HPC-NK cells
number of target cells killed
no cytokine
rhIL-2
rhIL-15
e
K562 spontaneous death
% of wells
number of target cells dead
no cytokine
rhIL-2
rhIL-15
f
THP-1 spontaneous death
% of wells
number of target cells dead
no cytokine
rhIL-2
rhIL-15
g
K562 serial killers
% of killed targets
no cytokine
rhIL-2
rhIL-15
h
THP-1 serial killers
% of killed targets
no cytokine
rhIL-2
rhIL-15

Supplementary Figure 2: ***rhIL-2 and rhIL-15 show similar serial killing properties of HPC-NK cells against leukemia.***

A-B. Percentage of serial killers after 12h co-culture of HPC-NK cells and (A) K562 (n=3) or (B) THP-1 (n=3) with no cytokine, 1000 U/ml rhIL-2, or 1 nM rhIL-15. At least 125 NK cells were analyzed. C-D. Percentage of wells showing the number of (C) K562 (n=3) or (D) THP-1 (n=3) cells killed in the presence of individual HPC-NK cells after 12h co-culture with no cytokine (open), 1000 U/ml rhIL-2 (light grey), or 1 nM rhIL-15 (dark grey). At least 125 NK cells were analyzed. E-F. Percentage of wells showing spontaneous (E) K562 (n=3) or (F) THP-1 (n=3) cell death after 12h culture without HPC-NK cells and with no cytokine (open), 1000 U/ml rhIL-2(light grey) or 1 nM rhIL-15 (dark grey). At least 173 target cells were analyzed. G-H. Percentage of killed (G) K562 (n=3) or (H) THP-1 (n=3) cells killed by serial killers after 12h co-culture with HPC-NK cells and with no cytokine, 1000 U/ml rhIL-2, or 1 nM rhIL-15. At least 126 killed target cells were analyzed. Graphs show mean ± SEM. Repeated measures one-way ANOVA with Bonferroni correction was used for A-B, G-H and repeated measures two-way ANOVA with Bonferroni correction for C-F to test for statistical significance.

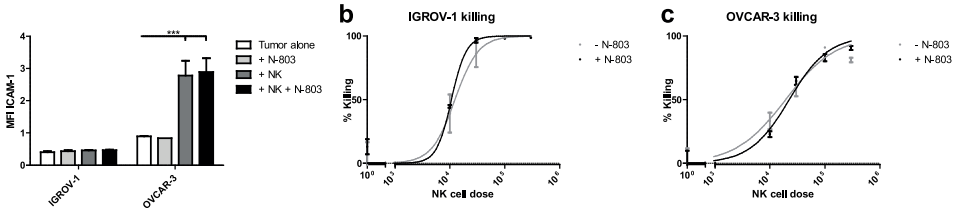

Supplementary Figure 3: ***N-803 does not increase HPC-NK cell-mediated killing of OC cells in monolayers overnight.***

(A) MFI of ICAM-1 expression after overnight culture of OC cell lines IGROV-1 and OVCAR-3, addition of N-803 and/or HPC-NK cells (n=3). B-C. Percentage of (B) IGROV-1 or (C) OVCAR-3 killing after overnight co-culture with HPC-NK cells and no cytokine (grey) or 1 nM N-803 (black) (n=1 containing quadriplos). Graphs show mean ± SD for B-C/SEM for A. One-way ANOVA with Bonferroni correction was used for all subfigures (repeated measures for A) to test for statistical significance.

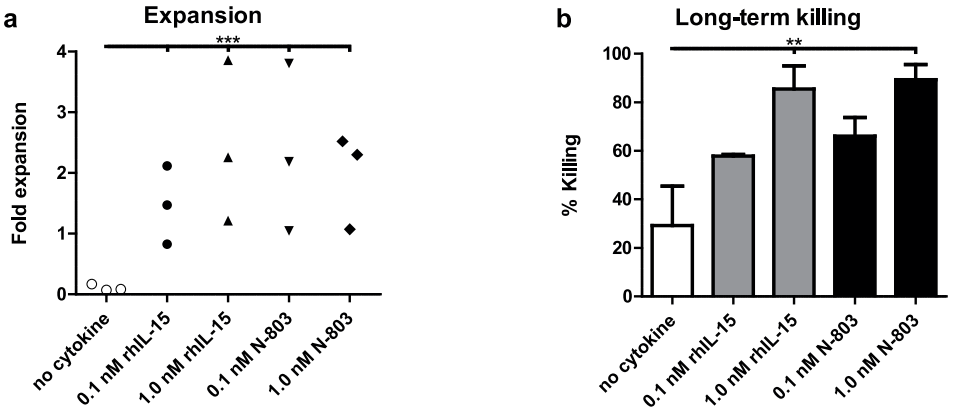

Supplementary Figure 4: ***rhIL-15 and N-803 expand HPC-NK cells and dose-dependently increase HPC-NK cell-mediated long-term OC spheroid killing.***

A. Fold expansion of HPC-NK cells in the presence of a SKOV-3 spheroid after 1 week co-incubation with 0.1 or 1 nM rhIL-15 or N-803 or no cytokine (n=3). B. Percentage of SKOV-3 spheroid killing after 1 week co-culture with HPC-NK cells and no cytokine, or 0.1 or 1 nM rhIL-15 or N-803 (n=3). Graph B shows mean ± SEM. Repeated measures one-way ANOVA with Bonferroni correction was used (after log transformation for A) to test for statistical significance.

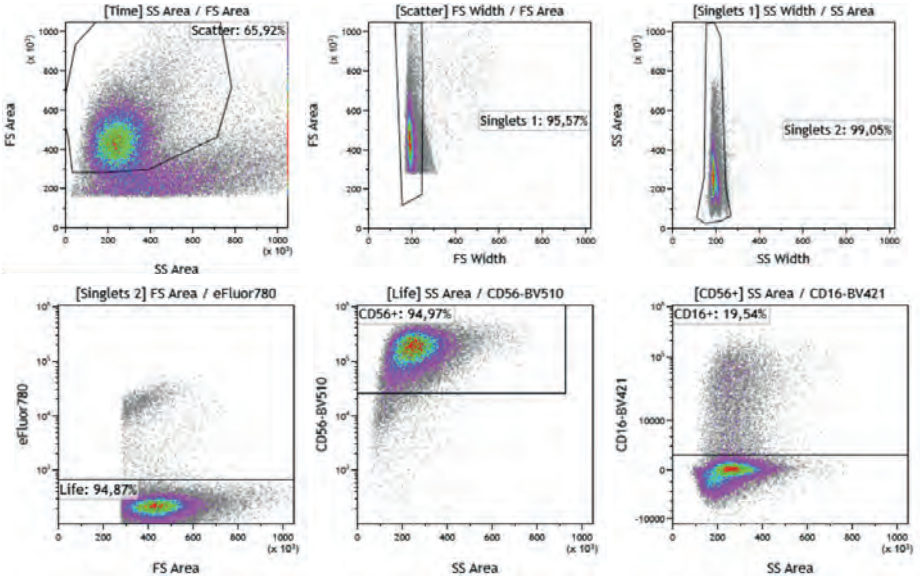

Supplementary Figure 5: ***CD16 expression in HPC-NK cells before injection into NSG mice.***

The gating strategy was based on time, lymphocyte size, doublet discrimination and dead cell exclusion using viability dye eFluor780. Next, CD56+ cells were gated and CD16 expression was determined.

Chapter 4

Comprehensive phenotyping of peritoneal NK cells in high-grade epithelial ovarian cancer reveals distinct subpopulations with an exhausted phenotype involving PD1, TIGIT and CD96

Ralph J.A. Maas, Diede van Ens, Jolanda Brummelman*, Janneke S. Hoogstad-van Evert*, Anniek B. van der Waart, Paul K.J.D. de Jonge, Rob Woestenenk, Petra L.M. Zusterzeel, Nelleke Ottevanger, Joop H. Jansen, Harry Dolstra[#] , Willemijn Hobo[#]

*[#]these authors contributed equally

Manuscript in submission

Abstract

Advanced epithelial ovarian cancer (EOC) patients have poor survival and EOC is frequently associated with ascites. This peritoneal ascites constitutes an attractive tumor microenvironment to study the characteristics of natural killer (NK) cells in EOC patients. Although several separate pathways have been studied in the past, we aimed to perform an analysis on the co-expression of a large number of activating and inhibitory receptors on NK cells versus the presence of soluble factors in ascites from the same EOC patients integrated in a single study. We used flow cytometry to characterize NK cells based on activation, differentiation and immune checkpoint markers within ascites of high-grade serous EOC patients compared to peritoneal NK cells from patients with benign disease. We employed FlowSOM single cell clustering analysis to identify peritoneal NK cell subpopulations and found two interesting groups of clusters. One group of clusters, with a more classical effector NK cell phenotype, was reduced in EOC ascites. In contrast, the second group of clusters was enriched in ascites of EOC patients and showed lower CD16, DNAM-1 and SIGLEC-7 expression. Interestingly, these latter clusters were also associated with increased expression of PD-1, TIGIT and/or CD96 suggesting an exhaustive phenotype. They were also significantly correlated to high levels of immune checkpoint mediators including soluble CD155 (PVR), CD112 (NECTIN-2), PD-L2, TIM-3, ULBP1 and MICA/B in ascites. The identification of NK cell clusters with an exhausted phenotype could aid in unraveling important immune checkpoint pathways interfering with NK cell anti-tumor reactivity in EOC patients and provide potential targets to augment NK cell immune checkpoint blockade therapies.

Introduction

Generally, epithelial ovarian carcinoma (EOC) does not show prominent symptoms at an early stage, which often results in late detection of advanced disease with a poor prognosis and a 5-year survival rate of only 28% [1]. Advanced EOC is frequently associated with ascites, an abnormal accumulation of fluid in the peritoneal cavity, which can negatively affect immune cells while promoting tumor cell growth and invasion [2, 3]. Importantly, EOC tumor cells often downregulate MHC class I, making them prone to NK cell attack, as we and others have demonstrated in previous studies [4, 5]. Furthermore, a higher NK cell percentage within the ascitic lymphocyte fraction is correlated with better survival of EOC patients [6]. Despite the susceptibility of EOC cells to killing by NK cells, the functionality of NK cells within the tumor microenvironment of the peritoneal cavity can be impaired. This dysfunction is established by amongst others suppressive immune cells, as well as inhibitory soluble factors produced by the local immune cells, stromal cells and/or EOC cells themselves [7-9]. A better understanding of the mechanisms and regulatory receptors underlying NK cell dysfunction in the EOC immune environment can pave the way for adjuvant immunotherapies to enhance potency of NK cell-based immunotherapeutic strategies to improve outcome for EOC patients with disease recurrence.

NK cells are generally characterized by CD56 and CD16 expression with the two major subsets described in peripheral blood. NK cells with a CD56^{bright}CD16^{-} phenotype are classically viewed as less mature and productive cytokine producers, while CD56^{dim}CD16^{+} NK cells are considered to be the more cytotoxic subset. Furthermore, NK cell activity is regulated by the sum of signals obtained via activating and inhibitory receptors [10]. Previously, we showed that a disturbed balance in DNAX Accessory Molecule-1 (DNAM-1) and T cell immunoreceptor with Ig and ITIM domains (TIGIT) expression on peritoneal NK cells in EOC patients results in skewing to a more inhibitory phenotype. Importantly, TIGIT blockade could partially rescue the decreased functionality [11]. Besides this, other NK cell receptors including natural killer group 2 member D (NKG2D), natural cytotoxicity receptors (NCRs), killer Ig-like receptors (KIRs) and Sialic acid-binding immunoglobulin-type lectins (SIGLECs) and other immune checkpoint receptors such as PD-1 have been implicated in regulating NK cell reactivity against EOC and other types of cancer [12-16]. Furthermore, soluble factors including suppressive cytokines present in the ascites may have an inactivating effect, causing phenotypical and functional changes in subsets of NK cells and eventually resulting in NK cell dysfunction [17]. However, to date, there are no comprehensive studies integrating NK cell regulatory receptor

phenotype data and their respective soluble ligand levels for studying peritoneal NK cells in high-grade EOC patients in a single analysis.

In this study, we applied 18-parameter flow cytometry panels with defined activation, differentiation and immune checkpoint markers to study peritoneal NK cell subsets in EOC patients compared to benign controls. FlowSOM analysis revealed interesting groups of NK cell clusters with the NK cell checkpoint panel. Interestingly, one of these cluster groups was enriched in EOC patient ascites, and was characterized by low CD16, DNAM-1 and SIGLEC-7 expression while PD-1, TIGIT and/or CD96 expression was increased indicative of an exhausted phenotype. Additionally, these clusters were associated with high ascitic levels of numerous soluble inhibitory immune checkpoints. Altogether, identification of NK cell clusters with an exhausted phenotype could aid in determining important immune checkpoint pathways interfering with NK cell anti-tumor reactivity in EOC patients. Additionally, it provides potential targets to augment NK cell adoptive transfer with immune checkpoint blockade.

Methods

Patient samples

Ascites fluid samples or peritoneal washings of patients with stage IIIc or IV high-grade serous EOC (Supplemental Table 1) were collected after written informed consent at primary debulking surgery. Study approval was given by the Regional Committee for Medical Research Ethics (CMO 2018-4845) and performed according to the Code for Proper Secondary Use of Human Tissue (Dutch Federation of Biomedical Scientific Societies, www.federa.org (http://www.federa.org)). Samples of abdominal washing fluid or free fluid from patients without any malignancy, planned for surgery of a benign cyst were used as controls. Controls were excluded in case of signs of active infection and had a serous cystadenoma, endometrioma, mucinous cystadenoma or fibroma (Supplemental Table 2). Cell-free ascitic fluid and mononuclear cells were subsequently isolated and cryopreserved, as previously described (Maas et al 2023, *manuscript submitted*).

Evaluation of the soluble fraction of ascites

Ascites or peritoneal washouts of benign and EOC patients were assessed previously (Maas et al 2023 *manuscript submitted*) for soluble TIM-3, GITRL, MICA, Trail-R2, Trail-R1, MICB, IP-10, CD137/41BB, IL-10, NECTIN-2, CD96 (Tactile),

IFN-gamma, TNF-alpha, IDO, Arginase, Perforin, PVR, IL-12p40, IL-15, TRAIL, PD-L2, Granzyme-B, ULBP-1, ULBP-3 and ULBP-4 by using Luminex (ProcartaPlex Thermo Fisher), and IL-1β, IL-1RA, IL-6, IL-8, TGF-β (R&D systems) and IL-2 (431801, Biolegend) were determined using corresponding commercial ELISA kits.

Flow cytometry (FCM)

For phenotypical analyses, 1 million cells were resupsended in 50 µL buffer with 25 µL human serum albumin (HSA) buffer (PBS/0.5% HSA, Sanquin Bloodbank) containing 0.1 mg/mL nanogam (human immunoglobulins, Sanquin Bloodbank) and 25 µL brilliant stain buffer (563794, BD Biosciences). Antibody mixtures were prepared in a total volume of 55 µL HSA buffer minus the volume of the antibodies (see Tables 1 and 2 for the full panels). The antibody mixture was cenrifuged at 14.000g for 2 min. Then, 50 µL was taken, added to the cell suspension and incubated at 4°C for 30 min. Cells were washed twice with 500 µL 0.5% HSA buffer and resuspended in 100 µL 0.5% HSA buffer for acquisition on a 6-laser Cytoflex LX flow cytometer (Beckman Coulter). Manual analysis was performed with Kaluza version 2.1 (Beckman Coulter) and Flowjo version 10 (BD).

High-dimensional flow cytometry data analysis

The antibodies within the panels were selected on brightness, potential spreading issues, consistency across panels to maximize resolution of the markers included the panels. Every lot-number of each antibody was titrated on PBMCs, to identify the highest signal-to-noise ratio and stain index, and to correct for lot-to-lot variation. The gain settings used on the Cytoflex LX were optimized to allow for optimal signal resolution by performing a gaintration using 8-peak beads (A79016, Spherotech).

Flow Cytometry Standard (FCS) 3.0 files were imported into Kaluza version 2.1, and analyzed by standard gating to remove aggregates and dead cells. Subsequently, the CD45^{+}CD3^{-}CD56^{+} NK cell population was identified in each panel. Next, these NK cell populations were exported to CSV files, imported in R (version 4.0.1) and analyzed according to Brummelman *et al*. [18]. In summary, data was arcsinh transformed using the transFlowVS function of the flowVS package (version 1.19.0) and scaled and centered using the scale function. Multi-dimensional scaling (MDS) plots, based on the median expression values of each marker, were generated using the plotMDS function from the limma package (version 3.44.3). Next, samples were downsampled (4,000 cells), concatenated and cell subpopulations were identified using the FlowSOM algorithm (version 1.20.0) [19]. The optimal number of metaclusters was k=30 (clusters with a frequency <0.5% were excluded and cluster 30

for the checkpoint panel was excluded as these were a small cluster of monocytes) for both panels. Heatmaps were created using the pheatmap package (version 1.0.12), whereupon hierachical clustering was performed using the Euclidean distance and Ward-linkage. Additional figures were generated using the ggplot2 package (version 3.3.2). Subsequently, cluster data were embedded in the FCS files, which were further analyzed in FlowJo software version 10 and Kaluza version 2.1 to determine the frequency of positive cells for each marker and the corresponding Mean Fluorescent intensity (MFI). The balloon plot, showing the manually determined frequencies and MFI of each marker per cluster was created in R using the ggpubr package (version 0.4.0).

StatisticsData analyses was conducted with Prism software (GraphPad, version 5.03 for Windows). For data with a normal distrubtion, the Student t-test (paired or unpaired) or One-way ANOVA (with or without repeated measure) were used, as indicated in the figure legends. Non-normally distributed data was analyzed with a Wilcoxon signed-rank, Mann-Whitney U, Kruskal-Wallis or Friedman test, as indicated in the figure legends. A p-value of <0.05 was considered statistically significant. To identify correlations between variables (*e.g.* frequency of immune cell subpopulations and cytokines), Spearman correlation analysis was performed and visualized in R using the corrplot package (version 0.84). A p-value of <0.05 was considered statistically significant.

Results

NK cells in ascites from EOC patients have lower activating receptor expression and higher inhibitory receptor expression compared to NK cells derived from patients with a benign disease

Here, we used two 18-color panels to characterize peritoneal NK cells of high-grade serous EOC patients in comparison to patients with a benign disease (benign controls). One panel consisted of classical NK cell subset markers including CD16, CD56, KIRs, NKG2A/NKG2C, NCRs and CD57 (named subset panel). The other panel focused more on inhibitory and stimulatory checkpoint receptors (named checkpoint panel) including NKG2A, DNAM-1, TIGIT, CD96, PD-1, TIM-3, SIGLEC-7, OX-40 and CD160 that were selected based on previously published and unpublished data [6, 11] (and Maas et al. 2024, *manuscript submitted*). Cells were gated on typical lymphocyte characteristics in the forward/sideward scatter and doublets, dead cells/debris and antibody-aggregates were excluded. From the resulting pre-enriched population of lymphocytes, NK cells were gated as $CD45^{+}CD56^{+}CD3^{-}$

cells (Supplemental Figure 1A). With a manual gating strategy we defined three major populations: CD56^{dim}CD16^{+}, CD56^{dim}CD16$^{-/dim}$ and CD56^{bright}CD16^{-} with a mean frequency ± SD of 23.9%±19.8%, 33.0%±18.0% and 28.5%±15.8%, respectively (Supplemental Figure 1B), without any significant difference in the proportion of these three NK cell subsets between EOC and benign patients. We also observed a CD56^{bright}CD16^{+} subset that was only present at low frequencies (mean=2.4%±4.0%) in few EOC patient samples. Therefore, we focussed further data analyses on the three major NK cell subsets identified with the established 18-color panels.

Next, we compared the phenotype of NK cells in ascites derived from 26 ascites samples from high-grade serous EOC patients and 11 benign peritoneal washings or ascites using manual gating (Figure 1, Supplemental figure 1C). The following stimulatory receptors, CD160 (all subsets), OX-40 (CD56^{dim}), DNAM-1 (CD56^{dim}), NKG2D (CD56^{bright}), NKp46 (CD56^{bright}) and NKp30 (CD56^{dim}) were significantly decreased in one or more of the defined NK cell subsets from EOC patient ascites (Figure 1). In contrast, only the inhibitory receptors CD96 (CD56^{dim}CD16^{+}) and TIM-3 (CD56^{bright}) were significantly higher expressed on peritoneal NK cell subsets from EOC patients compared to benign controls (Figure 1). On the other hand, SIGLEC-7 was significantly lower expressed by the CD56^{dim} NK cell subsets in EOC patients, and TIGIT was lower in the CD56^{bright} subset. Interestingly, CD69 expression was significantly higher on EOC-derived NK cells for both CD56^{dim} NK cell subsets as opposed to those of benign controls, indicating that in general the NK cells from EOC patients have a more activated phenotype. These data showed that most stimulatory NK cell receptors are significantly lower expressed, while inhibitory receptor expression such as CD96 and TIM-3 is significantly higher on EOC-derived NK cells as opposed to NK cells from benign abdominal fluids.

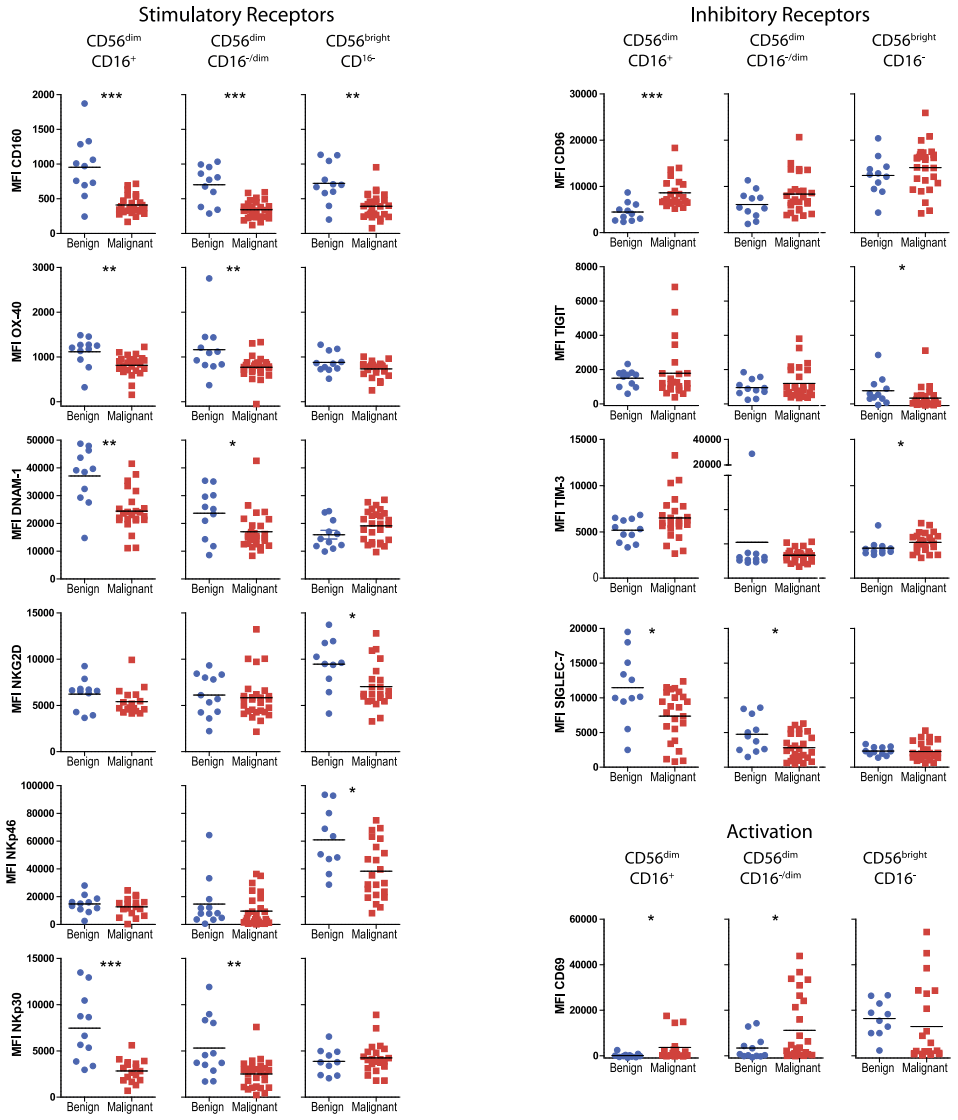

Figure 1: ***NK cell phenotype of different NK cells subsets defined by manual gating***

*Stimulatory receptors, inhibitory and activation markers are shown for $CD56^{dim}CD16^{+}$, $CD56^{dim}CD16^{-}$ and $CD56^{bright}CD16^{-}$ NK cells. A Mann-Whitney test was used for statistical analysis, * $p < 0.05$, ** $p < 0.01$ and *** $p < 0.001$*

FlowSOM clustering on the NK checkpoint panel revealed two distinct groups of NK cell clusters, one more abundant and one less abundant in EOC patients compared to benign controls

To identify NK cell clusters beyond the classical CD56 and CD16 defined subsets that are distinctive in EOC patients ascites, we further explored our dataset by using unbiased high-dimensional computational analysis to obtain more insight into co-expression of different receptors. Furthermore, we associated them with the cytokine milieu in ascites from EOC patients that was previously published (Maas et al 2023, *manuscript submitted*). First, we generated MDS plots to visualize the distribution of NK cell subsets of benign samples and EOC ascites and found that they did not cluster distinctly for either panel (Supplemental Figure 2A and B). In addition, hierarchical clustering on the heatmap did not reveal major differences between EOC patients and our benign control group (Supplemental Figure 2C and D). To better discriminate the different NK cell subpopulations present in our samples, we next performed FlowSOM clustering and visualized each cluster in a balloon plot (k=30, where clusters with a frequency <0.5% were excluded, Figure 2A and Supplemental figure 3A-B). The frequencies for all 30 clusters are shown in Supplemental figure 4A and B. For the subset panel some clusters were significantly enriched or decreased in EOC versus benign samples, however these clusters did not associate with each other (Supplemental figure 3A-B). As previously reported, CD16 and DNAM-1 were highly expressed in clusters found to be more frequent in benign peritoneal fluid (SP C3, C5 and C6), while CD56 expression in these clusters is low. Clusters enriched in ascites of EOC patients (SP C14, C15, C2, C25, C26 and C30) generally showed low CD16 and CD56 expression.

Next, we performed FlowSOM clustering on the checkpoint panel and visualized each cluster in a balloon plot (Figure 2A). Interestingly, we clearly observed two groups of NK cell clusters that were either increased or decreased in EOC patients compared to benign controls (Figure 2B). One group consisted of seven clusters (CP C6, C10, C11, C16, C19, C28 and C29) of which three clusters (CP C10, C19 and C29) were significantly enriched in EOC patient samples (Figure 2A, Supplemental Figure 4B). These NK cell clusters had a phenotype with lower expression of stimulatory receptors and high levels of inhibitory immune checkpoint receptors (Figure 2A-B). The second group consists of ten clusters (CP C4, C5, C7, C8, C9, C13, C14, C18, C20 and C24) of which four (CP C7, C9, C13 and C18) were significantly lower present in EOC patients (Figure 2C, Supplemental figure 4). Notably, these two different groups of clusters were negatively correlated with each other (Figure 2C). Phenotypically, the group of clusters more abundant in EOC patients was characterized by low expression levels of stimulatory receptors such as CD16,

DNAM-1 and CD160 while displaying higher levels of inhibitory receptors including PD-1, TIGIT and/or CD96 (Figure 2A-B). On the other hand, $CD56^{dim}$ NK cell clusters (CP C7, C9, C13 and C18) with high CD16, SIGLEC-7 and DNAM-1 expression and low levels of PD-1, TIGIT and CD96 were significantly decreased in EOC patients compared to benign controls (Figure 2A-B). Altogether, these data showed the presence of peritoneal NK cell subsets in EOC patients exhibiting low expression of stimulatory receptors and increased expression of PD-1, TIGIT and/or CD96, suggestive of a more exhausted phenotype.

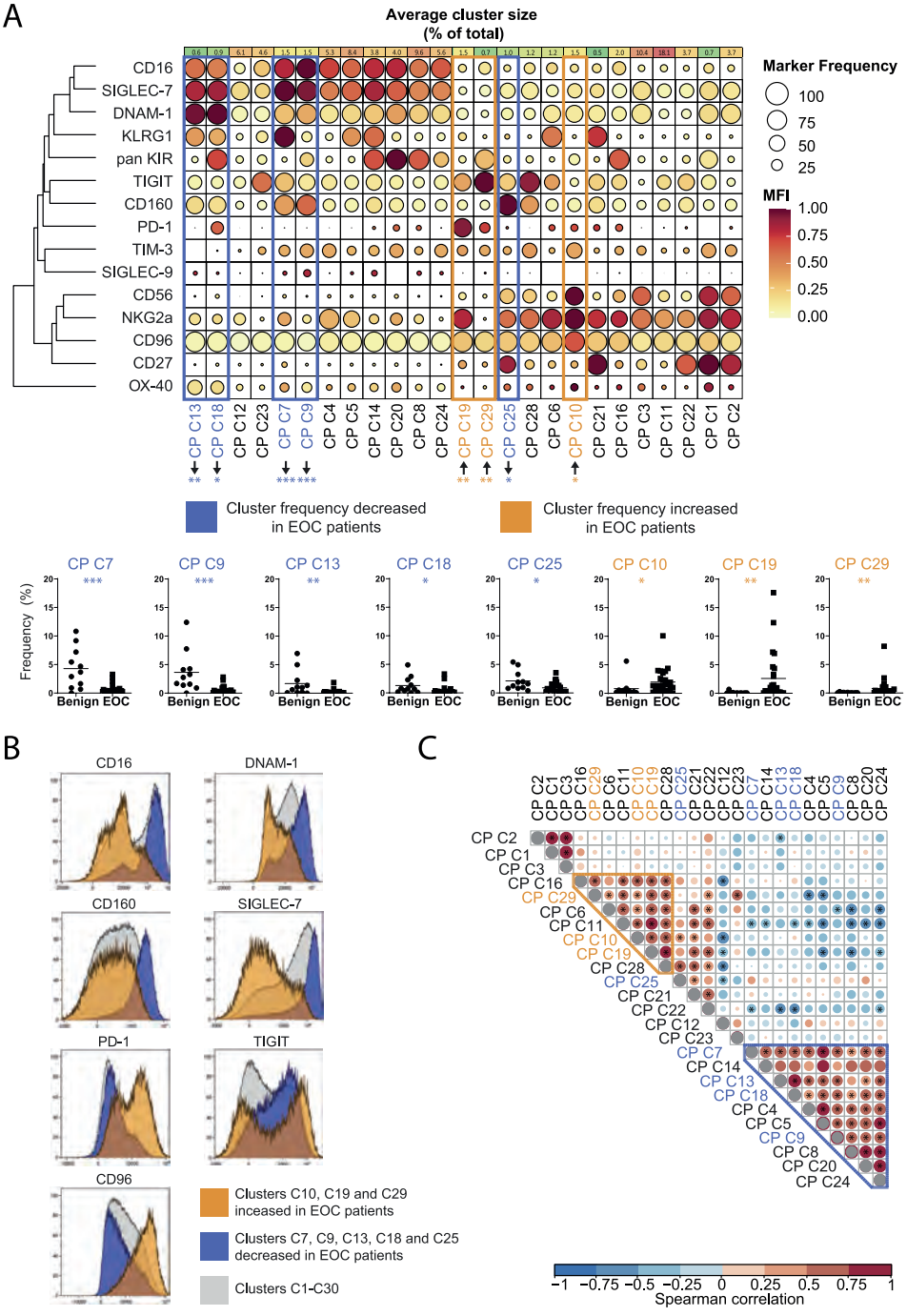
A
Average cluster size
(% of total)
CD16
SIGLEC-7
DNAM-1
KLRG1
pan KIR
TIGIT
CD160
PD-1
TIM-3
SIGLEC-9
CD56
NKG2a
CD96
CD27
OX-40
Marker Frequency
100
75
50
25
MFI
1.00
0.75
0.50
0.25
0.00
CP C13 CP C18 CP C12 CP C23 CP C7 CP C9 CP C4 CP C5 CP C14 CP C20 CP C8 CP C24 CP C19 CP C29 CP C25 CP C28 CP C6 CP C10 CP C21 CP C16 CP C3 CP C11 CP C22 CP C1 CP C2
Cluster frequency decreased in EOC patients
Cluster frequency increased in EOC patients
CP C7
CP C9
CP C13
CP C18
CP C25
CP C10
CP C19
CP C29
Frequency (%)
Benign EOC
B
CD16
DNAM-1
CD160
SIGLEC-7
PD-1
TIGIT
CD96
Clusters C10, C19 and C29 inceased in EOC patients
Clusters C7, C9, C13, C18 and C25 decreased in EOC patients
Clusters C1-C30
C
CP C2 CP C1 CP C3 CP C16 CP C29 CP C6 CP C11 CP C10 CP C19 CP C28 CP C25 CP C21 CP C22 CP C12 CP C23 CP C7 CP C14 CP C13 CP C18 CP C4 CP C5 CP C9 CP C8 CP C20 CP C24
−1 −0.75 −0.5 −0.25 0 0.25 0.5 0.75 1
Spearman correlation

Figure 2: ***FlowSOM clustering shows distinct clusters of NK cells in peritoneal fluids of benign and EOC patients***

(A)*Scaled MFI values of FlowSOM clusters checkpoint panel in a balloon plot. Each row represents a marker, while columns represent a cluster. Balloon size represents frequency while balloon color represents MFI (red is high MFI, yellow is low MFI). On top of the balloon plot the cluster size is presented as percent of total where red indicate large clusters and green small clusters. Statistical difference between cluster frequency of benign (significance indicated in blue) and EOC (significance indicated in orange) patients was calculated using a Mann Whitney test.* ***(B)*** *Histogram overlay of clusters C10, C19 and CD29 in orange with C7, C9, C13, C18 and CD25 in blue and with all clusters taken together in grey. On the y-axis the percentage of the maximum signal and on the x-axis the MFI for each marker.* ***(C)*** *Spearman correlogram of FlowSOM clusters of checkpoint panel fraction of EOC ascites. A heat map is used to indicate the Spearman's rank correlation coefficient of associations between biomarkers. Red indicates a positive correlation, and blue indicates a negative correlation. * $p < 0.05$,* ** $p < 0.01$, *** $p < 0.001$*, CP = checkpoint panel. Orange clusters have a significantly increased frequency in EOC patients while blue clusters have a significantly decreased frequency in EOC patients compared to controls.*

FlowSOM clusters from the NK checkpoint panel enriched in EOC patient samples strongly correlate to soluble inhibitory NK cell factors in ascites fluids

Next, we investigated whether soluble factors in ascites that may influence NK cell function correlated distinctively to the phenotype of peritoneal NK cells from EOC patients. For this, we used previously reported Luminex and ELISA data of ascites from the same patients and correlated this to the FlowSOM clustering data (Maas et al 2023, *manuscript submitted*). Overall, the NK subset panel did not show evident correlation patterns with the assessed soluble factors and the established FlowSOM clusters (Supplemental Figure 5). In contrast, both groups of clusters defined with the NK checkpoint panel were significantly associated with numerous soluble factors assessed within ascites (Figure 3). Interestingly, three of the clusters (CP C10, C19 and C29) enriched in EOC patients significantly correlated with high levels of soluble CD155 (PVR), CD112 (NECTIN2), ULBP1, MICA/B, PD-L2, IDO, TIM-3, TRAILR2, IL12p40, perforin, CD96 and IP10 in the ascitic fluid. These clusters also have the highest levels of PD-1, TIGIT and/or CD96, and lack CD16 and DNAM-1, suggestive of a more exhausted phenotype. In contrast, the group of clusters with a more classical effector NK cell phenotype that were less abundant in EOC patients showed negative correlation with many of the assessed factors including effector molecules granzyme B, IL-15 and soluble ligands for stimulatory receptors DNAM-1 (namely PVR and NECTIN-2) and NGK2D (namely MICA/B and ULBP1; Figure 3). Only, soluble Arginase levels positively correlated with this latter group of NK cell subsets (Figure 3). In conclusion, the group of NK cell subsets which were more abundant in EOC patient ascites display a more dysfunctional phenotype with less activating/stimulatory receptors and high inhibitory checkpoint expression and strongly correlated to (inhibitory) NK cell regulating factors in ascites.

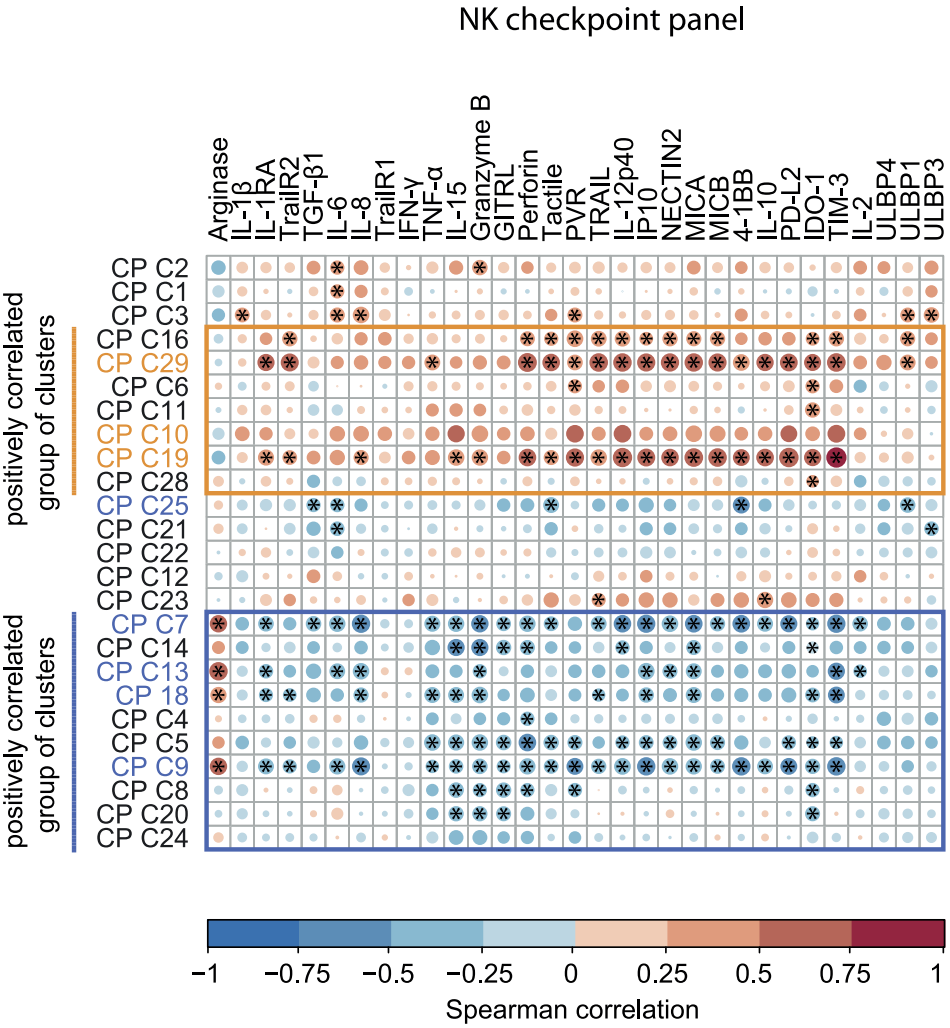

Figure 3: ***Correlogram of soluble factor levels in ascites versus FlowSOM clusters for both NK subset and checkpoint panels***

*Spearman correlogram of cytokine levels versus checkpoint panel FlowSOM clusters. A heat map is used to indicate the Spearman's rank correlation coefficient of associations between biomarkers. Red indicates a positive correlation, and blue indicates a negative correlation. * $p < 0.05$ CP = checkpoint panel. Orange clusters have a significantly increased frequency in EOC patients while blue clusters have a significantly decreased frequency in EOC patients compared to controls.*

Discussion

EOC is sensitive to NK cell-mediated cytotoxicity and the frequency of NK cells is associated with survival of EOC patients [6]. However, the phenotypical changes of these NK cells towards a more exhausted phenotype and their association with cytokines and inhibitory soluble factors has not been studied extensively. Here, we investigated ascites-derived NK cells with comprehensive 18-color flow cytometry panels, using both manual gating and unsupervised clustering analysis. Furthermore, we correlated these clusters to soluble factor levels to better understand the potential mechanisms underlying distinctive NK cell phenotype and function in EOC patients compared to patients with benign diseases. Thereby, we aimed to identify interesting pathways involved in NK cell dysfunction that might be targeted to augment NK cell-based therapies for EOC. Our analysis revealed two distinct groups of clusters of NK cell subpopulations using the established NK checkpoint panel. One displayed an activated phenotype that was decreased in EOC patients compared to benign samples and negatively correlated to the presence of various soluble factors in ascites. In contrast, the second group of NK cell subpopulations that were more abundant in EOC patients displayed a more exhausted phenotype which strongly correlated to the inhibitory cytokine milieu in EOC patient-derived ascites. However, a caveat in this analysis is the difference in peritoneal fluid material: in the benign control group a mix of ascites and peritoneal washings were used, while the samples of the EOC group mostly consisted of ascitic fluids.

Some of the findings highlighted in this study are in line with findings from previous research and were also revealed by manual gating analysis of the data such as decreased DNAM-1, NKp30, NKp46 but not NKG2D expression on NK cells within ascites of EOC patients compared to benign controls [6, 11]. Although certain markers from clustering analysis overlap with manual gating such as low DNAM-1 expression in EOC patients compared to the benign controls, unsupervised clustering analysis revealed additional distinctive co-expression patterns and NK cell subset abundance in EOC ascites. For example, while PD-1 expression was manually not identified to be increased in EOC patients, by utilizing comprehensive clustering methods we found a group of high PD-1 expressing NK cell clusters which shared a common phenotype.

Decreased DNAM-1, SIGLEC-7, CD160, CD56 and CD16 expression and increased PD-1, TIGIT and/or CD96 appeared to be the major characteristic of the NK cell subsets that were more abundant in EOC patient-derived ascites. In this regard, decrease of the inhibitory receptor SIGLEC-7 was not expected within these clusters as most other inhibitory receptors were expressed at higher levels. Interestingly,

SIGLEC-7^{+} PB-derived NK cells were shown to be highly functional NK cells when stimulated with K562 or PMA/Ionomycin. Additionally, in human immunodeficiency virus (HIV) infections loss of SIGLEC-7 defines a dysfunctional subset of NK cells associated with high levels of HIV-1 viremia [20]. Therefore, it appears that although SIGLEC-7 is considered an inhibitory receptor [21], SIGLEC-7+ NK cells can be highly functional. Furthermore, DNAM-1 is an important stimulatory receptor known to be downregulated in EOC which strongly limits NK cell functionality [11]. Similarly, CD160 is important for IFN-γ production by NK cells and CD160+ NK cells are known to be impaired by TGF-β1 signaling in hepatocellular carcinoma [22]. To date little is known about CD160 expression on NK cells within EOC patients. We demonstrated, both with manual gating analysis and with our FlowSOM clustering, that CD160+ NK cells are strongly reduced in EOC patient-derived NK cells. Based on the low levels of stimulatory receptors and high levels of inhibitory receptor expression, these NK cell subsets enriched in EOC are likely exhausted and dysfunctional. This is supported by numerous other studies that reported expression of PD1 and CD96 inhibitory checkpoint levels to be high on dysfunctional NK cells, which could be reverted by PD-1 and/or CD96 receptor blockade [11, 23, 24]. Nevertheless, these findings needs to be functionally confirmed in a follow-up study.

Clusters that were significantly more abundant in EOC patients correlated with soluble PVR, NECTIN-2, ULBP1, MICA/B, TIM-3 and PD-L2 levels. DNAM-1 is one of the most potent stimulatory NK cell receptors and its soluble ligands (PVR and NECTIN-2) were positively correlated to these clusters which can interfere with DNAM-1 signaling [25]. Similarly, ULBP1, MICA/B which are ligands for NKG2D, another potent stimulatory receptor were positively correlated to the clusters that were significantly more abundant in EOC patients. For NKG2D soluble ligands are also known to inhibit NKG2D mediated activation [13]. Interestingly, NKG2D levels were similar across most clusters, while DNAM-1 expression was low especially in PVR-high samples, suggesting soluble PVR receptor-binding induced downregulation which is a known mechanism of action for soluble PVR resulting in dysfunctional NK cells [26, 27]. TIM-3 is an important inhibitory checkpoint receptor expressed on the surface of T and NK cells but in its soluble form relates to T cell exhaustion and reduced IL-2 production [28, 29]. The soluble form of TIM-3 was also associated with, but not a unique trait for the group of clusters that was significantly more abundant in EOC patients, indicating soluble TIM-3 might not be the major soluble factor responsible for the phenotype of these clusters. PD-L2 is also associated to the group of NK cell clusters increased in EOC patients. PD-L2 expression on tumor cells has been shown to associate to tumor metastasis and poor prognosis in solid cancer patients after surgery [30]. More specifically, soluble PD-L2 levels were found to be related to platinum-resistance in EOC patients [31]. Although the PD-1 pathway is

mostly known for T cell exhaustion, some recent evidence suggests that PD-1 may also be expressed on healthy and EOC-associated NK cells [32]. Pesce et al. described that PD-1^+ NK cells have a reduced cytokine response and lower degranulation capacity upon stimulation with tumor cells, including OC cell line OVCAR-5 [32]. Further research of these soluble factors on NK cell functionality, phenotype and subset abundance in EOC patients is warranted.

In conclusion, we were able to identify important NK cell regulators and describe distinctive NK cell subsets with an exhausted phenotype that were more abundant in EOC ascites. Further unraveling of the mechanisms underlying NK cell dysfunction by identification of the cell surface receptors increased in EOC patients and their correlation to the soluble factor milieu in ascites of advanced EOC patients can aid future studies in determining important inhibitory and stimulatory NK cell receptors. These insights can pave the way to augment NK cell-based therapies in EOC patients.

Table 1 : ***NK Subset panel***

Marker/Dye combination	Manufacturer	Catalog number	Clone	Host species, Isotype	Laser (nm)	Filters
CD45 BUV395	BD Biosciences	563792	HI30	Mouse IgG1	355	385/26
CD16 BUV496	BD Biosciences	612944	3G8	Mouse IgG1	355	525/40
CD69 BUV737	BD Biosciences	612817	FN50	Mouse IgG1	355	740/35
CD56 BV421	Biolegend	318328	HCD56	Mouse IgG1	405	450/45
CD158b BV510	BD Biosciences	743452	CH-L	Mouse IgG2b	405	525/40
CD3 BV605	BioLegend	300460	UCHT1	Mouse IgG1	405	610/20
CD159c (NKG2C) BV711	BD Biosciences	748164	134591	Mouse IgG1	405	710/50
CD314 (NKG2D) BV785	BioLegend	320830	1D11	Mouse IgG1	405	780/60
CD158a,h FITC	BioLegend	339504	HP-MA4	Mouse IgG2b	488	525/40
CD57 PerCP-Cy5.5	BioLegend	393312	QA17A04	Mouse IgG1	488	690/50
CD226 (DNAM-1) PE	BioLegend	338306	11A8	Mouse IgG1	561	585/42
CD335 (NKp46) PE-Dazzle594	Biolegend	331930	9E2	Mouse IgG1	561	610/20
CD337 (NKp30) PE-Cy5	Beckman Coulter	A66904	Z25	Mouse IgG1	561	675/30
CD336 (NKp44) PE-Cy7	BioLegend	325116	P44-8	Mouse IgG1	561	763/40
CD159a (NKG2A) APC	Beckman Coulter	A60797	Z199	Mouse IgG2b	633	660/10
CD158e1 (KIR3DL1) AF700	BioLegend	312712	DX9	Mouse IgG1	633	712/25
CD62L APC-Fire750	BioLegend	304846	DREG-56	Mouse IgG1	633	763/40
Live/dead ViaKrome808	Beckman Coulter	C36628	N/A	N/A	808	885/40

Table 2 : ***Checkpoint panel***

Marker/Dye combination	Manufacturer	Catalog number	Clone	Host species, Isotype	Laser (nm)	Filters
CD45 BUV395	BD Biosciences	563792	HI30	Mouse IgG1	355	385/26
CD16 BUV496	BD Biosciences	612944	3G8	Mouse IgG1	355	525/40
CD3 BUV737	BD Biosciences	612750	UCHT1	Mouse IgG1	355	740/35
CD56 BV421	Biolegend	318328	HCD56	Mouse IgG1	405	450/45
CD226 (DNAM-1) BV510	Biolegend	338330	11A8	Mouse IgG1	405	525/40
CD366 (TIM-3) BV605	Biolegend	345018	F38-2E2	Mouse IgG1	405	610/20
CD270 (PD-1) BV711	Biolegend	329928	EH12.2H7	Mouse IgG1	405	710/50
CD134 (OX40) BV786	BD Biosciences	743285	Ber-ACT35 (ACT35)	Mouse IgG1	405	780/60
KLRG-1 FITC	Miltenyi Biotech	130-120-425	REA261	recombinant/humanized IgG1	488	525/40
KIR a/h PerCP-Cy5-5	Biolegend	339514	HP-MA4	Mouse IgG2b	488	690/50
KIRb PerCP-Cy5-5	Biolegend	312614	DX27	Mouse IgG2a	488	690/50
KIRe1 PerCP-Cy5-5	Biolegend	312718	DX9	Mouse IgG1	488	690/50
NKG2a PE	Beckman Coulter	IM3291U	Z199	Mouse IgG2b	561	585/42
CD96 PE-Dazzle594	Biolegend	338414	NK92.39	Mouse IgG1	561	610/20
CD27 PE-Cy5	eBiosciences	12-2589-42	7-3 (7)	Mouse IgG1	561	675/30
CD160 PE-Cy7	Biolegend	341212	BY55	Mouse IgM	561	763/40
TIGIT APC	R&D systems	FAB7898A	741182	Mouse IgG2b	633	660/10
SIGLEC-9 AF700	R&D systems	FAB1139N-100	191240	Mouse IgG2a	633	712/25
SIGLEC-7 APC-Fire750	Biolegend	339208	6-434	Mouse IgG1	633	763/40
Live/dead ViaKrome808	Beckman Coulter	C36628	N/A	N/A	808	885/40

References

1. Siegel RL, Miller KD, Fuchs HE, Jemal A. Cancer Statistics, 2021. CA Cancer J Clin. 2021;71(1):7-33.

2. Ahmed N, Stenvers KL. Getting to know ovarian cancer ascites: opportunities for targeted therapy-based translational research. Front Oncol. 2013;3:256.

3. Kim S, Kim B, Song YS. Ascites modulates cancer cell behavior, contributing to tumor heterogeneity in ovarian cancer. Cancer Sci. 2016;107(9):1173-8.

4. Kärre K, Ljunggren HG, Piontek G, Kiessling R. Selective rejection of H–2-deficient lymphoma variants suggests alternative immune defence strategy. Nature. 1986;319(6055):675-8.

5. Hoogstad-van Evert JS, Cany J, van den Brand D, Oudenampsen M, Brock R, Torensma R, et al. Umbilical cord blood CD34(+) progenitor-derived NK cells efficiently kill ovarian cancer spheroids and intraperitoneal tumors in NOD/SCID/IL2Rg(null) mice. Oncoimmunology. 2017;6(8):e1320630.

6. Hoogstad-van Evert JS, Maas RJ, van der Meer J, Cany J, van der Steen S, Jansen JH, et al. Peritoneal NK cells are responsive to IL-15 and percentages are correlated with outcome in advanced ovarian cancer patients. Oncotarget. 2018;9(78):34810-20.

7. James FR, Jiminez-Linan M, Alsop J, Mack M, Song H, Brenton JD, et al. Association between tumour infiltrating lymphocytes, histotype and clinical outcome in epithelial ovarian cancer. BMC Cancer. 2017;17(1):657.

8. Zhang L, Conejo-Garcia JR, Katsaros D, Gimotty PA, Massobrio M, Regnani G, et al. Intratumoral T cells, recurrence, and survival in epithelial ovarian cancer. The New England journal of medicine. 2003;348(3):203-13.

9. Hwang WT, Adams SF, Tahirovic E, Hagemann IS, Coukos G. Prognostic significance of tumor-infiltrating T cells in ovarian cancer: a meta-analysis. Gynecol Oncol. 2012;124(2):192-8.

10. Mandal A, Viswanathan C. Natural killer cells: In health and disease. Hematol Oncol Stem Cell Ther. 2015;8(2):47-55.

11. Maas RJ, Hoogstad-van Evert JS, Van der Meer JM, Mekers V, Rezaeifard S, Korman AJ, et al. TIGIT blockade enhances functionality of peritoneal NK cells with altered expression of DNAM-1/TIGIT/CD96 checkpoint molecules in ovarian cancer. Oncoimmunology. 2020;9(1):1843247.

12. Trefny MP, Kaiser M, Stanczak MA, Herzig P, Savic S, Wiese M, et al. PD-1(+) natural killer cells in human non-small cell lung cancer can be activated by PD-1/PD-L1 blockade. Cancer Immunol Immunother. 2020;69(8):1505-17.

13. Dhar P, Wu JD. NKG2D and its ligands in cancer. Curr Opin Immunol. 2018;51:55-61.

14. Barrow AD, Martin CJ, Colonna M. The Natural Cytotoxicity Receptors in Health and Disease. Frontiers in Immunology. 2019;10.

15. Dębska-Zielkowska J, Moszkowska G, Zieliński M, Zielińska H, Dukat-Mazurek A, Trzonkowski P, et al. KIR Receptors as Key Regulators of NK Cells Activity in Health and Disease. Cells. 2021;10(7).

16. Jiang K-Y, Qi L-L, Kang F-B, Wang L. The intriguing roles of Siglec family members in the tumor microenvironment. Biomarker Research. 2022;10(1):22.

17. Yigit R, Massuger LF, Figdor CG, Torensma R. Ovarian cancer creates a suppressive microenvironment to escape immune elimination. Gynecol Oncol. 2010;117(2):366-72.

18. Brummelman J, Haftmann C, Núñez NG, Alvisi G, Mazza EMC, Becher B, et al. Development, application and computational analysis of high-dimensional fluorescent antibody panels for single-cell flow cytometry. Nature Protocols. 2019;14(7):1946-69.

19. Van Gassen S, Callebaut B, Van Helden MJ, Lambrecht BN, Demeester P, Dhaene T, et al. FlowSOM: Using self-organizing maps for visualization and interpretation of cytometry data. Cytometry A. 2015;87(7):636-45.

20. Brunetta E, Fogli M, Varchetta S, Bozzo L, Hudspeth KL, Marcenaro E, et al. The decreased expression of Siglec-7 represents an early marker of dysfunctional natural killer-cell subsets associated with high levels of HIV-1 viremia. Blood. 2009;114(18):3822-30.

21. Nicoll G, Ni J, Liu D, Klenerman P, Munday J, Dubock S, et al. Identification and Characterization of a Novel Siglec, Siglec-7, Expressed by Human Natural Killer Cells and Monocytes*. Journal of Biological Chemistry. 1999;274(48):34089-95.

22. Sun H, Xu J, Huang Q, Huang M, Li K, Qu K, et al. Reduced CD160 Expression Contributes to Impaired NK-cell Function and Poor Clinical Outcomes in Patients with HCC. Cancer Res. 2018;78(23):6581-93.

23. Lee J, Ahn E, Kissick HT, Ahmed R. Reinvigorating Exhausted T Cells by Blockade of the PD-1 Pathway. For Immunopathol Dis Therap. 2015;6(1-2):7-17.

24. Sun H, Huang Q, Huang M, Wen H, Lin R, Zheng M, et al. Human CD96 Correlates to Natural Killer Cell Exhaustion and Predicts the Prognosis of Human Hepatocellular Carcinoma. Hepatology. 2019;70(1):168-83.

25. Okumura G, Iguchi-Manaka A, Murata R, Yamashita-Kanemaru Y, Shibuya A, Shibuya K. Tumor-derived soluble CD155 inhibits DNAM-1–mediated antitumor activity of natural killer cells. Journal of Experimental Medicine. 2020;217(4).

26. Mantovani S, Varchetta S, Mele D, Maiello R, Donadon M, Soldani C, et al. Defective DNAM-1 Dependent Cytotoxicity in Hepatocellular Carcinoma-Infiltrating NK Cells. Cancers. 2022;14(16):4060.

27. Okumura G, Iguchi-Manaka A, Murata R, Yamashita-Kanemaru Y, Shibuya A, Shibuya K. Tumor-derived soluble CD155 inhibits DNAM-1-mediated antitumor activity of natural killer cells. J Exp Med. 2020;217(4):1.

28. da Silva RF, Yoshida A, Cardozo DM, Jales RM, Paust S, Derchain S, et al. Natural Killer Cells Response to IL-2 Stimulation Is Distinct between Ascites with the Presence or Absence of Malignant Cells in Ovarian Cancer Patients. Int J Mol Sci. 2017;18(5).

29. Avery L, Filderman J, Szymczak-Workman AL, Kane LP. Tim-3 co-stimulation promotes short-lived effector T cells, restricts memory precursors, and is dispensable for T cell exhaustion. Proceedings of the National Academy of Sciences. 2018;115(10):2455-60.

30. Yang H, Zhou X, Sun L, Mao Y. Correlation Between PD-L2 Expression and Clinical Outcome in Solid Cancer Patients: A Meta-Analysis. Front Oncol. 2019;9:47.

31. Buderath P, Schwich E, Jensen C, Horn PA, Kimmig R, Kasimir-Bauer S, et al. Soluble Programmed Death Receptor Ligands sPD-L1 and sPD-L2 as Liquid Biopsy Markers for Prognosis and Platinum Response in Epithelial Ovarian Cancer. Front Oncol. 2019;9:1015.

32. Pesce S, Greppi M, Tabellini G, Rampinelli F, Parolini S, Olive D, et al. Identification of a subset of human natural killer cells expressing high levels of programmed death 1: A phenotypic and functional characterization. Journal of Allergy and Clinical Immunology. 2017;139(1):335-46.e3.

Supplemental data

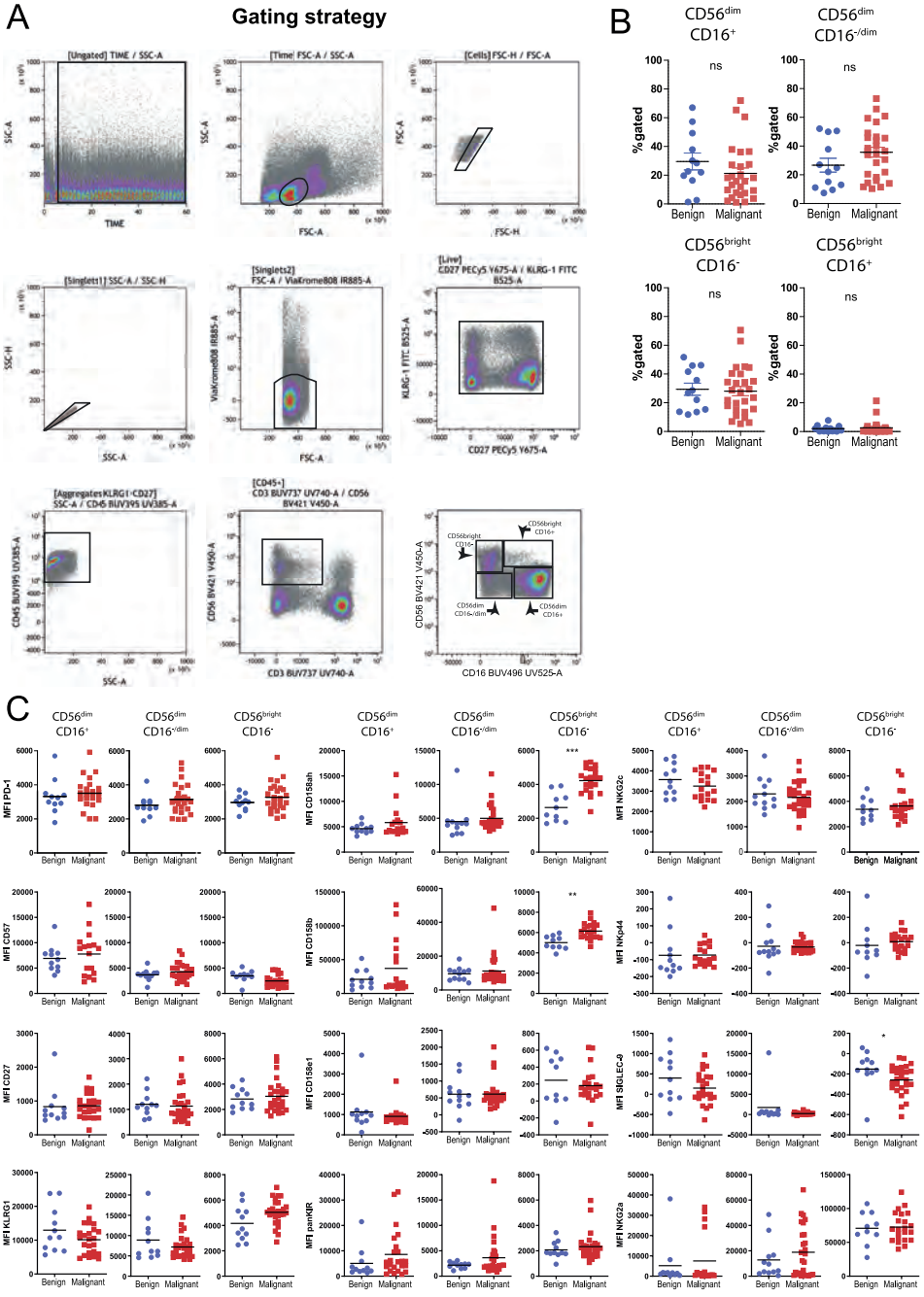

Supplemental Figure 1: ***NK cell gating strategy and cleanup***

(A) *Flow cytometry data of a healthy donor is shown as an example to demonstrate the gating strategy used to gate NK cells. First we gated on a steady cell input using a time gate. Then lymphocytes were selected using forward scatter (FSC-A) vs. side scatter (SSC-A). Doublets were excluded by plotting FSC-Area vs FSC-Height and SSC-Area vs. SSC-Height. Dead cells were excluded with a viability dye and aggregates were removed using a gate on FITC and PE-Cy5. CD45+ cells were displayed and gated vs. SSC. NK cells were then defined as CD56^{+} and CD3^{-}.* ***(B)*** *Percentage of each subpopulation of NK cells based on CD56 and CD16 expression in benign and malignant patients. A Mann-Whitney test was used for statistical analysis, * $p < 0.05$, ** $p < 0.01$ and ***$p<0.001$* ***(C)*** *Activating receptors, Inhibitory and activation markers are shown for CD56^{dim}CD16^{+}, CD56^{dim}CD16^{-} and CD56^{bright}CD16^{-} NK cells. A Mann-Whitney test was used for statistical analysis, * $p < 0.05$, ** $p < 0.01$ and ***$p<0.001$*

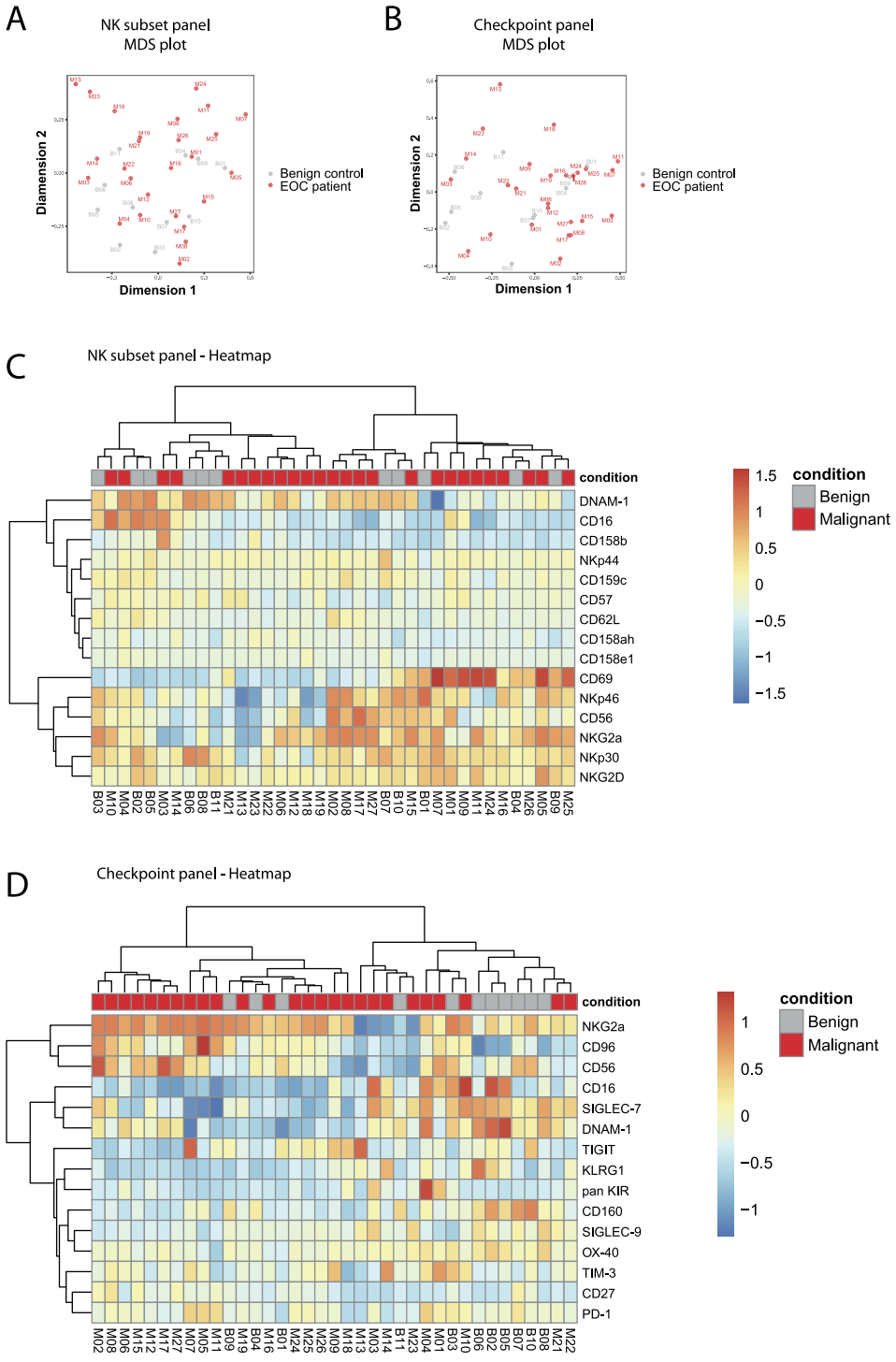
A
NK subset panel
MDS plot
Diamension 2
Dimension 1
Benign control
EOC patient
B
Checkpoint panel
MDS plot
Dimension 2
Dimension 1
Benign control
EOC patient
C
NK subset panel - Heatmap
condition
DNAM-1
CD16
CD158b
NKp44
CD159c
CD57
CD62L
CD158ah
CD158e1
CD69
NKp46
CD56
NKG2a
NKp30
NKG2D
1.5
1
0.5
0
−0.5
−1
−1.5
condition
Benign
Malignant
D
Checkpoint panel - Heatmap
condition
NKG2a
CD96
CD56
CD16
SIGLEC-7
DNAM-1
TIGIT
KLRG1
pan KIR
CD160
SIGLEC-9
OX-40
TIM-3
CD27
PD-1
1
0.5
0
−0.5
−1
condition
Benign
Malignant

Supplemental Figure 2: ***NK cells from benign and EOC patients cluster similarly based on phenotype in MDS and hierarchical clustering in a heatmap***

(A and B) *Multidimensional scaling (MDS), based on NK cell phenotype in NK subset* ***(A)*** *and checkpoint panel* ***(B)****, showing (dis)similarities in benign control samples (grey, n=11) and EOC patients (red, n=26).* ***(C and D)*** *Scaled expression levels in EOC patients (n=26) and benign control samples (n=11) visualized in a heatmap. Each row represents a different expression marker of NK subset* ***(C)*** *and checkpoint panel* ***(D)****, while columns represent EOC patients or benign controls (M=EOC patient and B=benign control). The scaled expression levels are reported and visualized with a color scale from blue (low levels) to red (high levels).*

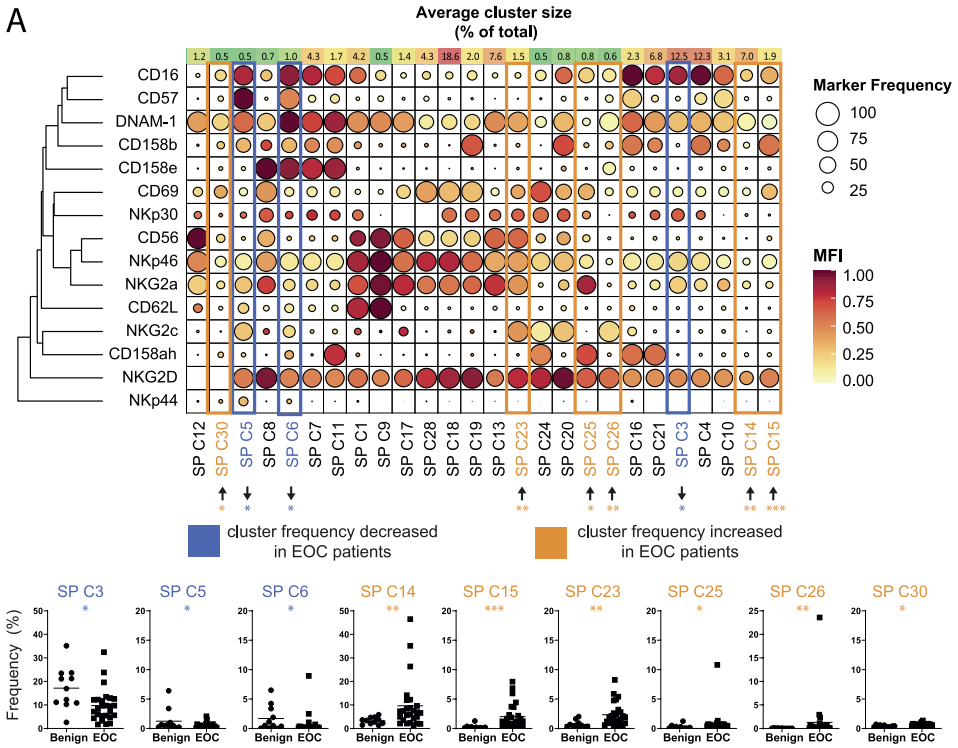
A
Average cluster size
(% of total)
Marker Frequency
100
75
50
25
MFI
1.00
0.75
0.50
0.25
0.00
CD16
CD57
DNAM-1
CD158b
CD158e
CD69
NKp30
CD56
NKp46
NKG2a
CD62L
NKG2c
CD158ah
NKG2D
NKp44
SP C12 SP C30 SP C5 SP C8 SP C6 SP C7 SP C11 SP C1 SP C9 SP C17 SP C28 SP C18 SP C19 SP C13 SP C23 SP C24 SP C20 SP C25 SP C26 SP C16 SP C21 SP C3 SP C4 SP C10 SP C14 SP C15
cluster frequency decreased in EOC patients
cluster frequency increased in EOC patients
SP C3 SP C5 SP C6 SP C14 SP C15 SP C23 SP C25 SP C26 SP C30
Frequency (%)
Benign EOC

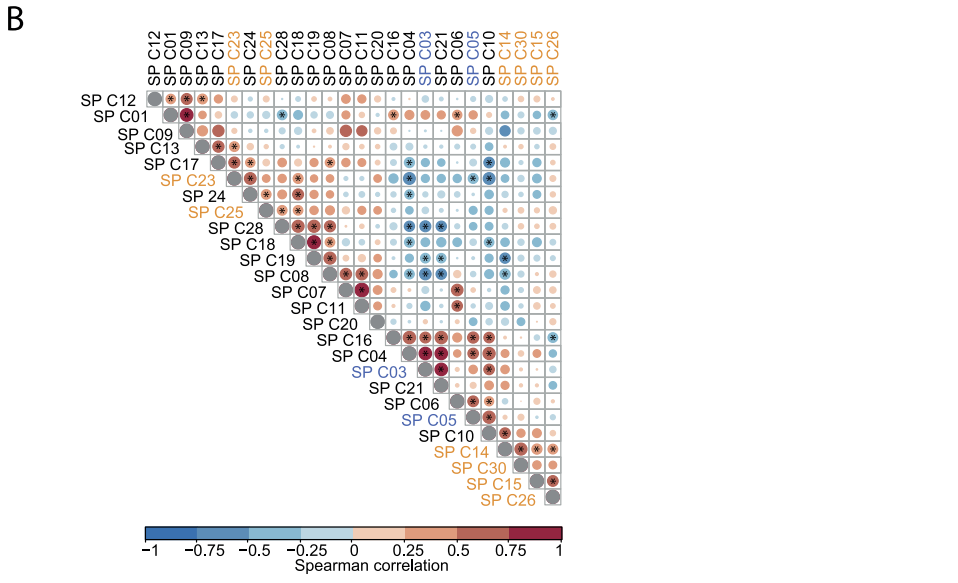
B
SP C12 SP C01 SP C09 SP C13 SP C17 SP C23 SP C24 SP C25 SP C28 SP C18 SP C19 SP C08 SP C07 SP C11 SP C20 SP C16 SP C04 SP C03 SP C21 SP C06 SP C05 SP C10 SP C14 SP C30 SP C15 SP C26
−1 −0.75 −0.5 −0.25 0 0.25 0.5 0.75 1
Spearman correlation

Supplemental Figure 3: ***FlowSOM clustering on NK cells from benign controls and EOC patients***
(A) *Scaled MFI values of FlowSOM clusters for NK subset in a balloon plot. Each row represents a marker, while columns represent a cluster. Balloon size represents frequency while balloon color represents MFI (red is high MFI, yellow is low MFI). On top of the balloon plot the cluster size is presented as percent of total where red indicate large clusters and green small clusters. Statistical difference between cluster frequency of benign control (significance indicated in blue) and EOC patient (significance indicated in orange) patients was calculated using a Mann Whitney test.* ***(B)*** *Spearman correlogram of FlowSOM clusters within NK subset panel. A heat map is used to indicate the Spearman's rank correlation coefficient of associations between biomarkers. Red indicates a positive correlation, and blue indicates a negative correlation.* $*\ p < 0.05$, $**\ p < 0.01$, $***\ p < 0.001$, *SP = NK Subset Panel*

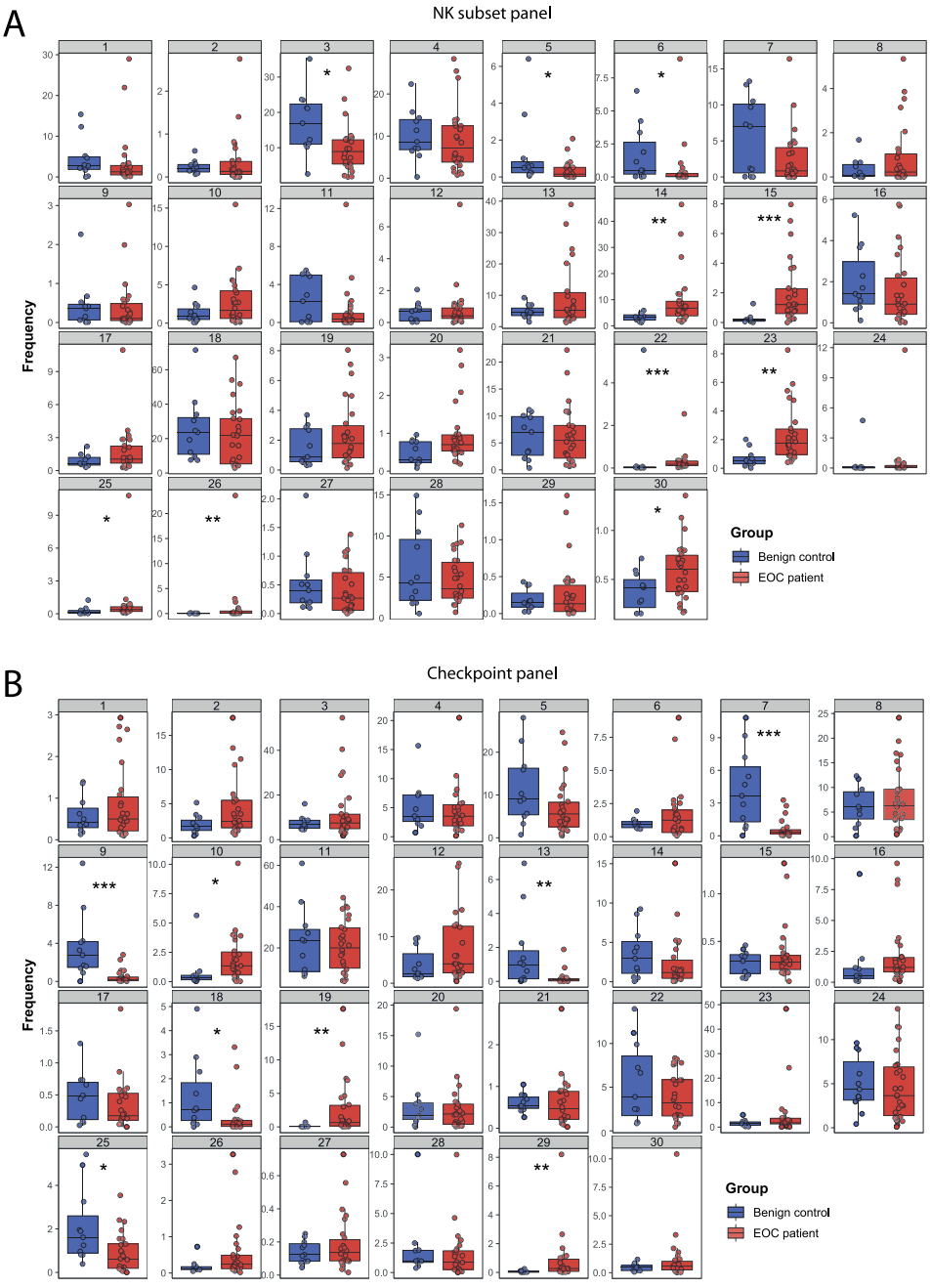

Supplemental Figure 4: ***Frequencies of FlowSOM clusters in both NK subset and checkpoint panels***
Box and whiskers plots showing the percentage of FlowSOM clusters in the NK subset panel ***(A)*** *and checkpoint panel* ***(B)****, showing different cell cluster distribution in benign control samples (blue, n=11), and EOC patients (red, n=26). Kruskal-Wallis with Dunn's Multiple Comparison Test was used for statistical analysis * $p < 0.05$, * $p < 0.05$, ** $p < 0.01$ and *** $p < 0.001$*

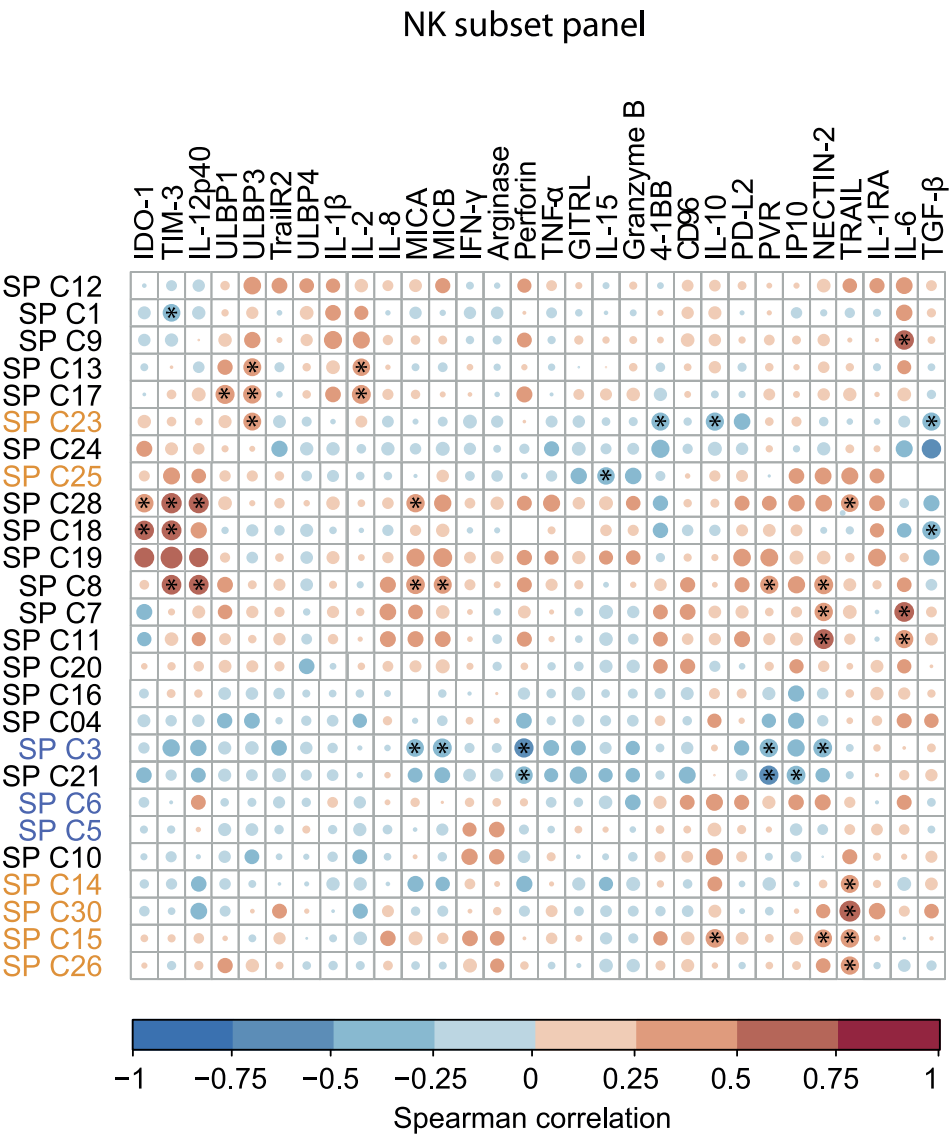

Supplemental Figure 5: ***Correlogram of cytokine levels in peritoneal fluids versus FlowSOM clusters NK subset panel***

*Spearman correlogram of cytokine levels versus NK subset FlowSOM. A heat map is used to indicate the Spearman's rank correlation coefficient of associations between biomarkers. Red indicates a positive correlation, and blue indicates a negative correlation. * $p < 0.05$*

Supplemental Table 1: ***EOC patient characteristics***

Number	Age (years)	Fluid type	FIGO Stadium	PFS (months)*	OS (months)*	CA-125 (U/ml) Serum
M01	75	ascites	IV	1.5	7.8	468
M02	56	ascites	IIIc	6.8	12.5	2200
M03	69	ascites	IIIc	20.0	53.8	198
M04	52	ascites	IV	4.1	9.4	1223
M05	63	ascites	IIIc	20.5	26.2	4889
M06	64	ascites	IV	0	8.6	1800
M07	61	ascites	IIIc	20.5	55.5	2380
M08	52	ascites	IV	5.2	Unknown	5700
M09	59	washing	IIIc	8.4	29.4	1304
M10	45	ascites	IV	0	1.7	1400
M11	69	ascites	IIIc	25.1	31.4	899
M12	67	ascites	IV	9.1	10.6	1560
M13	76	ascites	IIIc	23.9	41.3	928
M14	93	ascites	IV	0	1.22	412
M15	61	ascites	IIIc	Unknown	Unknown	10000
M16	64	ascites	IIIc	5.8	37.0	352
M17	52	ascites	IV	21.0	31.1	1621
M18	63	ascites	IIIc	18.0	30.4	344
M19	64	ascites	IIIc	3.6	29.0	31
M20	47	ascites	IIIc	18.9	18.9	1484
M21	72	ascites	IV	5.7	21.6	1018
M22	36	ascites	IIIc	22.0	22.0	1116
M23	61	ascites	IV	0	14.5	10000
M24	74	ascites	IV	1.1	1.1	1175
M25	76	ascites	IIIb	22.1	22.1	1516
M26	69	ascites	IIIc	10.2	18.6	215
M27	68	ascites	IIIc	14.2	16.5	1931
M28	50	ascites	IV	0	0.7	9909
M29	61	ascites	IIIc	0	2.5	5694
M30	57	ascites	IIIc	2.9	20.3	2118
M31	72	ascites	IV	6.9	7.6	1500

**At time of analysis, PFS = Progression free survival, OS = Overall survival*

Supplemental Table 2: ***Benign control patient characteristics***

Number	Age (years)	Fluid type	Pathology diagnosis	Endometriosis	Torsion/ infection	CA-125 (U/ ml) Serum
B1	53	ascites	Mucinous cystadenoma	-	-	60
B2	39	washing	Endometrioma	Yes	-	156
B3	62	ascites	Benign fibroma	-	Necrosis	284
B4	50	washing	Serous cystadenofibroma	-	-	25
B5	41	washing	Serous cystadenoma	-	-	10
B6	64	ascites	Serous cystadenoma	-	-	34
B7	47	washing	Mucineus cystadenoma	-	-	20
B8	65	washing	Mucinous cystadenoma	-	-	23
B9	47	washing	Serous cystadenoma	-	-	52
B10	41	washing	Mucinous cystadenoma	-	-	15
B11	54	washing	Serous cystadenoma	-	-	5

Chapter 5

TIGIT blockade enhances functionality of peritoneal NK cells with altered expression of DNAM-1/TIGIT/CD96 checkpoint molecules in ovarian cancer

Ralph J.A. Maas, Janneke S. Hoogstad-van Evert,* Jolien M.R. Van der Meer,* Vera Mekers, Somayeh Rezaeifard, Alan J. Korman, Paul K.J.D de Jonge, Jeannette Cany, Rob Woestenenk, Nicolaas P.M. Schaap, Leon F. Massuger, Joop H Jansen, Willemijn Hobo, and Harry Dolstra

*these authors contributed equally

Oncoimmunology. 2020;9(1):1843247.

Abstract

Advanced ovarian cancer (OC) patients have a poor 5-year survival of only 28%, emphasizing the medical need for improved therapies. Adjuvant immunotherapy could be an attractive approach since OC is an immunogenic disease and the presence of tumor-infiltrating lymphocytes has shown to positively correlate with patient survival. Among these infiltrating lymphocytes are natural killer (NK) cells, key players involved in tumor targeting, initiated by signaling via activating and inhibitory receptors. Here, we investigated the role of the DNAM-1/TIGIT/CD96 axis in the anti-tumor response of NK cells toward OC. Ascites-derived NK cells from advanced OC patients showed lower expression of activating receptor DNAM-1 compared to healthy donor peripheral blood NK cells, while inhibitory receptor TIGIT and CD96 expression was equal or higher, respectively. This shift to a more inhibitory phenotype could also be induced in vitro by co-culturing healthy donor NK cells with OC tumor spheroids, and *in vivo* on intraperitoneally infused NK cells in SKOV-3 OC bearing NOD/SCID-IL2Rγnull (NSG) mice. Interestingly, TIGIT blockade enhanced degranulation and interferon gamma (IFNγ) production of healthy donor CD56dim NK cells in response to OC tumor cells, especially when DNAM-1/CD155 interactions were in place. Importantly, TIGIT blockade boosted functional responsiveness of CD56dim NK cells of OC patients with a baseline reactivity against SKOV-3 cells. Overall, our data show for the first time that checkpoint molecules TIGIT/DNAM-1/CD96 play an important role in NK cell responsiveness against OC, and provides rationale for incorporating TIGIT interference in NK cell-based immunotherapy in OC patients.

Introduction

Patients with ovarian carcinoma (OC) are mostly diagnosed at advanced stage, as many women do not show clear symptoms at an early stage. This late detection of advanced disease is associated with poor prognosis and poor quality of life [1]. Current therapy for OC is debulking surgery combined with chemotherapy, yet the 5-year survival for advanced OC is only 28% [2]. Adjuvant immunotherapy could be a complementary approach since OC is considered to be an immunogenic disease and the presence of tumor-infiltrating lymphocytes (TILs) positively correlates with survival [3]. Several reports showed that prolonged survival associated mainly with the presence of CD8+ cytotoxic T cells [4,5], yet it has also been described that CD103+ tumor-infiltrating NK cells often co-infiltrate with CD8+CD103+ T cells suggesting both T and NK cell involvement in anti-OC immune responses [6]. Recently, we observed that a higher NK cell percentage within the ascitic lymphocyte fraction was correlated with enhanced survival of OC patients [5]. Furthermore, multiple studies have demonstrated that OC cells are susceptible to killing by activated NK cells [7–9]. Hence, increasing NK cell immunity in OC patients by immunotherapeutic strategies could be an attractive strategy. Boosting peritoneal NK cell responses with IL-15 receptor-mediated stimulation and intraperitoneal NK cell adoptive transfer are being explored as therapeutic approaches in OC [10–12]. However, intrinsic and adoptive NK cell antitumor immunity in OC patients can be attenuated by immunosuppressive cells and cytokines within the tumor microenvironment [13–16]. Identification of and interference with these immunosuppressive pathways may further improve the efficacy of NK cell-based immunotherapy.

NK cells are generally characterized according to their expression of CD56 and CD16 surface antigens in $CD56^{dim}CD16^{hig}$h and $CD56^{bright}CD16^{neg}$ NK cells. According to the tissue type and the pathological conditions, the frequency and distribution of these NK cell populations may vary [17,18]. Furthermore, cytokines and other soluble factors present in ascitic fluid of OC patients can have a strong effect on the phenotype and distribution of different subsets of NK cells [19]. For instance, transforming growth factor (TGF)-β exerts immune-suppressive action on NK cells and can partially convert healthy peripheral blood $CD56^{dim}CD16^{high}$ NK cells to $CD56^{bright}CD16^{low/neg}$ [19]. Functionally, NK cells are regulated by the net balance of signals perceived by their activating and inhibiting receptors which enables NK cells to effectively kill target cells that have increased expression of stress-induced ligands or lack sufficient inhibitory signals, while maintaining self-tolerance [18,19]. These NK cell receptors can be grouped in MHC class I-specific receptors versus non-MHC binding receptors. Important non-MHC binding activating receptors on NK cells are

DNAX Accessory Molecule-1 (DNAM-1), NKG2D, and natural cytotoxicity receptors (NCRs), while inhibitory receptors including T cell immunoglobulin and ITIM domain (TIGIT) keep the NK cell response in check [20]. TIGIT shares its ligands CD155 (or poliovirus receptor/PVR) and CD112 (or Nectin-2) with DNAM-1. CD96 (or TACTILE) also binds CD155, but in human NK cell signaling its function remains elusive. CD155 and CD112 are mainly expressed by antigen-presenting cells (APCs), activated T cells, fibroblasts, and endothelial cells in healthy tissues [21,22]. Furthermore, CD112/CD155 are upregulated upon cellular stress and are therefore highly expressed on several types of cancer amongst which OC.23,24 CD112 binds to DNAM-1 but only weakly to TIGIT, while CD155 has high affinity for both TIGIT and DNAM-1 [25–27]. NK cell cytotoxicity is triggered by DNAM-1 crosslinking, resulting in Fyn-mediated phosphorylation of the cytoplasmic tyrosine residues [28]. TIGIT signaling is mediated via immunoreceptor tyrosine-based inhibitory (ITIM) and immunoglobulin tail tyrosine (ITT)-like motifs, through which inhibitory signals are conducted that impair cytotoxicity, granule polarization, and cytokine secretion in NK cells [29,30]. The DNAM-1/TIGIT/CD96 axis on NK cells was recently elaborately reviewed by Sanchez-Correa et al. [31].

DNAM-1 on NK cells is downregulated in most cancer types including OC, colon carcinoma, and acute myeloid leukemia (AML) [32–35]. Carlsten et al. showed that DNAM-1 is an important activating NK cell receptor in OC and that CD155 expression on patient-derived OC tumor cells correlates with a reduction in DNAM-1 expression [34]. Similarly, reduced expression of DNAM-1 on NK cells from AML patients was observed, which was negatively correlated with CD112 expression on blasts [32]. Moreover, NK cells expressing high levels of TIGIT were associated with poor survival in AML patients [36]. These $TIGIT^{high}$ NK cells were found to be more susceptible to myeloid-derived suppressor cell (MDSC) inhibition compared to $TIGIT^{low}$ NK cells [37]. Furthermore, TIGIT could be upregulated through recombinant human (rh)IL-15 stimulation, which was associated with lower IFNγ production [37,38]. These studies underscore the importance of TIGIT as an important inhibitory receptor on NK cells with clinical impact, reflected by the promising efficacy of TIGIT blockade on NK cell reactivity in colon and breast cancer [39,40].

In this report, we investigated the role of TIGIT in the functional impairment of NK cells in OC patients. We demonstrated that NK cells from healthy donors, as well as OC patients, exhibit high expression of TIGIT, while DNAM-1 is strongly reduced on ascites-derived NK cells from patients. Moreover, we showed that this DNAM-1 downregulation on NK cells is mediated by OC tumor cell exposure. Most importantly, we showed augmented tumor reactivity of NK cells from both healthy

donors and OC patients following TIGIT blockade, thereby providing a rationale for incorporating TIGIT interference in NK cell-based immunotherapy in OC patients.

Methods

Patient samples

Malignant ascites fluid samples were collected after written informed consent at first surgery of patients with stage IIIc or IV high-grade serous papillary OC at the Radboud University Medical Center (Radboudumc). Study approval was given by the Regional Committee for Medical Research Ethics (CMO 2018–4845) and performed according to the Code for Proper Secondary Use of Human Tissue (Dutch Federation of Biomedical Scientific Societies, www.federa.org). The progression-free survival (PFS) and overall survival (OS) at time of analysis, CA-125 levels, and treatment status are shown for individual patients in Table 1. Ascites was filtered using a 100 μm filter, centrifuged, and cells were resuspended in phosphate-buffered saline (PBS). Subsequently, mononuclear cells were isolated using a Ficoll-Hypaque (1.077 g/mL; GE Healthcare, 17–1440–03) density gradient. For the benign controls, samples were collected at benign gynecological surgeries. The main indication for diagnostic laparoscopy was abdominal pain and samples were included only if pathological findings were absent. Detection of cysts, endometriosis, and adhesions at laparoscopy was exclusion criteria. All samples were cryopreserved in dimethyl sulfoxide (DMSO)-containing medium and used after thawing.

Patient Characteristics							CD56dim NK cell population								
Patient no.	**EOC Stage**	**CA125 (U/mL)**	**Treatment**	**Complete**	**PFS (months)**	**OS (months)**	**DNAM-1 (%gated)**	**DNAM-1 (ΔMFI)**	**TIGIT (%gated)**	**TIGIT (ΔMFI)**	**Responder (≥10% CD107a)**	**CD107a Control**	**CD107a TIGIT blockade**	**IFNγ control**	**IFNγ TIGIT blockade**
1	3c	1304	Interval debulking	Complete	8.4	29.4	NA	NA	NA	NA	Yes	14	22	4	7
2	4	1800	Interval debulking	Complete	0	8.6	79	0.90	38	1.8	Yes	10	21	3	8
3	3c	358	Primary debulking	Optimal	0	28.8	46	0.40	48	2.7	Yes	26	34	8	9
4	3c	1242	Primary debulking	Optimal	0	13.7	43	0.30	33	1	No	4	5	1	2
5	4	1400	chemotherapy	Treatment not continued	0	1.7	55	0.40	37	2.6	No	3	5	1	0
6	3c	2380	Primary debulking	Optimal	20.5	55.5	15	0.10	78	4.8	Yes	22	27	3	4
7	3c	928	Interval debulking	Complete	23.9	41.3	23	0.30	69	4.8	No	1	1	0	0
8	4	1223	Interval debulking	Optimal	4.1	9.4	81	1.17	29	1.79	Yes	37	51	34	46
9	4	1430	Interval debulking	Optimal	12.2	54.6	59	0.64	16	0.88	Yes	38	51	27	35
10	3c	2528	Primary debulking	Complete	17.2	54	61	0.60	34	1.3	NA	NA	NA	NA	NA

Table 1: ***Ovarian cancer patient characteristics and DNAM-1/TIGIT expression profile***

Characteristics of ovarian cancer patients from whom NK cells were phenotyped and functionally assessed. Patient samples were obtained at diagnosis. EOC, Epithelial Ovarian Cancer; PFS, Progression-Free Survival; OS, Overall Survival; MFI, Median Fluorescence Intensity; NA, not applicable.

NK cell isolations

Peripheral blood mononuclear cells (PBMCs) were obtained from healthy donor buffy coats (Sanquin Blood Bank, Nijmegen, the Netherlands) by density gradient Ficoll-Hypaque centrifugation. NK cells were isolated from PBMCs of healthy donors or cryopreserved ascites-derived mononuclear cells using a magnetic bead-based NK cell enrichment kit (StemCell Technologies, #19055) according to manufacturer's instructions. Further purification of ascites-derived NK cells was performed via fluorescence-activated cell sorting (FACS) based on lymphocyte sized forward/side scatter using the FACS Aria (BD Bioscience) to eliminate any remaining tumor cells. All isolations resulted in ≥90% purity..

Cell culture

The OC cell lines SKOV-3 (RRID:CVCL_0532) and IGROV-1 (RRID:CVCL_1304) were cultured in Roswell Park Memorial Institute medium 1640 (RPMI; Gibco, #11875091) supplemented with 10% fetal calf serum (FCS; Integro), and OVCAR-3 (RRID:CVCL_0465) was cultured with RPMI supplemented with 20% FCS and 1 µg/mL bovine albumin (Sigma, #I0516). K562 (RRID:CVCL_0004) was cultured in Iscove's Modified Dulbecco's medium (IMDM; Gibco, #12440061) containing 10% FCS. Cell lines were tested for mycoplasma contamination with MycoAlertTM Mycoplasma Detection Kit (Lonza, #LT07-418) every 6 months. All cell lines were cultured for a maximum of 3 months. SKOV-3 and K562 were purchased from the ATCC. IGROV-1 and OVCAR-3 were a kind gift from Prof. Dr. OC Boerman, Department of Nuclear Medicine, Radboud University Medical Center, Nijmegen, the Netherlands. Primary low-grade serous OC cell line ASC009 was generated by NTRC in Oss, the Netherlands, from primary ascites material and a kind gift from Guido Zaman.

Multicellular tumor spheroids

OC tumor spheroids were generated by seeding 3×10^4 (SKOV-3), 6×10^4 (IGROV-1) and 12×10^4 (OVCAR-3) cells/well in a volume of 100 µL/well of culture medium in 96-well plates pre-coated with 1% agarose in Dulbecco's Modified Eagle Medium/Nutrient Mixture F-12 medium (DMEM/F12; Invitrogen 11330–057, adjusted from

Giannattasio *et al.* and Friedrich *et al*. [41, 42]. Tumor spheroids were used for functional assays upon reaching a solid state at 4 days after initial seeding. For phenotypical analysis, 26.000 NK cells were seeded with concentrations of rhIL-15 ranging from 0.01 to 10nM (Immunotools) and re-treated with the same rhIL-15 dose on day 3. After 7 days, spheres were harvested, trypsinized with TrypLE™ Express (Thermofisher, #12605028) for 45 minutes, washed and analyzed.

Ovarian cancer tissue

Tissue was transferred to DMEM/F12 medium (Invitrogen 11330–057) supplemented with 10% FCS and 1% Penicillin-Streptomycin at 4°C. The next day, the tissue was mechanically minced using a scalpel and filtered through a 70 µm cell strainer to obtain a single cell suspension. For phenotypical analysis, 50.000-100.000 NK cells and the same number of OC tissue cells were seeded with concentrations of rhIL-15 (Immunotools) ranging from 0.01 to 10nM and re-supplemented with the same rhIL-15 dose on day 4. After 7 days, suspension cells were harvested, washed and analyzed.

Flow cytometry (FCM)

For phenotypical analysis, cells were incubated with antibodies in FCM buffer (PBS/ 0.5% bovine serum albumin) for 20 min at 4°C. After washing, cells were resuspended in FCM buffer and analyzed on a Gallios flow cytometer (Beckman Coulter). The following fluorochrome-conjugated monoclonal antibodies and life/dead stains were used: DNAM-1-FITC (clone DX11, BD Bioscience, #559788), TIGIT-APC (clone 741182, R&D systems, #FAB7898A), CD96-BV421 (clone NK92.39, Biolegend, #338418), CD96-PE-Dazzle (clone NK92.39, Biolegend, #338414) CD19-FITC (clone HD37, DAKO, #F0768), CD3-ECD (clone UCHT1, Beckman coulter, #A07748), CD14-PECy7 (clone HCD14, Biolegend, #325618), CD56-BV510 (clone HCD56, Biolegend, #318340), CD45-AF700 (clone HI30, Biolegend, #304024), KLRG-1 FITC (clone REA261, Miltenyi Biotec, #130-103-640), LIGHT PE (clone 7-3(7), eBioscience, #12-2589-42), CD160 PE-Cy7 (clone BY55, Biolegend, #341211), 4-1BB APC (clone 4B4-1, BD Bioscience, #220890), CD57 BV421 (clone NK-1, BD Bioscience, #563896, SIGLEC-9 FITC (clone REA492, Miltenyi Biotec, #130-107-607), SIGLEC-7 APC (clone 6-434, Biolegend, #339206), NKG2C PE (clone 134591.0, R&D Systems, #FAB138P), NKG2D PE-Cy7 (clone 1D11, Biolegend, 320812), NKp46 BV421 (clone 9E2, Biolegend, #331914), NKG2a APC (clone Z199, Beckman Coulter, #A60797), PD-1 BV421 (clone EH12.1, BD Bioscience, #562516), BTLA PE (clone J168-540, BD Bioscience, #558485), OX-40 PE-Cy7 (clone Ber-ACT35, Biolegend, #350011), 2B4

FITC (clone C1.7, Biolegend, #329506), CD112 PE-Cy7 (clone TX31, Biolegend, #337414), CD155 BV421 (clone SKII.4, Biolegend, 337631), fixable viability dye eFluor780 (eBiosciences, #65-0865-14) and 7-AAD (Sigma, #A9400-1MG). All flow cytometric data was analyzed with Kaluza 2.1 software from Beckman Coulter.

NK cell activity assay

Isolated NK cells were plated in a flat bottom 96 wells plate (Corning Star) at 100.000 cells/well and cultured overnight in IMDM supplemented with 10% FCS in the presence of 1nM rhIL-15 (Immunotools). The next day, NK cells were co-cultured with OC cell lines SKOV-3, IGROV-1, OVCAR-3 or K562 target cells (100.000 cells per well for all cell lines) in the presence of 10 ?g/ml anti-TIGIT hIgG1.3 FC silenced blocking antibody (Bristol-Myers Squibb), hIgG 1.3 FC silenced isotype control (Bristol-Myers Squibb), anti-DNAM-1 (clone 11A8, Biolegend, #338302), anti-CD96 (clone NK92.39, Biolegend, #338402) or hIgG1 (clone MOPC, BioXcell, BE0083). In addition, CD107a-PECy7 (clone H4A3, Biolegend, #328618) and Brefeldin A (BD, #555029) were added to the culture. All conditions were performed in triplicate. After 4h, cells were harvested and washed with PBS. After subsequent staining for CD56-APC (clone HCD56, Biolegend, #318310), CD45-AF700 and eFluor780 for 20 minutes at 4°C, cells were intracellularly stained for IFNγ-FITC (clone B27, BD Bioscience, #554700) with fixation/permeabilization buffer (eBioscience, #00-5123-43, #005223-56 and #00-8333-56) according to manufacturer's instructions. Cells were analysed on the Gallios flow cytometer.

In vivo SKOV-3 NK cell phenotype tumor model

All *in vivo* experiments were approved by the Radboudumc animal care and user committee (DEC 2015–123). Ten 6–20 weeks old female NOD/SCID/IL2Rgnull (NSG) mice (Jackson laboratories), with an average weight of 25 g, were divided randomly into two groups. One group received an intraperitoneal (i.p.) infusion with 1.0 × 106 SKOV-3-GFP-Luc cells and the control group received a PBS injection. Bioluminescence imaging (BLI) was performed weekly until saturation. For this, mice were injected i.p. with 150 mg/kg D-luciferin (PerkinElmer 122796), anesthetized with isoflurane and after 10 min bioluminescence images were collected in an IVIS using the Living Image processing software. Regions of Interest (ROIs) were drawn around the abdominal area, and measurements were automatically generated as integrated flux of photons (photons/s). After 49 days, all mice received i.p. peripheral blood NK cell infusion (3.8 × 106 cells/mouse) derived from a healthy donor. In addition, all mice received i.p. recombinant human rhIL-15 (2.5 μg/mouse, Immunotools, 11340158) every 2 days. Fourteen days after NK cell infusion, mice

were sacrificed and an abdominal lavage was performed with 8 mL PBS. NK cells from this lavage were used for NK cell activity assays and phenotyping.

In vivo SKOV-3 NK cell plus TIGIT blockade tumor model

Forty-five 6–20 weeks old female NOD/SCID/IL2Rgnull (NSG) mice (Jackson laboratories), with an average weight of 24 g, were divided randomly into three groups. All groups received an intraperitoneal (i.p.) infusion with 0.2 × 106 SKOV-3-GFP-Luc cells. BLI imaging was performed weekly as described above. After 4 days, two groups received an i.p. peripheral blood NK cell infusion (5.4 × 106 cells/mouse) derived from a healthy donor. In addition, all mice received i.p. recombinant human rhIL-15 (2.5 µg/mouse, Immunotools, 11340158) every 2 days and weekly injections of nanogram. Mice receiving NK cells were also injected twice weekly with either isotype control B12-LALAPG Fc silenced antibodies (custom ordered, Evitrea) or anti-TIGIT hIgG1.3 Fc silenced blocking antibodies (Bristol-Myers Squibb). Control mice not receiving NK cells were also treated with isotype control B12-LALAPG Fc silenced antibodies. Thirty-three days after SKOV-3 tumor cell infusion, mice were sacrificed and an abdominal lavage was performed as described above. Harvested cells were quantified using Flow-Count Fluorospheres (Beckman Coulter, 7547053) according to manufacturer's instructions. NK cells from this lavage were used for an NK cell activity assay.

StatisticsData analysis was conducted by Prism software (GraphPad, version 5.03 for Windows) and SPICE software (version 5). For normally distributed data the Student t-test (paired or unpaired) or One-way ANOVA (with or without repeated measure) was used where applicable as stated in the figure legends. Non-normally distributed data were tested with a Wilcoxon signed-rank test, Mann-Whitney test, Kruskal-Wallis or Friedman test where applicable as stated in the figure legends. For statistical comparison of SPICE pie charts, the built-in test in SPICE software was used, applying 1,000,000 permutations. A p-value of <0.05 was considered statistically significant.

Results

Peritoneal NK cells of OC patients consist of multiple distinct CD56dim subpopulations which have reduced DNAM-1 expression

Flow cytometric analysis was performed on peritoneal NK cells from OC patients, peritoneal NK cells from patients with benign conditions, and peripheral blood NK cells from healthy donors to determine the DNAM-1, TIGIT, and CD96 expression levels on CD56 positive NK cell subsets. For this, we analyzed $CD56^{dim}$ and $CD56^{bright}$ NK cells derived from ascites of high-grade serous OC patients (N = 9) and compared them to healthy donors (N = 10, Figures 1A-C). $CD56^{dim}$ and $CD56^{bright}$ NK cells were defined as shown in Supplemental fig S1A-E for malignant ascites of patients, healthy donor peripheral blood and benign peritoneal fluid. We confirmed that DNAM-1 expression was significantly reduced in both peritoneal $CD56^{dim}$ and $CD56^{bright}$ NK cells from OC patients (51.8% ± 23.4% and 64.1% ± 13.6%, respectively; Figure 1B) compared to healthy donor NK subsets (90.9% ± 7.7 and 91.8% ± 7.4%, respectively; Figure 1B). Notably, TIGIT expression was similar for ascites-derived NK cells and healthy donor NK cells, with higher expression on $CD56^{dim}$ compared to $CD56^{bright}$ NK cells Figure 1B. Expression of CD96 was significantly higher in both $CD56^{dim}$ and $CD56^{bright}$ NK cell subsets in ascites (84.2% ± 9.3% and 95.1% ± 3.0%, respectively; Figure 1B) compared to healthy donor NK cells (44.1% ± 28.2% and 78.8% ± 13.6%, respectively; Figure 1B). In a separate experiment, we also assessed the phenotype of peritoneal fluid NK cells of benign patients and found intermediate DNAM-1 positivity in CD56dim and CD56bright NK cells (69.7% ± 25.8% and 62.4% ± 11.7%, respectively) as shown in Supplemental fig S1F. CD96, similarly to DNAM-1 was moderately positive in $CD56^{dim}$ and $CD56^{bright}$ NK cells in benign peritoneal fluid (50.7% ± 26.6% and 90.1% ± 8.7%, respectively). Unfortunately, TIGIT expression of benign patients could not be compared directly because of a different fluorescence intensity of the antibody used in the two different studies. These data reveal that the balance shifts toward higher expression of inhibitory receptor CD96 while activating receptor DNAM-1 is reduced on peritoneal NK cells of OC patients.

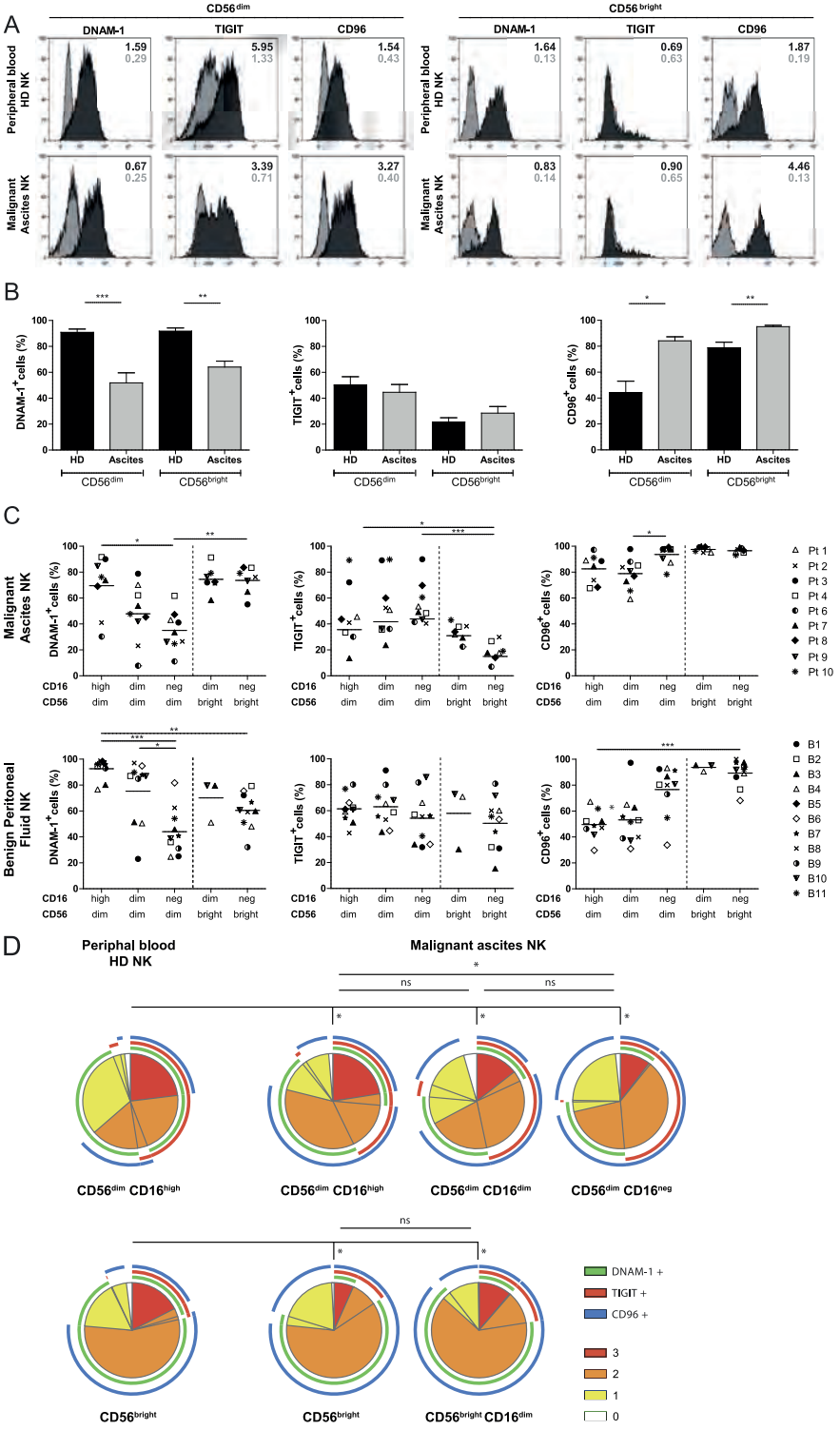
A
CD56dim
CD56bright
DNAM-1
TIGIT
CD96
Peripheral blood HD NK
Malignant Ascites NK
1.59
0.29
5.95
1.33
1.54
0.43
1.64
0.13
0.69
0.63
1.87
0.19
0.67
0.25
3.39
0.71
3.27
0.40
0.83
0.14
0.90
0.65
4.46
0.13
B
DNAM-1+cells (%)
TIGIT+cells (%)
CD96+cells (%)
HD
Ascites
C
Malignant Ascites NK
Benign Peritoneal Fluid NK
CD16
CD56
high
dim
neg
bright
Pt 1
Pt 2
Pt 3
Pt 4
Pt 6
Pt 7
Pt 8
Pt 9
Pt 10
B1
B2
B3
B4
B5
B6
B7
B8
B9
B10
B11
D
Peripheral blood HD NK
Malignant ascites NK
ns
CD56dim CD16high
CD56dim CD16high
CD56dim CD16dim
CD56dim CD16neg
CD56bright
CD56bright
CD56bright CD16dim
DNAM-1 +
TIGIT +
CD96 +
3
2
1
0

Figure 1: ***NK cell phenotype of the DNAM-1/TIGIT/CD96 pathway in healthy donors and ovarian cancer patients***

(A) *DNAM-1, TIGIT and CD96 expression of healthy donor (HD) peripheral blood and OC patient ascites-derived $CD56^{dim}$ and $CD56^{bright}$ NK cells of a representative HD and OC patient, respectively. In grey the isotype control and in black the marker of interest are depicted. Numbers in the plot represent the median fluorescence intensity.* ***(B)*** *DNAM-1, TIGIT and CD96 expression on $CD56^{dim}$ and $CD56^{bright}$ NK cells of 10 HDs and 9 OC patients. Data is shown as mean+SEM. Kruskal-Wallis with Dunn's Multiple Comparison Test was used for statistical analysis, * $p < 0.05$, ** $p < 0.01$ and *** $p < 0.001$.* ***(C)*** *DNAM-1, TIGIT and CD96 expression in 5 NK subsets, defined by characteristic CD56 and CD16 expression patterns, of 11 benign peritoneal fluids (bottom three panels) and 9 malignant ascites (top three panels). Datapoints with less than 100 events are excluded from the graphs. For a detailed number of cells per datapoint refer to Supplemental fig 1G. Kruskal-Wallis with Dunn's Multiple Comparison Test was used for statistical analysis, * $p < 0.05$, ** $p < 0.01$ and *** $p < 0.001$.* ***(D)*** *Co-expression patterns were determined with SPICE software. The pies depict the average proportion of cells expressing DNAM-1, TIGIT and CD96, and the arcs indicate which receptors are expressed by the corresponding pies. Statistical differences were analyzed using the built-in statistical tool. *$p < .05$; $n = 10$ for HD and $n=9$ for OC patients.*

As expected in healthy donors we observed a clear distinction between $CD56^{dim}$ $CD16^{high}$ and $CD56^{bright}$ $CD16^{neg}$ NK cell subsets, but for peritoneal-derived NK cells, we found altered CD56 and CD16 expression patterns (Supplemental fig S1E). Based on a minimum of 100 events, three distinct populations of $CD56^{dim}$ NK cells were defined; i.e. $CD56^{dim}$ $CD16^{high}$, $CD56^{dim}$ $CD16^{low}$ and $CD56^{dim}$ $CD16^{neg}$ NK cells, each having different expression patterns of DNAM-1, TIGIT and CD96 (Figure 1C, Supplemental fig S1G). In addition, we found the $CD56^{bright}$ $CD16^{neg}$ NK cell subset besides a small $CD56^{bright}$ population with low CD16 expression in some donors, which exhibit similar expression levels of DNAM-1, TIGIT, and CD96. The conventional $CD56^{dim}$ $CD16^{high}$ NK cells seemed similar in OC patients and healthy donors, but with slightly lower DNAM-1 expression and higher CD96 expression in OC. Interestingly, within the three ascites-derived $CD56^{dim}$ populations, DNAM-1 expression gradually decreased in parallel with decreasing CD16 expression Figure 1C. In contrast, CD96 expression significantly increased with loss of CD16 expression, while TIGIT expression remained unaltered and is exclusively expressed by the $CD56^{dim}$ populations in malignant ascites. $CD56^{dim}CD16^{high}$ NK cells from benign patients resemble healthy donor peripheral blood NK cells with a high percent of DNAM-1 and low percent CD96 relative to malignant ascites-derived NK cells. However, $CD56^{dim}$ $CD16^{low}$ NK cells from benign peritoneal fluid have an equally low percent DNAM-1 and increased percent CD96 as observed in OC patients Figure 1C. To look at these co-expression profiles from a different angle, we performed SPICE analysis. This analysis demonstrated that healthy donor $CD56^{dim}$ NK cells had significantly different co-expression patterns of DNAM, TIGIT, and CD96 compared to the three ascites-derived $CD56^{dim}$ NK cell subsets as healthy donor NK cells expressed more DNAM-1 and less CD96 Figure 1D. Within the three different OC subsets, the $CD56^{dim}$ $CD16^{high}$ NK cells were significantly different

from $CD56^{dim}$ $CD16^{neg}$ NK cells but not $CD56^{dim}$ $CD16^{low}$ NK cells which is mainly attributed by DNAM-1 expression which is high on $CD56^{dim}$ $CD16^{high}$, intermediate on $CD56^{dim}$ $CD16^{low}$ and lowest on $CD56^{dim}$ $CD16^{neg}$ NK cells. As a result, $CD56^{dim}$ $CD16^{neg}$ OC derived NK cells showed an enlarged population with TIGIT/CD96 co-expression whereas the majority of CD16+ NK cells had more CD96/DNAM-1 co-expression indicating that $CD56^{dim}$ $CD16^{neg}$ have a more inhibitory phenotype and $CD56^{dim}$ $CD16^{high}$ a more activatory phenotype these populations have a more inhibitory and activating phenotype, respectively.

Collectively, these data demonstrate that peritoneal NK cells in OC patients display an altered expression pattern of the DNAM-1/TIGIT/CD96 axis compared to healthy donor NK cells that is indicative of a more inhibitory or exhausted phenotype.

Expression of DNAM-1/TIGIT/CD96 axis members on NK cells is increased upon rhIL-15 stimulation and shifts to a more inhibitory phenotype upon engagement with OC tumor cells

To further investigate the effect of OC cells on DNAM-1/TIGIT/CD96 expression levels by NK cells, we co-cultured healthy donor NK cells for one week with OC spheroids, generated from the cell lines SKOV-3, IGROV-1, and OVCAR-3, in the presence of increasing rhIL-15 concentrations to support NK cell survival. DNAM-1, TIGIT, and CD96 expression levels were all upregulated on $CD56^{dim}$ NK cells by rhIL-15, in a dose-dependent manner Figure 2A. Stimulation with either of the OC spheroids resulted in a strong decrease of DNAM-1 expression Figure 2A. In contrast, TIGIT and CD96 expression were not significantly affected by SKOV-3, IGROV-1, or OVCAR-3 spheroids at lower rhIL-15 concentrations. However, with higher levels of rhIL-15, also a trend in reduced CD96 and TIGIT expression was observed in the presence of SKOV-3 and/or IGROV-1 spheroids. In a similar 2D model with primary ascites-derived cell line ASC009, we found comparable results Figure 2B. To validate these results with primary high-grade OC material from a patient, we made a cell suspension of a small piece of tumor tissue and performed a co-culture with healthy donor NK cells for one week in the presence of rhIL-15. Indeed, we found that DNAM-1 was strongly reduced in the presence of primary tumor cells Figure 2C. Also, TIGIT expression was somewhat decreased, but CD96 was not affected. In addition to DNAM-1, TIGIT, and CD96, we also looked at other NK cell checkpoint molecules but found no significant differences between NK cells cultured with or without spheroids (Supplemental fig S2A). There was a trend toward lower NKG2D expression, but this was not significant. We also visualized these expression patterns in SPICE and again no differences between NK cells cultured with or without spheroids were seen.

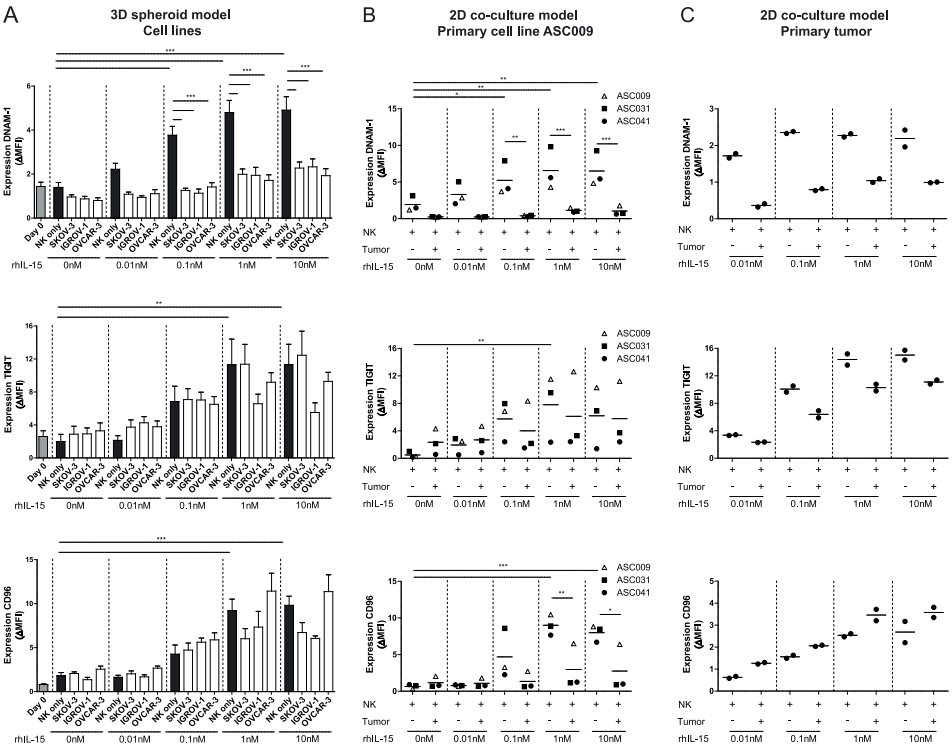

Figure 2: ***DNAM-1, TIGIT and CD96 are dose-dependently upregulated by rhIL-15 and DNAM-1 is downregulated by OC tumor cells***

(A) *DNAM-1 (n = 8), TIGIT (n = 6) and CD96 (n = 5) expression on NK cells of healthy donors co-cultured with SKOV-3, IGROV-1 or OVCAR-3 spheroids and increasing rhIL-15 concentrations for 7 days. Data is shown as mean+SEM. One-Way ANOVA with Bonferroni correction was used for statistical analysis, * p < .05, ** p < .01 and *** p < .001.* ***(B)*** *DNAM-1, TIGIT and CD96 expression on healthy donor NK cells co-cultured with a patient-derived primary tumor cell line and increasing rhIL-15 concentrations for 7 days cultured in duplicate.* ***(C)*** *DNAM-1, TIGIT and CD96 expression on healthy donor NK cells co-cultured with patient-derived tumor cells and increasing rhIL-15 concentrations for 7 days cultured in duplicate*

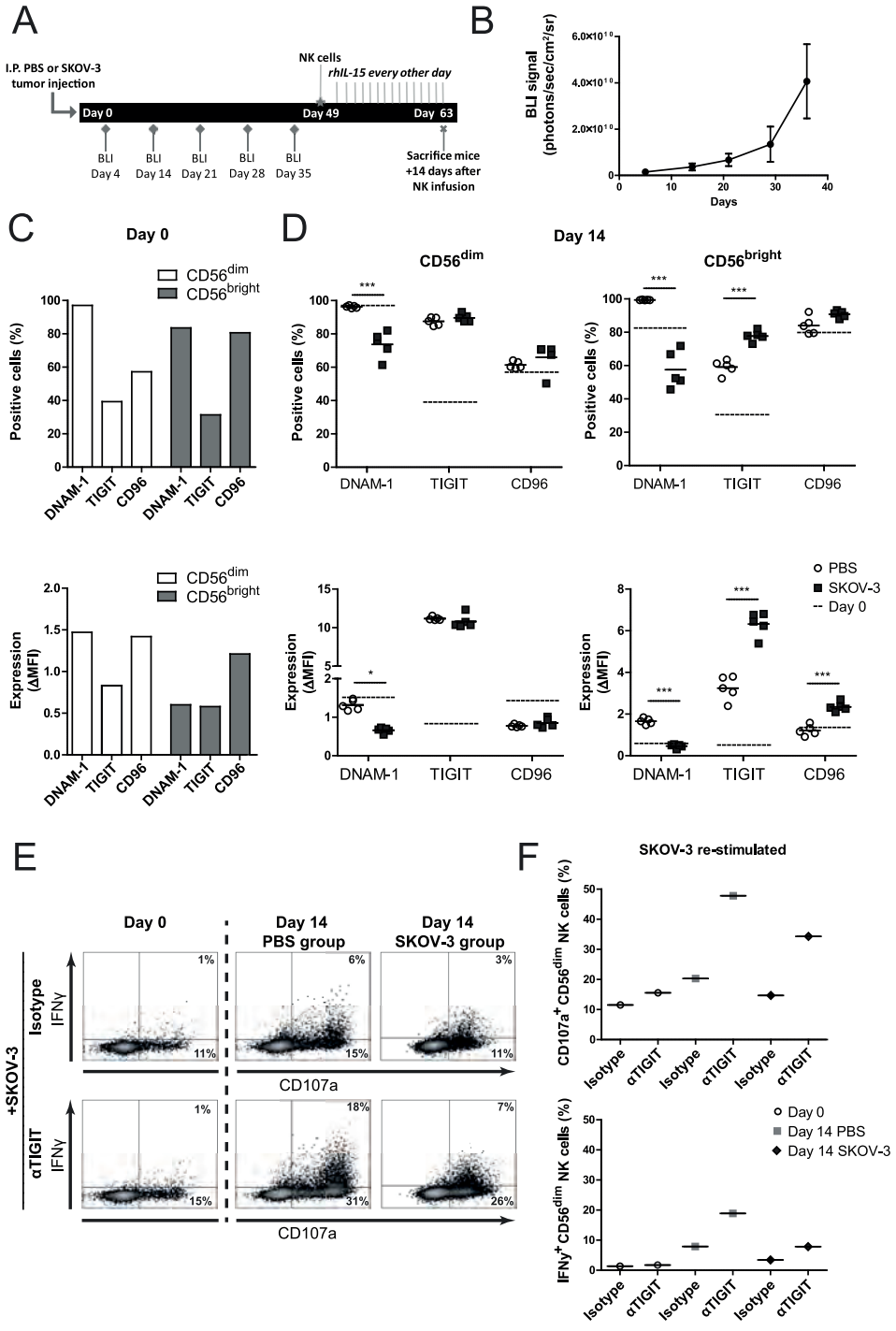
A
I.P. PBS or SKOV-3 tumor injection
NK cells
rhIL-15 every other day
Day 0
Day 49
Day 63
BLI Day 4
BLI Day 14
BLI Day 21
BLI Day 28
BLI Day 35
Sacrifice mice +14 days after NK infusion
B
BLI signal (photons/sec/cm²/sr)
Days
C
Day 0
CD56dim
CD56bright
Positive cells (%)
Expression (ΔMFI)
DNAM-1
TIGIT
CD96
D
Day 14
CD56dim
CD56bright
PBS
SKOV-3
Day 0
E
Day 0
Day 14 PBS group
Day 14 SKOV-3 group
+SKOV-3
Isotype
αTIGIT
IFNγ
CD107a
F
SKOV-3 re-stimulated
CD107a+CD56dim NK cells (%)
IFNγ+CD56dim NK cells (%)
Isotype
αTIGIT
Day 0
Day 14 PBS
Day 14 SKOV-3

Figure 3: ***SKOV-3 tumor bearing mice have significantly reduced DNAM-1 expression in CD56^{dim} and CD56^{bright} NK cells***

(A) *Schematic overview of the mouse experiment.* ***(B)*** *Bioluminescence imaging (BLI) signal of the SKOV-3 tumor-bearing mice over time (n = 5).* ***(C)*** *Expression of DNAM-1, TIGIT and CD96 on CD56dim (left) and CD56bright (right) NK cells by flow cytometric measurement on day 0. The top graphs depict percentage positive cells and the bottom graphs depict ΔMFI.* ***(D)*** *Expression of DNAM-1, TIGIT and CD96 on intraperitoneal NK cells harvested 14 days after adoptive transfer in SKOV-3 tumor-bearing NSG mice and control mice. Day 0 data is represented by dotted lines as a reference. The top graphs depict percentage positive cells and the bottom graphs depict ΔMFI. Cumulative data are shown (lines indicate mean, n = 5 per group). A One-Way ANOVA with Bonferroni correction was used for statistical analysis, * $p < .05$ and *** $p < .001$.* ***(E)*** *Representative plots are shown of CD107a and IFNγ expression by CD56dim NK cells after 4 h co-culture with SKOV-3 target cells, low dose rhIL-15 and TIGIT blockade or matching isotype control. (F) The percentage of CD107a and IFNγ expressing CD56dim NK cells are shown on day 0 and day 14. Day 14 results are pooled NK cells from 5 different mice from either tumor-bearing or control mice*

Next, we investigated whether engagement of NK cells with OC tumors *in vivo* also alters DNAM-1/TIGIT/CD96 expression levels. For this, SKOV-3 tumor-bearing NSG mice were infused intraperitoneally with healthy donor NK cells Figures 3A and b. rhIL-15 was given every other day to support NK cell persistence, and after 14 days NK cells were harvested by peritoneal lavage. Flow cytometry analysis showed that NK cells from SKOV-3 bearing mice had significant lower DNAM-1 expression on both CD56^{dim} and CD56^{bright} NK cells compared to NK cells from non-tumor bearing control mice Figures 3C-D. TIGIT expression of CD56dim NK cells was not affected by *in vivo* exposure to SKOV-3 tumors. Similarly to the in vitro OC spheroid model, rhIL-15 had a potent stimulatory effect on TIGIT expression as the ΔMFI (delta Median Fluorescence Intensity) was strongly increased at day 14 compared to day 0. DNAM-1 and CD96 levels were similar on the day of infusion and harvesting. To determine the functional implication of TIGIT expression *in vivo* on non-exposed and OC-exposed NK cells, we analyzed their reactivity at the single-cell level upon ex vivo re-stimulation with SKOV-3 cells in the absence and presence of TIGIT blocking antibody Figures 3E-F. Interestingly, TIGIT blockade increased degranulation and IFNγ production activity of NK cells harvested from either SKOV-3 tumor-bearing mice or control mice Figures 3E-F. To assess, the importance of other checkpoint molecules besides DNAM-1 and TIGIT, we assessed expression levels of 4–1BB, CD57, 2B4, NKG2D, NKp46, LIGHT, CD160, BTLA, OX-40, PD-1, NKG2a, SIGLEC-7, SIGLEC-9, and KLRG-1: only KLRG-1 showed a decrease in the presence of tumor (Supplemental fig S2B).

Altogether, these data indicate that DNAM-1 and TIGIT are both upregulated by NK cells in response to rhIL-15 in a dose-dependent manner, while DNAM-1 expression is strongly decreased following exposure to OC cell line spheroids or patient-derived tumor cells.

TIGIT blockade effectively enhances degranulation and IFNγ production by OC-reactive CD56^{dim} NK cells

We next analyzed the effects of TIGIT versus DNAM-1 blockade on NK cell responses against OC in more detail. First, we addressed this for healthy donor NK cells, as these cells appear more functional based on their phenotype and have higher DNAM-1 compared to ascites-derived NK cells Figure 1. Hereto, mononuclear cells (MNCs) or CD56-enriched cells (by negative selection) were rested overnight with low dose (1 nM) rhIL-15. This revealed that DNAM-1 is somewhat upregulated on CD56^{dim} NK cells in the isolated fraction, while TIGIT was significantly enhanced only in CD56^{dim} NK cells in the non-selected MNC situation (Supplemental fig S3A-B). Notably, CD96 was upregulated on both CD56^{dim} and CD56^{bright} NK cells in all tested conditions. Interestingly, malignant ascites-derived NK cells showed similar expression patterns as healthy donor NK cells (Supplemental fig S4A-C). As overnight resting of enriched NK cells in the presence of rhIL-15 did not affect TIGIT expression, we continued with 1 nM rhIL-15 for subsequent TIGIT blocking studies using the three different OC cell lines as targets. Unstimulated NK cells and rhIL-15 stimulated NK cells showed little to no degranulation and IFNγ production, whereas NK cells stimulated with K562 and rhIL-15 showed a strong response in both degranulation and IFNγ (Supplemental fig S5A). Fold change of CD107a and IFNγ response was calculated compared to tumor cell stimulation in the presence of rhIL-15. TIGIT blockade resulted in a 36% (± 16%) increase in degranulation and 31% (± 14%) increase in IFNγ production against SKOV-3 by healthy donor CD56^{dim} NK cells Figure 4A. In contrast, CD56^{bright} NK cells did not respond to TIGIT blockade as these cells lack TIGIT expression (Supplemental fig S5B). As expected, DNAM-1 blockade effectively inhibited the degranulation and IFNγ response of CD56dim Figure 4A and CD56^{bright} (Supplemental fig S4A-B) NK cells toward SKOV-3. Simultaneous TIGIT and DNAM-1 co-blockade still impaired degranulation and IFNγ production by healthy donor NK cells, indicating that DNAM-1 triggering is more dominant in regulating OC-reactivity of NK cells (Supplemental fig S5C). Notably, single CD96 blockade, or co-blockade of CD96 with TIGIT or DNAM did not affect NK cell functionality. Similar results were found with the OC cell lines IGROV-1 and OVCAR-3 (Figure 4B and Supplemental fig S5D).

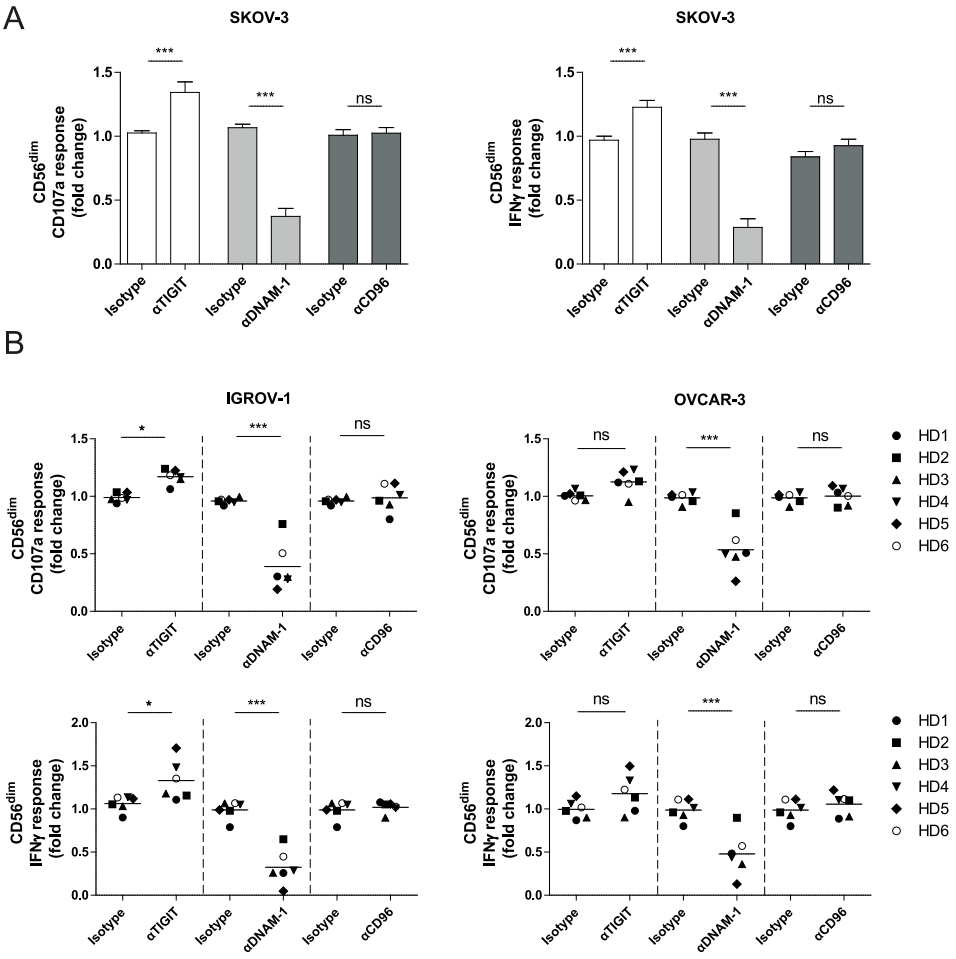

Figure 4: ***CD56^{dim} NK cell degranulation towards OC cell lines is boosted by TIGIT blockade and inhibited by DNAM-1 blockade***

(A) *Healthy donor CD56dim NK cells fold change for CD107a and IFNγ after 4 h stimulation with SKOV-3 target cells, low dose rhIL-15, and TIGIT, DNAM-1 and/or CD96 blockade or matching isotype controls. Fold change in CD107a and IFNγ expression on CD56^{dim} cells following antibody treatment is calculated relatively to the condition with low dose rhIL-15 and 4 h SKOV-3 stimulation only. Cumulative data are shown as mean+SEM (n = 6)* ***(B)*** *IGROV-1 and OVCAR-3 stimulation for 4 h in the presence of TIGIT and/or DNAM-1 blockade or matching isotype controls. Fold change in CD107a and IFNγ expression on CD56^{dim} cells following antibody treatment is calculated relatively to the condition with low dose rhIL-15 and 4 h IGROV-1 or OVCAR-3 stimulation only −3 (n = 6 for IGROV-1 and n = 6 for OVCAR). A One-Way repeated measure ANOVA with Bonferroni correction was used for statistical analysis, * p < .05, ** p < .01 and *** p < .001*

We observed that TIGIT blockade was most effective in improving NK cell reactivity against SKOV-3 and IGROV-1, but less prominent for the OVCAR-3 cell line. This correlated with CD155 expression but not CD112, as CD155 was absent on

OVCAR-3 in contrast to high levels observed on both SKOV-3 and IGROV-1, while all three cell lines had medium to high expression of CD112 Table 2. To elucidate which TIGIT/DNAM-1 ligand, CD112, or CD155, is most dominant in NK cell reactivity against OC tumor cells, siRNA-treated SKOV-3 cells were used with substantially reduced CD112 or CD155 expression (Supplemental fig S6A). Decreased siRNA-mediated CD155 expression significantly lowered NK cell reactivity against SKOV-3 cells, whereas CD112 knockdown did not have a clear effect (Supplemental fig S6B-C).

Table 2 : ***Ovarian cancer (primary) cell line characteristics***

Cell line	CD112 Expression (ΔMFI±SD)	CD155 Expression (ΔMFI±SD)
SKOV-3	49.7 (±8.0)	1040 (±197)
IGROV-1	31.3 (±15.5)	1050 (±350)
OVCAR-3	24.7 (±15.3)	783 (±215)
ASC009	22.7 (±4.9)	1567 (±116)

CD112 and CD155 expression of ovarian cancer cell lines. SKOV-3, OVCAR-3, IGROV-1 and ASC009 were all acquired on three different time points. Data shown is the average ΔMFI with standard deviation.

Together, these data demonstrate that TIGIT blockade enhances degranulation and IFNγ production of healthy donor $CD56^{dim}$ NK cells in response to OC tumor cells, especially when appropriate DNAM-1/CD155 interactions are in place.

$CD56^{dim}$ NK cell functionality can be elevated by TIGIT blockade in an *in vivo* mouse model and in a subset of OC patients

Having demonstrated that healthy donor NK cell reactivity against OC tumor cells can be boosted by TIGIT blockade, we next investigated whether this effect was also apparent in more clinically relevant models. For this, SKOV-3 tumor-bearing NSG mice were infused intraperitoneally with healthy donor NK cells and treated with TIGIT blockade or isotype control twice weekly Figure 5A. rhIL-15 support was given during the 4 weeks in which we acquired tumor load weekly by BLI. NK cell treated mice showed significantly less tumor load compared to no treatment ($P < .05$, Figure 5B). Importantly, NK cell treatment combined with TIGIT blockade resulted in a stronger reduction in tumor load compared to no treatment ($P < .001$). The number of NK cells harvested at day 33 was similar for both groups Figure 5C. In addition, we performed a degranulation assay on NK cells harvested from each mouse and found that NK cells from mice that had been treated with TIGIT blockade had a

significant higher capacity to degranulate and secreted more IFNγ compared to mice that received the isotype control Figure 5D. When NK cells from isotype control treated mice were re-stimulated with SKOV-3, subsequent ex vivo TIGIT blockade strongly enhanced their CD107a and IFNγ levels Figure 5e. DNAM-1 blockade and DNAM-1/TIGIT co-blockade, resulted in a similar reduced degranulation capacity as we observed in our in vitro model.

Finally, we investigated TIGIT blockade in ascites-derived NK cells. For this, ascites samples were selected that were collected at diagnosis or first surgery of patients with stage III or IV high-grade serous papillary OC. Patient-derived CD56 positive NK cells were isolated and cultured overnight with low dose (1 nM) rhIL-15 and stimulated with K562 or OC target cells for 4 h. Though heterogeneous, similar degranulation and IFNγ responses against K562 were observed overall for ascites-derived and healthy donor $CD56^{dim}$ NK cells figure 5F. In contrast, ascites-derived NK cells from several OC patients showed impaired responsiveness to SKOV-3 as compared to healthy donors Figure 5G.

Based on the SKOV-3 degranulation response, patients were grouped in responders (≥10% CD107a+ $CD56^{dim}$ cells) and non-responders (<10% CD107a+ $CD56^{dim}$ cells; Figure 5G and Table 1). Next, we compared the response against K562 for both non-responders versus responders. Also here we noticed that $CD56^{dim}$ NK cells from non-responders exhibited impaired tumor responsiveness, indicating a more general impairment of the NK cells in these particular patients (Supplemental fig S7A and B). Notably, TIGIT blockade was unable to rescue the NK functionality in these non-responders Figure 5H. Most importantly, TIGIT blockade of $CD56^{dim}$ NK cells in responders resulted in significantly enhanced degranulation and IFNγ production activity Figure 5H. Simultaneous blockade of TIGIT and DNAM-1 reversed this effect, and again inhibited the degranulation and IFNγ production by ascites-derived NK cells. This indicates that also in this setting DNAM-1 triggering is more dominant in NK-mediated targeting of OC tumor cells. Altogether, our data demonstrate that TIGIT blockade boosts functional responsiveness of $CD56^{dim}$ NK cells in patients with baseline reactivity against OC tumor cells.

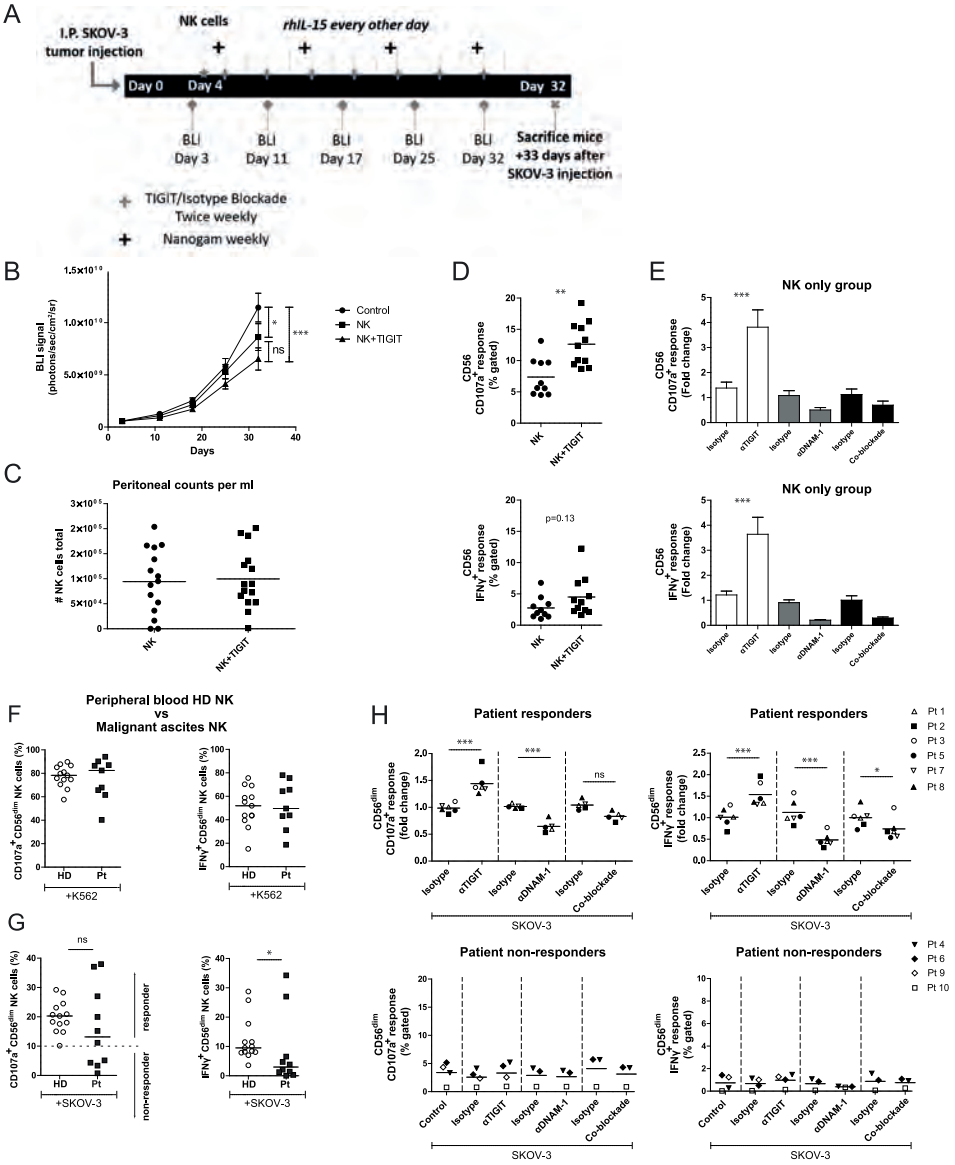

Figure 5: ***TIGIT blockade boosts functional responsiveness of CD56^{dim} NK cells of OC patients with a baseline reactivity against SKOV-3 cells***

(A) *Schematic overview of the mouse experiment.* ***(B)*** *Bioluminescence imaging (BLI) signal of SKOV-3 tumor-bearing mice over time in "control", "NK" only and "NK+TIGIT" blockade groups (n = 15 per group).* ***(C)*** *Total number of peritoneal NK cells harvested from "NK" only and "NK+TIGIT" blockade groups as measured by flow cytometry (average of bead and volume count cytoflex).* ***(D)*** *Percent CD107a (top graph) and IFNγ (bottom graph) from peritoneal NK cells harvested from "NK" only and "NK+TIGIT" groups which were re-stimulated ex-vivo with SKOV-3 for 4 h in the presence of low dose rhIL-15.* ***(E)*** *Percent CD107a (top graph) and IFNγ (bottom graph) from peritoneal NK cells harvested from "NK" only group re-stimulated with SKOV-3 in the presence of low dose rhIL-15 in combination with TIGIT, DNAM-1, TIGIT/DNAM-1 co-blockade or corresponding isotype control(s).* ***(F-G)*** *Percentage CD107a+ and*

IFNγ+ CD56^{dim} NK cells upon overnight treatment with low dose rhIL-15 (1 nM) and subsequent 4 h stimulation with K562 ***(F)*** *or SKOV-3* ***(G)****. Based on a cutoff of 10% CD107a expression on CD56^{dim} NK cells co-cultured with SKOV-3 and rhIL-15 (without additional treatment) patients were subdivided in responder (≥10%) and non-responder (<10%) cohorts. Cumulative data of healthy donors (HD; n = 10) and ovarian cancer patients (Pt; n = 9) are shown with median. The Mann-Whitney test was used for statistical analysis, * p < .05. (h) CD56^{dim} NK cells positive for CD107a and IFNγ after 4 h stimulation with SKOV-3 target cells, low dose rhIL-15 (1 nM), and TIGIT and/or DNAM-1 blockade or matching isotype controls. Cumulative data shown for SKOV-3 responders only (lines indicate mean, n = 6). A One-Way ANOVA with Bonferroni correction was used for statistical analysis, * p < .05 and *** p < .001*

Discussion

NK cells are regulated via activating and inhibitory receptors, and the net balance of these signals determines whether an NK cell will tolerate or kill a target cell [43,44]. Due to this nature, NK cells have the ability to recognize and destruct tumor cells with increased expression of stress-induced activating ligands and a lack of inhibitory signals. Interestingly, many studies have demonstrated that OC cells are susceptible to killing by activated NK cells [7–9], hinting that NK cell-based immunotherapy could be an attractive adjuvant treatment for OC patients. However, NK cell antitumor immunity in OC patients can be attenuated by immunosuppressive cells and cytokines within the tumor microenvironment [13–16]. Here, we investigated the role of the DNAM-1/TIGIT/CD96 axis on NK cells in the context of OC. We found that peritoneal NK cells of OC patients consist of different CD56^{dim} subpopulations with reduced DNAM-1 and high TIGIT and CD96 expression, which to a lesser extent can also be found for benign patient peritoneal fluid-derived NK cells. This shift to a more inhibitory phenotype could also be induced in vitro by co-culturing healthy donor NK cells with OC tumor spheroids and *in vivo* upon infusion into SKOV-3 OC bearing NSG mice. Other important NK cell receptors such as PD-1, NKG2a, and OX-40 were not affected by interaction with OC cells and spheroids. Interestingly, we were able to counteract DNAM-1 downregulation by adding rhIL-15 to the NK cell-tumor co-cultures, which resulted in a dose-response increase of DNAM-1, TIGIT, and CD96.

The 5 subsets with different DNAM-1/TIGIT/CD96 expression patterns detected in benign and malignant ascites can be induced by a number of factors. First, a study after hematopoietic stem cell transplantation showed that cryopreserved peripheral blood-derived NK cells show a population of CD56^{dim}CD16^{neg} NK cells that decreases after time which was not observed with fresh cells [45]. However, they could replicate this finding using fresh cells that were stored at room temperature for 24 h indicating a relationship between NK cell viability and this CD56^{dim}CD16^{neg} population. Other studies have shown that TGF-β is able to convert a subset of CD56$^{dim/bright}$CD16^{high} NK cells to a CD56$^{dim/bright}$CD16$^{low/neg}$ phenotype [46,47].

Additionally, TGF-β has been shown to downregulate DNAM-1 and increase CD96 expression on NK cells which is in agreement with our observations [46,48–50]. Since TGF-β is known to be present in ascites of OC patients this cytokine may play a role in the altered phenotype of the detected subsets. However, benign patients where the levels of TGF-β may be lower also showed a high frequency of $CD56^{dim}CD16^{neg}$ NK cells. Additionally, CD96 levels on peritoneal NK cells of benign patients appear similar to healthy donor peripheral blood NK cells. Therefore, other factors, such as NK cell activation status, NK cell viability, cytokine stimulation, and tumor cell interaction may be involved to the observed phenotypical alterations in peritoneal NK cells.

In order to functionally boost NK cell reactivity against OC cells, we tested TIGIT blockade. First, in healthy donors, we found that TIGIT blockade enhanced degranulation and IFNγ production of healthy donor $CD56^{dim}$ NK cells in response to OC tumor cells, especially when DNAM-1/CD155 interactions were in place. In our models, CD96 blockade did not improve nor hamper NK cell functionality, though we cannot exclude the possibility that the used CD96 antibody clone and/or ex vivo model-related factors have impacted the results. Most interestingly, we observed that TIGIT blockade boosted functional responsiveness of CD56dim NK cells of OC patients with a baseline reactivity against SKOV-3 OC cells.

Inhibitory phenotypes on NK cells, or on other cell types, are commonly described in the context of cancer as for example melanoma patients have an increased proportion of $CD56^{dim}$ $CD16^{neg}$ NK cells in tumor biopsies and their prevalence negatively correlated with lytic ability [51]. Our results suggest that these $CD56^{dim}$ $CD16^{neg}$ cells have a more inhibitory phenotype compared to $CD56^{dim}$ $CD16^{high}$ and $CD16^{low}$ NK cells as they had the lowest DNAM-1 levels, high TIGIT expression and the highest CD96 expression of the three $CD56^{dim}$ subsets in both OC patients and patients with benign conditions. CD96+ NK cells have recently been described to be functionally exhausted with impaired cytokine production which, together with DNAM-1 downregulation, supports that $CD56^{dim}$ $CD16^{neg}$ NK cells acquired a more inhibitory phenotype [50]. CD96 was also strongly increased by NK cells in SKOV-3 OC bearing NSG mice indicating that, next to TIGIT, it may be an interesting target for future blocking studies in OC. Loss of CD16 in the $CD56^{dim}$ $CD16^{neg}$ and $CD16^{low}$ populations could be due to protein downregulation or CD16 shedding after degranulation as a result of tumor cell contact since CD16 shedding is known to strongly correlate with increased CD107a expression [52,53]. In turn, DNAM-1 also decreases upon tumor cell contact [34]. Therefore, it is possible that $CD56^{dim}$ $CD16^{high}$ NK cells may become $CD56^{dim}$ $CD16^{low}$ and later $CD56^{dim}$ $CD16^{neg}$ during

continuous OC tumor engagement but future studies will have to elucidate this phenomenon in more detail.

In our assays, we used rhIL-15 for NK cell survival and found that TIGIT and DNAM-1 expression was increased by rhIL-15 in a dose-dependent manner which is in accordance with literature [37,54,55]. However, after co-incubation of healthy donor NK cells with OC tumor cell spheroids, DNAM-1 expression was strongly reduced and levels were comparably low as ascites-derived NK cells of OC patients. This is in line with our previous results and other studies showing a reduced expression of DNAM-1 on NK cells in OC patients [34,35]. We validated these findings in an *in vivo* model and found that DNAM-1 expression on adoptively transferred NK cells was reduced in SKOV-3 OC bearing mice compared to mice without tumor. In contrast, TIGIT was strongly upregulated in all mice due to rhIL-15 administration to boost NK cell persistence, which is in accordance with our in vitro data where we also found increased TIGIT levels upon rhIL-15 stimulation. Carlsten et al. showed that CD155 expression specifically reduces DNAM-1 on NK cells by demonstrating that a cell line overexpressing CD155 induced a DNAM-1 reduction whereas CD155 negative cells did not. In addition, they showed that CD155 expression on OC tumor cells from patients negatively correlates with NK cell DNAM-1 expression and that co-culture of NK cells and OC cell lines results in DNAM-1 downregulation in a contact-dependent manner [9,34]. These data fit with our findings but we did not find a correlation between CD155 expression and DNAM-1 downregulation, as OVCAR-3 which had the lowest CD155 expression, equally downregulated DNAM-1 compared to SKOV-3 and IGROV-1 which had high CD155 expression levels. This suggests that, besides CD155, ligation with other ligands such as CD112 or other factors may also reduce DNAM-1 expression on NK cells. This is supported by a study in AML patients where blast CD112 expression was negatively correlated with DNAM-1 expression on NK cells [32].

Our data show for the first time that TIGIT blockade can enhance NK cell responsiveness toward OC. A beneficial effect of TIGIT blockade on NK cells has already been demonstrated in colon cancer and breast cancer [39,40]. We determined that in SKOV-3 tumor-bearing mice TIGIT blockade yielded more active NK cells compared to control NK cells that did not receive TIGIT blockade. Compared to untreated SKOV-3 tumor-bearing mice, the tumor load was more significantly decreased in NK cell and TIGIT blockade treated mice compared to mice that only received NK cells. Similarly, we observed that TIGIT blockade was able to improve degranulation and IFNγ production activity of $CD56^{dim}$ NK cells from patients with an in vitro baseline response toward SKOV-3 tumor cells. This supports that TIGIT blockade in OC could be a potential immunotherapy for patients with high-grade OC

who are now faced with limited treatment options. Our cohort of OC patients was too small to find a correlation between clinical parameters and in vitro responders versus non-responders, but a subset of patients evidently showed strongly diminished NK cell reactivity toward OC cells (e.g. SKOV-3). However, these non-responders also showed an impaired response toward K562 target cells, which lack MHC-I expression and are thereby highly sensitive to NK cell attack. It would be interesting to determine the in vitro SKOV-3 response of OC patients in the ongoing clinical trial with TIGIT blockade (NCT03628677) and verify whether they observe a similar distribution of responders/non-responders and whether this correlates with clinical outcome of TIGIT blockade. Besides validating our findings it would also be intriguing to unravel the mechanisms underlying non-responsiveness of patient-derived NK cells. One possibility is that these NK cells have a strong inhibitory signature and express few activating receptors leading to an inability to respond to OC tumor cells which we currently investigate in a larger cohort. Another explanation could be that factors in ascitic fluid mediated such a strong inhibitory response that tumor exposure could not re-activate these NK cells. Notably, we found that TIGIT blockade alone was not sufficient to rescue these non-responding NK cells of OC patients. To further investigate the interactions within the DNAM-1/TIGIT pathway we performed co-blockade experiments and observed a net inhibition of NK cell function. Therefore, we concluded that DNAM-1 is the dominant receptor within this checkpoint axis in our OC models. To obtain the highest clinical benefit of TIGIT blockade, probably DNAM-1 needs to be concomitantly upregulated. Accordingly, we demonstrated that TIGIT responsiveness was highest in non-tumor bearing mice, which can be attributed to higher DNAM-1 expression, as compared to tumor-bearing mice. The importance of the DNAM-1 receptor in the context of OC is underscored by our previous study where we showed that OC patients with poor OS have lower DNAM-1 expression on ascites NK cells than patients with a better OS [35].

Overall, our data show that checkpoint molecules TIGIT/DNAM-1 play an important role in NK cell responsiveness against OC, and provides rationale for incorporating TIGIT interference in NK cell-based immunotherapy in OC patients. We demonstrate that DNAM-1 expression can be upregulated by rhIL-15 suggesting that TIGIT checkpoint blockade efficacy in OC patients may be optimal in combination with rhIL-15-based stimulation. TIGIT blockade Is a highly appealing strategy to boost NK cell functionality as multiple ongoing clinical trials (NCT02794571, NCT03119428, NCT03563716, and NCT03628677) currently investigate the safety, tolerability, and efficacy of TIGIT blockade in patients with advanced metastatic cancers. Since NK cell-based transfer strategies have been shown safe without causing toxicity in multiple cancer types, NK cell adoptive transfer in combination with TIGIT blockade and rhIL-15 could be a promising immunotherapeutic approach in OC patients.

References

1. Ahmed N, Stenvers KL. *Getting to know ovarian cancer ascites: opportunities for targeted therapy-based translational research.* Front Oncol. 2013;3:256.

2. Siegel RL, Miller KD, Jemal A. *Cancer statistics, 2017. CA* Cancer J Clin. 2017;67(1):7–16.

3. James FR, Jiminez-Linan M, Alsop J, Mack M, Song H, Brenton JD, Pharoah PDP, Ali HR. *Association between tumour infiltrating lymphocytes, histotype and clinical outcome in epithelial ovarian cancer*. BMC Cancer. 2017;17(1):657.

4. Zhang L, Conejo-Garcia JR, Katsaros D, Gimotty PA, Massobrio M, Regnani G, Makrigiannakis A, Gray H, Schlienger K, Liebman MN, et al. *Intratumoral T cells, recurrence, and survival in epithelial ovarian cancer*. N Engl J Med. 2003;348(3):203–213.

5. Hwang WT, Adams SF, Tahirovic E, Hagemann IS, Coukos G. *Prognostic significance of tumor-infiltrating T cells in ovarian cancer: a meta-analysis*. Gynecol Oncol. 2012;124(2):192–198.

6. Webb JR, Milne K, Watson P, deLeeuw RJ, Nelson BH. *Tumor-infiltrating lymphocytes expressing the tissue resident memory marker CD103 are associated with increased survival in high-grade serous ovarian cancer.* Clin Cancer Res. 2014;20(2):434–444.

7. Geller MA, Knorr DA, Hermanson DA, Pribyl L, Bendzick L, Mccullar V, Miller JS, Kaufman DS. *Intraperitoneal delivery of human natural killer cells for treatment of ovarian cancer in a mouse xenograft model.* Cytotherapy. 2013;15(10):1297–1306.

8. Felices M, Chu S, Kodal B, Bendzick L, Ryan C, Lenvik AJ, Boylan KLM, Wong HC, Skubitz APN, Miller JS, et al. *IL-15 super-agonist (ALT-803) enhances natural killer (NK) cell function against ovarian cancer.* Gynecol Oncol. 2017;145(3):453–461.

9. Carlsten M, Björkström NK, Norell H, Bryceson Y, van Hall T, Baumann BC, Hanson M, Schedvins K, Kiessling R, Ljunggren H-G, et al. *DNAX accessory molecule-1 mediated recognition of freshly isolated ovarian carcinoma by resting natural killer cells*. Cancer Res. 2007;67(3):1317–1325.

10. Geller MA, Cooley S, Judson PL, Ghebre R, Carson LF, Argenta PA, Jonson AL, Panoskaltsis-Mortari A, Curtsinger J, McKenna D, Dusenbery K, et al. *A phase II study of allogeneic natural killer cell therapy to treat patients with recurrent ovarian and breast cancer.* Cytotherapy. 2011;13(1):98–107.

11. Yang Y, Lim O, Kim TM, Ahn Y-O, Choi H, Chung H, Min B, Her JH, Cho SY, Keam B, et al. *Phase I study of random healthy donor-derived allogeneic natural killer cell therapy in patients with malignant lymphoma or advanced solid tumors*. Cancer Immunol Res. 2016;4(3):215–224.

12. Hoogstad-van Evert J, Bekkers R, Ottevanger N, Schaap N, Hobo W, Jansen JH, Massuger L, Dolstra H. *Intraperitoneal infusion of ex vivo-cultured allogeneic NK cells in recurrent ovarian carcinoma patients (a phase I study)*. Medicine (Baltimore). 2019;98(5):e14290.

13. Yigit R, Massuger LFAG, Figdor CG, Torensma R. *Ovarian cancer creates a suppressive microenvironment to escape immune elimination.* Gynecol Oncol. 2010;117(2):366–372.

14. Yigit R, Figdor CG, Zusterzeel PLM, Pots JM, Torensma R, Massuger LFAG. *Cytokine analysis as a tool to understand tumour-host interaction in ovarian cancer.* Eur J Cancer. 2011;47(12):1883–1889.

15. Rodriguez GM, Galpin K, McCloskey C, Vanderhyden B. *The Tumor Microenvironment of Epithelial Ovarian Cancer and Its Influence on Response to Immunotherapy*. Cancers (Basel). 2018;10(8):242.

16. Giuntoli RL 2nd, Webb TJ, Zoso A, Rogers O, Diaz-Montes TP, Bristow RE, Oelke M. *Ovarian cancer-associated ascites demonstrates altered immune environment: implications for antitumor immunity.* Anticancer Res. 2009;29(8):2875–2884.

17. Fogel LA, Yokoyama WM, French AR. *Natural killer cells in human autoimmune disorders.* Arthritis Res Ther. 2013;15(4):216.

18. Mandal A, Viswanathan C. *Natural killer cells: in health and disease.* Hematol Oncol Stem Cell Ther. 2015;8(2):47–55.

19. Baci D, Bosi A, Gallazzi M, Rizzi M, Noonan DM, Poggi A, Bruno A, Mortara L. *The ovarian cancer tumor immune microenvironment (TIME) as target for therapy: a focus on innate immunity cells as therapeutic effectors.* Int J Mol Sci. 2020;21(9):3125.

20. Kwon HJ, Kim N, Kim HS. *Molecular checkpoints controlling natural killer cell activation and their modulation for cancer immunotherapy.* Exp Mol Med. 2017;49(3):e311.

21. Sakisaka T, Takai Y. *Biology and pathology of nectins and nectin-like molecules.* Curr Opin Cell Biol. 2004;16(5):513–521.

22. Fuchs A, Colonna M. *The role of NK cell recognition of nectin and nectin-like proteins in tumor immunosurveillance.* Semin Cancer Biol. 2006;16(5):359–366.

23. Cerboni C, Fionda C, Soriani A, Zingoni A, Doria M, Cippitelli M, Santoni A. *The DNA damage response: a common pathway in the regulation of NKG2D and DNAM-1 ligand expression in normal, infected, and cancer cells.* Front Immunol. 2013;4:508.

24. Smazynski J, Hamilton PT, Thornton S, Milne K, Wouters MCA, Webb JR, Nelson BH. *The immune suppressive factors CD155 and PD-L1 show contrasting expression patterns and immune correlates in ovarian and other cancers.* Gynecol Oncol. 2020;158(1):167–177.

25. Martinet L, Smyth MJ. *Balancing natural killer cell activation through paired receptors.* Nat Rev Immunol. 2015;15(4):243.

26. Deuss FA, Gully BS, Rossjohn J, Berry R. *Recognition of nectin-2 by the natural killer cell receptor T cell immunoglobulin and ITIM domain (TIGIT)*. J Biol Chem. 2017;292(27):11413–11422.

27. Wang H, Qi J, Zhang S, Li Y, Tan S, Gao GF. *Binding mode of the side-by-side two-IgV molecule CD226/DNAM-1 to its ligand CD155/Necl-5.* Proc Natl Acad Sci U S A. 2019;116(3):988–996.

28. Shibuya A, Campbell D, Hannum C, Yssel H, Franz-Bacon K, McClanahan T, Kitamura T, Nicholl J, Sutherland GR, Lanier LL, et al. *DNAM-1, a novel adhesion molecule involved in the cytolytic function of T lymphocytes*. Immunity. 1996;4(6):573–581.

29. Stanietsky N, Simic H, Arapovic J, Toporik A, Levy O, Novik A, Levine Z, Beiman M, Dassa L, Achdout H, et al. *The interaction of TIGIT with PVR and PVRL2 inhibits human NK cell cytotoxicity.* Proc Natl Acad Sci U S A. 2009;106(42):17858–17863.

30. Liu S, Zhang H, Li M, Hu D, Li C, Ge B, Jin B, Fan Z. *Recruitment of Grb2 and SHIP1 by the ITT-like motif of TIGIT suppresses granule polarization and cytotoxicity of NK cells*. Cell Death Differ. 2013;20(3):456–464.

31. Sanchez-Correa B, Valhondo I, Hassouneh F, Lopez-Sejas N, Pera A, Bergua JM, Arcos MJ, Bañas H, Casas-Avilés I, Durán E, et al. *DNAM-1 and the TIGIT/PVRIG/TACTILE Axis: novel immune checkpoints for natural killer cell-based cancer immunotherapy.* Cancers (Basel). 2019;11(6):877.

32. Sanchez-Correa B, Gayoso I, Bergua JM, Casado JG, Morgado S, Solana R, Tarazona R. *Decreased expression of DNAM-1 on NK cells from acute myeloid leukemia patients.* Immunol Cell Biol. 2012;90(1):109–115.

33. Zhang Z, Wu N, Lu Y, Davidson D, Colonna M, Veillette A. *DNAM-1 controls NK cell activation via an ITT-like motif*. J Exp Med. 2015;212(12):2165–2182.

34. Carlsten M, Norell H, Bryceson YT, Poschke I, Schedvins K, Ljunggren HG, Kiessling R, Malmberg KJ, et al. *Primary human tumor cells expressing CD155 impair tumor targeting by down-regulating DNAM-1 on NK cells*. J Immunol. 2009;183(8):4921–4930.

35. Hoogstad-van Evert JS, Maas RJ, Van Der Meer J, Cany J, Van Der Steen S, Jansen JH, Miller JS, Bekkers R, Hobo W, Massuger L, Dolstra H, et al. *Peritoneal NK cells are responsive to IL-15 and percentages are correlated with outcome in advanced ovarian cancer patients*. Oncotarget. 2018;9(78):34810–34820.

36. Hattori N, Kawaguchi Y, Sasaki Y, Shimada S, Murai S, Abe M, Baba Y, Watanuki M, Fujiwara S, Arai N, et al. *Monitoring TIGIT/DNAM-1 and PVR/PVRL2 immune checkpoint expression levels in allogeneic stem cell transplantation for acute myeloid leukemia*. Biol Blood Marrow Transplant. 2019;25(5):861–867.

37. Sarhan D, Cichocki F, Zhang B, Yingst A, Spellman SR, Colley S, Verneris MR, Blazar BR, Miller JS, et al. *Adaptive NK cells with low TIGIT expression are inherently resistant to myeloid-derived suppressor cells.* Cancer Res. 2016;76(19):5696–5706.

38. Wang F, Hou H, Wu S, Tang Q, Liu W, Huang M, Yin B, Huang J, Mao L, Lu Y, Sun Z, et al. *TIGIT expression levels on human NK cells correlate with functional heterogeneity among healthy individuals.* Eur J Immunol. 2015;45(10):2886–2897.

39. Zhang Q, Bi J, Zheng X, Chen Y, Wang H, Wu W, Wang Z, Wu Q, Peng H, Wei H, Sun R, et al. *Blockade of the checkpoint receptor TIGIT prevents NK cell exhaustion and elicits potent anti-tumor immunity.* Nat Immunol. 2018;19(7):723–732.

40. Xu F, Sunderland A, Zhou Y, Schulick RD, Edil BH, Zhu Y. *Blockade of CD112R and TIGIT signaling sensitizes human natural killer cell functions.* Cancer Immunol Immunother. 2017;66(10):1367–1375.

41. Giannattasio A, Weil S, Kloess S, Ansari N, Stelzer EHK, Cerwenka A, Steinle A, Koehl U, Koch J. *Cytotoxicity and infiltration of human NK cells in in vivo-like tumor spheroids.* BMC Cancer. 2015;15(1):351.

42. Friedrich J, Seidel C, Ebner R, Kunz-Schughart LA. *Spheroid-based drug screen: considerations and practical approach*. Nat Protoc. 2009;4(3):309–324.

43. Kiessling R, Klein E, Wigzell H. *"Natural" killer cells in the mouse. I. Cytotoxic cells with specificity for mouse Moloney leukemia cells. Specificity and distribution according to genotype.* Eur J Immunol. 1975;5(2):112–117.

44. Herberman RB, Nunn ME, Lavrin DH. *Natural cytotoxic reactivity of mouse lymphoid cells against syngeneic acid allogeneic tumors. I. Distribution of reactivity and specificity.* Int J Cancer. 1975;16(2):216–229.

45. Lugthart G, van Ostaijen-ten Dam MM, van Tol MJD, Lankester AC, Schilham MW. *CD56(dim)CD16$^-$ NK cell phenotype can be induced by cryopreservation.* Blood. 2015;125(11):1842–1843.

46. Xu Y, Sun J, Sheard MA, Tran HC, Wan Z, Liu WY, Asgharzadeh S, Sposto R, Wu HW, Seeger RC, et al. *Lenalidomide overcomes suppression of human natural killer cell anti-tumor functions by neuroblastoma microenvironment-associated IL-6 and TGFβ1.* Cancer Immunol Immunother. 2013;62(10):1637–1648.

47. Allan DS, Rybalov B, Awong G, Zúñiga-Pflücker JC, Kopcow HD, Carlyle JR, Strominger JL. *TGF-β affects development and differentiation of human natural killer cell subsets.* Eur J Immunol. 2010;40(8):2289–2295.

48. Tran HC, Wan Z, Sheard MA, Sun J, Jackson JR, Malvar J, Xu Y, Wang L, Sposto R, Kim ES, et al. *TGFβR1 blockade with galunisertib (LY2157299) enhances anti-neuroblastoma activity of the anti-GD2 antibody dinutuximab (ch14.18) with natural killer cells.* Clin Cancer Res. 2017;23(3):804–813.

49. Wilson EB, El-Jawhari JJ, Neilson AL, Hall GD, Melcher AA, Meade JL, Cook GP. *Human tumour immune evasion via TGF-β blocks NK cell activation but not survival allowing therapeutic restoration of anti-tumour activity*. PLoS One. 2011;6(9):e22842.

50. Sun H, Huang Q, Huang M, Wen H, Lin R, Zheng M, Qu K, Li K, Wei H, Xiao W, et al. *Human CD96 correlates to natural killer cell exhaustion and predicts the prognosis of human hepatocellular carcinoma.* Hepatology. 2019;70(1):168–183.

51. Vujanovic L, Chuckran C, Lin Y, Ding F, Sander CA, Santos PM, Lohr J, Mashadi-Hossein A, Warren S, White A, et al. *CD56(dim) CD16(-) natural killer cell profiling in melanoma patients receiving a cancer vaccine and interferon-alpha.* Front Immunol. 2019;10:14.

52. Romee R, Foley B, Lenvik T, Wang Y, Zhang B, Ankario D, Luo X, Cooley S, Verneris M, Walcheck B, Miller J, et al. *NK cell CD16 surface expression and function is regulated by a disintegrin and metalloprotease-17 (ADAM17).* Blood. 2013;121(18):3599–3608.

53. Grzywacz B, Kataria N, Verneris MR. *CD56dimCD16+ NK cells downregulate CD16 following target cell induced activation of matrix metalloproteinases*. Leukemia. 2007;21(2):356–359.

54. Szczepanski MJ, Szajnik M, Welsh A, Foon KA, Whiteside TL, Boyiadzis M. *Interleukin-15 enhances natural killer cell cytotoxicity in patients with acute myeloid leukemia by upregulating the activating NK cell receptors.* Cancer Immunol Immunother. 2010;59(1):73–79.

55. de Rham C, Ferrari-Lacraz S, Jendly S, Schneiter G, Dayer J-M, Villard J. *The proinflammatory cytokines IL-2, IL-15 and IL-21 modulate the repertoire of mature human natural killer cell receptors.* Arthritis Res Ther. 2007;9(6):R125.

Supplemental data

Supplemental Methods: siRNA targeting and silencing of CD112 and CD155

Three different siRNA's targeting CD112 or CD155 were purchased from Invitrogen. In a pilot experiment the most efficient siRNA's were chosen for further experimentation. The most efficient siRNA targeting CD112 had the following sequence: sense 5'-CCUGAUACCUGUGACCCUCUCUGUA-3', antisense 5'-UACAGAGAGGGUCACAGGUAUCAGG-3'. And for CD155 the following sequence: sense 5'-*GCUGUGAGCAGAGAGAACAGCUCUU*-3', antisense 5'-AAGAGCUGUUCUCUCUGCUCACAGC-3'. Non-coding siRNA was used as a negative control (Med GC siRNA, Invitrogen, #12935300). siRNA transfection was performed in a 48 wells plate. During the siRNA transfection, SKOV-3 cells were cultured in serum free X-VIVO-15 without phenol red (Lonza, #BE04-774Q) at 250.000 cells per well. siRNA was precomplexed for 15 minutes with transfection reagent SAINT-RED (Synvolux Therapeutics, #SR-1003-04). Lipoplexes were formed at a ratio of 1 µg siRNA to 10 µl 0.75mM SAINT-RED supplemented with serum-free phenol red-free X-VIVO-15 to a total volume of 50 µl for 15 minutes at room temperature. Subsequently, lipoplexes were added to the cells and co-incubated for 3h at 37°C in 250 µl serum-free phenol red-free X-VIVO-15. Afterwards, 250 µl X-VIVO-15 medium/20% human serum (HS, PAA Laboratories) was added. After 24h, cells were washed and re-plated in a 6 well plate (Corning Costar) in IMDM/10% Fetal Calf Serum (FCS). Two days after re-plating, cells were harvested, counted and used in assays. Cells were stained for CD112-PE (clone TX31, Biolegend, #337409), CD155-APC (clone 300907, R&D systems, #FAB25301A) and Sytox Blue Dead Cell Stain (Invitrogen, #S34857).

Supplemental figures

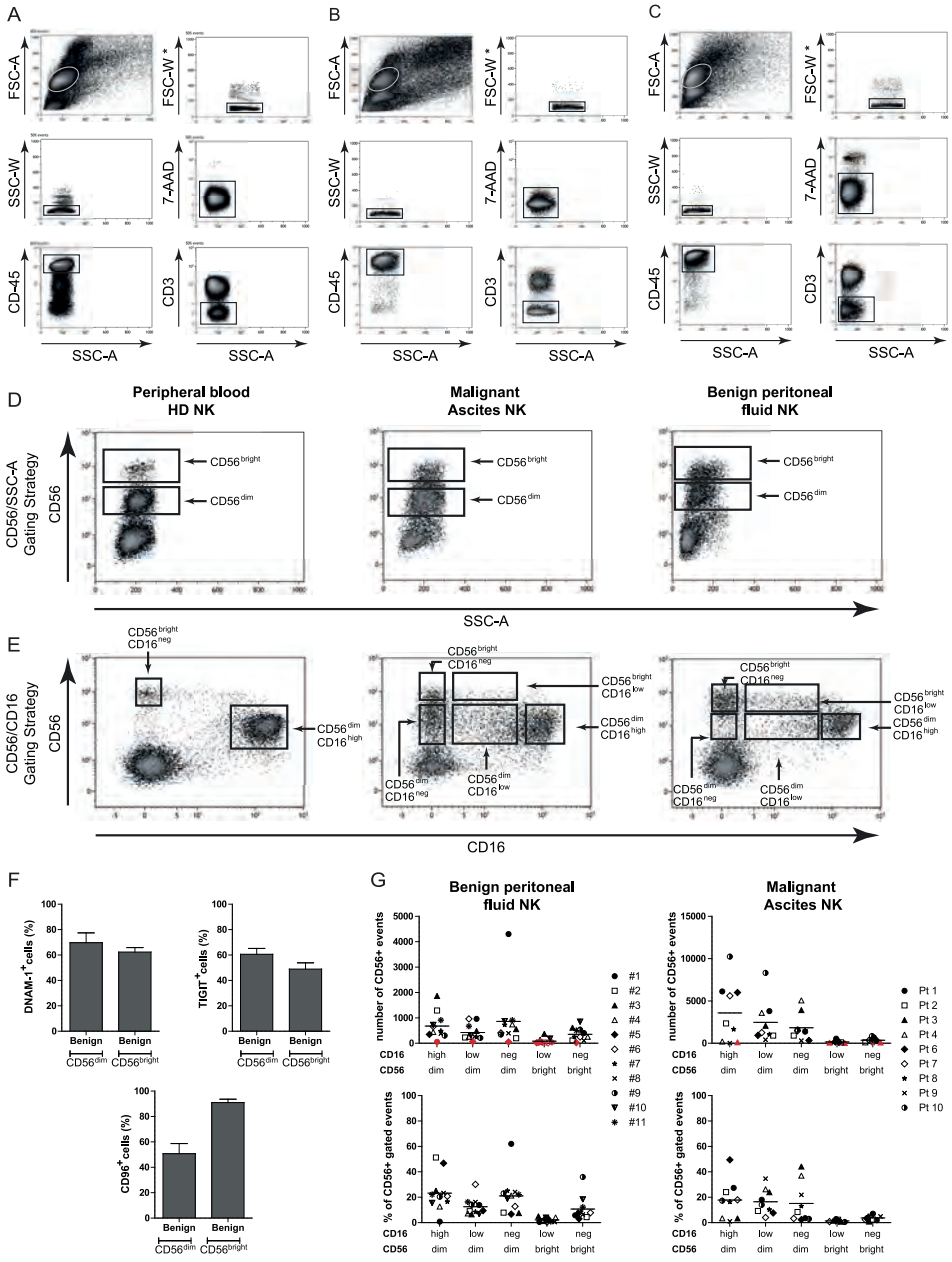

Supplemental figure 1: ***Supplemental figure 1: Gating strategy of healthy donor and ascites derived NK cells based on CD56 expression or CD56/CD16 co-expression patterns***

NK cells were gated on lymphocyte size based on forward/side scatter, followed by doublet discrimination and dead cell exclusion using a viability dye. Subsequently, $CD45^{+}CD3^{-}$ cells were used for NK cell gating based on CD56 or CD56/CD16 (co-)expression. ***(A)*** *Representative NK gating strategy based on CD56 expression for one healthy donor (peripheral blood) and one ovarian cancer patient (ascites).* ***(B)*** *Representative NK gating strategy based on CD56 expression on y-axis and CD16 expression on x-axis. Arrows indicate subsets.*

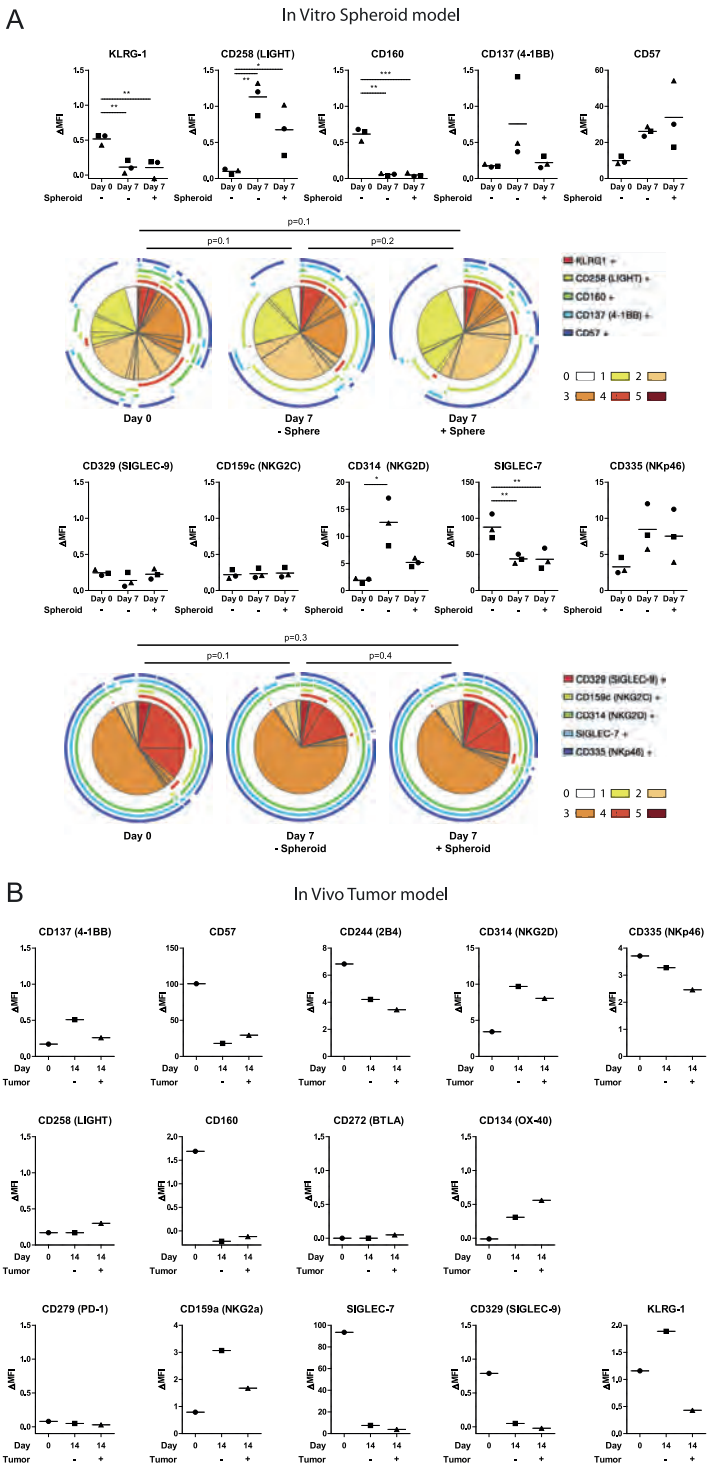
A
In Vitro Spheroid model
KLRG-1
CD258 (LIGHT)
CD160
CD137 (4-1BB)
CD57
ΔMFI
Day 0 Day 7 Day 7
Spheroid - - +
p=0.1
p=0.1
p=0.2
KLRG1 +
CD258 (LIGHT) +
CD160 +
CD137 (4-1BB) +
CD57 +
0 1 2
3 4 5
Day 0
Day 7
- Sphere
Day 7
+ Sphere
CD329 (SIGLEC-9)
CD159c (NKG2C)
CD314 (NKG2D)
SIGLEC-7
CD335 (NKp46)
p=0.3
p=0.1
p=0.4
CD329 (SIGLEC-9) +
CD159c (NKG2C) +
CD314 (NKG2D) +
SIGLEC-7 +
CD335 (NKp46) +
Day 0
Day 7
- Spheroid
Day 7
+ Spheroid
B
In Vivo Tumor model
CD137 (4-1BB)
CD57
CD244 (2B4)
CD314 (NKG2D)
CD335 (NKp46)
CD258 (LIGHT)
CD160
CD272 (BTLA)
CD134 (OX-40)
CD279 (PD-1)
CD159a (NKG2a)
SIGLEC-7
CD329 (SIGLEC-9)
KLRG-1
ΔMFI
Day 0 14 14
Tumor - +

Supplemental figure 2: ***Other NK cell receptor pathways are not affected by the presence of tumor cells In Vitro and In Vivo***

(A) *KLRG-1, LIGHT, CD160, 4-1BB and CD57 expression in the top panel and SIGLEC-9, NKG2C, NKG2D, SIGLEC-7 and NKp46 in the bottom panel on NK cells of healthy donors co-cultured with SKOV-3 spheroids and 10nM IL-15 for 7 days. One-Way repeated measure ANOVA with Bonferroni correction was used for statistical analysis of scatter plots, * $p < 0.05$, ** $p < 0.01$ and *** $p < 0.001$. Co-expression patterns were determined with SPICE software. The pies depict the average proportion of cells expressing 0 to 5 of the receptors, and the arcs indicate which receptors are expressed by the corresponding pies. Statistical differences were analyzed using the built-in statistical tool. *$p < 0.05$, $n = 3$ for each group.* ***(B)*** *ΔMFI of 4-1BB, CD57, 2B4, NKG2D, NKp46, LIGHT, CD160, BTLA, OX-40, PD-1, NKG2a, SIGLEC-7, SIGLEC-9 and KLRGI-1 on pooled intraperitoneal NK cells from 5 mice harvested 14 days after adoptive transfer in SKOV-3 tumor bearing NSG mice and control mice.*

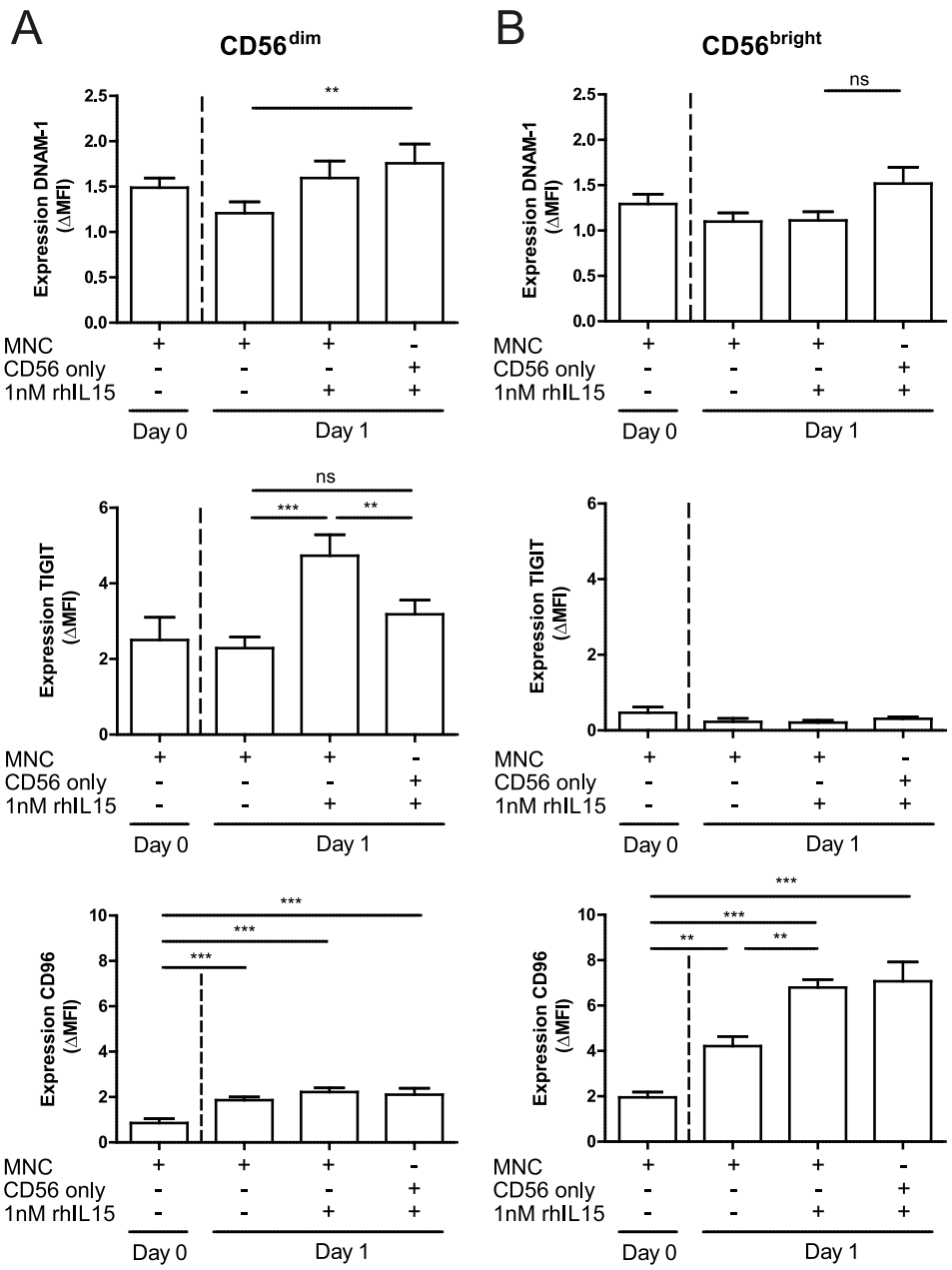

Supplemental figure 3: ***Effect of overnight IL-15 stimulation on DNAM-1, TIGIT and CD96 expression on total versus isolated healthy donor NK cells***

$CD56^{dim}$ ***(A)*** *and* *$CD56^{bright}$* ***(B)*** *NK cell expression of DNAM-1 (n=10), TIGIT (n=10) and CD96 (n=7). MNC (mononuclear cell fraction) non-isolated fraction of ascites derived cells and CD56 bead isolated NK cells from the MNC fraction (CD56 only). Data are expressed as mean+SEM. A One-Way repeated measure ANOVA with Bonferroni correction was used for statistical analysis, ** $p < 0.01$ and *** $p < 0.001$.*

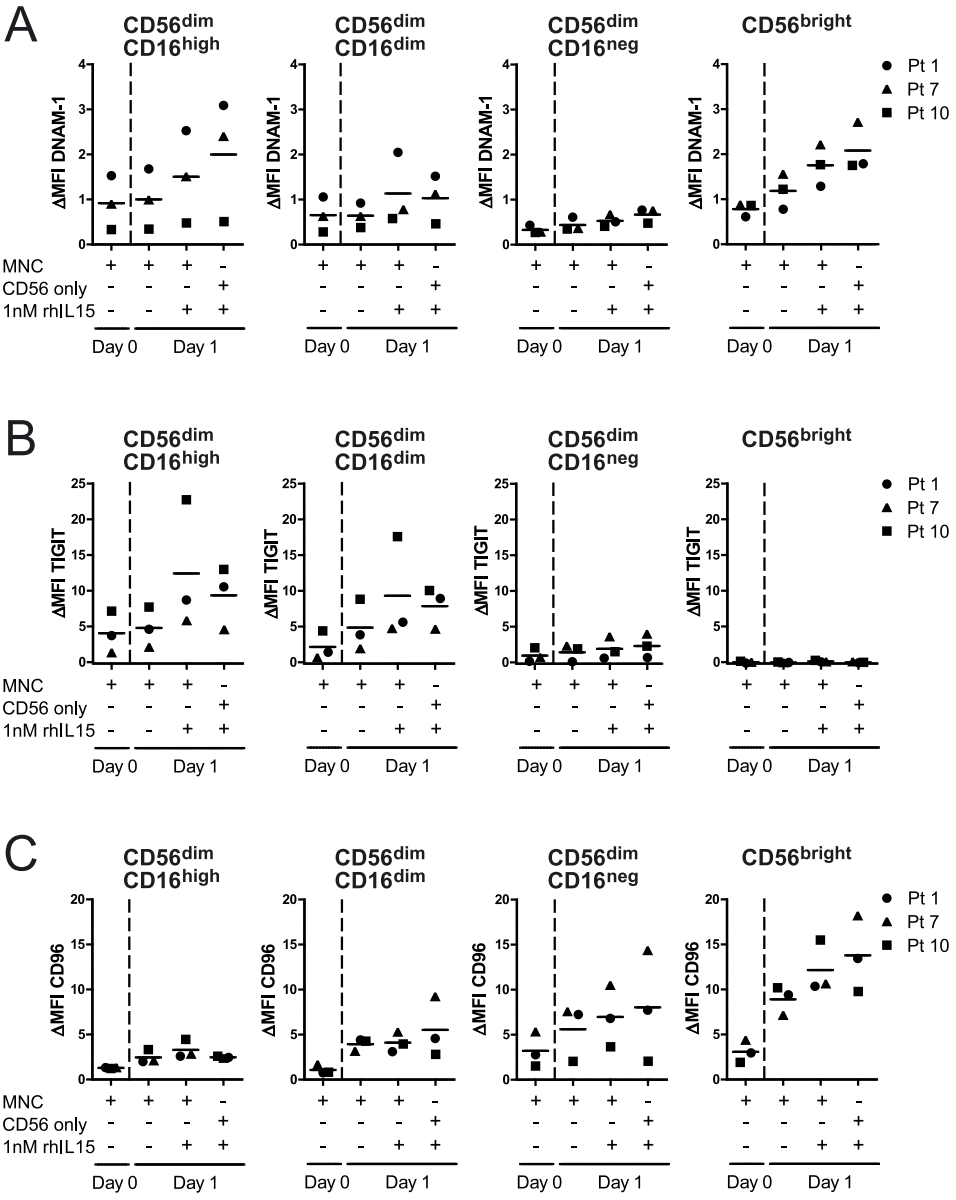

Supplemental figure 4: ***Effect of overnight IL-15 stimulation on DNAM-1, TIGIT and CD96 expression on total versus isolated OC patient derived NK cells***

DNAM-1 ***(A)****, TIGIT* ***(B)*** *and CD96* ***(C)*** *expression by CD56^{dim} CD16^{high}, CD56^{dim} CD16^{dim}, CD56^{dim} CD16^{neg}, CD56^{bright} CD16^{dim} and CD56^{bright} CD16^{neg} NK cells in ascites of OC patients. MNC refers to total ascitic mononuclear cell fraction after ficoll. CD56 only refers to bead isolated NK cells from the MNC fraction. Data are expressed as ΔMFI (lines indicate the mean, n=3).*

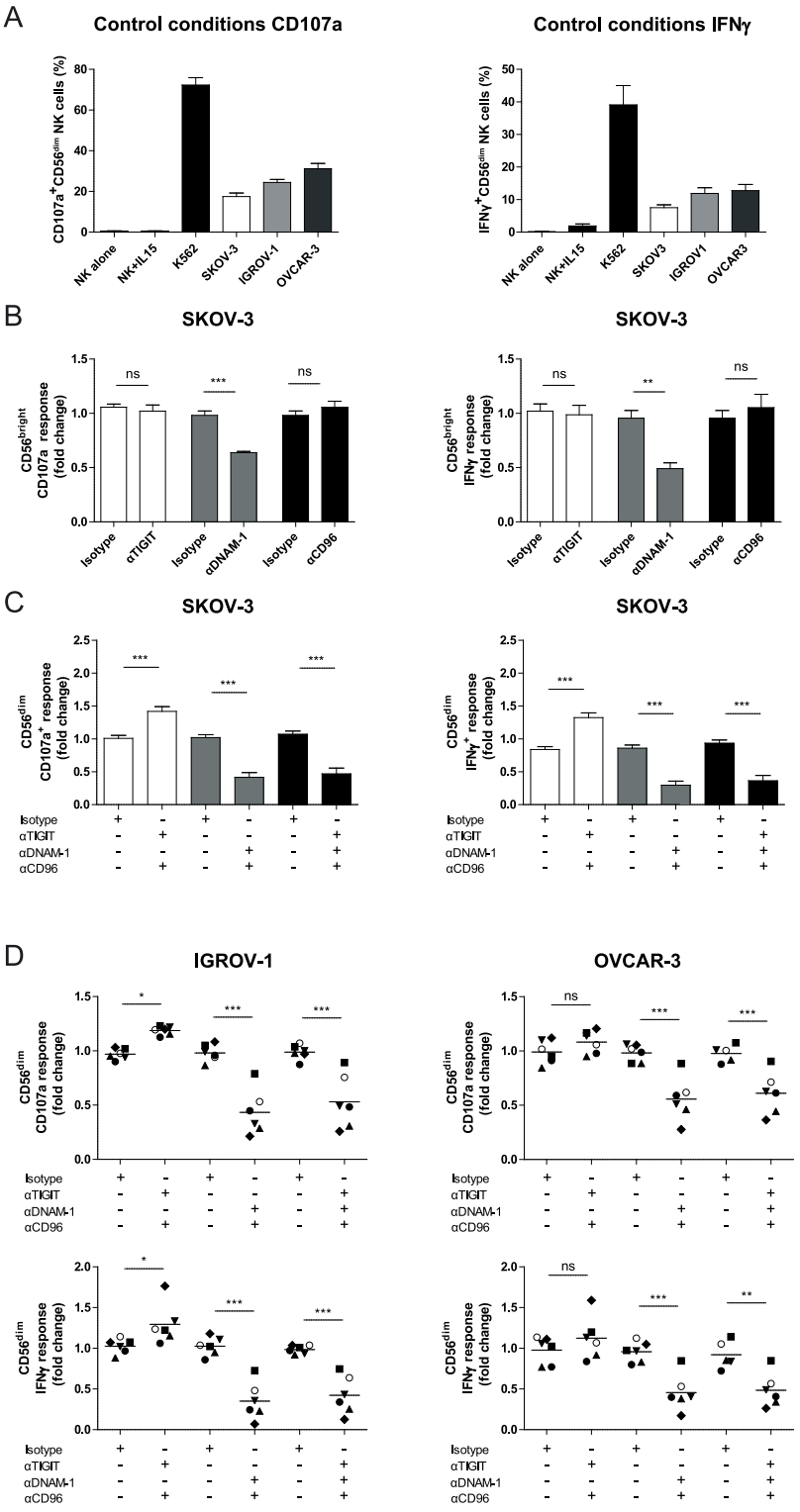
A
Control conditions CD107a
Control conditions IFNγ
CD107a+CD56dim NK cells (%)
IFNγ+CD56dim NK cells (%)
NK alone
NK+IL15
K562
SKOV-3
IGROV-1
OVCAR-3
SKOV3
IGROV1
OVCAR3
B
SKOV-3
CD56bright CD107a response (fold change)
CD56bright IFNγ response (fold change)
Isotype
αTIGIT
αDNAM-1
αCD96
C
CD56dim CD107a+ response (fold change)
CD56dim IFNγ+ response (fold change)
D
IGROV-1
OVCAR-3
CD56dim CD107a response (fold change)
CD56dim IFNγ response (fold change)

Supplemental figure 5: ***NK function cannot be reinvigorated by TIGIT blockade in CD56bright NK cells and co-blockade of DNAM-1/TIGIT results in a strong inhibition of CD56dim NK cells whereas CD96/TIGIT does not mediate increased functionality***

NK cells were cultured overnight with low dose IL-15 (1nM), followed by 4h stimulation with SKOV-3 in the presence of blocking antibodies or matching isotype controls. ***(A)*** *Fold change in CD107a and IFNγ expression of $CD56^{bright}$ NK cells mediated by DNAM-1, TIGIT or CD96 blocking or matching isotype control relative to no treatment (i.e. only SKOV-3 and IL-15 stimulation).* ***(B)*** *Fold change in CD107a and IFNγ expression of $CD56^{dim}$ NK cells mediated by DNAM-1, TIGIT and/or CD96 co-blocking or matching isotype control relative to no treatment (i.e. only SKOV-3 and IL-15 stimulation)* ***(C)*** *same as (B) but with IGROV-1 and OVCAR-3 as stimulus. Cumulative data are shown as mean+SEM (n=6) for (A), (B) and (C).*
*A One-Way ANOVA with Bonferroni correction was used for statistical analysis, * $p < 0.05$, ** $p < 0.01$ and *** $p < 0.001$.*

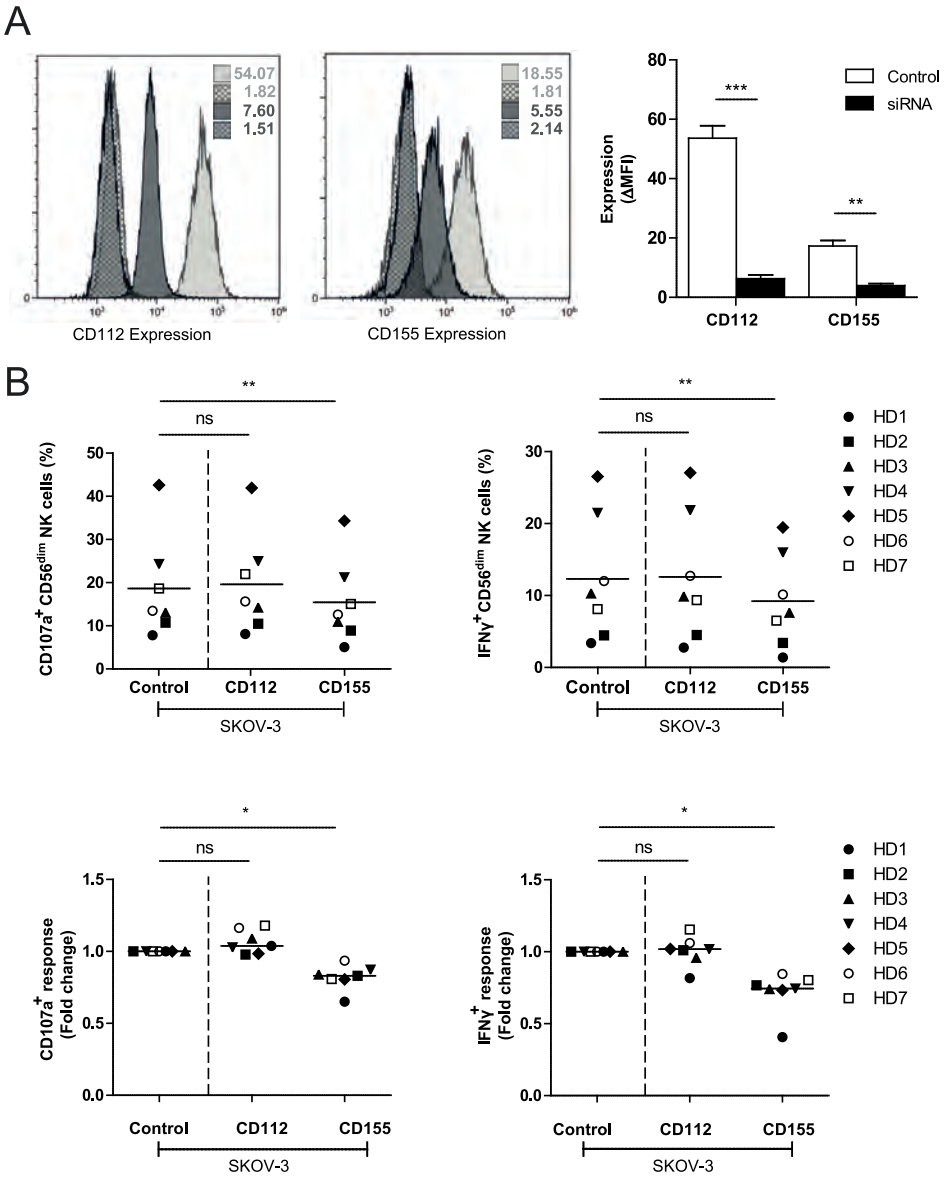

Supplemental figure 6: ***CD155 can be effectively silenced on SKOV-3 cells, resulting in impaired degranulation and IFNγproduction by CD56^{dim} NK cells***

(A) *Representative histograms of CD112 and CD115 expression (smooth) versus isotype control (boxed) by SKOV-3 cells treated with (light gray) or without siRNA (dark gray).* ***(B)*** *Cumulative data is expressed as mean+SEM (n=7). A One-Way repeated measure ANOVA with Bonferroni correction was used for statistical analysis, ** $p < 0.01$ and *** $p < 0.001$.* ***(B-C)*** *CD56^{dim} NK cells stimulated with siRNA-treated SKOV-3 cells (i.e. control, CD112 or CD155 siRNA).* ***(B)*** *%CD107a and IFNγ positive CD56^{dim} NK cells (line indicates mean, n=7).* ***(C)*** *Fold change in CD107a and IFNγ of CD56^{dim} NK cells mediated by CD112 or CD155 siRNA treated SKOV-3 cells relative to corresponding siRNA control SKOV-3 cells (lines indicate mean, n=7). TheFriedman test was used for statistical analysis, * $p < 0.05$.*

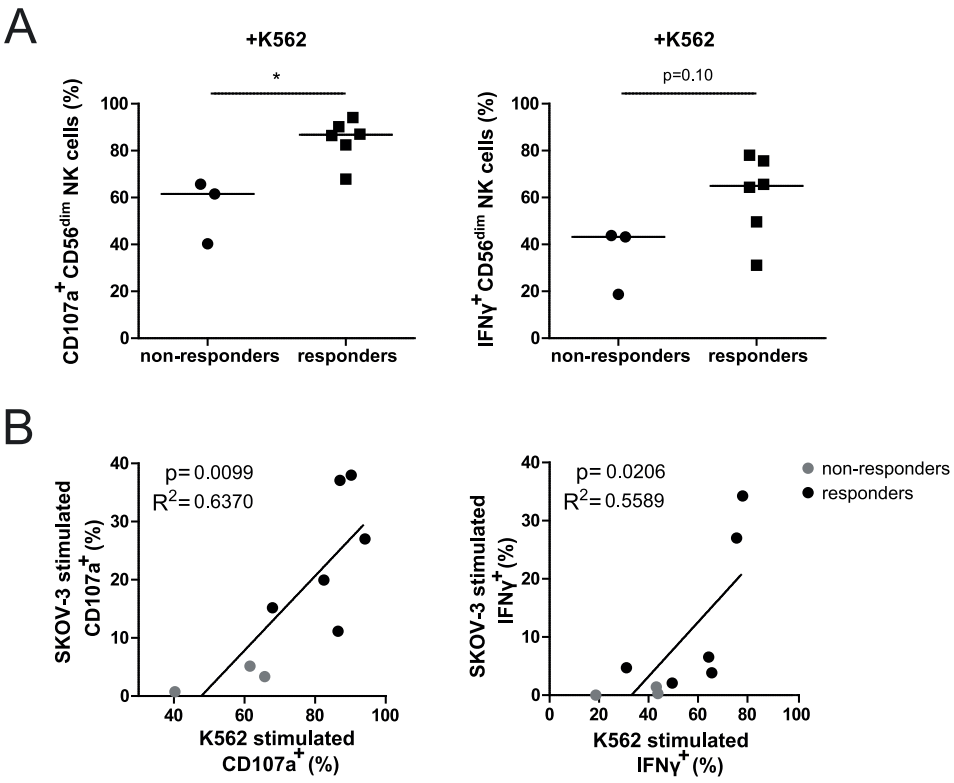

Supplemental figure 7: ***CD56^{dim} NK cells from non-responders to SKOV-3 also exhibit impaired degranulation capacity towards K562***

Patients were subdivided in responder and non-responder cohorts based on CD56^{dim} NK cell response towards SKOV-3 (≥10% CD107a, n=6) and non-responders (<10% CD107a, n=4). ***(A)*** *CD56^{dim} NK cells of SKOV-3 non-responders were stimulated with K562. %CD107a and IFNγ-positive NK cells are depicted (line indicates median). The Mann-Whitney test was used for statistical analysis, * p < 0.05.* ***(B)*** *Correlation between CD56^{dim} NK cell response towards SKOV-3 and K-562 for CD107a and IFNγ.* ***(C)*** *Non-responder CD56^{dim} NK cell CD107a and IFNγ positivity towards SKOV-3 with low dose IL-15 in the presence of TIGIT and/or DNAM-1 blocking antibodies or matching isotype controls (lines indicate mean, n=4).*

Chapter 6

Increased peritoneal TGF-β1 is associated with ascites-induced NK-cell dysfunction and reduced survival in high-grade epithelial ovarian cancer

Ralph J.A. Maas, Janneke S. Hoogstad-van Evert, Iris M Hagemans, Jolanda Brummelman, Diede van Ens, Paul K.J.D. de Jonge, Laura Hooijmaijers, Shweta Mahajan, Anniek B. van der Waart, Charlotte K.J.C. Hermans, Janne de Klein, Rob Woestenenk, Antonius E. van Herwaarden, Nicolaas P.M. Schaap, Somayeh Rezaeifard, Daniele V.F. Tauriello, Petra L.M. Zusterzeel, Nelleke Ottevanger, Joop H. Jansen, Willemijn Hobo*, Harry Dolstra*

*these authors contributed equally

Front Immunol. 2024 Sep 23;15:1448041.

Abstract

Natural killer (NK) cell therapy represents an attractive immunotherapy approach against recurrent epithelial ovarian cancer (EOC), as EOC is sensitive to NK cell-mediated cytotoxicity. However, NK cell antitumor activity is dampened by suppressive factors in EOC patient ascites. Here, we integrated functional assays, soluble factor analysis, high-dimensional flow cytometry cellular component data and clinical parameters of advanced EOC patients to study the mechanisms of ascites-induced inhibition of NK cells. Using a suppression assay, we found that ascites from EOC patients strongly inhibits peripheral blood-derived NK cells and CD34+ progenitor-derived NK cells, albeit the latter were more resistant. Interestingly, we found that higher ascites-induced NK cell inhibition correlated with reduced progression-free and overall survival in EOC patients. Furthermore, we identified transforming growth factor (TGF)-β1 to correlate with ascites-induced NK cell dysfunction and reduced patient survival. In functional assays, we showed that proliferation and anti-tumor reactivity of CD34+ progenitor-derived NK cells are significantly affected by TGF-β1 exposure. Moreover, inhibition of TGF-β1 signalling with galunisertib partly restored NK cell functionality in some donors. For the cellular components, we showed that the secretome is associated with a different composition of CD45+ cells between ascites of EOC and benign reference samples with higher proportions of macrophages in the EOC patient samples. Furthermore, we revealed that higher TGF-β1 levels are associated with the presence of M2-like macrophages, B cell populations and T-regulatory cells in EOC patient ascites. These findings reveal that targeting TGF-β1 signalling could increase NK cell immune responses in high-grade EOC patients.

Introduction

The prognosis of epithelial ovarian carcinoma (EOC) is poor, with a five-year overall survival (OS) of 32% in advanced-stage disease [1]. Since EOC patients frequently have vague symptoms, 70% of patients presents with advanced stage III or IV disease. Often EOC is accompanied by ascites, an abnormal accumulation of fluid in the peritoneal cavity due to lymphatic obstruction and increased vascular permeability [2]. Ascites promotes tumor cell growth and invasion, and contains immune cells such as lymphocytes and macrophages as well as stromal/tissue-resident cells [3, 4]. Furthermore, ascites comprises a large variety of soluble factors released by these cells, thereby playing an important role in influencing anti-tumor immunity within the abdominal cavity [5]. The amount of ascites, as well as the cellular and soluble factor make-up varies from patient to patient [6]. A more detailed insight into this immune environment could aid in understanding which dominant factors contribute to suppression of anti-tumor immune responses in EOC patients.

Immunotherapy could be a complementary approach to existing EOC treatments, as it is considered to be an immunogenic tumor type. The presence of tumor-infiltrating lymphocytes (TILs) positively correlates with survival, whereas the presence of regulatory T cells (Tregs) is associated with decreased survival [7-9]. As ovarian tumor cells often downregulate MHC class I while expressing natural killer (NK) cell activating ligands, they are prone to NK cell-mediated immune responses [10-12]. Furthermore, a high NK cell percentage within ascites correlates with better survival of EOC patients [13]. Hence, boosting NK cell immunity through immunotherapeutic strategies may improve outcome in advanced EOC patients. Nevertheless, NK cell function can be dampened by immunosuppressive cells and soluble mediators within the ascites. For instance, the NK cell inhibitory effect of TGF-β1 and IL-10 in ascites was already described in the early 90's [14, 15]. Furthermore, several studies have shown that exposure to soluble or cell bound B7-H6, PVR (CD155) and MIC-A/B results in downregulation of the NK cell activating receptors NKp30, DNAM-1 and NKG2D [16-20].

To further elucidate mechanisms impairing NK cell function in the local EOC environment, we combined NK-cell functional data, soluble factor analysis, high-dimensional flow cytometry assessment of cellular components and clinical parameters of 31 advanced EOC patients and 16 benign peritoneal fluids in integrated analyses. We found strong inhibitory effects on healthy donor-derived NK cells by EOC patient ascites, that were correlated to patient progression-free (PFS) survival, overall survival (OS) and serum CA-125 levels. Using soluble factor analysis, we revealed that TGF-β1 was a discrete inhibitory factor correlating to ascites-induced

NK cell dysfunction. Furthermore, we showed that blocking TGF-β1 signalling using galunisertib partially rescued NK cell functionality. Galunisertib is a small molecule inhibitor that binds the intracellular serine-threonine kinase domain of TGFβR1 and thereby prevents phosphorylation SMAD2/3 signalling and nuclear translocation which disrupts TGFβ1-mediated signalling Moreover, using multicolor flow cytometry we identified tumor-associated macrophages (TAMs), B cell populations and Tregs to be the main cell types associated with the suppressive factor profile found in ascites of advanced EOC patients. Altogether, our data provide a rationale for anti-TGF-β1 treatment strategies to augment NK cell responses in high-grade EOC patients.

Materials and Methods

Patient samples

EOC patient ascites fluid samples of patients with FIGO stage III or IV high-grade serous EOC were collected after written informed consent at first surgery at the Radboud University Medical Center or Canisius Wilhelmina Hospital. All high grade FIGO stage III or IV EOC patients with ascites were asked to participate in this study. Ascites was collected at diagnosis or during primary surgery. Diagnosis of high grade EOC was based on histology. Study approval was given by the Regional Committee for Medical Research Ethics (CMO 2018-4845) and performed according to the Code for Proper Secondary Use of Human Tissue (Dutch Federation of Biomedical Scientific Societies, www.federa.org). The PFS and OS at time of analysis, CA-125 levels (serum and peritoneal) and treatment status are shown for the patient cohort in Supplemental Table 1 and individual patients in Supplemental Table 2. The median time of follow up was 21.6 months (16.5-53.8 months). Samples of abdominal washing fluid or free fluid from patients without any malignancy, planned for surgery of a benign cyst were used as a relevant reference sample. We chose both abdominal washings and ascites of benign indications to be able to visualize the differences in soluble factors in a cancer microenvironment versus a benign one. Benign samples were excluded in case of signs of active infection and had a serous cystadenoma, endometrioma, mucinous cystadenoma or fibroma (Supplemental Table 3). Ascites samples were filtered using a 100 μm filter and centrifuged. Cell-free ascites supernatant was stored at -20°C for secretome analysis and NK cell activity assays. Cells were resuspended in phosphate buffered saline (PBS) for subsequent mononuclear cell isolation using a Ficoll-Hypaque (1.077 g/mL; GE Healthcare, 17-1440-03) density gradient. Cells were cryopreserved in Iscove's Modified Dulbecco's medium (IMDM; Gibco, #12440061) supplemented with 10% dimethyl sulfoxide (DMSO) and 10% fetal calf serum (FCS, Integro) and used after thawing.

NK cell isolations

Peripheral blood mononuclear cells (PBMCs) were obtained from healthy donor buffy coats (Sanquin Blood Supply Foundation, Nijmegen, the Netherlands) by density gradient Ficoll-Hypaque centrifugation and frozen for phenotypic analysis (n=14, Mean age (SD) 47(±17) years) or used fresh for subsequent NK cell isolation used in functional assays. Peripheral blood (PB)-NK cells were isolated from PBMCs of healthy donors using a magnetic bead-based NK cell enrichment kit (StemCell Technologies, #19055) according to manufacturer's instructions. All isolations resulted in ≥90% purity, as measured by flowcytometry.

HPC-NK cell culture

CD34+ hematopoietic progenitor cells (HPCs) were isolated from umbilical cord blood (UCB). UCB was collected at caesarean sections after informed consent (approved by the Radboudumc Committee for Medical Research Ethics CMO 2014/226), in accordance with institutional guidelines and regulations, and the Declaration of Helsinki. CD34+ HPCs were isolated from mononuclear cells after Ficoll–Hypaque density-gradient centrifugation and subsequent CD34-positive immunomagnetic bead selection (Miltenyi Biotec, 130046702). CD34+ HPCs were expanded and differentiated into HPC-NK cells in a 5-week culture protocol, as described previously [21]. HPC-NK cells (≥70% CD56+) were used immediatly after culture, or after cryopreservation followed by 5-8 days of culture in NK MACS basal medium plus supplement (NK MACS, Miltenyi Biotec, 130–114-429) containing 10% human serum (HS), 50 ng/ml recombinant human (rh)IL-15 (Immunotools, 11340155) and 0.2 ng/ml rhIL-12 (Miltenyi Biotec, 130–096-704).

Tumor cell culture

SKOV-3 (RRID:CVCL_0532) was cultured in Roswell Park Memorial Institute medium 1640 (RPMI; Gibco, #11875091) supplemented with 10% (FCS; Integro). K562 (RRID:CVCL_0004) was cultured in IMDM (Gibco, #12440061) containing 10% FCS. Cell lines were tested for mycoplasma contamination with MycoAlertTM Mycoplasma Detection Kit (Lonza, #LT07-418) every six months. Cell lines were purchased from the ATCC and cultured for a maximum of 3 months.

Determination of soluble factors in ascites and serum

Ascites of EOC and benign patients was assessed for soluble factors by Luminex and ELISA. Flow cytometry and high-dimensional data analysis was performed as

described in the supplementary information. NK functionality assays were performed with peripheral blood-derived and CD34+ progenitor-derived NK cells. For details see Supplementary information.

StatisticsData analysis was conducted using Prism software (GraphPad, version 5.03 for Windows). For normally distributed data, the Student t-test (paired or unpaired) or One-way ANOVA (with or without repeated measure) was used, as stated in the figure legends. Non-normally distributed data was tested with a Wilcoxon signed-rank test, Mann-Whitney test, Kruskal-Wallis or Friedman test, as indicated in the figure legends. To identify correlations between variables (e.g. frequency of immune cell subpopulations and soluble factors), Spearman correlation analysis was performed and visualized in R using the corrplot package (version 0.84). A p-value of <0.05 was considered statistically significant.

Results

Inhibition of NK cell functionality by EOC ascites is correlated with reduced patient survival

Soluble factors in ascites have been demonstrated to impair immune cell function within the tumor microenvironment (TME) of EOC patients. To assess the inhibitory effect on NK cell function, we pre-treated PB or hematopoietic progenitor-derived (HPC) NK cells with various amounts of patient-derived ascites in the presence or absence of IL-15. After overnight exposure, NK cells were challenged with tumor cells and evaluated for CD107a-based degranulation and IFN-γ response. Dose-dependent inhibitory effects were observed when NK cells were pre-treated with increasing amounts of ascites both with or without rhIL-15 (Supplemental Figure 1), whereas the presence of ascites had no negative effects when co-incubated during the 4h tumor cell stimulation without pre-incubation (Supplemental Figure 2). As the most prominent effects were seen with the presence of 50% ascites during the 16h pre-treatment, we used this concentration for all subsequent PB-NK and HPC-NK inhibition assays.

After defining the optimal conditions to demonstrate the inhibitory effects in the in vitro assay, we tested the inhibitory properties of peritoneal fluids from 31 EOC patients and 16 benign reference patients for inhibition of NK cells towards SKOV-3 or K562 target cells with both NK cell sources (Figure 1A). We found that peritoneal fluids, regardless of their origin, strongly inhibited NK cell functionality (degranulation activity and IFN-γ production) in all tested conditions compared to the

PBS control condition. Only in the K562-stimulated HPC-NK cells the effect on CD107a degranulation was not statistically significant (Figure 1A). Viability of NK cells in this assay was 82±7% for HPC-NK cells and 97±3% for PB-NK cells across all different conditions indicating that the large volume of non-media does not affect NK cell viability. Interestingly, the different NK-cell sources were not equally affected, as HPC-NK cells were significantly more resistant to ascites-mediated suppression than PB-NK cells for all tested parameters (Figure 1B). Furthermore, ascites-mediated suppression had more impact on NK-cell responses towards SKOV-3 target cells than against MHC class I-negative K562 cells (Figure 1C).

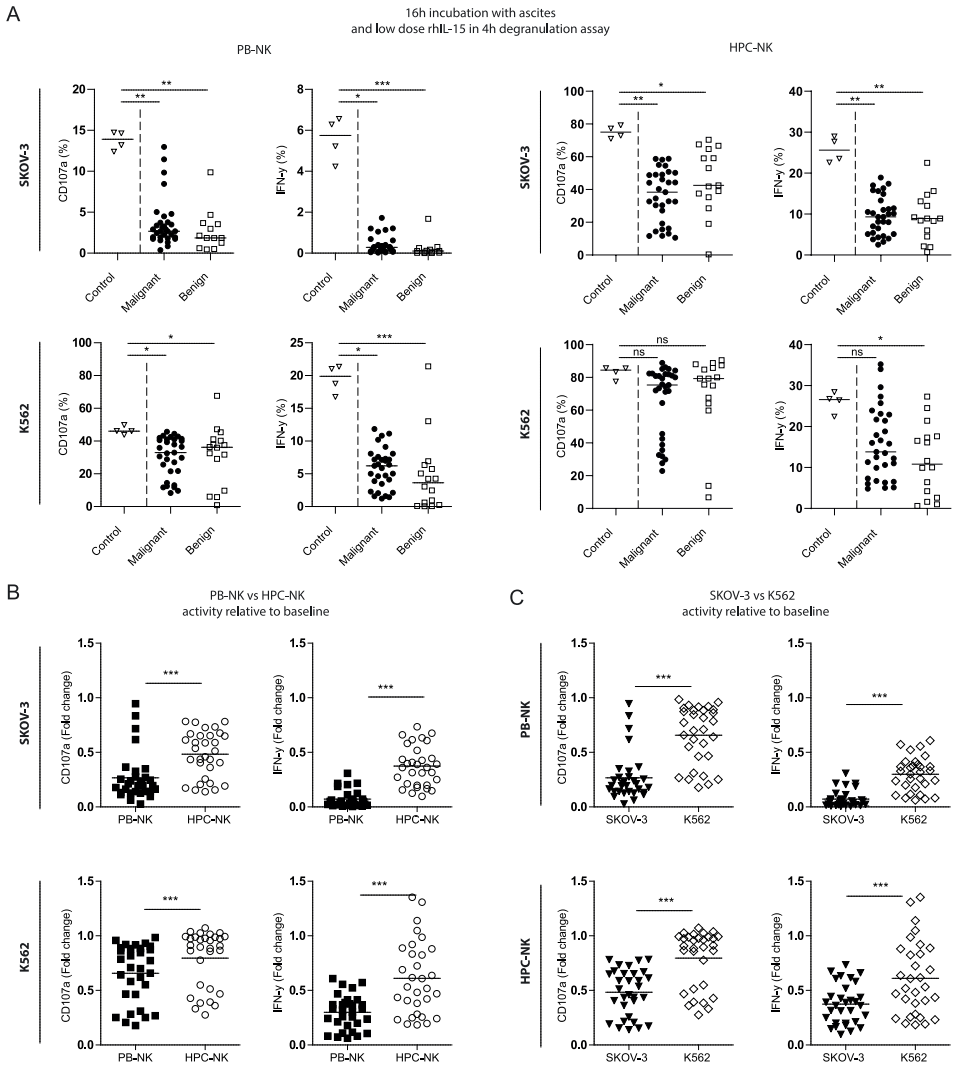

Figure 1: ***Ascites from EOC patients inhibits NK cell activity***

(A) *Percent positive CD107a and IFN-γ PB-derived (left) and HPC-derived (right) NK cells stimulated with SKOV-3 (top) or K562 (bottom) target cells in the presence of PBS (open triangles), EOC patient ascites (filled circles, n=31) or benign fluid (open squares, n=15). Cells were incubated overnight with aforementioned fluids with addition of 1nM rhIL-15 and challenged with target cells for 4 hours. For control quadruplicates are shown, and for EOC patient and benign control fluids the average of duplicates are depicted and were used for statistics. Kruskal-Wallis with Dunn's Multiple Comparison Test was used for statistical analysis, * $p < 0.05$, ** $p < 0.01$ and *** $p < 0.001$.* ***(B) and (C)*** *Fold change CD107a and IFN-γ inhibition of the same assay compared to control of EOC patient ascites (n=31) with for (B) HPC-derived (open circles) and PB-derived (filled squares) NK cells stimulated with SKOV-3 (top) and K562 (bottom) or for (C) stimulated with SKOV-3 (filled triangles) and K562 (open diamonds) on PB-NK (top) or HPC-NK cells (bottom). Wilcoxon signed-rank test was used for statistical analysis, *** $p < 0.001$ (C).*

The inhibitory effects were consistent across different parameters between the different functional read-outs (i.e. PB-NK vs. HPC-NK, SKOV-3 vs. K562, and CD107a vs. IFN-γ, Figure 2A). Next, we assessed the correlation between ascites-mediated NK cell dysfunction and clinical parameters of the advanced EOC patients (Figure 2B). The mean age of the selected EOC patient cohort (n=31) was 63±11 years and 53±10 years for the benign reference group (n=12; excluding 4 patients of whom age and CA-125 levels were not available). The median OS and PFS of the advanced EOC patient cohort at time of analysis was 18.9 and 6.9 months, respectively, with seven of the patients still alive at time of analysis (Supplemental Table 1, Supplemental Table 2). Interestingly, ascites-induced impairment of PB-NK cell reactivity against either K562 or SKOV-3 target cells was significantly correlated with lower PFS (Figure 2B and C; ρ= -0.54 for K562 and -0.51 for SKOV-3) and OS (ρ=-0.40 for both K562 and SKOV-3). Similarly, ascites-induced HPC-NK dysfunction in response to K562 targets was negatively associated with PFS (Figure 2B and C; ρ=-0.42). Furthermore, we observed a positive correlation between ascites-induced NK cell dysfunction and higher CA-125 levels in the serum of EOC patients (Figure 2B and D). CD107a degranulation activity was more strongly correlated to serum CA-125 levels for both PB-NK cells (ρ=0.35 and 0.55 for K562 and SKOV-3, respectively) and HPC-NK cells (ρ=0.53 and 0.51 for K562 and SKOV-3, respectively). For IFN-γ production only HPC-NK inhibition significantly correlated to both CA-125 serum and peritoneal levels (ρ=0.53 and 0.56, respectively; Figure 2D). Collectively, these data demonstrate that ascites from EOC patients contains soluble inhibitory factors that potently impair NK cell function, which significantly correlates to reduced survival and higher serum CA-125 levels.

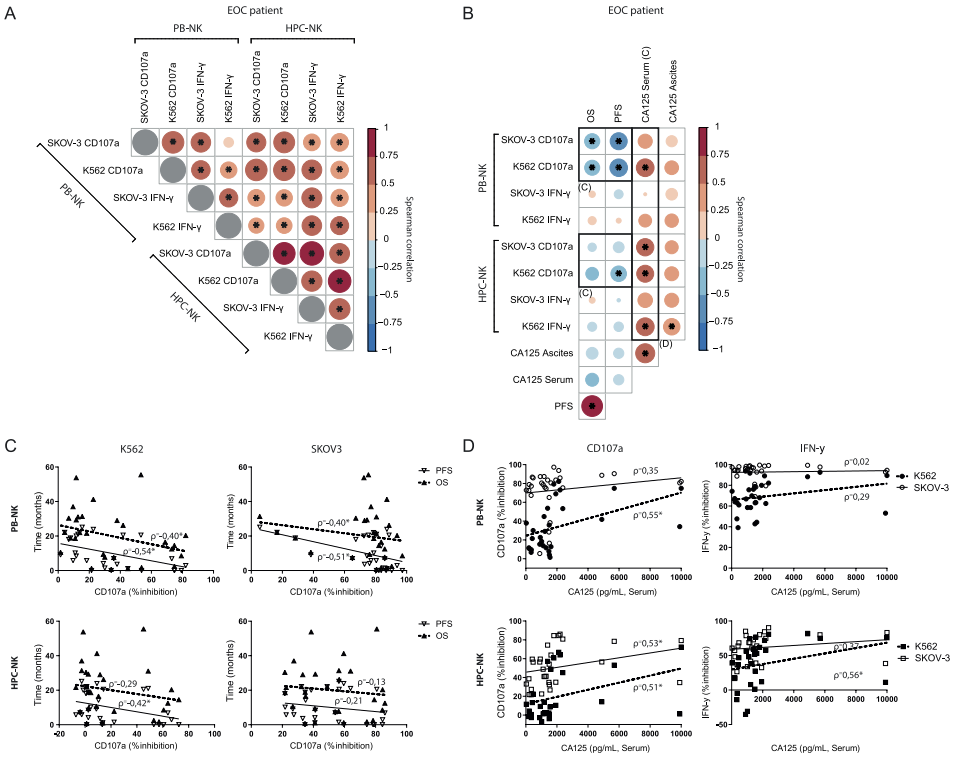

Figure 2: ***Inhibitory properties of ascites on NK cells correlates to patient survival and CA-125 levels***

(A–B) *Spearman correlograms of mean fold change of suppression by EOC patient ascites between all tested conditions, i.e. HPC-NK vs PB-NK, SKOV-3 vs K562 and CD107a vs IFN-γ* ***(A)****, or those conditions versus OS, PFS, CA-125 (serum and ascites)* ***(B)****; with color intensity and circle size indicating the Spearman's rank correlation coefficient between biomarkers, and * denoting $p < 0.05$.* ***(C)*** *Scatter plots illustrating the relationship between PFS and OS in months versus PB-NK CD107a (top) or IFN-γ (right) response to SKOV-3 (left) and K562 (right). Spearman's rank correlation coefficient (ρ) shown, * $p < 0.05$* ***(D)*** *Scatter plots illustrating the relationship between CD107a (left) or IFN-γ (right) and CA-125 serum levels in PB-NK (top) and HPC-NK cells (bottom).*

High TGF-β1 concentration is correlated with EOC ascites-mediated NK cell dysfunction

After establishing that soluble factors in ascites can potently induce NK cell dysfunction, we sought to find dominant inhibitory factors in ascites that could impair NK cell reactivity. For this, we examined peritoneal fluids in 25-plex Luminex and ELISAs in parallel with NK cell suppression assays (Figure 3A). Although we observed that the general cytokine profiles of benign and EOC patient ascites fluids were mostly similar, there were individual soluble factors that were significantly different (Figure 3A and B). We verified that IL-6 concentration, a cytokine previously associated with poor outcome in EOC patients [22], was significantly elevated in EOC patient ascites compared to benign ascites. Furthermore, soluble ligands for activating NK cell receptors such as MIC-B (NKG2D ligand) and Nectin-2 (DNAM-1 ligand) were higher in EOC patient ascites along with the immune inhibitory cytokines IL-10 and TGF-β1 compared to benign ascites (Figure 3B). Besides an increase in inhibitory mediators, markers of immune activation (including IP-10, TRAIL, perforin and IL-12p40 levels) were elevated in malignant ascites samples, soluble factors not shown in Figure 3B were not statistically significantly different between malignant and benign reference samples.

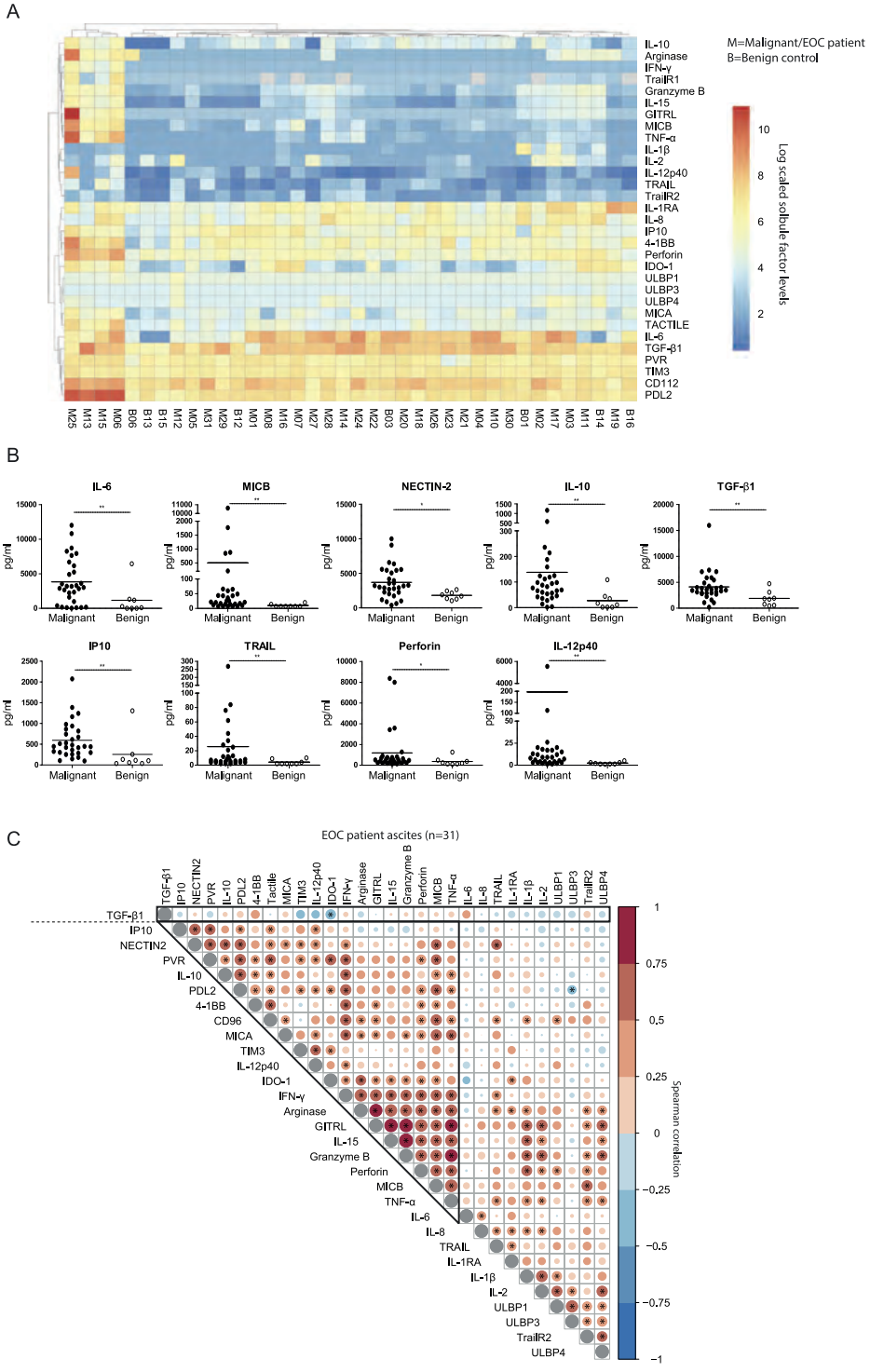
A
IL-10
Arginase
IFN-γ
TrailR1
Granzyme B
IL-15
GITRL
MICB
TNF-α
IL-1β
IL-2
IL-12p40
TRAIL
TrailR2
IL-1RA
IL-8
IP10
4-1BB
Perforin
IDO-1
ULBP1
ULBP3
ULBP4
MICA
TACTILE
IL-6
TGF-β1
PVR
TIM3
CD112
PDL2
M=Malignant/EOC patient
B=Benign control
Log scaled solbule factor levels
10
8
6
4
2
M25 M13 M15 M06 B06 B13 B15 M12 M05 M31 M29 B12 M01 M08 M16 M07 M27 M28 M14 M24 M22 B03 M20 M18 M26 M23 M21 M04 M10 M30 B01 M02 M17 M03 M11 B14 M19 B16
B
IL-6
MICB
NECTIN-2
IL-10
TGF-β1
IP10
TRAIL
Perforin
IL-12p40
pg/ml
Malignant
Benign
C
EOC patient ascites (n=31)
TGF-β1
IP10
NECTIN2
PVR
IL-10
PDL2
4-1BB
CD96
MICA
TIM3
IL-12p40
IDO-1
IFN-γ
Arginase
GITRL
IL-15
Granzyme B
Perforin
MICB
TNF-α
IL-6
IL-8
TRAIL
IL-1RA
IL-1β
IL-2
ULBP1
ULBP3
TrailR2
ULBP4
Spearman correlation
1
0.75
0.5
0.25
0
−0.25
−0.5
−0.75
−1

Figure 3: ***TGF-β1 as a discrete suppressive cytokine in EOC patient ascites***
(A) *Log scaled soluble cytokine levels by Luminex or ELISA on of EOC patient (n=31) and benign control (n=16) peritoneal fluids visualized in a heatmap. Each row represents a different cytokine, while columns represent patients or donors (M=malignant and B=benign). The log scaled cytokine level of patients or donors is reported and visualized with a color scale from blue (low levels) to red (high levels).* ***(B)*** *Cytokine levels of significantly different cytokines in the panel of EOC patient and benign control ascites fluids. A Mann-Whitney test was used for statistical analysis, * $p < 0.05$ and ** $p < 0.01$.* ***(C)*** *Spearman correlogram of mean fold change of suppression by EOC patient ascites in all tested condition and clinical parameters versus cytokine levels. A heat map is used to indicate the Spearman's rank correlation coefficient (ρ) of associations between biomarkers. Red indicates a positive correlation, and blue indicates a negative correlation. * $p < 0.05$*

To define patterns of co-existence for the different soluble mediators in ascites of advanced EOC patients, we correlated their concentrations (Figure 3C). Most mediators were positively correlated, indicating that soluble factor levels accumulate in a joint fashion with 19 soluble factors strongly positively correlating together and to a lesser extent with the remaining 10 soluble factors. Notably, TGF-β1 was not part of this cluster, as correlations with other determined mediators were lacking, and only IDO-1 was negatively correlated. Next, we assessed correlations between ascites-induced NK cell dysfunction and clinical parameters with the levels of determined soluble factors in ascites in our patient cohort (Figure 4A). Interestingly, the presence of high peritoneal TGF-β1 concentrations correlated to a decreased NK cell functionality. Soluble 4-1BB exhibited a similar, but weaker, correlation with ascites-mediated NK cell dysfunction (Figure 4A). Conversely, high levels of ULBP-4 were positively correlated with NK cell-mediated EOC reactivity, although, only in 9 out of 31 tested ascites samples the ULBP-4 concentration was above the limit of detection (data not shown). When focusing on associations with clinical parameters, we observed that IL-15, GITRL and granzyme-B were positively correlated to PFS. Surprisingly, IDO-1 also positively correlated to PFS and OS (Figure 4A). In contrast, TGF-β1 and IL-6 negatively correlated with PFS, and TGF-β1 negatively associated with OS as well. None of the assessed cytokines were significantly correlated to serum and peritoneal levels of CA-125 (Figure 4A). Finally, we analyzed the most and least NK cell inhibitory ascites (defined by quartiles of CD107a and IFN-γ activity relative to the baseline functionality) for their TGF-β1 concentration (Figure 4B, C and D). This confirmed that TGF-β1 was significantly increased in the strongest NK cell inhibitory EOC ascites samples. Taken together, these data suggest that TGF-β1 is a soluble factor that strongly negatively correlates to ascites-induced NK-cell dysfunction and decreased survival in EOC patients.D). This confirmed that TGF-β1 was significantly increased in the strongest NK cell inhibitory EOC ascites samples. Taken together, these data indicate that TGF-β1 appears to be a discrete soluble strongly negatively correlating to ascites-induced NK-cell dysfunction and decreased survival in EOC patients.

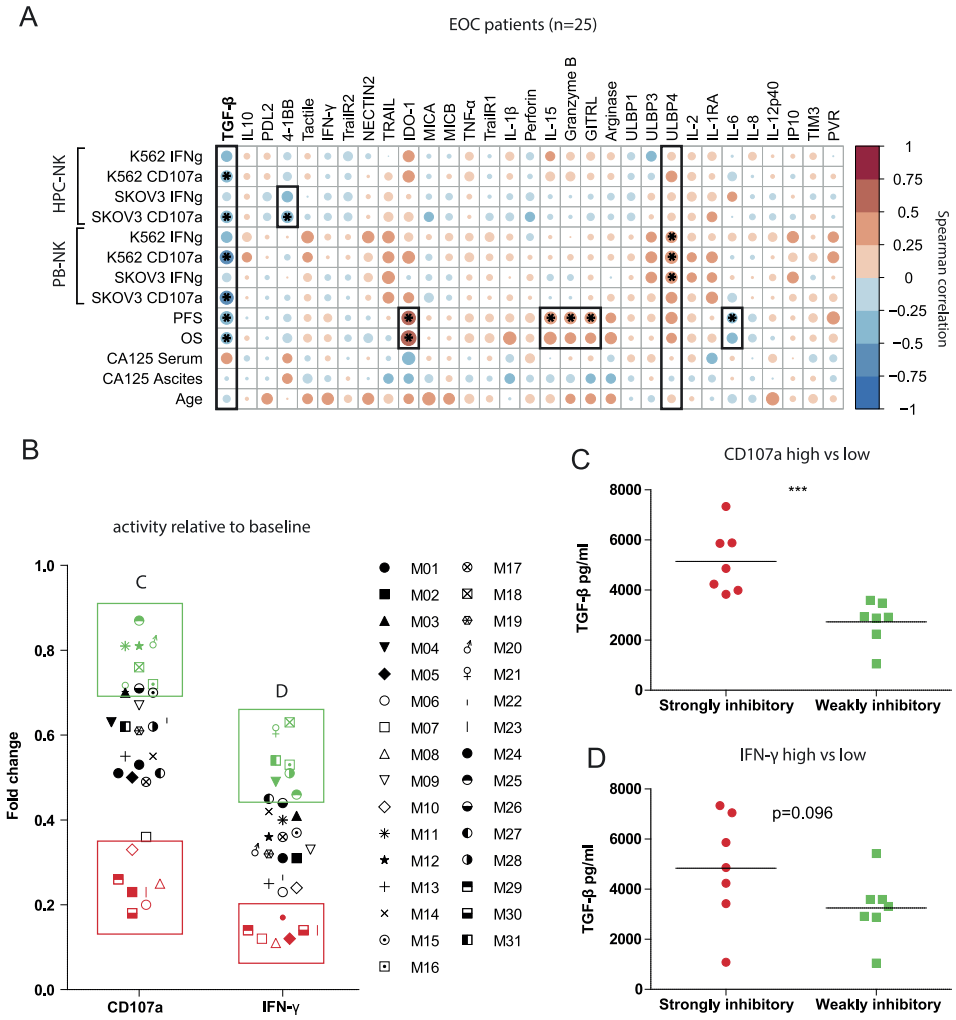

Figure 4: ***TGF-β1 is a main driver of ascites -induced NK cell inhibition***

(A) *Spearman correlogram of mean fold change of suppression by EOC patient ascites, PFS, OS, CA-125 levels in serum and peritoneal fluids and age versus soluble cytokine levels. A heat map is used to indicate the* ρ^2 *of associations between biomarkers. Red indicates a positive correlation, and blue indicates a negative correlation.* ***(B)*** *Mean fold change CD107a and IFN-γ inhibition of all conditions for each EOC patient ascites. All red labelled patients indicate the 25% strongest inhibitory ascites', and all green labelled patients indicate the 25% least inhibitory ascites'.* ***(C and D)*** *TGF-β1 levels of most and least inhibitory ascites' defined in (B) based on CD107a (C) and IFN-γ (D). A Mann-Whitney test was used for statistical analysis,* $* p < 0.05$, $*** p < 0.001$.

TGF-β1 inhibits HPC-NK cell proliferation and functionality

As a distinct role of TGF-β1 in mediating EOC ascites-induced NK-cell dysfunction was found in our association studies, we further wanted to elucidate the effects of TGF-β1 and its interference on modulating NK-cell EOC reactivity. First, we assessed expression of TGF-βR2, which is part of the heterotetrametric receptor complex, on the surface of HPC-NK cells and observed that TGF-βR2 was highly expressed by HPC-NK cells (Figure 5A). Next, we evaluated to what extent rhTGF-β1 inhibits HPC-NK cell proliferation induced by IL-2/IL-15 stimulation and if galunisertib (LY2157299), an affordable and readily available TGF-βR1 kinase inhibitor, can interfere with TGF-β1-mediated effects of proliferation. Indeed, TGF-β1 reduced HPC-NK cell proliferation that could partly be restored by galunisertib (Figure 5B). In addition, pre-treatment with rhTGF-β1 significantly impaired HPC-NK cell-mediated IFN-γ production within the CD107a degranulating population upon target cell challenge (Figure 5C). Interestingly, galunisertib partially restored rhTGF-β1-induced reduction of IFN-γ responses against K562 and/or SKOV-3 target cells in 4 out of 5 donors (Supplemental Figure 3). These data indicate that TGF-β1 could severely hamper functionality of therapeutic NK-cell products and that blockade of TGF-βR1 receptor signalling can partly rescue NK cell dysfunction by TGF-β1.

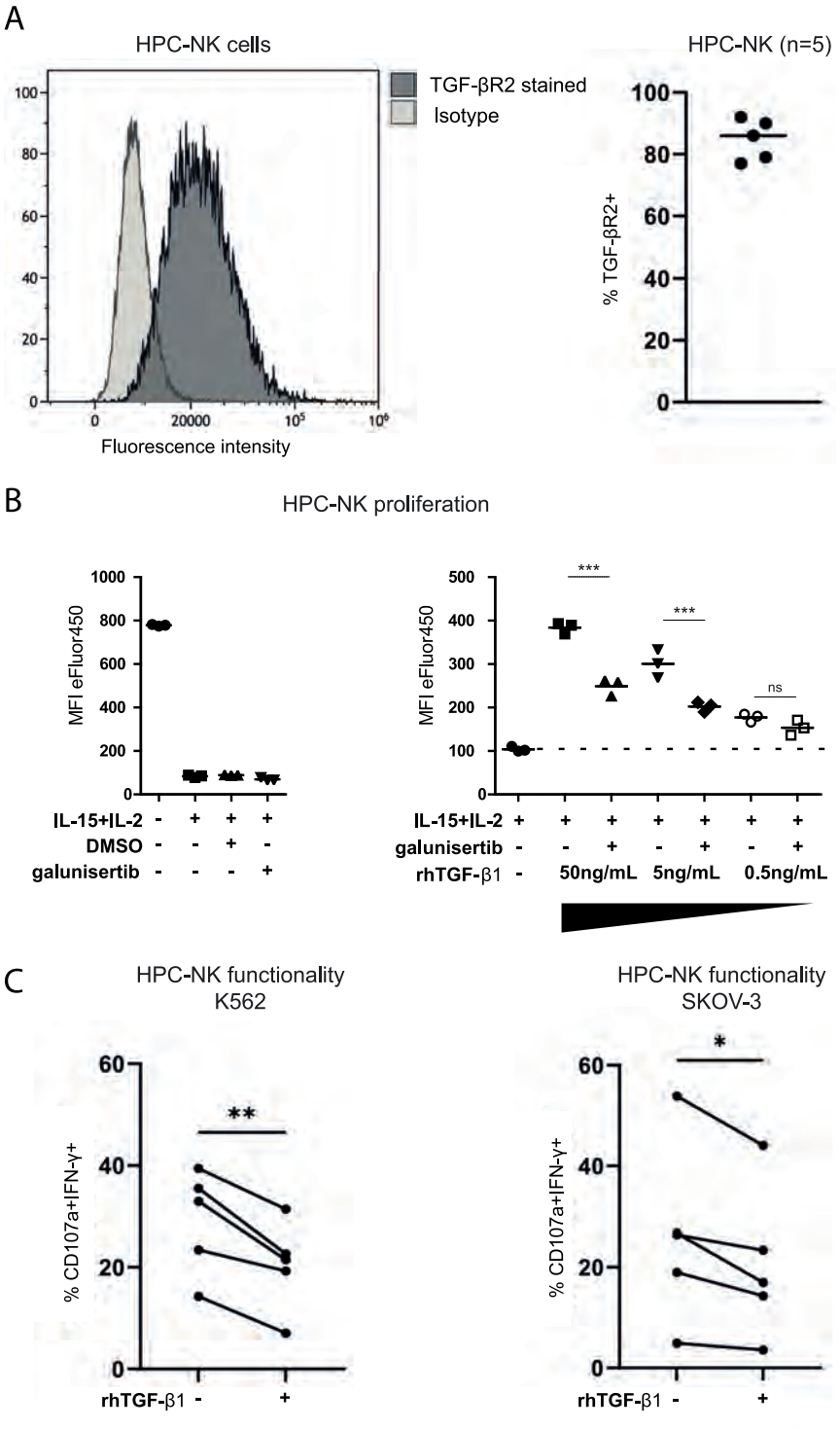
A
HPC-NK cells
TGF-βR2 stained
Isotype
Fluorescence intensity
HPC-NK (n=5)
% TGF-βR2+
B
HPC-NK proliferation
MFI eFluor450
IL-15+IL-2
DMSO
galunisertib
rhTGF-β1
50ng/mL
5ng/mL
0.5ng/mL
***
ns
C
HPC-NK functionality
K562
HPC-NK functionality
SKOV-3
% CD107a+IFN-γ+
rhTGF-β1
**
*

Figure 5: ***TGF-β1 inhibits NK cell functionality but can be rescued by a TGF-β1 small molecule inhibitor***

(A) *TGF-βR2 expression (black) and isotype control (light grey) unstimulated HPC-NK cells in histograms (left) and the percentage of TGF-βR2+ HPC-NK cells shown for 5 different donors (right).* ***(B)*** *Cell Proliferation Dye-stained HPC-NK cells in a proliferation assay measured by a decrease in eFluor450 fluorescence. The left panel shows triplicate unstimulated, IL-2+IL-15 stimulated (with or without DMSO or galunisertib) controls with eFluor450 MFI on y-axis. The right panels shows reference triplicates of HPC-NK cells stimulated with IL-2+IL-15 control with or without decreasing amounts (50, 5 or 0.5ng/mL) of rhTGF-β1 with or without galunisertib. Both panels include data from the same experiment. The Friedman test was used to calculate statistical significance.* ***(C)*** *Percentage of HPC-NK cells that are double positive for CD107a and IFN-γ after stimulation with K562 or SKOV-3 cells in the presence or absence of TGF-β1(n=5). One-way ANOVA with post-hoc Bonferroni test was used for statistical analysis. ns, not significant, *p<0.05, **p<0.01, ***p<0.0001.*

M2-like TAMs, B cells and Tregs are associated with the secretome including TGF-β1 in EOC patient ascites

Following the soluble factor analysis, we focused on the cellular compartment in the same cohort of EOC patient and benign reference fluids. For this, we set up an 18-color flow cytometry panel (Supplemental Table 4) to assess the immune composition (including T cell subsets, B cells, NK cells, macrophages, monocytic subsets and granulocytic cells) within the peritoneal fluids. PBMC from healthy donors were used as reference in peripheral blood. In benign peritoneal fluids, the fraction of CD45+ hematopoietic cells was 97±3%, while this was 82±15% in ascites of EOC patients, indicating the presence of tumor cells or other non-hematological cells in EOC patient ascites (Figure 6A). Notably, the percentage of CD14+CD33+CD16+ and CD14+CD33+CD163+ macrophages in EOC patient ascites was significantly higher (16.3±13.0% and 38.4±20.1%, respectively) compared to the percentages found in benign fluids (5.7±8.8% and 20.3 ±20.5%, respectively). No significant differences were found in the percentages of classical CD14+CD33+CD16- or CD14+CD33+CD163- monocytes, which was 25.1±13.7% and 2.2±1.8% respectively in EOC patients compared with 21.8±19.9% and 7.0±7.2% in benign fluids. Furthermore, no difference was found in the proportion of lymphocytes within the CD45+ population between EOC and benign fluids, which was 48.9±22.5% and 39.2±29.4%, respectively. The frequency of CD4+ T cells was slightly lower in EOC ascites, while the frequency of CD19+ B cells was slightly higher (Figure 6A).

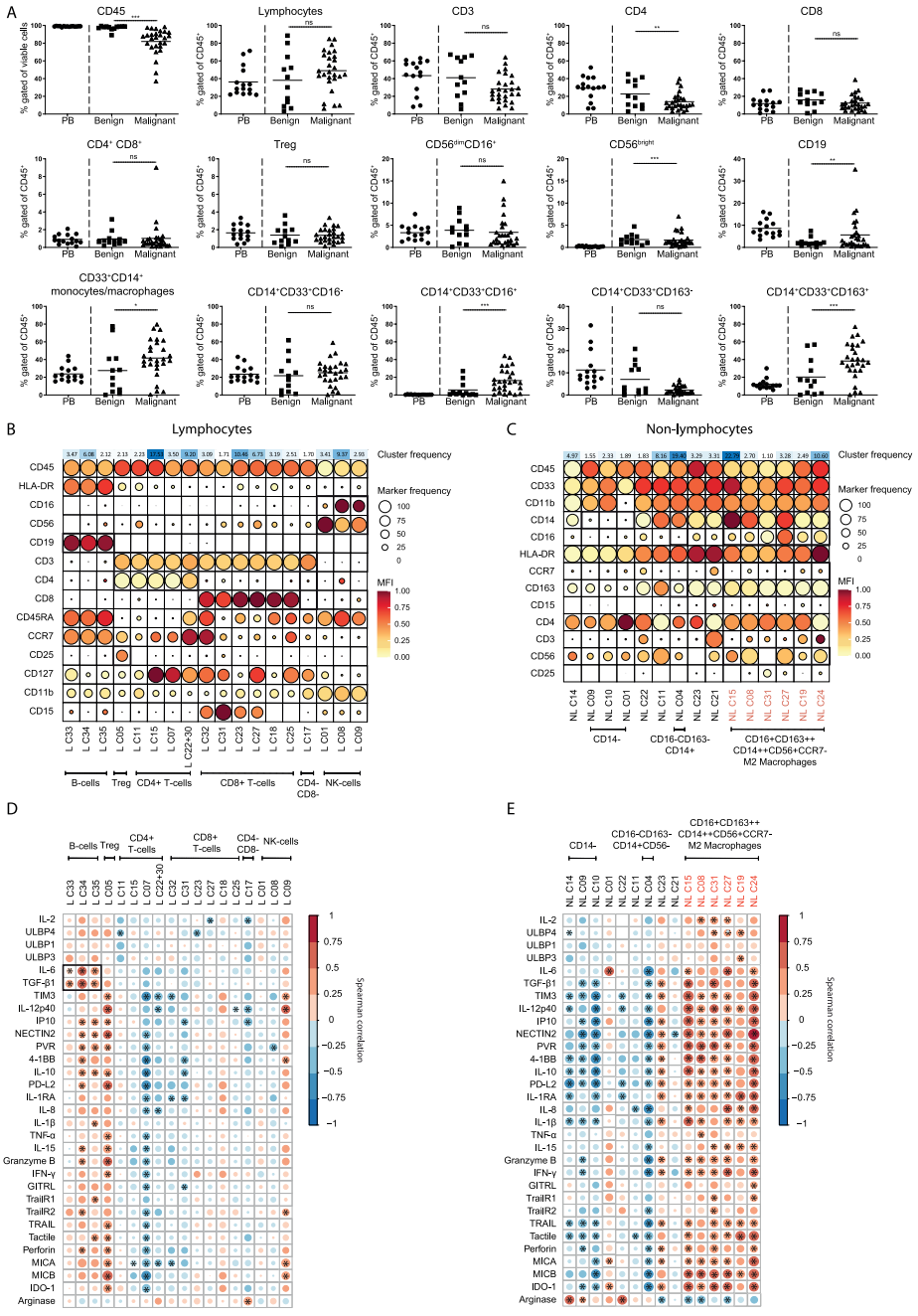
A
CD45
Lymphocytes
CD3
CD4
CD8
CD4+ CD8+
Treg
CD56dimCD16+
CD56bright
CD19
CD33+CD14+ monocytes/macrophages
CD14+CD33+CD16-
CD14+CD33+CD16+
CD14+CD33+CD163-
CD14+CD33+CD163+
% gated of viable cells
% gated of CD45+
PB
Benign
Malignant
ns
B
Lymphocytes
Cluster frequency
Marker frequency
MFI
CD45
HLA-DR
CD16
CD56
CD19
CD3
CD4
CD8
CD45RA
CCR7
CD25
CD127
CD11b
CD15
B-cells
Treg
CD4+ T-cells
CD8+ T-cells
CD4- CD8-
NK-cells
C
Non-Lymphocytes
CD45
CD33
CD11b
CD14
CD16
HLA-DR
CCR7
CD163
CD15
CD4
CD3
CD56
CD25
CD14-
CD16-CD163-CD14+
CD16+CD163++ CD14++CD56+CCR7- M2 Macrophages
D
IL-2
ULBP4
ULBP1
ULBP3
IL-6
TGF-β1
TIM3
IL-12p40
IP10
NECTIN2
PVR
4-1BB
IL-10
PD-L2
IL-1RA
IL-8
IL-1β
TNF-α
IL-15
Granzyme B
IFN-γ
GITRL
TrailR1
TrailR2
TRAIL
Tactile
Perforin
MICA
MICB
IDO-1
Arginase
Spearman correlation
E

Figure 6: ***M2 like macrophages, Tregs and B cells are associated to the secretome including TGF-β1 in EOC patient ascites***

(A) *Frequency of cell populations within CD45$^+$ cells in PBMCs (as circulating reference, PB), benign peritoneal fluids and malignant ascites based on manual gating, Kruskal-Wallis with Dunn's Multiple Comparison Test was used for statistical analysis, ** $p < 0.01$, *** $p < 0.001$.* ***(B and C)*** *Scaled MFI values of FlowSOM clusters for the lymphocyte (B) and non-lymphocyte (C) fraction of malignant ascites in a balloon plot. Each row represents a marker, while columns represent a cluster. Balloon size represents frequency while balloon color represents MFI (red is high MFI, yellow is low MFI). On top of the balloon plot the cluster size is presented as percent of total where red indicate large clusters and green small clusters. All clusters smaller than 1% of the total cell population were excluded to prevent overfitting of rare populations.* ***(D and E)*** *Spearman correlogram of cytokine levels versus clusters of the lymphocyte (D) and non-lymphocyte (E) fraction of EOC patient ascites. A heat map is used to indicate the Spearman's rank correlation coefficient (ρ) of associations between biomarkers. Red indicates a positive correlation, and blue indicates a negative correlation. All clusters smaller than 1% of the total cell population were excluded to prevent overfitting of rare populations. ns, not significant, * $p < 0.05$, L, lymphocyte and NL, non-lymphocyte.*

Next, we performed multidimensional scaling (MDS) on the leukocyte dataset to visualize the differences in distribution of cellular populations in healthy donor PB compared to benign reference or EOC patient peritoneal fluids (Supplemental Figure 4A). For the non-lymphocyte (NL) fraction we gated on CD45+CD33+ cells and for the lymphocyte (L) on CD45+CD33- cells, and the MFI of each marker was used to calculate the MDS plot. Healthy donor PB samples clearly clustered separately from EOC patient ascites samples, while benign samples are distributed between the EOC patient ascites samples and healthy donor PB samples. For the CD45+ NL fraction of the leukocyte panel, we found a similar pattern but the differences between each group were less pronounced. Hierarchical clustering of surface marker intensities across the samples corresponded with results from the MDS, showing a clear difference between benign reference and EOC patients which was especially clear in the NL fraction (Supplemental Figure 4B). To further define the cell population landscape in ascites, we used the FlowSOM (k=35) clustering approach. We found separate clusters for both the L and NL fractions, and excluded all clusters smaller than 1% of the total cell population to prevent overfitting of rare populations (Figure 6B and C). For the L fraction, we found three clusters that were enriched in EOC patients, namely CD4+CD25++CD127- Tregs (L C05), CD56dimCD16low NK cells (L C09) and a cluster of CD19+ B cells (L C34) (Figure 6B, Figure 7A). The two clusters enriched in benign peritoneal fluid were a CD3+CD4+ T cell cluster (L C07) and a CD3+CD8+ T cell cluster (L C31). For the NL fraction, we found a large meta-cluster of CD14+CD163+CD197-CD16+/-CD56+/- M2-like macrophages (NL C08, NL C23, NL C31, NL C33, NL C34, NL C30, NL C26 and NL C29, Figure 6C, Figure 7B). To determine which of these cell populations were associated with the secretory compartment in EOC ascites, we correlated the FlowSOM clustering data with the soluble factor levels. Interestingly, the TGF-β1 and IL-6 concentration was

significantly associated with all CD19+ B-cell clusters (L C33, L C34 and L C35, Figure 6D). In addition, these CD19+ B cell clusters also associated with other inhibitory and activating factors, including IL-10 and soluble ligands for DNAM-1 (NECTIN2 and PVR). This association was partially shared with the CD4+CD25+ +CD127- Treg cluster (L C05) and a CD56dim NK cell cluster (L C09) with reduced CD16 expression typically found in EOC ascites [23], although not all correlations were similar. Notably, the strongest association with the secretory milieu in ascites was with CD14+CD163+CD197-CD16+/-CD56+/- M2-like macrophages including TGF-β1 (NL C08, NL C15, NL C19, NL C24, NL C27 and NL C31, Figure 6E). A cluster of (classical) CD14+CD163-CD16-CD56- monocytes, found mostly in PB (NL C04), was negatively correlated with several soluble factors.

Altogether these findings indicate that the presence of CD14+CD163+CD197-CD16+/-CD56+/- M2-like macrophages encompasses the major difference between the cellular make-up of benign versus EOC ascites. Interestingly, these M2-like TAMs strongly correlate with the inhibitory secretome of EOC patient ascites, including TGF-β1. Besides these M2-like macrophages, B cells and Tregs are also associated with the secretome found in EOC patient ascites.

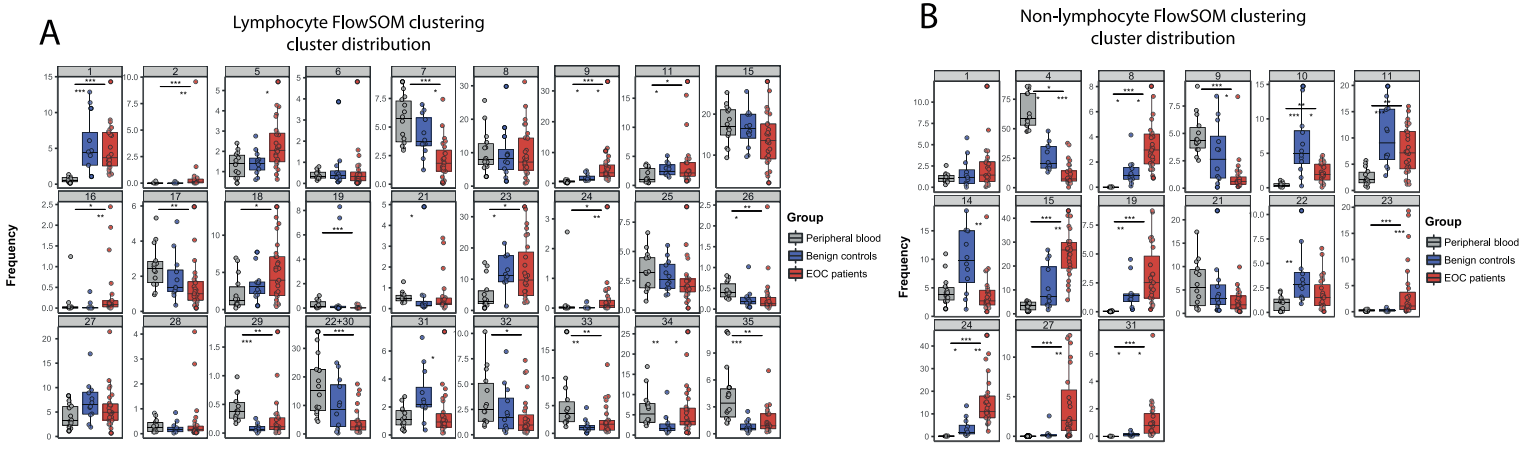

Figure 7: ***(A and B)*** *Box and whiskers plots showing the percentage of FlowSOM clusters, based on the lymphocyte fraction (A) and non-lymphocyte fraction (B), showing different cell cluster distribution in healthy donors (grey, n=14), benign patients (blue, n=12) and patients with malignancy (red, n=27). All clusters smaller than 1% of the total cell population were excluded to prevent overfitting of rare populations. Kruskal-Wallis with Dunn's Multiple Comparison Test was used for statistical analysis * $p < 0.05$, * $p < 0.05$, ** $p < 0.01$ and *** $p < 0.001$*

Discussion

EOC patient ascites is a major factor contributing to recurrence and poor prognosis in EOC patients. This ascites contains a variety of soluble and cellular components that influence the function of tumor-targeting lymphocytes [5, 24]. Although significant NK-cell numbers are present in EOC ascites, their antitumor activity is inhibited by soluble mediators and membrane-bound receptors [25]. Furthermore, it is well known that ascites can impair the functionality of NK cells [5], and can thereby hamper the antitumor efficacy of NK-cell therapeutic products in EOC patients. Nevertheless, we and others have previously shown that ascites-induced NK-cell dysfunction can be reinvigorated by for instance IL-15 receptor-mediated stimulation [13, 26]. To further elucidate mechanisms impairing NK cell function in the local EOC environment, we now combined NK-cell functional data, soluble factor analysis, high-dimensional flow cytometry assessment of cellular components and clinical parameters of advanced EOC patients in integrated analyses. Using an activation assay, we examined the effects of ascites on CD107a and IFN-γ expression of NK cells after stimulation with tumor target cells. Interestingly, we found that strong inhibitory effects of EOC patient ascites on CD107a degranulation from healthy donor-derived NK cells were associated to reduced PFS and OS in a cohort of 31 high-grade serous EOC patients. One explanation why survival was significantly associated to CD107a degranulation but not IFN-γ is that the baseline IFN-γ response to SKOV-3 is low, especially for healthy-donor PB-NK cells thus reducing demonstration of the inhibitory potential of ascites. Further, for most ascites fluids maximum IFN-γ inhibition was achieved, and a stronger OC cell stimulus in a future study might overcome this limitation. Moreover, we observed a positive correlation between ascites-induced NK-cell dysfunction and higher CA-125 levels in the serum of the EOC patients. Previous reports have already shown that CA-125 present in EOC patient ascites inhibits NK-cell antitumor activity [27]. However, our data show a stronger correlation between ascites-induced NK-cell dysfunction and CA-125 serum levels rather than peritoneal levels. Furthermore, we revealed that TGF-β1 was a suppressive factor associated to ascites-induced NK-cell dysfunction, reduced patient survival and the presence of a higher frequency of M2-like macrophages. In functional assays, we showed that NK cell proliferation and function is significantly affected by TGF-β1, and inhibition of TGF-βR1 signalling by galunisertib partly restored NK-cell functionality. Although we tried to capture the major soluble factors and pathways that are known to impact NK cell function such as IL-15, IL-10 and ligands for activating receptors such as DNAM-1 and NKG2D we did not find a significant association of any other factor with both functional and patient survival data. As TGF-β1 is only partly responsible for our findings there may be important factors that we failed to include in our study or that our study was not power enough to identify.

Nonetheless, these results show that TGF-β1 is an important factor in EOC ascites capable of dampening NK-cell antitumor activity.

Other factors that were significantly elevated in EOC patient ascites compared to benign ascites included IL-6 and IL-10 as well as soluble ligands for activating NK cell receptors such as MIC-B (NKG2D ligand) and Nectin-2 (DNAM-1 ligand). High ascites levels of IL-6 have previously been associated with poor outcome in EOC patients [28]. For inhibitory cytokine IL-10, 2 out of 3 studies showed that IL-10 levels in ascites were not associated with prognosis [28]. Our study did not show an association of IL-10 levels to patient survival either. Shedding of ligands for activating receptors such as MIC-A and MIC-B can help evasion of tumor cells from NK-cell attack [29], and we found that elevated MIC-B levels are increased in EOC ascites compared to benign ascites. Recent data suggests similar mechanisms where soluble PVR, a DNAM-1 ligand, inhibited DNAM-1-mediated NK-cell activation [20]. In contrast, we found that soluble ULBP-4 in ascites, a different NKG2D ligand, was associated to increased NK-cell activity similar to a recent study where ULBP4 was associated with higher T-cell function in Multiple Sclerosis patients [30]. Although benign ascites samples also showed strong inhibitory effects on NK cells, our sample size was too small to perform comprehensive correlative studies and we may have missed important inhibitory soluble factors in our analysis. The mechanisms underlying these observations will be further studied in follow-up investigations.

Many of the soluble inhibitory factors assessed are not secreted by NK cells, but other immune cells that regulate immunity, including NK cells, in ascites. We also evaluated the frequencies and phenotype of a variety of immune cells in order to identify the cell populations that correlate with the suppressive factors present in ascites. We found a lower fraction CD45+ hematopoietic cells in patients with malignancy, which corresponds to increased frequency of tumor and stroma cells present in ascites [13]. Another evident observation was the high proportion of M2-like TAMs, which has also been described and reviewed extensively [31]. Presence of these TAMs was associated with high levels of TGF-β, IL-6, IL-10 and TNF-α in ascites [32], which we confirmed in our study. It is well-known that TGF-β is a major driver for the polarization towards M2-like TAMs [33]. In addition, we observed that other soluble factors were associated with these TAMs, including IL-12p40, IL-15, IP10 and soluble IDO-1. Since our study is solely associative, future research is required to elucidate the source of these factors. Generally, IDO-1 expression is known to be up-regulated in cancer and serves as an immunosuppressive and immune evasive mechanism by tumor cells [34]. A recent study on IDO-1 in EOC demonstrated elevated levels of IDO-1 metabolism in ascites compared to healthy controls [35]. In contrast, we did not observe an increase for soluble IDO-1 in our

study, but we compared EOC patient ascites to benign reference fluids, while Grobben et al. used healthy donor plasma as controls potentially explaining the discrepancy in results. Furthermore, our study revealed a positive correlation between survival of EOC patients and increased IDO-1 levels. Moreover, in a phase III trial IDO-1 inhibition did not show survival benefits in unresectable or metastatic melanoma patients [36]. Therefore, the mechanism behind IDO-1 signalling in cancer remains to be further investigated as IDO-1 has been associated strongly with ascites and survival of EOC patients.

Besides M2-like TAMs we observed associations of (sub)populations of B cells and Tregs and high levels of soluble mediators in EOC patient ascites. Regulatory (CD25+) B cells have already been described, and few studies have highlighted the importance of B cells in EOC [37]. One study on regulatory IL-10-producing B cells in EOC patients showed that their frequencies correlated positively with Tregs [38]. These IL-10-producing B cells also suppressed IFN-γ production by effector T cells. Furthermore, Tregs are known to be associated to an inhibitory TME. Our study confirms that Tregs in EOC are associated with the secretome, although these Tregs did not significantly correlate to TGF-β1 concentrations they did to IL-10. The high proportion of CD56dimCD16low NK cells in ascites was previously reported to be associated to EOC [23]. Although TGF-β1 is known to downregulate NK-cell phenotype and function, we found no correlation between the CD56dimCD16low NK-cell phenotype and TGF-β1.

Others have shown that TGF-β1 can promote cancer progression, which is primarily mediated through its effects on the local TME. Here, we revealed that TGF-β1 in EOC ascites contributes to induction of NK-cell dysfunction. CD34 HPC-derived NK cells were susceptible to rhTGF-β1 added to the culture leading to reduced proliferation and functionality. Importantly, addition of the TGF-βR1 inhibitor galunisertib partly mitigated this inhibitory effect, but this effect was donor dependent. Moreover, while galunisertib was positively evaluated in some (pre-)clinical studies [39, 40], systemic TGF-β inhibition yielded poor results overall that were attributed in part to cardiovascular toxic side effects and formation of benign tumors [33, 41]. In combination with our data, this shows that a more effective and controlled inhibition of TGF-β1 signalling is needed for sustained activity of NK cells in the TME. This is currently being explored by others via overexpression of a dominant-negative TGF-βR2 (TGFβRDN) or CRISPR-Cas9-mediated knockout of TGFBR2 in adoptive T- and NK-cell therapy products [42, 43]. Recently, a phase I trial with prostate cancer-directed CAR T cells armored with a TGFβRDN to block TGF-β signalling was conducted illustrating both feasibility and importance of interfering with the TGF-β pathway [44]. Another study in glioblastoma-bearing mice

treated with allogeneic NK cells showed that TGFBR2 knockout prevented NK-cell dysfunction and tumor growth [45]. The same group is currently evaluating NK cells with deleted TGF-βR2 for treatment of glioblastoma in a phase I trial (NCT04991870). This CRISPR/Cas9 TGF-βR2 deletion can easily be implemented in our protocol for ex vivo-generated HPC-NK cells. In combination with the aforementioned TGF-β receptor gene editing strategies, this provides a promising approach to improve current EOC treatment with adoptive NK cell therapy.

In this study, we primarily used CD34+ HPC-derived NK cells that have already been shown to be able to efficiently kill ovarian cancer cells in vitro and in vivo [46], and these cells are currently tested in a phase I study in EOC patients (NCT03539406). Importantly, we revealed that galunisertib significantly rescued HPC-NK cell function when challenged with TGF-β in vitro. Furthermore, while both HPC-NK cells and healthy donor PB-NK cells were potently impaired by ascites of EOC patients, we found that HPC-NK cells were more resistant to ascites-mediated suppression indicating their high functionality and lower vulnerability to TME-mediated suppression. This finding is in line with a previous report where we showed that HPC-NK cells have superior EOC reactivity compared to PB-NK cells, which could be related to the increased granzyme-B release by HPC-NK cells and higher serial killing potential [21, 47]. Furthermore, we found TGF-βR2 expression to be higher on PB-NK cells than on HPC-NK cells (data not shown).

In conclusion, our results demonstrate that high peritoneal TGF-β1 concentrations were negatively correlated to EOC patient survival. Furthermore, we found that NK-cell function is strongly impaired by ascites from high-grade EOC patients, and that TGF-β1 plays an important role in this effect. We showed that inhibition of the TGF-β signalling pathway by small molecule inhibitor galunisertib partly rescued NK-cell function. Taken together, these results provide a rationale for improvement of NK-cell function via inhibition of TGF-β1 signalling. Since systemic anti-TGF-β has shown limited success in clinical trials so far, a more potent approach with fewer side effects is warranted. We envision implementing CRISPR/Cas9 gene editing in our 5-week culture protocol to improve our HPC-NK cell therapeutic product to achieve this.

References

1. Siegel RL, Giaquinto AN, Jemal A. *Cancer statistics, 2024. CA:* A Cancer J Clin. (2024) 74(1):12–49.

2. Ahmed N, Stenvers KL. *Getting to know ovarian cancer ascites: opportunities for targeted therapy-based translational research.* Front Oncol. (2013) 3:256.

3. Lane D, Goncharenko-Khaider N, Rancourt C, Piché A. *Ovarian cancer ascites protects from TRAIL-induced cell death through alphavbeta5 integrin-mediated focal adhesion kinase and Akt activation.* Oncogene. (2010) 29(24):3519–31.

4. Puiffe ML, Le Page C, Filali-Mouhim A, Zietarska M, Ouellet V, Tonin PN, et al. *Characterization of ovarian cancer ascites on cell invasion, proliferation, spheroid formation, and gene expression in an in vitro model of epithelial ovarian cancer.* Neoplasia. (2007) 9(10):820–9.

5. Rickard BP, Conrad C, Sorrin AJ, Ruhi MK, Reader JC, Huang SA, et al. *Malignant ascites in ovarian cancer: cellular, acellular, and biophysical determinants of molecular characteristics and therapy response.* Cancers (Basel). (2021) 13(17):4318.

6. Kim S, Kim B, Song YS. *Ascites modulates cancer cell behavior, contributing to tumor heterogeneity in ovarian cancer.* Cancer Sci. (2016) 107:1173–8.

7. Siegel RL, Miller KD, Jemal A. Cancer statistics, 2017. CA Cancer J Clin. (2017) 67(1):7–30.

8. Curiel TJ, Coukos G, Zou L, Alvarez X, Cheng P, Mottram P, et al. *Specific recruitment of regulatory T cells in ovarian carcinoma fosters immune privilege and predicts reduced survival.* Nat Med. (2004) 10(9):942–9.

9. Ghiringhelli F, Ménard C, Terme M, Flament C, Taieb J, Chaput N, et al. *CD4+CD25+ regulatory T cells inhibit natural killer cell functions in a transforming growth factor-beta-dependent manner*. J Exp Med. (2005) 202(8):1075–85.

10. Kärre K, Ljunggren HG, Piontek G, Kiessling R. *Selective rejection of H–2-deficient lymphoma variants suggests alternative immune defence strategy.* Nature. (1986) 319(6055):675–8.

11. Marijt KA, Sluijter M, Blijleven L, Tolmeijer SH, Scheeren FA, van der Burg SH, et al. *Metabolic stress in cancer cells induces immune escape through a PI3K-dependent blockade of IFNγ receptor signaling.* J Immunother Cancer. (2019) 7(1):152.

12. Labani-Motlagh A, Israelsson P, Ottander U, Lundin E, Nagaev I, Nagaeva O, et al. *Differential expression of ligands for NKG2D and DNAM-1 receptors by epithelial ovarian cancer-derived exosomes and its influence on NK cell cytotoxicity.* Tumour Biol. (2016) 37(4):5455–66.

13. Hoogstad-van Evert JS, Maas RJ, van der Meer J, Cany J, van der Steen S, Jansen JH, et al. *Peritoneal NK cells are responsive to IL-15 and percentages are correlated with outcome in advanced ovarian cancer patients*. Oncotarget. (2018) 9(78):34810–20.

14. Hirte H, Clark DA. *Generation of lymphokine-activated killer cells in human ovarian carcinoma ascitic fluid: Identification of transforming growth factor-β as a suppressive factor.* Cancer Immunology Immunotherapy. (1991) 32(5):296–302.

15. Gotlieb WH, Abrams JS, Watson JM, Velu TJ, Berek JS, Martínez-Maza O. *Presence of interleukin 10 (IL-10) in the ascites of patients with ovarian and other intra-abdominal cancers.* Cytokine. (1992) 4(5):385–90.

16. da Silva RF, Yoshida A, Cardozo DM, Jales RM, Paust S, Derchain S, et al. *Natural killer cells response to IL-2 stimulation is distinct between ascites with the presence or absence of Malignant cells in ovarian cancer patients*. Int J Mol Sci. (2017) 18(5):856.

17. Carlsten M, Norell H, Bryceson YT, Poschke I, Schedvins K, Ljunggren HG, et al. *Primary human tumor cells expressing CD155 impair tumor targeting by down-regulating DNAM-1 on NK cells*. J Immunol. (2009) 183(8):4921–30.

18. Pesce S, Tabellini G, Cantoni C, Patrizi O, Coltrini D, Rampinelli F, et al. *B7-H6-mediated downregulation of NKp30 in NK cells contributes to ovarian carcinoma immune escape. Oncoimmunology*. (2015) 4(4):e1001224.

19. Coudert JD, Zimmer J, Tomasello E, Cebecauer M, Colonna M, Vivier E, et al. *Altered NKG2D function in NK cells induced by chronic exposure to NKG2D ligand-expressing tumor cells.* Blood. (2005) 106(5):1711–7.

20. Okumura G, Iguchi-Manaka A, Murata R, Yamashita-Kanemaru Y, Shibuya A, Shibuya K. *Tumor-derived soluble CD155 inhibits DNAM-1-mediated antitumor activity of natural killer cells.* J Exp Med. (2020) 217(4):1.

21. Van der Meer JMR, Maas RJA, Guldevall K, Klarenaar K, de Jonge P, Evert JSH, et al. *IL-15 superagonist N-803 improves IFNγ production and killing of leukemia and ovarian cancer cells by CD34(+) progenitor-derived NK cells*. Cancer Immunol Immunother. (2021) 70(5):1305–21.

22. Browning L, Patel MR, Horvath EB, Tawara K, Jorcyk CL. *IL-6 and ovarian cancer: inflammatory cytokines in promotion of metastasis.* Cancer Manag Res. (2018) 10:6685–93.

23. Maas RJ, Hoogstad-van Evert JS, Van der Meer JM, Mekers V, Rezaeifard S, Korman AJ, et al. *TIGIT blockade enhances functionality of peritoneal NK cells with altered expression of DNAM-1/TIGIT/CD96 checkpoint molecules in ovarian cancer. Oncoimmunology.* (2020) 9(1):1843247.

24. Yigit R, Figdor CG, Zusterzeel PL, Pots JM, Torensma R, Massuger LF. *Cytokine analysis as a tool to understand tumour-host interaction in ovarian cancer.* Eur J Cancer. (2011) 47(12):1883–9.

25. Sivori S, Della Chiesa M, Carlomagno S, Quatrini L, Munari E, Vacca P, et al. *Inhibitory receptors and checkpoints in human NK cells, implications for the immunotherapy of cancer.* Front Immunol. (2020) 11.

26. Felices M, Lenvik TR, Kodal B, Lenvik AJ, Hinderlie P, Bendzick LE, et al. *Potent cytolytic activity and specific IL15 delivery in a second-generation trispecific killer engager.* Cancer Immunol Res. (2020) 8(9):1139–49.

27. Patankar MS, Jing Y, Morrison JC, Belisle JA, Lattanzio FA, Deng Y, et al. *Potent suppression of natural killer cell response mediated by the ovarian tumor marker CA125.* Gynecol Oncol. (2005) 99(3):704–13.

28. Fahmi MN, Pradjatmo H, Astuti I, Nindrea RD. *Cytokines as prognostic biomarkers of epithelial ovarian cancer (EOC): A systematic review and meta-analysis.* Asian Pac J Cancer Prev. (2021) 22(2):315–23.

29. Xing S, Ferrari de Andrade L. *NKG2D and MICA/B shedding: a 'tag game' between NK cells and Malignant cells.* Clin Transl Immunol. (2020) 9(12):e1230.

30. Carmena Moratalla A, Carpentier Solorio Y, Lemaitre F, Farzam-Kia N, Levert A, Zandee SEJ, et al. *Stress signal ULBP4, an NKG2D ligand, is upregulated in multiple sclerosis and shapes CD8(+) T-cell behaviors*. Neurol Neuroimmunol Neuroinflamm. (2022) 9(1):e1119.

31. Nowak M, Klink M. *The role of tumor-associated macrophages in the progression and chemoresistance of ovarian cancer*. Cells. (2020) 9(5):1299.

32. Chen Y, Tan W, Wang C. *Tumor-associated macrophage-derived cytokines enhance cancer stem-like characteristics through epithelial-mesenchymal transition.* OncoTargets Ther. (2018) 11:3817–26.

33. Tauriello DVF, Sancho E, Batlle E. *Overcoming TGFβ-mediated immune evasion in cancer.* Nat Rev Cancer. (2022) 22(1):25–44.

34. Wang D, Saga Y, Mizukami H, Sato N, Nonaka H, Fujiwara H, et al. *Indoleamine-2,3-dioxygenase, an immunosuppressive enzyme that inhibits natural killer cell function, as a useful target for ovarian cancer therapy.* Int J Oncol. (2012) 40(4):929–34.

35. Grobben Y, den Ouden JE, Aguado C, van Altena AM, Kraneveld AD, Zaman GJR. *Amino acid-metabolizing enzymes in advanced high-grade serous ovarian cancer patients: value of ascites as biomarker source and role for IL4I1 and IDO1.* Cancers. (2023) 15(3):893.

36. Long GV, Dummer R, Hamid O, Gajewski TF, Caglevic C, Dalle S, et al. *Epacadostat plus pembrolizumab versus placebo plus pembrolizumab in patients with unresectable or metastatic melanoma (ECHO-301/KEYNOTE-252): a phase 3, randomised, double-blind study.* Lancet Oncol. (2019) 20(8):1083–97.

37. Brisslert M, Bokarewa M, Larsson P, Wing K, Collins LV, Tarkowski A. *Phenotypic and functional characterization of human CD25+ B cells.* Immunology. (2006) 117(4):548–57.

38. Wei X, Jin Y, Tian Y, Zhang H, Wu J, Lu W, et al. *Regulatory B cells contribute to the impaired antitumor immunity in ovarian cancer patients.* Tumour Biol. (2016) 37(5):6581–8.

39. Kelley RK, Gane E, Assenat E, Siebler J, Galle PR, Merle P, et al. *A phase 2 study of galunisertib (TGF-β1 receptor type I inhibitor) and sorafenib in patients with advanced hepatocellular carcinoma*. Clin Trans Gastroenterol. (2019) 10(7):e00056.

40. Zhang Q, Hou X, Evans BJ, VanBlaricom JL, Weroha SJ, Cliby WA. *LY2157299 monohydrate, a TGF-βR1 inhibitor, suppresses tumor growth and ascites development in ovarian cancer.* Cancers (Basel). (2018) 10(8):260.

41. Teixeira AF, Ten Dijke P, Zhu HJ. *On-target anti-TGF-β Therapies are not succeeding in clinical cancer treatments: what are remaining challenges?* Front Cell Dev Biol. (2020) 8:605.

42. Yvon ES, Burga R, Powell A, Cruz CR, Fernandes R, Barese C, et al. *Cord blood natural killer cells expressing a dominant negative TGF-β receptor: Implications for adoptive immunotherapy for glioblastoma.* Cytotherapy. (2017) 19(3):408–18.

43. Fix SM, Forget MA, Sakellariou-Thompson D, Wang Y, Griffiths TM, Lee M, et al. *CRISPR-mediated TGFBR2 knockout renders human ovarian cancer tumor-infiltrating lymphocytes resistant to TGF-β signaling.* J Immunother Cancer. (2022) 10(7):e003750.

44. Narayan V, Barber-Rotenberg JS, Jung IY, Lacey SF, Rech AJ, Davis MM, et al. *PSMA-targeting TGFβ-insensitive armored CAR T cells in metastatic castration-resistant prostate cancer: a phase 1 trial.* Nat Med. (2022) 28(4):724–34.

45. Shaim H, Shanley M, Basar R, Daher M, Gumin J, Zamler DB, et al. *Targeting the αv integrin/TGF-β axis improves natural killer cell function against glioblastoma stem cells*. J Clin Invest. (2021) 131(14):e142116.

46. Hoogstad-van Evert JS, Cany J, van den Brand D, Oudenampsen M, Brock R, Torensma R, et al. *Umbilical cord blood CD34(+) progenitor-derived NK cells efficiently kill ovarian cancer spheroids and intraperitoneal tumors in NOD/SCID/IL2Rg(null) mice*. Oncoimmunology. (2017) 6:e1320630.

47. Subedi N, Verhagen LP, de Jonge P, Van Eyndhoven LC, van Turnhout MC, Koomen V, et al. *Single-cell profiling reveals functional heterogeneity and serial killing in human peripheral and ex vivo-generated CD34+ Progenitor-derived natural killer cells*. Adv Biol (Weinh). (2022) p:e2200207.

Supplemental Data

Supplemental tables

Supplemental table 1: ***Supplemental Overview patient characteristics.***

		Malignant (n=31)	Benign (n=16)
	Mean age (SD)	63 (11) years	53 (10) years*
	Median PFS (SD)	6.9 (8.9) months	N/A
	Median OS (SD)	18.9 (14.9) months	N/A
	Serum CA-125 (SD)	2432 (2879) U/mL	244 (636) U/mL**
	Peritoneal CA-125 (SD)	17589 (23098) U/mL	1026 (1891) U/mL
	FIGO stage 3b/c	n=18	N/A
	FIGO stage 4	n=13	N/A
	Alive* **	n=7	N/A
	NACT	n=21	N/A
Treatment type	**PDS**	n=7	N/A
	No treatment	n=2	N/A
	Poor	n=2	N/A
Response	**Mixed**	n=5	N/A
	Good	n=19	N/A
Ascites	**Yes**	n=30	n=8
	No	n=1	n=8

**Age is known for n=12; **CA-125 serum levels have been quantified in n=12; ***At time of analysis, SD = Standard deviation, PFS = Progression free survival, OS = Overall survival, NACT = neoadjuvant chemotherapy, PDS = Primary debulking, N/A = Not applicable*

Supplemental table 2: ***Individual EOC patient characteristics.***

Paper	Age (years)	FIGO stage	PFS (months)*	OS (months)*	Alive	CA125 U/ mL (Serum)	CA-125 U/ mL (Peritoneal)	NACT/PDS
M01	75	IV	1.5	7.8	No	468	15000	NACT
M02	56	IIIc	6.8	12.5	No	2200	7500	NACT
M03	69	IIIc	20.0	53.8	No	198	1100	PDS
M04	52	IV	4.1	9.4	No	1223	22500	NACT
M05	63	IIIc	20.5	26.2	No	4889	37000	NACT
M06	64	IV	0	8.6	No	1800	4550	NACT
M07	61	IIIc	20.5	55.5	No	2380	26500	PDS
M08	52	IV	5.2	Unknown	Unknown	5700	55000	NACT
M09	59	IIIc	8.4	29.4	No	1304	4450	NACT
M10	45	IV	0	1.7	No	1400	18000	None
M11	69	IIIc	25.1	31.4	No	899	4100	NACT
M12	67	IV	9.1	10.6	No	1560	7000	NACT
M13	76	IIIc	23.9	41.3	No	928	1400	NACT
M14	93	IV	0	1.2	No	412	850	PDS
M15	61	IIIc	Unknown	Unknown	Unknown	10000	12500	NACT
M16	64	IIIc	5.8	37.0	No	352	4650	N/A
M17	52	IV	21.0	31.1	Yes	1621	14000	NACT
M18	63	IIIc	18.0	30.4	Yes	344	1700	PDS
M19	64	IIIc	3.6	29.0	No	31	3250	PDS
M20	47	IIIc	18.9	18.9	Yes	1484	6500	PDS
M21	72	IV	5.7	21.6	Yes	1018	7500	NACT

Paper	Age (years)	FIGO stage	PFS (months)*	OS (months)*	Alive	CA125 U/ mL (Serum)	CA-125 U/ mL (Peritoneal)	NACT/PDS
M22	36	IIIc	22.0	22.0	No	1116	85000	PDS
M23	61	IV	0	14.5	No	10000	95000	NACT
M24	74	IV	1.1	1.1	No	1175	15000	NACT
M25	76	IIIb	22.1	22.1	Yes	1516	18500	NACT
M26	69	IIIc	10.2	18.6	Yes	215	2050	NACT
M27	68	IIIc	14.2	16.5	Yes	1931	2250	NACT
M28	50	IV	0	0.7	No	9909	27000	None
M29	61	IIIc	0	2.5	No	5694	34000	NACT
M30	57	IIIc	2.9	20.3	No	2118	8500	NACT
M31	72	IV	6.9	7.6	No	1500	2900	NACT

**At time of analysis, SD = Standard deviation, PFS = Progression free survival, OS = Overall survival,NACT = neoadjuvant chemotherapy, PDS = Primary debulking*

Supplemental table 3: ***Individual benign patient characteristics.***

Number	Age (years)	Fluid type	Pathology diagnosis	Endometriosis	Torsion/infection	CA-125 (U/ml) Serum	CA-125 (U/ml) Peritoneal
B1	53	ascites	Mucinous cystadenoma	-	-	60	750
B2	39	washing	Endometrioma	Yes	-	156	425
B3	62	ascites	Benign fibroma	-	Necrosis	284	500
B4	50	washing	Serous cystadenofibroma	-	-	25	700
B5	41	washing	Serous cystadenoma	-	-	10	80
B6	64	ascites	Serous cystadenoma	-	-	34	550
B7	47	washing	Mucineus cystadenoma	-	-	20	230
B8	65	washing	Mucinous cystadenoma	-	-	23	280
B9	47	washing	Serous cystadenoma	-	-	52	300
B10	41	washing	Mucinous cystadenoma	-	-	15	600
B11	54	washing	Serous cystadenoma	-	-	5	210
B12	69	ascites	Benign not further defined	-	-	2249	1400
B13*	Unknown	ascites	Benign not further defined	Unknown	Unknown	Unknown	435
B14*	Unknown	ascites	Benign not further defined	Unknown	Unknown	Unknown	8000
B15*	Unknown	ascites	Benign not further defined	Unknown	- Unknown	Unknown	1050
B16*	Unknown	ascites	Benign not further defined	Unknown	Unknown	Unknown	900

*Age and CA-125 of samples B13-B16 are unknown and their benign diagnosis not further defined

Supplemental Table 4: ***Antibodies for leukocyte subset panel.***

Marker/ Dye combination	Manufacturer	Catalog number	Clone	Host species, Isotype	Laser	Filters
CD3 FITC	BioLegend	300406	UCHT1	Mouse IgG1	488	525/40
CD4 BV510	BioLegend	317444	OKT4	Mouse IgG2b	405	525/40
CD8 BUV737	BD Biosciences	612755	SK1	Mouse IgG1	355	740/35
CD45RA PE-Cy7	BioLegend	304126	HI100	Mouse IgG2b	561	763/43
CD197 (CCR7) BV605	BioLegend	353224	G043H7	Mouse IgG2a	405	610/20
CD127 (IL-7Rα) APC	BioLegend	351316	A019D5	Mouse IgG1	638	660/10
CD25 BV786	BD Biosciences	563701	M-A251	Mouse IgG1	405	780/60
CD19 PE-Cy5	Beckman Coulter	A07771	J3-119	Mouse IgG1	561	675/30
CD56 BV711	BioLegend	318336	HCD56	Mouse IgG1	405	710/50
CD16 BUV496	BD Biosciences	612944	3G8	Mouse IgG1	355	525/40
CD45 BUV395	BD Biosciences	563792	HI30	Mouse IgG1	355	385/26
CD33 BV421	BioLegend	303416	WM53	Mouse IgG1	405	450/45
HLA-DR APC-R700	BD Biosciences	565127	G46-6	Mouse IgG2a	638	712/25
CD15 APC-Fire750	BioLegend	323042	W6D3	Mouse IgG1	638	763/40
CD14 PerCP-Cy5.5	Biolegend	301824	M5E2	Mouse IgG2a	488	690/50
CD11b PE	Beckman Coulter	IM2581U	Bear1	Mouse IgG1	561	585/42
CD163 PE-CF594	BD Biosciences	562670	GHI/61	Mouse IgG1	561	610/20
Live/ dead ViaKrome808	Beckman Coulter	C36628	N/A	N/A	808	885/40

Supplemental figures

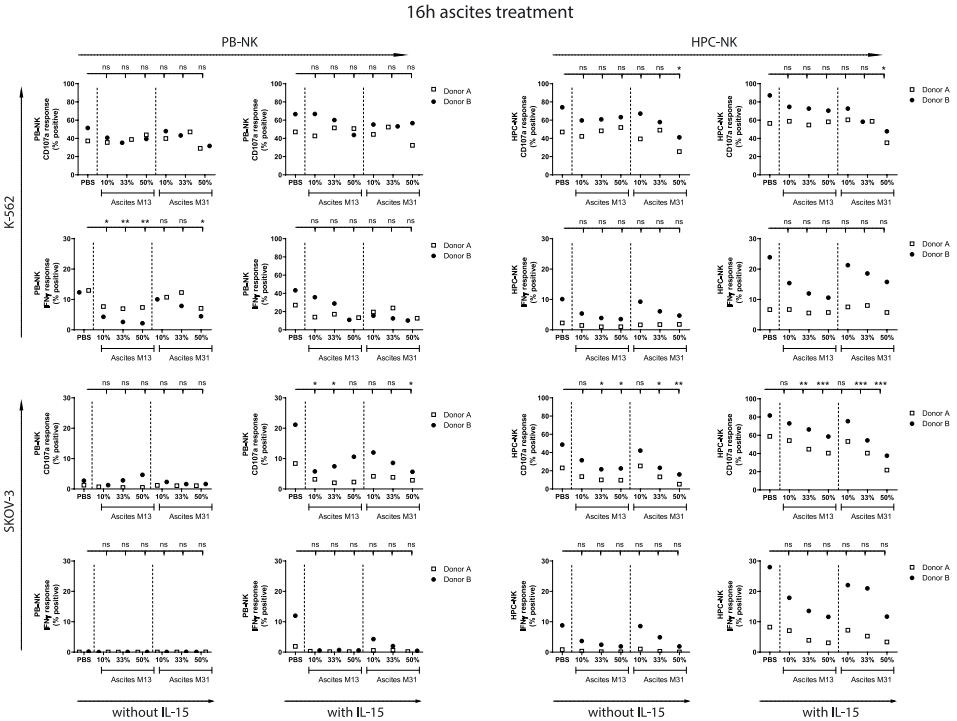

Supplemental figure 1: ***The effect of ascites from two OC patients with overnight co-incubation on NK cell activity***

Percent positive CD107a and IFN-γ on HPC-derived (right) or PB-NK cells (left) stimulated with SKOV-3 (bottom) or K562 (top) target cells in the presence of PBS control or malignant ascites (M13 and M31). Cells were incubated overnight with aforementioned fluids with or without addition of 1nM rhIL-15. After overnight incubation NK cells were challenged with target cells for 4h . Experiment was performed in duplicate, averages are shown.

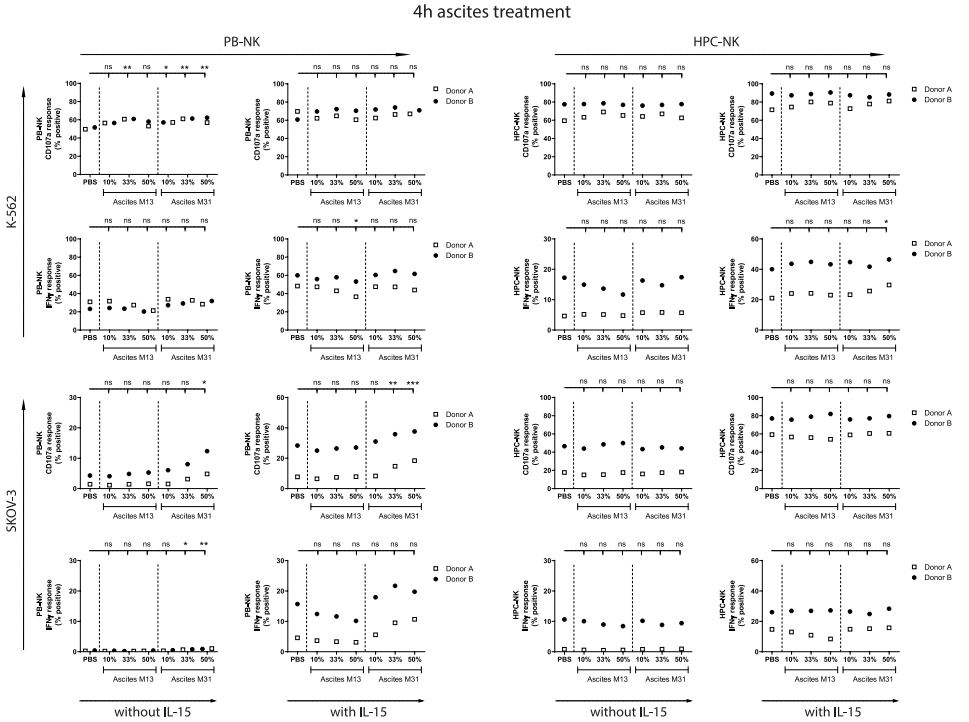

Supplemental figure 2: ***The effect of ascites from two OC patients with 4h co-incubation on NK cell activity***

Percent positive CD107a and IFN-γ on HPC-derived (right) or PB-NK cells (left) stimulated with SKOV-3 (bottom) or K562 (top) target cells in the presence of PBS control or malignant ascites (M13 and M31).Cells were incubated for 4h with aforementioned fluids with or without addition of 1nM rhIL-15 and target cells. Experiment was performed in duplicate, averages are shown.

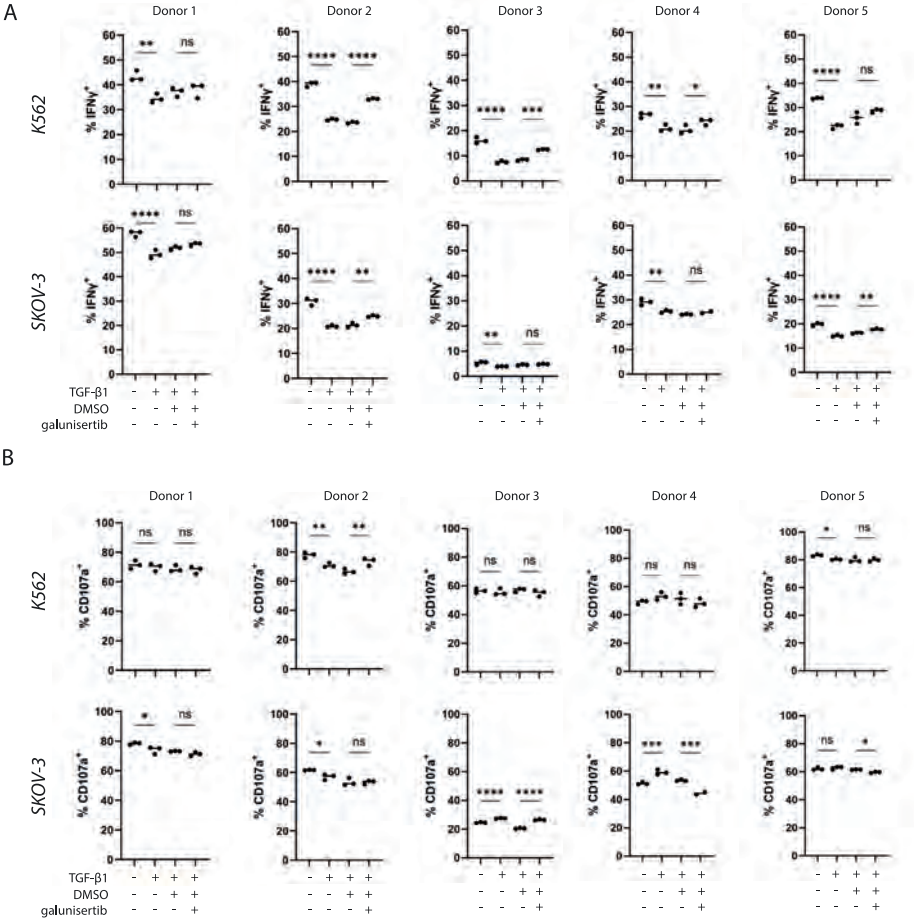

Supplemental figure 3: ***TGF-β1 inhibits NK cell IFN-γ responses and can be rescued by a TGF-β1 small molecule inhibitor in a subset of donors***

Percent positive IFN-γ ***(A)*** *and CD107a* ***(B)*** *positive of five different HPC-derived NK cell donors stimulated with SKOV-3 (bottom) or K562 (top) target cells in the presence or absence of rhTGF-β1, DMSO and galunisertib. Experiment was performed in triplicate.*

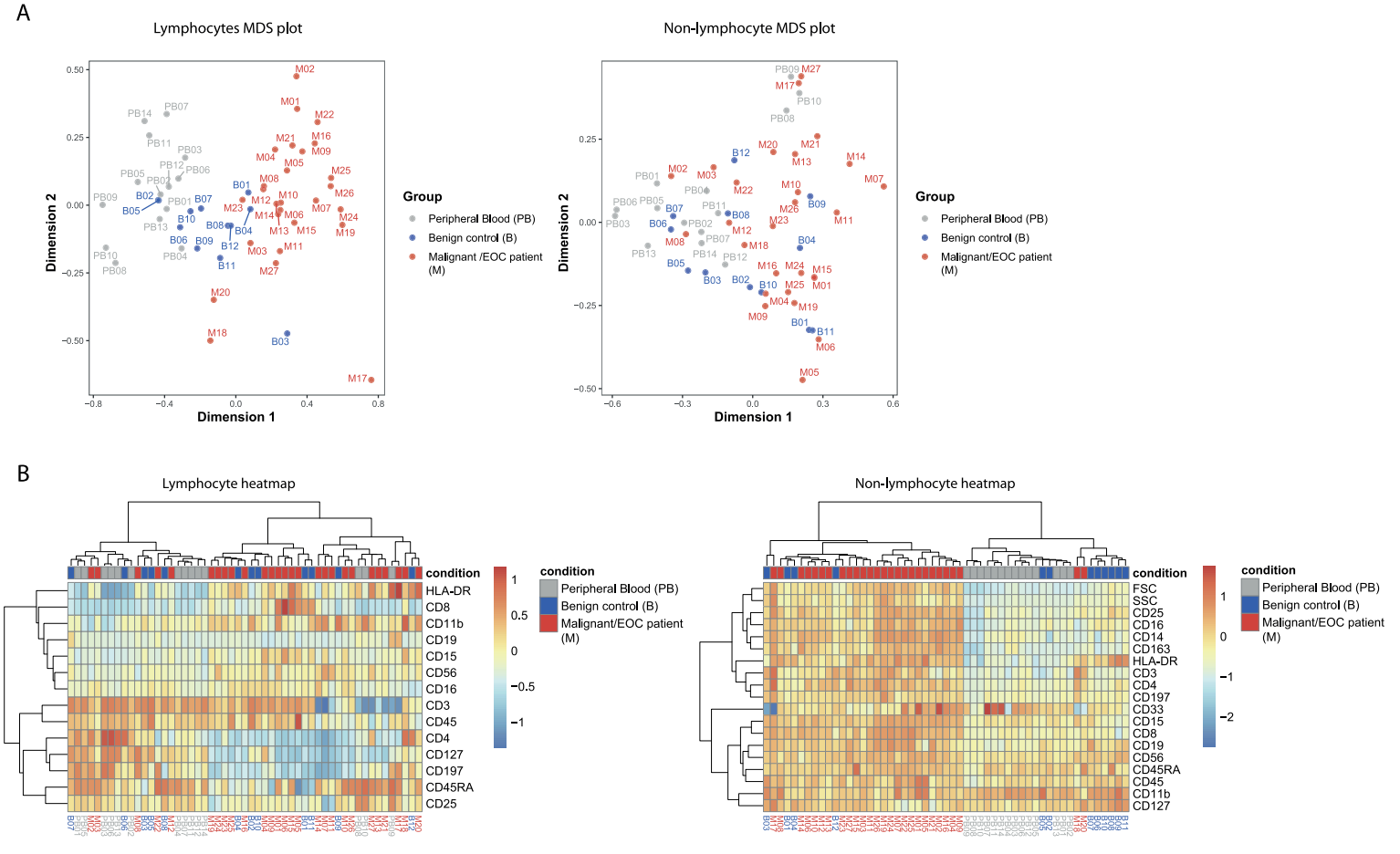
A
Lymphocytes MDS plot
Dimension 1
Dimension 2
Group
Peripheral Blood (PB)
Benign control (B)
Malignant /EOC patient (M)
Non-lymphocyte MDS plot
Dimension 1
Dimension 2
Group
Peripheral Blood (PB)
Benign control (B)
Malignant/EOC patient (M)
B
Lymphocyte heatmap
condition
HLA-DR
CD8
CD11b
CD19
CD15
CD56
CD16
CD3
CD45
CD4
CD127
CD197
CD45RA
CD25
condition
Peripheral Blood (PB)
Benign control (B)
Malignant/EOC patient (M)
Non-lymphocyte heatmap
condition
FSC
SSC
CD25
CD16
CD14
CD163
HLA-DR
CD3
CD4
CD197
CD33
CD15
CD8
CD19
CD56
CD45RA
CD45
CD11b
CD127
condition
Peripheral Blood (PB)
Benign control (B)
Malignant/EOC patient (M)

Supplemental figure 4: ***PCA clustering and hierarchical clustering of healthy donors, benign patients and malignant patients***

(A) *Principal component analysis (PCA), based on the lymphocyte distribution (left) and non-lymphocyte population (right), showing (dis)similarities in healthy donors (grey, n=14), benign patients (blue, n=12) and patients with malignancy (red, n=27) are shown.* ***(B)*** *Scaled expression levels in healthy donors (n=14) of Malignant (n=26) and benign (n=12) visualized in a heatmap. Each row represents a different expression marker, while columns represent patients or donors (H=healthy donor, M=malignant and B=benign). The scaled expression levels are reported and visualized with a color scale from blue (low levels) to red (high levels).*

Healthy donor

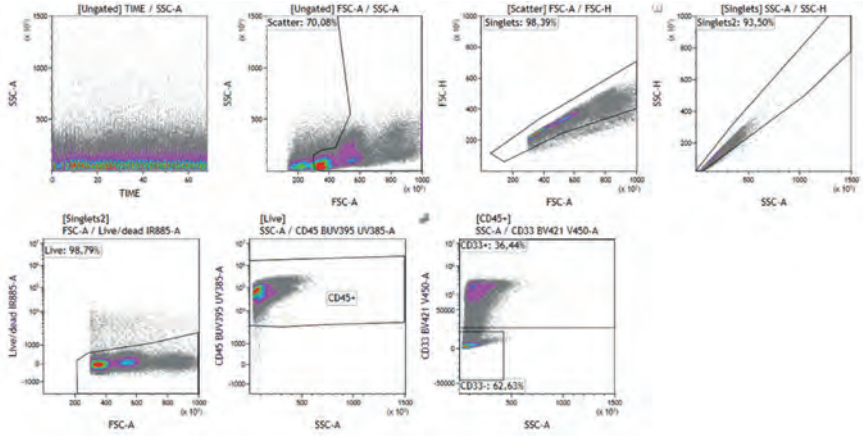

Benign reference

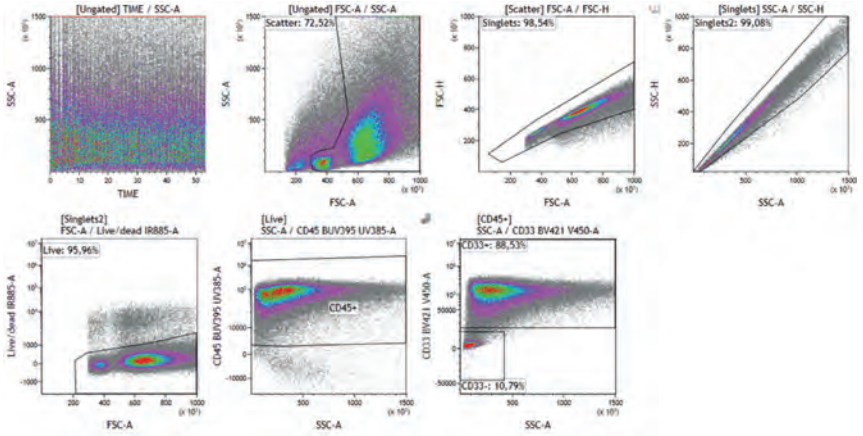

EOC patient

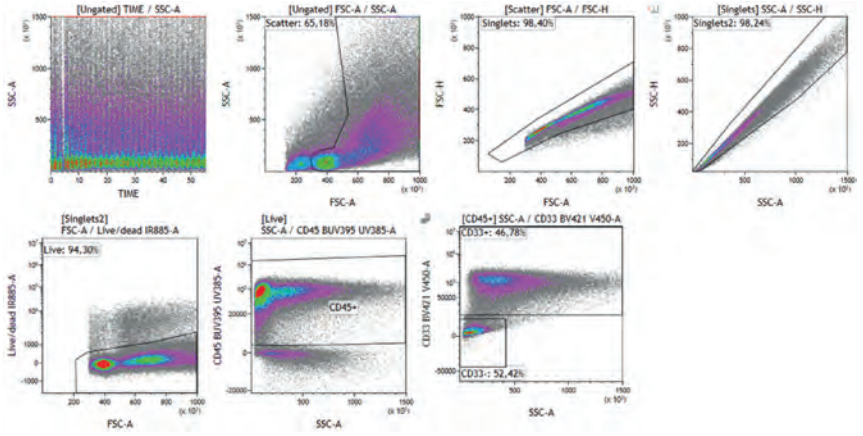

Supplemental figure 5: ***flow cytometry gating strategy for export to high dimensional analysis in R***
Representative flow cytometry gating strategy of a healthy donor (top), benign (middle) and EOC patient (bottom) is shown as an example to demonstrate the gating strategy used to gate CD45+CD33+ and CD45+CD33- cells for the FlowSOM analysis. First we gated on a steady cell input using a time gate. Then debris was excluded based on forward scatter (FSC-A) vs. side scatter (SSC-A). Doublets were excluded by plotting FSC-Area vs FSC-Height and SSC-Area vs. SSC-Height. Dead cells were excluded with a viability dye. CD45+ cells were displayed and gated vs. SSC. CD33+ and CD33- cells were then defined based on CD33 expression.

Chapter 7

Summary, general discussion and future perspectives

Summary

Ovarian cancer (OC) is a disease with relatively poor prognosis with a five-year overall survival (OS) of 25% for advanced-stage disease [1]. Epithelial ovarian cancer (EOC), which accounts for approximately 90% of ovarian cancers, encompasses various subtypes such as serous, endometrioid, clear-cell and mucinous carcinomas. Since the symptoms of OC are often vague the majority of patients presents with advanced stage (FIGO stage III or IV) disease and ascites. Ascitis is fluid accumulated in the peritoneal cavity containing various cells and soluble factors leading to reduced survival and poor quality of life by promoting tumor growth and invasion, and inhibiting the immune system. Current treatment options consist of surgical debulking followed by chemotherapy or debulking after neoadjuvant chemotherapy. The major hurdle with this approach is that 80% of patients develop a recurrence within 3 years [2]. One of the most promising adjuvant treatment methods for these patients is immunotherapy, as EOC has shown to be a relatively immunogenic tumor. In more detail: presence of tumor infiltrating cytotoxic lymphocytes is associated with prolonged survival, while presence of regulatory T cells is correlated with decreased survival [3-5]. Although the majority of immunotherapy-based treatment strategies has revolved around T cell-based strategies there is evidence that an NK cell-based approach for this disease might have advantages over T cells. The main goal of the research presented in this thesis was to identify the role of NK cells in EOC and to identify critical pathways that regulate NK cell function which could be targeted to improve NK cell based immunotherapy development in EOC.

Natural Killer (NK) cells are innate cytotoxic lymphocytes, not reliant on specific antigen specific receptors that bind antigens presented by the major histocompatibility complex (MHC). Instead, activation of NK cells is regulated by the sum of intracellular signals from inhibitory and activating receptors expressed on the NK cell surface upon interaction with their ligands on the tumor cells. A strong activation signal for NK cells is the lack or reduced expression of missing self-signals from MHC-1 molecules, a mechanism often used by tumor cells to evade T cell recognition, thereby making NK cells ideal candidates for immune cell-based treatment strategies. However, patient's autologous NK cells are often present in low numbers and may be strongly inhibited by the suppressive tumor-immune environment. Besides boosting naturally occurring autologous NK cells, adjuvant adoptive immunotherapy exploiting allogeneic donor NK cells is a compelling strategy. Different NK cell sources are investigated for this purpose, but this thesis focused mostly on naturally occurring peripheral blood (PB)-derived NK cells and

$CD34^+$ hematopoietic progenitor (HPC)-derived NK cells cultured *ex vivo* in a 35 day culture protocol. These allogeneic HPC-NK cells can be generated as an "off-the-shelf" immunotherapy product and have the added benefit of being more effective killers than NK cells derived from PB [6]. Adoptive NK cell therapy can be further boosted by cytokine stimulation, blocking inhibitory pathways and by genetic engineering.

The aim of this thesis was to identify major determinants that regulate NK cell activity against EOC. We employed comprehensive multicolor flowcytometry panels and soluble factor analysis combined with functional assays to identify major inhibitory NK cell pathways that affect NK cell function in EOC. To boost NK cell function we used a combination of cytokine stimulation with blockade of the identified inhibitory pathways crucial for NK cell reactivity against EOC.

In **Chapter 2,** we investigated the role of NK cells in FIGO advanced stage IIIc or IV high-grade serous papillary EOC and demonstrated that the frequency of NK cells within ascites is related to OS and progression-free survival. However, expression of activation markers DNAM-1, NKp30, NKp46, but not NKG2D and 2B4 on NK cells from high-grade EOC were significantly lower than benign peritoneal fluid NK cells. Using an *in vitro* activation assay we demonstrated that boosting by IL-15 or IL-15 superagonist N-803 can reinvigorate NK cell degranulation and IFN-γ production against EOC tumor targets. Superagonist N-803, consists of a modified IL-15 with enhanced binding and activating properties with an added IgG Fc region to significantly extend its half-life *in vivo* compared to recombinant human (rh) IL-15. By demonstrating the correlation between NK cell percentage and outcome in EOC patients and that NK cell functionality can be boosted by IL-15 based stimulation we provided additional rationale for future NK cell-based immunotherapy approaches.

Chapter 3 further explores the therapeutic potential of N-803 in boosting HPC-NK cells functionality against EOC and acute myeloid leukemia (AML). We found that N-803 increases IFN-γ production and proliferation of HPC-NK cells. In AML models, serial killer capabilities were also improved and increased intercellular adhesion molecule 1 (ICAM-1) expression on the AML cells enhanced their susceptibility to NK cell-mediated killing. In EOC models there was no increase in serial killing with addition of N-803-, although CXCL10 expression by the EOC tumor cells was significantly upregulated which could in turn augment NK cell infiltration and attraction through CXCR3 expressed on HPC-NK cells. In EOC tumor bearing mice treated with HPC-NK cells, N-803 or rhIL-15 were both able to support HPC-NK cell persistence, which significantly reduced tumor growth compared to the control group that did not receive NK cell boosting. Altogether, these data provide

rationale for N-803-based cytokine support in both EOC and AML to support NK cell survival and to improve NK cell-mediated anti-tumor activity following adoptive NK cell transfer.

In **Chapter 4,** we developed two 18-color flow cytometry panels to characterize NK cell subsets based on activation, differentiation and immune checkpoint marker expression, and compared NK cells derived from ascites of 26 high-grade (FIGO stage III and IV) serous EOC patients to NK cells from 11 abdominal washing fluid or free benign fluid from patients without any malignancy. Using FlowSOM clustering we revealed two interesting groups of clusters using the NK checkpoint panel, focused on inhibitory and activating receptors such as DNAM-1, TIGIT, PD-1 and SIGLEC-7. No differences in NK cell subset composition nor abundance were found with the NK subset panel, that mainly contained classical NK cell subset markers including KIRs, NKG2A/NKG2C and NCRs. One group of clusters identified with the NK checkpoint panel was enriched in benign ascites and resembled PB-NK cells. The second group of clusters was enriched in malignant ascites and was associated with lower levels of the activation receptors DNAM-1 and CD16, and higher inhibitory checkpoint molecule expression of TIGIT, TIM-3 and/or PD-1. Interestingly, the group of clusters increased in benign patients negatively correlated to most soluble factors in ascites, whereas the group of clusters increased in malignant patients positively correlated to the majority of soluble factors found in the EOC patients ascites. In this chapter, we demonstrated that high-dimensional flow cytometry data analysis can pinpoint NK cell clusters and receptors linked to the cytokine environment in ascites. This insight can guide future immune checkpoint blockade studies by highlighting relevant NK cell receptor pathways for EOC.

The importance of the tumor ligand expression for activating receptors was further studied in **Chapter 5** as this aids NK cells in recognizing and eliminating the tumor cells. Here, we investigated the tumor and NK cell interaction with a focus on the DNAM-1, TIGIT and CD96 pathway, as we had identified DNAM-1 as one of the major activating receptors that is downregulated on NK cells derived from malignant EOC ascites. While DNAM-1 is significantly downregulated on EOC patient-derived NK cells, TIGIT expression was equal and CD96 showed higher expression compared to healthy PB-NK cells. We were able to reproduce the DNAM-1 downregulation *in vitro* with healthy donor PB-NK cells though co-culture with an EOC mono-layer, EOC spheroids and *in vivo* in EOC tumor bearing mice. Other NK cell receptors like PD-1, NKG2A and OX40 were not altered by this tumor and NK cell interaction. Enhancing NK cell activity through IL-15 administration reversed the effects by upregulating DNAM-1 expression in a dose-dependent manner, but also led to increased expression of TIGIT and CD96. Checkpoint inhibition using TIGIT

blockade resulted in increased degranulation and IFN-γ production by healthy PB-NK cells. More importantly, TIGIT blockade on EOC patient-derived NK cells increased their EOC reactivity. In tumor bearing mice treated with rhIL-15 and PB-NK cells, TIGIT blockade resulted in reduced tumor load compared to untreated mice highlighting the importance of favorably modulating the DNAM-1/TIGIT/CD96 pathway to augment NK cell-based tumor reactivity in EOC.

Besides direct interactions of tumor ligand with NK cell receptors, we further investigated the inhibitory role of the immune cells and soluble factors in the tumor microenvironment (ascites) of EOC. Ascites is known to promote tumor cell growth and invasion, and contains a variety of immune cells. In **Chapter 6,** we performed multiplexing and ELISA's on malignant and benign ascites. We used the same ascites to determine the inhibitory properties on NK cell function and degranulation, and correlated this to the characterized soluble factor levels and clinical outcome parameters including OS and progression free survival. Notably, we found that HPC-NK cells were more resistant to the inhibitory effects from ascites compared to PB-NK cells. TGF-β1 turned out to be a dominant suppressive cytokine that correlated with ascites-induced NK cell dysfunction and reduced patient survival. Blockade of TGF-β1 signaling with small molecule inhibitor galunisertib partly restored NK cell functionality. Besides a detrimental effect on NK cell function and association to poor clinical outcome, TGF-β1 was also associated with the presence of inhibitory cell types such as M2-like macrophages, (regulatory) B cell populations and regulatory T cells. These findings illustrate the importance of the TGF-β1 pathway in advanced EOC and provide evidence that NK cell-based immunotherapies for EOC might benefit from TGF-β1 interference, which would ideally be applied in the local tumor microenvironment.

Collectively, this thesis provides further rationale that NK cell-based immunotherapy is an attractive adjuvant treatment strategy for EOC patients, who currently have limited treatment options after recurrence. We showed that IL-15 based boosting is critical to sustain and activate NK cells as well as to prolong their persistence *in vivo*. Furthermore, both tumor cells, immune suppressive cells such as myeloid-derived suppressor cells, M2-like macrophages and regulatory T cells, and inhibitory soluble factors present in ascites can induce downmodulation of activating receptor expression and upregulation of inhibitory checkpoint receptors. A key inhibitory soluble factor in ascites is TGF-β1 while TIGIT signaling is an important inhibitory checkpoint molecule that reduces NK cell function in the peritoneal cavity. Therefore, both IL-15 based boosting as well as interference with the inhibitory TIGIT and TGF-β1 signaling pathways provide appealing strategies to limit EOC-induced NK cell inhibition and improve NK cell-based immunotherapy strategies.

General Discussion and Future Perspectives

The importance of NK cell immunity in EOC

In **Chapter 2** of this thesis, we demonstrated that the frequency of NK cells in ascites from EOC patients is associated to survival. Our study was the first to report a positive relationship between the NK cell frequency within ascites and clinical outcome parameters. Dong et al. had previously described a negative association between NK cell (and B cell) infiltration in EOC and survival in 2006 [7]. The main difference compared to our study is that we assessed NK cell frequency in ascites and did not investigate the percentage of NK cells infiltrating tumor tissue. Another critical difference is that we used CD56 and CD16 to define our CD3- NK cell populations, whereas Dong et al. used CD16 and CD3 negative gating to define NK cells. Notably, we and others have observed that CD16 expression can be downregulated on peritoneal NK cell subsets in EOC compared to healthy PB-NK reference samples. Therefore, CD16 is a subset marker for NK cells but not a pan-NK cell marker. Furthermore, we found that CD56, the main marker to distinguish NK cells from other lymphocytes, can also be expressed by EOC [8]. Henriksen et al. [9] and Li et al. [10] used CD57 as marker to define NK cell infiltrating populations. Henriksen et al. found high numbers of $CD57^+$ cells and $CD8^+$ T cells to associate with favorable OS, while Li et al. demonstrated tumor infiltration of $CD8^+$ T cells to associate with favorable OS but not $CD57^+$ NK cells. Some dissimilarities between these studies may explain this discrepancy, but both studies used CD57 to define NK cells while terminally differentiated effector T cells can also express CD57. Therefore, CD57 alone is not sufficient to accurately define NK cells, further illustrated in **Chapter 6** where we found only ~10% ascites-derived NK cells to be $CD57^+$. Unfortunately, it remains technically challenging to stain for CD56 using immunohistochemical staining in tumor tissue. Therefore, the role of NK cells in tumor tissue may not have been accurately assessed in all previously published studies. To date, our study remains the only one that defined NK cells by CD56 and CD16, and to describe a positive association to peritoneal $CD3^-CD56^+$ NK cell frequency and EOC patient survival. Two other observations in **Chapter 2** paved the way for the research in the following Chapters. The first is that IL-15 boosting *in vitro* was able to reinvigorate degranulation and IFN-γ production of patient's NK cells obtained from the peritoneal cavity. We further explored the potential for this treatment strategy in **Chapter 3** with IL-15 super-agonist N-803 demonstrating superior NK cell killing capacity and reduced tumor growth, respectively. Finally, we established that activating markers NKp30, NKp46 and DNAM-1 on NK cells were significantly lower in EOC patients compared to healthy PB-NK cells, in line with previous studies [11, 12]. The only discrepancy here is that we did not find this

association with activating receptor NKG2D, while other studies did. We further investigated this association in a larger dataset including many other important NK cell regulating inhibitory and activating receptors in **Chapter 4.** Here, we found that NKG2D was indeed significantly lower compared to NK cells from benign controls in $CD56^{bright}$ $CD16^{-}$ NK cells, but not in $CD56^{dim}$ NK cells.

A substantial part of the data generated in this thesis is based on experiments using human cancer cell lines. The main cell lines used for this thesis were SKOV-3, IGROV-1 and OVCAR-3 (Table 1).

Table 1: ***EOC cell line properties used in this thesis***

Cell line	SKOV-3	IGROV-1	OVCAR-3
Ascites production *in vivo*	Yes	No	No
Histology	Clear cell/non-serous	Endometrioid/non-serous	High grade serous
Age at sampling (years)	64	47	60
Genome ancestry	European	European	European
Tissue origin	Ascites	Primary tumor	Ascites

However, cell lines may not adequately represent primary cells and ideally hypotheses should be confirmed using primary material. Another issue is contamination of cell lines, as 24% of cell lines distributed by cell banks in 2010 were contaminated with mycoplasma [13]. In our lab, we tested for mycoplasma every 6 months, so the results in this thesis are with mycoplasma-negative cell lines. We have generated cultures from primary material, which proved challenging, but we have used these primary cells to confirm our findings in **Chapter 5**. There are also advantages to using cell lines, including ease of use, being an unlimited supply of material and allowing experiments worldwide to be more easily reproduced and compared. Although many studies, including some experiments in this thesis, are performed with 2D cultures of cell lines 3D spheroid cultures are more clinically relevant. Spheroids better mimic the natural cell–cell and cell–ECM interactions which can affect cytotoxicity results for example [14]. The morphology and physiology of cells in spheroids also correspond more to *in vivo* EOC compared to 2D cultures [15]. Yet, spheroids cannot be a replacement for *in vivo* models. As indicated in Table 1, SKOV-3 which was used for the majority of experiments in this thesis represents a non-serous histology. For future studies it would be relevant to include a more clinically relevant cell line model of the high-grade serous EOC type, as that would be most representative for the majority of the EOC patients. Some potentially interesting cell lines include

OVCAR-3, OVCAR-4, OVCAR-8, COV362 and COV318 as these are all reported to grow intraperitoneally and are reportedly of the high-grade serous subtype [16-19]. Unfortunately, OVCAR-3 cannot stably express luciferase, the enzyme used to quantify tumor burden *in vivo [16]*. And OVCAR-8 was later reported to be of the non-serous subtype instead of high-grade serous [18]. High-grade serous tumors are characterized by TP53 mutations, but although OVCAR-8 is TP53 mutated it behaves similarly to other non-serous cell lines [20]. The downside for OVCAR-4 is that it is a relatively slow growing tumor compared to the other cell lines [21]. Another potential disadvantage of OVCAR-3 and OVCAR-4 is their reported inability to produce ascites *in vivo* [16, 21]. However, other studies did find OVCAR-3 to produce ascites *in vivo* [22, 23]. OVCAR-8 on the other hand does produce ascites *in vivo* and has a fast disease progression compared to other cell lines making this an excellent choice to include in future EOC studies although, unfortunately, its origin and histology is not clearly defined as high-grade serous [20, 24]. COV362 and COV318, similar to OVCAR-8 are interesting with intraperitoneal tumor growth reported *in vivo*, they have some native ascites producing capacity but this capacity was enhanced in both COV362 and COV318 luciferase cell lines [16]. Contradictory, Mitra et al. reported no intraperitoneal tumor growth for COV362 [21]. In short, OVCAR-3, OVCAR-4, OVCAR-8, COV362 and COV318, seem attractive choices for future studies.

NK cell persistence and boosting through cytokine support in EOC

As demonstrated in **Chapter 2**, NK cells in the tumor microenvironment (TME) of EOC are strongly inhibited due to, in part, the soluble factors and tumor cell interactions further described in **Chapter 6**. Several cytokines can potentially provide a boosting signal to NK cells, the most studied being IL-2 and IL-15 [25-27]. Other cytokines such as IL-12, IL-18, IL-21 and IFN-α can also boost NK cell activity [28-30]. From studies with receptor knockout mice we know that IL-2, IL-18, IL-21 and IL-2Ra are less critical for NK cell development, as these mice have normal numbers of NK cells in their peripheral blood albeit with reduced effector functions [31-33]. However, IL-15 and IL-15Ra knockout mice have a significant reduction in NK cell numbers [34, 35]. Knockout of the other cytokines each individually have some effect on either NK cell function and/or maturation, but IL-15 appears to be the major cytokine associated to NK cell numbers and persistence. One advantage to IL-2 is that this is the cytokine most commonly used in clinical trials to boost NK cell and T cell persistence. However, the main disadvantage of IL-2 support are the side effects, which include skewing the differentiation and maintenance of regulatory T cells, which may subsequently dampen immune responses [36]. For these reasons we decided to further explore IL-15-based boosting of NK cells in **Chapter 3**. N-803

is a modified IL-15 molecule with an activating mutation with enhanced binding properties, an IL-15Rα sushi domain for trans-presentation and an IgG1 Fc tail to increase the half-life [37-39]. Normally, IL-15Rα is expressed on the surface of antigen presenting cells and forms a complex with IL-15, which is then recognized by the β and γ receptor chains located on the surface of NK cells and $CD8^+$ T cells. Both trans and cis (no IL-15Rα binding involved) presentations of IL-15 play an important role in the regulation, activation and proliferation of NK cells [40-42]. Several clinical trials with N-803 have been conducted or are still ongoing [43-45]. For example, Foltz et al. used N-803 in a phase I study combined with rituximab in patients with indolent Non-Hodgkin Lymphoma [46]. In agreement with other clinical studies conducted to date, N-803 was safe and well tolerated. Interestingly, they found durable clinical responses including rituximab-refractory patients [46]. Continuous IL-2 and IL-15 administration is known to support NK cell survival *in vivo*, but there are potential issues with either cytokine that need to be further addressed. A major potential issue of continuous high IL-15 stimulation is NK cell exhaustion. This was first described by Felices et al. who found that continuous exposure to IL-15 in an AML model resulted in a defect *ex vivo* NK cell expansion/survival, diminished inflammatory function and decreased killing [47]. The underlying mechanism was identified to be sustained mTOR signaling, as the mTOR inhibitor rapamycin was able to reverse these effects. Another study confirmed these results in an *in vivo* AML model [48]. A more recent study by Mishra et al. revealed that blockade of ADAM17 increased NK cell proliferation and CD62L expression in response to IL-15 stimulation [49]. ADAM17 is a protease that can cleave cell surface proteins, resulting in shedding, which in turn rapidly reduces receptor density on the cell surface [50, 51]. Blockade of ADAM17 could be a strategy to overcome NK cell IL-15 induced exhaustion [49]. Another potential hurdle for IL-15 based allogeneic NK cell support is that is also boosts the patient' $CD8^+$ T cells which may subsequently recognize and eliminate the donor NK cells. Berrien-Elliott et al. compared IL-2 and N-803 infusion in patients with relapsed/refractory AML treated with CD3-depleted/enriched NK cells in a phase 1 dose escalation trial [52]. Patients treated with IL-2 had better clinical responses compared to N-803. Interestingly, allogeneic NK cells supported with N-803 showed higher absolute counts at peak expansion, which corresponds with data published by us and others. However, on day 21 there was a strong decline in NK cell numbers in the N-803 treated patients, possibly due to $CD8^+$ T cell-mediated elimination. Indeed, patient autologous T cells were significantly increased in the peripheral blood and bone marrow of N-803 treated patients compared to IL-2 treated patients. To overcome some of these problems, local administration of IL-15 might be applied. In this regard, several studies, as early as 2018, have demonstrated that it is feasible to generate chimeric antigen receptor (CAR) NK cells that overexpress IL-15 which can support NK cell

survival and activation [53-57]. One recent clinical study with allogeneic anti-CD19 CAR-NK cells, derived from umbilical cord blood, expressing IL-15 and inducible caspase 9, acting as a safety switch, demonstrated the feasibility of this approach in refractory CD19-positive cancers [56]. These patients showed an objective response to treatment with CAR-NK cells without developing major toxic side-effects. Another approach is to engineer CAR-T and CAR-NK cells overexpressing IL-15 and IL-15 receptor alpha (IL-15Rα) to establish local transpresentation, which was shown to result in less IL-15-induced toxicity and enhanced anti-tumor activity [57, 58]. Silvestre et al. transduced NK-92 cells with a CD19 CAR alone, CD19 CAR with IL-15 or CD19 CAR with both IL-15 and IL-15Rα. The CD19 CAR-NK cells harbouring IL-15/IL-15Rα showed significantly increased *in vitro* tumor killing activity compared to cells expressing IL-15 alone [57]. These strategies, most likely in combination with other innovative engineering strategies such as CRISPR/Cas9 mediated deletion of β2M to disrupt the HLA-I complex and to prevent host rejection. Ideally in combination with overexpression of HLA-E to prevent rejection by allogeneic NK cells which might improve effectiveness and longevity of NK cell-based immunotherapy [59, 60].

NK cell exhaustion, receptor checkpoint expression and soluble factors in ascites

The sum of activating and inhibitory receptor signals is critical in the regulation of NK cell functionality and determines whether a target cell is subsequently killed or spared [61, 62]. Despite the often used common differentiation markers (*i.e.* CD3-, CD56+ and CD16) to define NK cells, NK cells represent a diverse population characterized by a wide array of activating and inhibitory receptors, of which the expression is influenced by the local environment and the specific stimuli they encounter [63]. In **Chapter 4**, we applied two extensive 18-color panels to further characterize NK cell subsets in high-grade EOC patient ascites and compared them to benign control samples. Using unsupervised clustering, we found that lower DNAM-1, SIGLEC-7 and CD16 expression turned out to be the major characteristic of significant clusters found in EOC ascites. In **Chapter 5,** we investigated DNAM-1 and CD16 expression with the major focus on the DNAM-1/CD96/TIGIT pathway in more detail. DNAM-1 has been shown to be one of the key activating receptors involved in NK cell-dependent anti-tumor responses [64-67]. DNAM-1^+ NK cells are more pro-inflammatory, proliferate more and have a better anti-tumor response [68]. In **Chapter 5**, we showed that DNAM-1 levels on NK cells significantly decrease upon *in vitro* co-culture with EOC cells, but can be increased by IL-15 stimulation. However, whether this phenomenon is based on cell-cell interaction, soluble ligands or cytokine mediated signaling remains to be investigated. Soluble (s)CD155

suppresses DNAM-1-mediated degranulation of NK cells and binds with greater affinity to DNAM-1 compared to inhibitory receptors TIGIT and CD96 [69]. Given the importance of the DNAM-1 pathway in EOC, one might expect elevated levels of sCD155 in ascites of high-grade EOC patients, but levels were not significantly increased compared to benign control samples in our study. Though, this does not implicate that there is no suppressive role for sCD155 in ascites, as benign fluids also exerted some inhibitory activity and in both fluid types the sCD155 levels were well above the detection limit. CD155 is up-regulated in tumors and favors tumor cell proliferation and migration. In contrast, when expressed on the surface of tumor cells, CD155 can bind activating receptor DNAM-1 and induce tumor cell killing. CD155 and CD112 are often elevated in various solid and hematological malignancies, correlating with a worse OS and disease stage [70-77]. Although we reported in **Chapter 5** that CD155 and CD112 are both highly expressed by EOC cells, we did not find a significant association between sCD155 nor sCD112 in ascites of EOC patients and OS in **Chapter 4**. Soluble ligands for DNAM-1 might be an important factor that tip the scale in favor of tumor cell proliferation and migration, while impairing NK cell killing. Interestingly, sCD112 was significantly increased in ascites from malignant EOC patients compared to benign controls. For sCD112 less is known in literature about its mechanism of action and binding properties. Further research is required to potentially open a window for new therapeutic strategies targeting soluble DNAM-1 ligands. Blockade of CD155 has already been suggested as a therapeutic approach alongside allogeneic NK cell therapy to enhance NK cell activation, cytotoxicity, and graft-versus-tumor effects [78].

Besides increasing NK cell activity through augmenting DNAM-1 signaling, another attractive strategy is to block inhibitory TIGIT signaling. Similar checkpoint blockade strategies targeting inhibitory receptors PD-1 and CTLA-4 showed impressive clinical responses [79-81]. Expression of TIGIT correlates with NK and T cell dysfunction and more importantly with poor prognosis in several types of cancers [82-84]. In **Chapter 5,** we explored TIGIT blockade on NK cells and found promising results in our *in vitro* and *in vivo* models. This is corresponds with the finding that TIGIT deficiency, or prophylactic antibody blockade, yields a modest level of protection against primary tumor growth in mice [64, 85-87]. This is in line with our results, as we found a modest increase in NK cell-mediated anti-tumor responses upon TIGIT blockade. Similar to T cell exhaustion, NK cell exhaustion is a gradual process consisting of different stages that may be unique per disease or even per patient [88]. Therefore, future clinical studies may consider rescuing exhausted NK cells through personalized modalities. For example, focusing on EOC specifically, evaluation of both the soluble component in ascites and the cellular exhaustion markers (NK and tumor cells) can guide the selection of checkpoint blockade targets. The second

modality to overcome the current modest effects of single antibody blockade is the combination of multiple checkpoint blockers that are preferably selected on an individual basis. In unpublished data with our *in vitro* degranulation assay using the SKOV-3 cell line we found that co-blockade of TIGIT and KIR worked well together, but also individually, by increasing IFN-γ (left) and CD107a (right) responses in healthy donor-derived NK cells (N=7) (Figure 1). In addition, we also explored TIM-3 blockade but could not find differences in NK-cell mediated SKOV-3 reactivity in the presence or absence of blockade (Figure 1).

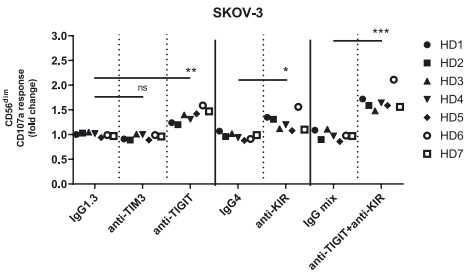

Figure 1: ***KIR and/or TIGIT blockade, in contrast to TIM-3, significantly boosted IFN-γ and CD107a on CD56^{dim} NK cells from healthy donors (HD) in response to SKOV-3 EOC cells. SKOV-3 stimulation for 4 h on HD PBMC derived NK cells in the presence of anti-TIM-3 (10 µg/mL), anti-TIGIT (10 µg/mL) and/or anti-KIR (10 µg/mL) or matching isotype controls***. *Fold change in IFN-γ (left) and CD107a (right) expression gated on CD56^{dim} cells following antibody treatment is calculated relative to the condition of NK cells supported with low dose rhIL-15 and subjected to 4 h SKOV-3 stimulation (n = 7). A One-Way repeated measures ANOVA with Bonferroni correction was used for statistical analysis, * $p < 0.05$, ** $p < 0.01$ and *** $p < 0.001$*

As confirmed in **Chapter 5**, TIGIT is one of the important checkpoint inhibitors on NK cells in the context of EOC reactivity, while other inhibitory checkpoints such as KIRs or PD-1 might be more relevant/dominant in other diseases. Using the same assay set-up we assessed TIM-3, TIGIT and KIR blockade in an acute myeloid leukemia model (THP-1 cells) with healthy donor derived NK cells (N=7, Figure 2).

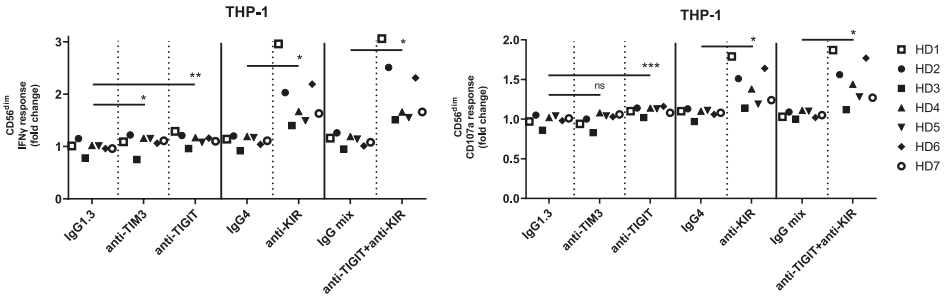

Figure 2: ***Anti-KIR strongly boosts NK cells while TIM-3 and TIGIT blockade have modest effects on PB-NK cells in response to THP-1 AML cells (4 h) in the presence of anti-TIM-3 (10 µg/mL), anti-TIGIT (10 µg/mL) and/or anti-KIR (10 µg/mL) or matching isotype controls.*** *Fold change in IFN-γ (left) and CD107a (right) expression gated on CD56^{dim} cells following antibody treatment is calculated relatively to the condition with low dose rhIL-15 (5 ng/mL) and 4 h THP-1 stimulation only (n = 7). A One-Way repeated measure ANOVA with Bonferroni correction was used for statistical analysis, * p < 0.05, ** p < 0.01 and *** p < 0.001*

Here, both TIM-3 and TIGIT blockade did not show significant differences, while KIRs appeared to be important inhibitory checkpoint molecule(s) resulting in increased NK cell reactivity against THP-1 cells when blocked.

The hypothesis that monoblockade is unlikely to yield significant clinical responses is supported by a clinical study in elderly patients with acute myeloid leukemia (AML), which demonstrated that KIR mono-blockade (lirilumab) therapy did not improve disease-free survival [89]. Interestingly, combined rituximab (anti-CD20 antibody) treatment with anti-KIR showed significantly better results compared to either treatment alone in a syngeneic murine lymphoma model [90]. Another strategy to overcome inhibition through checkpoint molecules for allogeneic treatment strategies would be to engineer NK cells without expression of these inhibitory receptors. CRISPR/Cas9 technology has revolutionized genome editing, allowing knockout of specific genes with a targeted guide RNA. This guide RNA forms a complex with the Cas9 protein, which can subsequently bind and cleave the DNA region of interest resulting in a double-strand break. The DNA repair mechanism is error prone and can hence cause frameshift mutations resulting in an early stop codon which disrupts gene function [91]. A CRISPR/Cas9-based approach could be employed to knock out inhibitory receptors, such as TIGIT or KIRs, on NK cells prior to infusion.

Similarly, NKG2A blockade (monalizumab) is being clinically evaluated and yielded poor results as monotherapy in patients with recurrent/metastatic squamous cell carcinoma of the head and neck. No objective response rate (ORR) was observed and the study did not meet its primary objective [92]. More importantly, a study with

monalizumab monotherapy in patients with gynecologic malignancies also did not meet the protocol-defined criteria [93]. Both groups reported that future studies should include co-blockade strategies. One such example is the UPSTREAM study, where monalizumab is combined with anti-PD-L1 (durvalumab). Interestingly, the COAST trial investigated anti-PD-L1 (durvalumab) treatment in patients with unresectable, stage III non–small cell lung cancer in combination with anti-CD73 (oleclumab) or anti-NKG2A (monalizumab) and reported a better ORR and prolonged progression free survival [94]. Our HPC-NK cells have relatively high levels of NKG2A with an average of 80% NKG2A$^+$ cells in the therapeutic product, and thus NKG2A blockade could be an interesting strategy to improve anti-tumor activity [95].

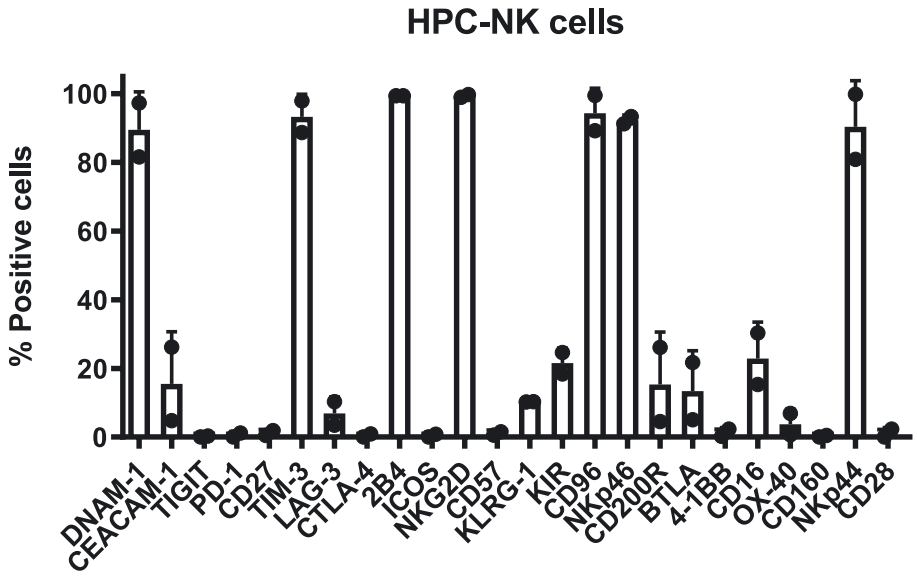

Figure 3: ***Checkpoint receptor expression on the HPC-NK cell end product. CD34$^+$ stem cells were isolated from cord blood, cryopreserved and thawed for HPC-NK cell generation within 5-6 weeks, as described previously [39]****. HPC-NK cells were then analyzed by flow cytometry for expression of DNAM-1, CEACAM-1, TIGIT, PD-1, CD27, TIM-3, LAG-3, CTLA-4, 2B4, ICOS, NKG2D, CD57, KLRG-1, pan-KIR, CD96, NKp46, CD200R, BTLA, 4-1BB, CD16, OX-40, CD160, NKp44 and CD28 (N=2).*

To further improve HPC-NK cell based therapies other checkpoint molecules besides NKG2A should further be explored. Since HPC-NK cells inherently lack or have low TIGIT expression after 35 days of culture, TIGIT blockade is likely not the most promising strategy to improve the efficacy of this therapeutic product (Figure 3). Based on the phenotype of HPC-NK cells potentially interesting targets include CD96 and KIR. As TIGIT and TIM-3 were initial targets of interest within the scope of this thesis, we further investigated their expression on HPC-NK cells. Even after 2 weeks

of NK cell expansion in SKOV-3 tumor bearing mice, we did not observe TIGIT expression on our HPC-NK cells (Figure 4). On the other hand, although TIM-3 was initially relatively highly expressed at the end of the culture (90% positive, Figure 3), it was downregulated *in vivo* as only 10% of HPC-NK cells was positive after 2 weeks of *in vivo* expansion. Interestingly, stimulation with IL-15 or N-803 retained TIM-3 expression *in vivo* to the 20-40% positive range depending on the stimulation used.

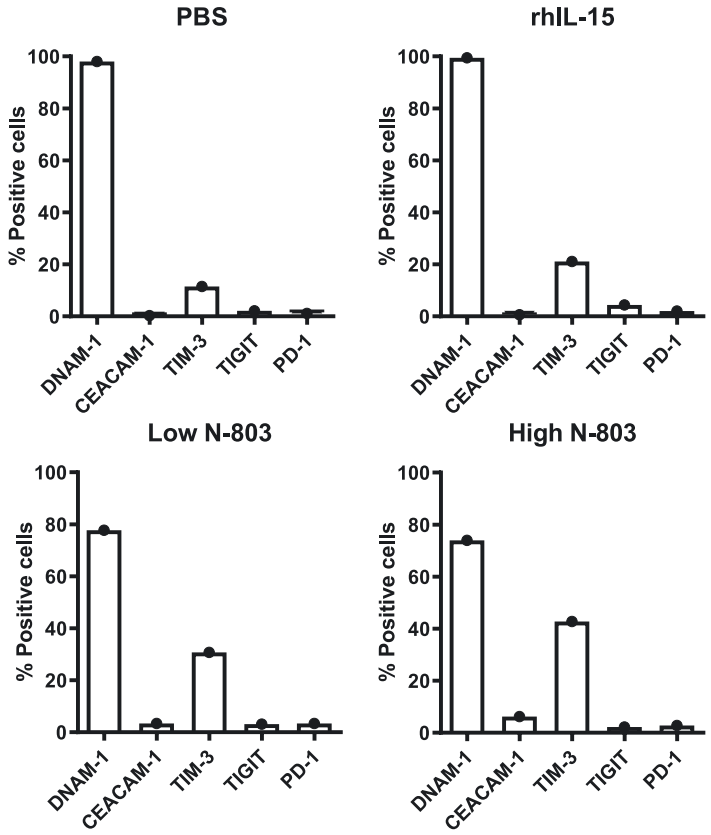

Figure 4: ***TIGIT checkpoint receptor expression on HPC-NK cells is not modulated by rhIL-15 or N-803 stimulation in vivo.*** *SKOV-3 tumor cells (0.2 million/mouse) were injected in 24 NOD scid gamma (NSG) mice (6-20 weeks old) 4 days prior to HPC-NK cell treatment (12 million/mouse). Cells were harvested by intraperitoneal washing at 15-16 days after infusion. HPC-NK cell survival and expansion was either not supported (N=6, PBS every other day), or induced with rhIL-15 (N=6, 2.5µg every other day), low dose N-803 (N=6, 50µg/kg twice weekly) or high dose N-803 (N=6, 200µg/kg twice weekly). Expression of DNAM-1, CEACAM-1, TIM-3, TIGIT and PD-1 was evaluated using flow cytometry on intraperitoneal HPC-NK cells at 15-16 days after adoptive transfer in SKOV-3 tumor-bearing NSG mice treated with PBS (top left), rhIL-15 (top right), low dose N-803 (bottom left) or high dose N-803 (bottom right). Data is presented as a single data point since cell counts were low and thus all cells from the same experimental group were pooled.*

CD96 expression is high on HPC-NK cells and is one of the receptors that is strongly upregulated on NK cells from EOC patients or healthy PB-derived NK cells upon tumor contact, as described in **Chapter 5.** It is also associated with poor prognosis in different types of cancer, including AML [96, 97]. The function of CD96 and the intracellular domains are different across mice and human. Murine CD96 has only an inhibitory domain similar to TIGIT, while human CD96 has both the inhibitory immunoreceptor tyrosine-based inhibitory motif (ITIM), but also a YXXM motif that could be both inhibitory or activating [98, 99]. Literature reports contradictory findings regarding the impact of CD96 blockade in the human setting, with the majority of studies describing no or a minimal effect, consistent with the data presented in Chapter 5 of this thesis. More research would be needed to reveal CD96's function and what the role of the YXXM motif is.

Alternatively, a checkpoint molecule not included in this analysis that might be interesting for further exploration is CD112R (also known as PVRL2). CD112R, as the name implies, binds CD112 which is a shared ligand with TIGIT. Yet, the binding affinity of CD112R to CD112 is much higher [100, 101]. Recent studies demonstrated this to be another major inhibitory pathway on NK cells and $CD8^+$ T cells [102]. Since CD112 is relatively highly expression on NK cells in epithelial ovarian cancer (EOC) compared to other cancers, co-blockade of TIGIT and CD112R could enhance NK cell-mediated reactivity against EOC as illustrated in an EOC model where co-blockade of TIGIT and CD112R led to robust IFN-γ responses [70]. Conversely, in a lung tumor model with low CD112 expression, TIGIT and PD-1 blockade was more effective, and additional CD112R blockade had no further impact [70]. This study illustrates the importance of ligand expression on the tumor cells and the respective checkpoint molecules expressed by effector cells to predict effectiveness of certain checkpoint inhibitor combinations. Although the aforementioned study was focused on $CD8^+$ T cells, similar results were demonstrated for NK cells. In this perspective, another group showed lack of effect of TIGIT blockade in an AML model, corresponding with our unpublished data, while CD112R blockade significantly increased NK cell mediated lysis of KG1a myeloid tumor cells [103]. It would be interesting to investigate the combination of KIR and CD112R blockade on those cells.

Besides CD112R, SIGLEC-7 is an interesting checkpoint receptor which, similar to CD96 and TIGIT, carries an ITIM motif [104]. SIGLEC-7 is an inhibitory lectin-type receptor on NK cells which inhibits NK cell cytotoxicity via Sia-containing ligands [105, 106]. In **Chapter 4,** SIGLEC-7 was a main determinant in driving clustering of peritoneal NK cells from EOC patients, together with CD16 and DNAM-1 which we identified in **Chapters 2 and 5**. We found high expression of SIGLEC-7 on EOC

patient ascites-derived NK cells in **Chapter 4**, while SIGLEC-9 expression was low. SIGLEC-7 defines a dysfunctional subset of NK cells associated with high levels of human immunodeficiency virus (HIV) load [107]. Nevertheless, SIGLEC-7$^+$ NK cells from peripheral blood of healthy adults were found to be highly functional [108]. Although this seems contradictory, the same group confirmed that agonistic antibodies to SIGLEC-7 did induce NK cell inhibition. To put this in perspective, much like PD-1 or TIGIT+, SIGLEC7$^+$ NK cells may not inherently be dysfunctional; rather, their functionality becomes significantly inhibited upon exposure to their respective ligands. SIGLEC-7 is mainly expressed on mature blood NK cells from healthy adults. It is difficult to dissect the difference between a mature and exhausted NK cell, as this is not just defined by receptor expression on the NK cell, but also dependent on the cytokine milieu and ligand expression of surrounding (cancer) cells [108]. In **Chapter 4**, we found a similar trend as Shao et al. reported, SIGLEC-7 was mostly expressed by peritoneal NK cell clusters that had high DNAM-1 and CD16. SIGLEC-7 in relation to cancer is poorly studied, a 2019 review identified potential functions, yet reported no specific studies on SIGLEC-7 expression in cancers. Our study is among the first to contribute to this field [109]. Since SIGLEC-7 blockade improves NK cell function and the ligands for SIGLEC-7 are known to be expressed by many tumors, it might be an interesting additional checkpoint molecule for future research on EOC and other cancers [110].

In **Chapter 6** of this thesis, we explored which soluble factors in ascites were dominant in NK cell inhibition in EOC and found TGF-β1 to be the main inhibitory pathway for both PB and HPC-NK cells. Interestingly, a study by Sun et al. suggested that DNAM-1 could be downregulated by soluble factors including TGF-β1 (37, 39, 45, 46). Interfering with the TGF-β pathway may thereby, besides its immediate NK cell boosting effect, also limit NK cell exhaustion.

The TGF-β receptor is a heterotetrameric complex of the TGF-β receptor 1 (TGFBR1) and TGFBR2. In **Chapter 6** we demonstrated that TGFBR2, in contrast to TIGIT, is expressed by HPC-NK cells. This makes interference of the TGF-β receptor a promising strategy to improve efficacy of HPC-NK cell based therapies. HPC-NK cells can be relatively easily genetically modified *ex vivo* before administration to a patient. It would be interesting to genetically modify the HPC-NK cells to be less sensitive to TGF-β inhibition. In this perspective, Yvon et al. used retroviral transduction to engraft a dominant negative TGF-β receptor II. These cells expressing a dominant negative TGF-β receptor II maintained both perforin expression and NKG2D/DNAM-1 expression in the presence of TGF-β with superior killing of glioblastoma tumor cells [111]. A similar strategy was used for CAR-T cells targeting mesothelin in a murine ovarian cancer model, resulting in improved functionality of

CAR-T cells in the presence of TGF-β [112]. To take this one step further, Wang et al. genetically modified NK-92 cells to express an extracellular and transmembrane domain of the TGF-β type II receptor with the intracellular domain of NK cell activating receptor NKG2D. Similarly to the dominant negative TGF-β receptor II, these NK cells were resistant to TGF-β-induced suppression and instead were activated and chemo-attracted by TGF-β1-producing tumor cells [113]. With a similar strategy, Shaim et al. used CRISPR/Cas9 gene editing to knock out the TGF-β type II receptor in NK cells and subsequently infused them to treat glioblastoma multiforme tumor bearing mice [114]. Their study revealed a notable decrease in tumor burden and improved OS when using TGF-β type II receptor knockout NK cells, compared to untreated tumor bearing mice. The reduction in tumor size was notably greater in mice treated with TGF-β type II receptor knockout NK cells than in those treated with wildtype NK cells combined with galunisertib. Altogether, these studies indicate that interference with the TGF-β pathway in NK cells could be employed to protect against TGF-β mediated immunosuppression and even result in stronger NK cell activation.

Conclusion

The main focus of this thesis was to identify important inhibitory pathways on NK cells and to explore ways to limit NK cell exhaustion in the EOC microenvironment with the ultimate goal to improve existing NK cell-based therapy in EOC patients, who currently have limited treatment options. We identified major cell populations and receptor pathways that are dysregulated in EOC patients and demonstrated that blockade of those identified inhibitory pathways restored NK cell function. From early data we learned that NK cells are important EOC cancer reactive effector cells and we found the DNAM-1/TIGIT pathway to be a major dysregulated pathway within EOC. Although our results are promising for new NK cell-based EOC cancer therapies, for optimal clinical responses a combination strategy needs to be further explored. Customizing combinations of checkpoint inhibitors for specific cancer types and patients, based on tumor characteristics, shows great potential as personalized medicine. Furthermore, we explored different cytokines to optimally support and boost NK cell function *in vivo*, for example with N-803 with an increased half-life and higher activity compared to IL-15. Alternatively, adoptive transfer of NK cells genetically engineered to express IL-15, to provide a more local effect with fewer side-effects, could be a promising strategy. Finally, we showed that TGF-β is one of the main inhibitory cytokines present in ascites. Since systemic blockade of TGF-β is associated with various potential side-effects, clever engineering of NK cells, perhaps in combination with IL-15, could render them less susceptible to TGF inhibition. In this thesis we established important novel insights into critical pathways for NK cell

activation and inhibition in the context of EOC. We provided rationale for incorporating IL-15, TIGIT and TGF-β-based strategies to further improve NK cell-based immunotherapy in EOC patients.

References

1. Matulonis UA, Sood AK, Fallowfield L, Howitt BE, Sehouli J, Karlan BY. *Ovarian cancer.* Nature Reviews Disease Primers. 2016;2(1):16061.

2. Fumita Y, Tanaka F, Saji F, Nakamuro K. *Immunosuppressive factors in ascites fluids from ovarian cancer patients.* Am J Reprod Immunol (1980). 1984;6(4):175-8.

3. Curiel TJ, Coukos G, Zou L, Alvarez X, Cheng P, Mottram P, et al. *Specific recruitment of regulatory T cells in ovarian carcinoma fosters immune privilege and predicts reduced survival.* Nat Med. 2004;10(9):942-9.

4. Sato E, Olson SH, Ahn J, Bundy B, Nishikawa H, Qian F, et al. *Intraepithelial CD8+ tumor-infiltrating lymphocytes and a high CD8+/regulatory T cell ratio are associated with favorable prognosis in ovarian cancer.* Proc Natl Acad Sci U S A. 2005;102(51):18538-43.

5. Leffers N, Gooden MJ, de Jong RA, Hoogeboom BN, ten Hoor KA, Hollema H, et al. *Prognostic significance of tumor-infiltrating T-lymphocytes in primary and metastatic lesions of advanced stage ovarian cancer.* Cancer Immunol Immunother. 2009;58(3):449-59.

6. Spanholtz J, Preijers F, Tordoir M, Trilsbeek C, Paardekooper J, de Witte T, et al. *Clinical-grade generation of active NK cells from cord blood hematopoietic progenitor cells for immunotherapy using a closed-system culture process.* PLoS One. 2011;6(6):e20740.

7. Dong HP, Elstrand MB, Holth A, Silins I, Berner A, Trope CG, et al. *NK- and B-cell infiltration correlates with worse outcome in metastatic ovarian carcinoma.* Am J Clin Pathol. 2006;125(3):451-8.

8. Maas RJ, Hoogstad-van Evert JS, Van der Meer JM, Mekers V, Rezaeifard S, Korman AJ, et al. *TIGIT blockade enhances functionality of peritoneal NK cells with altered expression of DNAM-1/TIGIT/CD96 checkpoint molecules in ovarian cancer. Oncoimmunology.* 2020;9(1):1843247.

9. Henriksen JR, Donskov F, Waldstrøm M, Jakobsen A, Hjortkjaer M, Petersen CB, et al. *Favorable prognostic impact of Natural Killer cells and T cells in high-grade serous ovarian carcinoma.* Acta Oncologica. 2020;59(6):652-9.

10. Li K, Mandai M, Hamanishi J, Matsumura N, Suzuki A, Yagi H, et al. *Clinical significance of the NKG2D ligands, MICA/B and ULBP2 in ovarian cancer: high expression of ULBP2 is an indicator of poor prognosis.* Cancer Immunol Immunother. 2009;58(5):641-52.

11. Belisle JA, Gubbels JA, Raphael CA, Migneault M, Rancourt C, Connor JP, et al. *Peritoneal natural killer cells from epithelial ovarian cancer patients show an altered phenotype and bind to the tumour marker MUC16 (CA125).* Immunology. 2007;122(3):418-29.

12. Nham T, Poznanski SM, Fan IY, Shenouda MM, Chew MV, Lee AJ, et al. *Ex vivo-expanded NK cells from blood and ascites of ovarian cancer patients are cytotoxic against autologous primary ovarian cancer cells.* Cancer Immunol Immunother. 2018;67(4):575-87.

13. Capes-Davis A, Theodosopoulos G, Atkin I, Drexler HG, Kohara A, MacLeod RAF, et al. *Check your cultures! A list of cross-contaminated or misidentified cell lines.* International Journal of Cancer. 2010;127(1):1-8.

14. Moshksayan K, Kashaninejad N, Warkiani ME, Lock JG, Moghadas H, Firoozabadi B, et al. *Spheroids-on-a-chip: Recent advances and design considerations in microfluidic platforms for spheroid formation and culture.* Sensors and Actuators B: Chemical. 2018;263:151-76.

15. Edmondson R, Broglie JJ, Adcock AF, Yang L. T*hree-dimensional cell culture systems and their applications in drug discovery and cell-based biosensors.* Assay Drug Dev Technol. 2014;12(4):207-18.

16. De Haven Brandon A, Box G, Hallsworth A, Court W, Matthews N, Herodek B, et al. *Identification of ovarian high-grade serous carcinoma cell lines that show estrogen-sensitive growth as xenografts in immunocompromised mice.* Scientific Reports. 2020;10(1):10799.

17. Anglesio MS, Wiegand KC, Melnyk N, Chow C, Salamanca C, Prentice LM, et al. *Type-specific cell line models for type-specific ovarian cancer research.* PLoS One. 2013;8(9):e72162.

18. Domcke S, Sinha R, Levine DA, Sander C, Schultz N. *Evaluating cell lines as tumour models by comparison of genomic profiles.* Nat Commun. 2013;4:2126.

19. Beaufort CM, Helmijr JC, Piskorz AM, Hoogstraat M, Ruigrok-Ritstier K, Besselink N, et al. *Ovarian cancer cell line panel (OCCP): clinical importance of in vitro morphological subtypes.* PLoS One. 2014;9(9):e103988.

20. Hallas-Potts A, Dawson JC, Herrington CS. *Ovarian cancer cell lines derived from non-serous carcinomas migrate and invade more aggressively than those derived from high-grade serous carcinomas.* Scientific Reports. 2019;9(1):5515.

21. Mitra AK, Davis DA, Tomar S, Roy L, Gurler H, Xie J, et al. *In vivo tumor growth of high-grade serous ovarian cancer cell lines*. Gynecol Oncol. 2015;138(2):372-7.

22. Hamilton TC, Young RC, Louie KG, Behrens BC, McKoy WM, Grotzinger KR, et al. *Characterization of a xenograft model of human ovarian carcinoma which produces ascites and intraabdominal carcinomatosis in mice*. Cancer Res. 1984;44(11):5286-90.

23. Bobbs AS, Cole JM, Cowden Dahl KD. *Emerging and Evolving Ovarian Cancer Animal Models.* Cancer Growth Metastasis. 2015;8(Suppl 1):29-36.

24. Shen YT, Wang L, Evans JC, Allen C, Piquette-Miller M. *Development of a Bioluminescent BRCA1-Deficient Xenograft Model of Disseminated, High-Grade Serous Ovarian Cancer.* Int J Mol Sci. 2019;20(10).

25. Björkström NK, Ljunggren H-G, Michaëlsson J. *Emerging insights into natural killer cells in human peripheral tissues.* Nature Reviews Immunology. 2016;16(5):310-20.

26. Wu Y, Tian Z, Wei H. *Developmental and Functional Control of Natural Killer Cells by Cytokines.* Frontiers in Immunology. 2017;8.

27. de Rham C, Ferrari-Lacraz S, Jendly S, Schneiter G, Dayer JM, Villard J. *The proinflammatory cytokines IL-2, IL-15 and IL-21 modulate the repertoire of mature human natural killer cell receptors.* Arthritis Res Ther. 2007;9(6):R125.

28. Skak K, Frederiksen KS, Lundsgaard D. *Interleukin-21 activates human natural killer cells and modulates their surface receptor expression.* Immunology. 2008;123(4):575-83.

29. Ellis TM, McKenzie RS, Simms PE, Helfrich BA, Fisher RI. *Induction of human lymphokine-activated killer cells by IFN-alpha and IFN-gamma.* J Immunol. 1989;143(12):4282-6.

30. Cooper MA, Fehniger TA, Caligiuri MA. *The biology of human natural killer-cell subsets.* Trends Immunol. 2001;22(11):633-40.

31. Kasaian MT, Whitters MJ, Carter LL, Lowe LD, Jussif JM, Deng B, et al. *IL-21 limits NK cell responses and promotes antigen-specific T cell activation: a mediator of the transition from innate to adaptive immunity*. Immunity. 2002;16(4):559-69.

32. Ma A, Koka R, Burkett P. *Diverse functions of IL-2, IL-15, and IL-7 in lymphoid homeostasis.* Annu Rev Immunol. 2006;24:657-79.

33. Chaix J, Tessmer MS, Hoebe K, Fuséri N, Ryffel B, Dalod M, et al. *Cutting edge: Priming of NK cells by IL-18.* J Immunol. 2008;181(3):1627-31.

34. Kennedy MK, Glaccum M, Brown SN, Butz EA, Viney JL, Embers M, et al. *Reversible defects in natural killer and memory CD8 T cell lineages in interleukin 15-deficient mice.* J Exp Med. 2000;191(5):771-80.

35. Lodolce JP, Boone DL, Chai S, Swain RE, Dassopoulos T, Trettin S, et al. *IL-15 receptor maintains lymphoid homeostasis by supporting lymphocyte homing and proliferation.* Immunity. 1998;9(5):669-76.

36. Ahmadzadeh M, Rosenberg SA. *IL-2 administration increases CD4+ CD25(hi) Foxp3+ regulatory T cells in cancer patients.* Blood. 2006;107(6):2409-14.

37. Zhu X, Marcus WD, Xu W, Lee HI, Han K, Egan JO, et al. *Novel human interleukin-15 agonists*. J Immunol. 2009;183(6):3598-607.

38. Han KP, Zhu X, Liu B, Jeng E, Kong L, Yovandich JL, et al. *IL-15:IL-15 receptor alpha superagonist complex: high-level co-expression in recombinant mammalian cells, purification and characterization.* Cytokine. 2011;56(3):804-10.

39. Van der Meer JMR, Maas RJA, Guldevall K, Klarenaar K, de Jonge P, Evert JSH, et al. *IL-15 superagonist N-803 improves IFNγ production and killing of leukemia and ovarian cancer cells by CD34(+) progenitor-derived NK cells.* Cancer Immunol Immunother. 2021;70(5):1305-21.

40. Neely GG, Epelman S, Ma LL, Colarusso P, Howlett CJ, Amankwah EK, et al. *Monocyte surface-bound IL-15 can function as an activating receptor and participate in reverse signaling.* J Immunol. 2004;172(7):4225-34.

41. Lodolce JP, Burkett PR, Koka RM, Boone DL, Ma A. *Regulation of lymphoid homeostasis by interleukin-15.* Cytokine Growth Factor Rev. 2002;13(6):429-39.

42. Schluns KS, Stoklasek T, Lefrançois L. *The roles of interleukin-15 receptor alpha: trans-presentation, receptor component, or both?* Int J Biochem Cell Biol. 2005;37(8):1567-71.

43. Margolin K, Morishima C, Velcheti V, Miller JS, Lee SM, Silk AW, et al. *Phase I Trial of ALT-803, A Novel Recombinant IL15 Complex, in Patients with Advanced Solid Tumors*. Clin Cancer Res. 2018;24(22):5552-61.

44. Wrangle JM, Velcheti V, Patel MR, Garrett-Mayer E, Hill EG, Ravenel JG, et al. *ALT-803, an IL-15 superagonist, in combination with nivolumab in patients with metastatic non-small cell lung cancer: a non-randomised, open-label, phase 1b trial.* Lancet Oncol. 2018;19(5):694-704.

45. Rosser CJ, Tikhonenkov S, Nix JW, Chan OTM, Ianculescu I, Reddy S, et al. *Safety, Tolerability, and Long-Term Clinical Outcomes of an IL-15 analogue (N-803) Admixed with Bacillus Calmette-Guérin (BCG) for the Treatment of Bladder Cancer.* Oncoimmunology. 2021;10(1):1912885.

46. Foltz JA, Hess BT, Bachanova V, Bartlett NL, Berrien-Elliott MM, McClain E, et al. *Phase I Trial of N-803, an IL15 Receptor Agonist, with Rituximab in Patients with Indolent Non-Hodgkin Lymphoma.* Clinical Cancer Research. 2021;27(12):3339-50.

47. Felices M, Lenvik AJ, McElmurry R, Chu S, Hinderlie P, Bendzick L, et al. *Continuous treatment with IL-15 exhausts human NK cells via a metabolic defect*. JCI Insight. 2018;3(3).

48. Bou-Tayeh B, Laletin V, Salem N, Just-Landi S, Fares J, Leblanc R, et al. *Chronic IL-15 Stimulation and Impaired mTOR Signaling and Metabolism in Natural Killer Cells During Acute Myeloid Leukemia.* Front Immunol. 2021;12:730970.

49. Mishra HK, Dixon KJ, Pore N, Felices M, Miller JS, Walcheck B. *Activation of ADAM17 by IL-15 Limits Human NK Cell Proliferation.* Frontiers in Immunology. 2021;12.

50. Arribas J, Esselens C. *ADAM17 as a therapeutic target in multiple diseases.* Curr Pharm Des. 2009;15(20):2319-35.

51. Zunke F, Rose-John S. *The shedding protease ADAM17: Physiology and pathophysiology*. Biochim Biophys Acta Mol Cell Res. 2017;1864(11 Pt B):2059-70.

52. Berrien-Elliott MM, Becker-Hapak M, Cashen AF, Jacobs M, Wong P, Foster M, et al. *Systemic IL-15 promotes allogeneic cell rejection in patients treated with natural killer cell adoptive therapy*. Blood. 2022;139(8):1177-83.

53. Christodoulou I, Ho WJ, Marple A, Ravich JW, Tam A, Rahnama R, et al. *Engineering CAR-NK cells to secrete IL-15 sustains their anti-AML functionality but is associated with systemic toxicities*. Journal for ImmunoTherapy of Cancer. 2021;9(12):e003894.

54. Lu T, Ma R, Dong W, Teng KY, Kollath DS, Li Z, et al. *Off-the-shelf CAR natural killer cells secreting IL-15 target spike in treating COVID-19.* Nat Commun. 2022;13(1):2576.

55. Liu E, Tong Y, Dotti G, Shaim H, Savoldo B, Mukherjee M, et al. *Cord blood NK cells engineered to express IL-15 and a CD19-targeted CAR show long-term persistence and potent antitumor activity.* Leukemia. 2018;32(2):520-31.

56. Liu E, Marin D, Banerjee P, Macapinlac HA, Thompson P, Basar R, et al. *Use of CAR-Transduced Natural Killer Cells in CD19-Positive Lymphoid Tumors.* New England Journal of Medicine. 2020;382(6):545-53.

57. Silvestre RN, Eitler J, de Azevedo JTC, Tirapelle MC, Fantacini DMC, de Souza LEB, et al. *Engineering NK-CAR.19 cells with the IL-15/IL-15Rα complex improved proliferation and anti-tumor effect in vivo.* Front Immunol. 2023;14:1226518.

58. Zhang Y, Zhuang Q, Wang F, Zhang C, Xu C, Gu A, et al. *Co-expression IL-15 receptor alpha with IL-15 reduces toxicity via limiting IL-15 systemic exposure during CAR-T immunotherapy.* Journal of Translational Medicine. 2022;20(1):432.

59. Guo Y, Xu B, Wu Z, Bo J, Tong C, Chen D, et al. *Mutant B2M-HLA-E and B2M-HLA-G fusion proteins protects universal chimeric antigen receptor-modified T cells from allogeneic NK cell-mediated lysis.* Eur J Immunol. 2021;51(10):2513-21.

60. Ren J, Liu X, Fang C, Jiang S, June CH, Zhao Y. *Multiplex Genome Editing to Generate Universal CAR T Cells Resistant to PD1 Inhibition*. Clin Cancer Res. 2017;23(9):2255-66.

61. Mandal A, Viswanathan C. *Natural killer cells: In health and disease.* Hematol Oncol Stem Cell Ther. 2015;8(2):47-55.

62. Baci D, Bosi A, Gallazzi M, Rizzi M, Noonan DM, Poggi A, et al. *The Ovarian Cancer Tumor Immune Microenvironment (TIME) as Target for Therapy: A Focus on Innate Immunity Cells as Therapeutic Effectors*. Int J Mol Sci. 2020;21(9).

63. Hayakawa Y, Huntington ND, Nutt SL, Smyth MJ. *Functional subsets of mouse natural killer cells*. Immunological Reviews. 2006;214(1):47-55.

64. Chan CJ, Martinet L, Gilfillan S, Souza-Fonseca-Guimaraes F, Chow MT, Town L, et al. *The receptors CD96 and CD226 oppose each other in the regulation of natural killer cell functions*. Nat Immunol. 2014;15(5):431-8.

65. Gilfillan S, Chan CJ, Cella M, Haynes NM, Rapaport AS, Boles KS, et al. *DNAM-1 promotes activation of cytotoxic lymphocytes by nonprofessional antigen-presenting cells and tumors*. J Exp Med. 2008;205(13):2965-73.

66. Iguchi-Manaka A, Kai H, Yamashita Y, Shibata K, Tahara-Hanaoka S, Honda S, et al. *Accelerated tumor growth in mice deficient in DNAM-1 receptor*. J Exp Med. 2008;205(13):2959-64.

67. Lakshmikanth T, Burke S, Ali TH, Kimpfler S, Ursini F, Ruggeri L, et al. *NCRs and DNAM-1 mediate NK cell recognition and lysis of human and mouse melanoma cell lines in vitro and in vivo.* J Clin Invest. 2009;119(5):1251-63.

68. Martinet L, Ferrari De Andrade L, Guillerey C, Lee JS, Liu J, Souza-Fonseca-Guimaraes F, et al. *DNAM-1 expression marks an alternative program of NK cell maturation*. Cell Rep. 2015;11(1):85-97.

69. Okumura G, Iguchi-Manaka A, Murata R, Yamashita-Kanemaru Y, Shibuya A, Shibuya K. *Tumor-derived soluble CD155 inhibits DNAM-1–mediated antitumor activity of natural killer cells*. Journal of Experimental Medicine. 2020;217(4).

70. Whelan S, Ophir E, Kotturi MF, Levy O, Ganguly S, Leung L, et al. *PVRIG and PVRL2 Are Induced in Cancer and Inhibit CD8(+) T-cell Function*. Cancer Immunol Res. 2019;7(2):257-68.

71. Stamm H, Klingler F, Grossjohann EM, Muschhammer J, Vettorazzi E, Heuser M, et al. *Immune checkpoints PVR and PVRL2 are prognostic markers in AML and their blockade represents a new therapeutic option.* Oncogene. 2018;37(39):5269-80.

72. Nishiwada S, Sho M, Yasuda S, Shimada K, Yamato I, Akahori T, et al. *Clinical significance of CD155 expression in human pancreatic cancer.* Anticancer Res. 2015;35(4):2287-97.

73. Bevelacqua V, Bevelacqua Y, Candido S, Skarmoutsou E, Amoroso A, Guarneri C, et al. *Nectin like-5 overexpression correlates with the malignant phenotype in cutaneous melanoma.* Oncotarget. 2012;3(8):882-92.

74. Masson D, Jarry A, Baury B, Blanchardie P, Laboisse C, Lustenberger P, et al. *Overexpression of the CD155 gene in human colorectal carcinoma.* Gut. 2001;49(2):236-40.

75. Iguchi-Manaka A, Okumura G, Kojima H, Cho Y, Hirochika R, Bando H, et al. *Increased Soluble CD155 in the Serum of Cancer Patients.* PLoS One. 2016;11(4):e0152982.

76. Iguchi-Manaka A, Okumura G, Ichioka E, Kiyomatsu H, Ikeda T, Bando H, et al. *High expression of soluble CD155 in estrogen receptor-negative breast cancer.* Breast Cancer. 2020;27(1):92-9.

77. Karabulut M, Gunaldi M, Alis H, Afsar CU, Karabulut S, Serilmez M, et al. *Serum nectin-2 levels are diagnostic and prognostic in patients with colorectal carcinoma*. Clin Transl Oncol. 2016;18(2):160-71.

78. Cho M, Phillips M, Song L, Erbe-Gurel A, Capitini CM. *CD155 axis modulation promotes natural killer cell-mediated graft-versus-tumor effects against osteosarcoma*. The Journal of Immunology. 2022;208(1_Supplement):62.06-62.06.

79. Kumagai S, Togashi Y, Kamada T, Sugiyama E, Nishinakamura H, Takeuchi Y, et al. *The PD-1 expression balance between effector and regulatory T cells predicts the clinical efficacy of PD-1 blockade therapies*. Nature Immunology. 2020;21(11):1346-58.

80. Rotte A. *Combination of CTLA-4 and PD-1 blockers for treatment of cancer.* Journal of Experimental & Clinical Cancer Research. 2019;38(1):255.

81. Dantoing E, Piton N, Salaün M, Thiberville L, Guisier F. *Anti-PD1/PD-L1 Immunotherapy for Non-Small Cell Lung Cancer with Actionable Oncogenic Driver Mutations.* Int J Mol Sci. 2021;22(12).

82. Tang W, Pan X, Han D, Rong D, Zhang M, Yang L, et al. *Clinical significance of CD8+ T cell immunoreceptor with Ig and ITIM domains+ in locally advanced gastric cancer treated with SOX regimen after D2 gastrectomy.* Oncoimmunology. 2019;8(6):e1593807.

83. Degos C, Heinemann M, Barrou J, Boucherit N, Lambaudie E, Savina A, et al. *Endometrial tumor microenvironment alters human NK cell recruitment, and resident NK cell phenotype and function.* Frontiers in immunology. 2019;10:877.

84. Harjunpää H, Guillerey C. *TIGIT as an emerging immune checkpoint*. Clinical & Experimental Immunology. 2020;200(2):108-19.

85. Guillerey C, Harjunpää H, Carrié N, Kassem S, Teo T, Miles K, et al. *TIGIT immune checkpoint blockade restores CD8(+) T-cell immunity against multiple myeloma.* Blood. 2018;132(16):1689-94.

86. Blake SJ, Stannard K, Liu J, Allen S, Yong MC, Mittal D, et al. *Suppression of Metastases Using a New Lymphocyte Checkpoint Target for Cancer Immunotherapy.* Cancer Discov. 2016;6(4):446-59.

87. Zhang Q, Bi J, Zheng X, Chen Y, Wang H, Wu W, et al. *Blockade of the checkpoint receptor TIGIT prevents NK cell exhaustion and elicits potent anti-tumor immunity.* Nat Immunol. 2018;19(7):723-32.

88. Beltra JC, Manne S, Abdel-Hakeem MS, Kurachi M, Giles JR, Chen Z, et al. *Developmental Relationships of Four Exhausted CD8(+) T Cell Subsets Reveals Underlying Transcriptional and Epigenetic Landscape Control Mechanisms. Immunity*. 2020;52(5):825-41.e8.

89. Vey N, Karlin L, Sadot-Lebouvier S, Broussais F, Berton-Rigaud D, Rey J, et al. *A phase 1 study of lirilumab (antibody against killer immunoglobulin-like receptor antibody KIR2D; IPH2102) in patients with solid tumors and hematologic malignancies*. Oncotarget. 2018;9(25):17675-88.

90. Kohrt HE, Thielens A, Marabelle A, Sagiv-Barfi I, Sola C, Chanuc F, et al. *Anti-KIR antibody enhancement of anti-lymphoma activity of natural killer cells as monotherapy and in combination with anti-CD20 antibodies.* Blood. 2014;123(5):678-86.

91. Xue C, Greene EC. *DNA Repair Pathway Choices in CRISPR-Cas9-Mediated Genome Editing.* Trends Genet. 2021;37(7):639-56.

92. Galot R, Le Tourneau C, Saada-Bouzid E, Daste A, Even C, Debruyne P, et al. *A phase II study of monalizumab in patients with recurrent/metastatic squamous cell carcinoma of the head and neck: The I1 cohort of the EORTC-HNCG-1559 UPSTREAM trial*. Eur J Cancer. 2021;158:17-26.

93. Tinker AV, Hirte HW, Provencher D, Butler M, Ritter H, Tu D, et al. *Dose-Ranging and Cohort-Expansion Study of Monalizumab (IPH2201) in Patients with Advanced Gynecologic Malignancies: A Trial of the Canadian Cancer Trials Group (CCTG): IND221.* Clin Cancer Res. 2019;25(20):6052-60.

94. Herbst RS, Majem M, Barlesi F, Carcereny E, Chu Q, Monnet I, et al. *COAST: An Open-Label, Phase II, Multidrug Platform Study of Durvalumab Alone or in Combination With Oleclumab or Monalizumab in Patients With Unresectable, Stage III Non-Small-Cell Lung Cancer*. J Clin Oncol. 2022;40(29):3383-93.

95. Cany J, van der Waart AB, Spanholtz J, Tordoir M, Jansen JH, van der Voort R, et al. *Combined IL-15 and IL-12 drives the generation of CD34(+)-derived natural killer cells with superior maturation and alloreactivity potential following adoptive transfer.* Oncoimmunology. 2015;4(7):e 1017701.

96. Du W, Hu Y, Lu C, Li J, Liu W, He Y, et al. *Cluster of differentiation 96 as a leukemia stem cell-specific marker and a factor for prognosis evaluation in leukemia.* Mol Clin Oncol. 2015;3(4):833-8.

97. Jiang Y, Xu P, Yao D, Chen X, Dai H. C*D33, CD96 and Death Associated Protein Kinase (DAPK) Expression Are Associated with the Survival Rate and/or Response to the Chemotherapy in the Patients with Acute Myeloid Leukemia (AML).* Med Sci Monit. 2017;23:1725-32.

98. Schneider H, Rudd CE. D*iverse mechanisms regulate the surface expression of immunotherapeutic target ctla-4*. Front Immunol. 2014;5:619.

99. Chambers CA. *The expanding world of co-stimulation: the two-signal model revisited.* Trends in Immunology. 2001;22(4):217-23.

100. Chauvin J-M, Zarour HM. *TIGIT in cancer immunotherapy*. Journal for ImmunoTherapy of Cancer. 2020;8(2):e000957.

101. Zhu Y, Paniccia A, Schulick AC, Chen W, Koenig MR, Byers JT, et al. I*dentification of CD112R as a novel checkpoint for human T cells.* J Exp Med. 2016;213(2):167-76.

102. Murter B, Pan X, Ophir E, Alteber Z, Azulay M, Sen R, et al. *Mouse PVRIG Has CD8(+) T Cell-Specific Coinhibitory Functions and Dampens Antitumor Immunity*. Cancer Immunol Res. 2019;7(2):244-56.

103. Li J, Whelan S, Kotturi MF, Meyran D, D'Souza C, Hansen K, et al. *PVRIG is a novel natural killer cell immune checkpoint receptor in acute myeloid leukemia*. Haematologica. 2021;106(12):3115-24.

104. Yamaji T, Mitsuki M, Teranishi T, Hashimoto Y. *Characterization of inhibitory signaling motifs of the natural killer cell receptor Siglec-7: attenuated recruitment of phosphatases by the receptor is attributed to two amino acids in the motifs*. Glycobiology. 2005;15(7):667-76.

105. Kawasaki Y, Ito A, Withers DA, Taima T, Kakoi N, Saito S, et al. *Ganglioside DSGb5, preferred ligand for Siglec-7, inhibits NK cell cytotoxicity against renal cell carcinoma cells.* Glycobiology. 2010;20(11):1373-9.

106. Nicoll G, Avril T, Lock K, Furukawa K, Bovin N, Crocker PR. *Ganglioside GD3 expression on target cells can modulate NK cell cytotoxicity via siglec-7-dependent and -independent mechanisms.* Eur J Immunol. 2003;33(6):1642-8.

107. Brunetta E, Fogli M, Varchetta S, Bozzo L, Hudspeth KL, Marcenaro E, et al. *The decreased expression of Siglec-7 represents an early marker of dysfunctional natural killer-cell subsets associated with high levels of HIV-1 viremia.* Blood. 2009;114(18):3822-30.

108. Shao JY, Yin WW, Zhang QF, Liu Q, Peng ML, Hu HD, et al. S*iglec-7 Defines a Highly Functional Natural Killer Cell Subset and Inhibits Cell-Mediated Activities.* Scand J Immunol. 2016;84(3):182-90.

109. Daly J, Carlsten M, O'Dwyer M. *Sugar Free: Novel Immunotherapeutic Approaches Targeting Siglecs and Sialic Acids to Enhance Natural Killer Cell Cytotoxicity Against Cancer.* Front Immunol. 2019;10:1047.

110. Jandus C, Boligan KF, Chijioke O, Liu H, Dahlhaus M, Démoulins T, et al. *Interactions between Siglec-7/9 receptors and ligands influence NK cell-dependent tumor immunosurveillance.* J Clin Invest. 2014;124(4):1810-20.

111. Yvon ES, Burga R, Powell A, Cruz CR, Fernandes R, Barese C, et al. *Cord blood natural killer cells expressing a dominant negative TGF-β receptor: Implications for adoptive immunotherapy for glioblastoma.* Cytotherapy. 2017;19(3):408-18.

112. Li K, Xu J, Wang J, Lu C, Dai Y, Dai Q, et al. *Dominant-negative transforming growth factor-β receptor-armoured mesothelin-targeted chimeric antigen receptor T cells slow tumour growth in a mouse model of ovarian cancer.* Cancer Immunology, Immunotherapy. 2023;72(4):917-28.

113. Wang Z, Guo L, Song Y, Zhang Y, Lin D, Hu B, et al. *Augmented anti-tumor activity of NK-92 cells expressing chimeric receptors of TGF-βR II and NKG2D.* Cancer Immunol Immunother. 2017;66(4):537-48.

114. Shaim H, Shanley M, Basar R, Daher M, Gumin J, Zamler DB, et al. *Targeting the αv integrin/ TGF-β axis improves natural killer cell function against glioblastoma stem cells*. J Clin Invest. 2021;131(14).

Appendix

Nederlandse samenvatting

Het immuunsysteem is een complex netwerk van verschillende afweercellen en signaalstoffen met als doel het lichaam te beschermen tegen schadelijke indringers - zoals bacteriën, schimmels en virussen - maar ook het herkennen en bestrijden van "afwijkende" kankercellen. Ons immuunsysteem bestaat uit twee onderdelen: het adaptief en het aangeboren immuunsysteem. De eerste werkt middels een antigeen-specifieke immuunrespons via T- en B-cellen die enkele weken nodig heeft om volledig op gang te komen. Het aangeboren immuunsysteem is het eerste verdedigingsmechanisme van het lichaam en reageert snel. Natural killer (NK) cellen maken deel uit van het aangeboren immuunsysteem. Dit betekent dat ze snel kunnen reageren op virus-geïnfecteerde cellen en kankercellen zonder voorafgaande blootstelling aan deze cellen of geheugen. Dit maakt ze een veelbelovende therapeutische mogelijkheid voor vormen van kanker die gevoelig zijn voor NK-cel reactiviteit zoals eierstokkanker. Eierstokkanker is een agressieve vorm van kanker die vaak laat wordt ontdekt door veelal vage klachten totdat de maligne cellen explosief gegroeid en gemetastaseerd zijn. In dit vergevorderde stadium is het moeilijk om patiënten te behandelen en hebben zij veelal een slecht prognose. Slechts 28% van deze gevorderd stadium patiënten leeft nog na vijf jaar. Ascites - een ophoping van vocht in de buikholte - is een veelvoorkomende complicatie die optreedt bij vergevorderde eierstokkanker. Ascites draagt bij aan de tumorgroei en bevat stoffen en suppressieve cellen die het immuunsysteem remmen, waaronder NK-cellen die proberen de tumoren aan te vallen. De huidige behandeling voor eierstokkanker is chirurgie om zoveel mogelijk tumor te verwijderen, in combinatie met voorafgaande en/of aanvullende chemotherapie. Maar ondanks deze intensieve behandeling keert de kanker in 80% van de patiënten terug.

Een veelbelovende en recente ontwikkeling in de behandeling van eierstokkanker is het versterken van het immuunsysteem van de patiënt om de terugkeer van de ziekte te voorkomen. Eierstokkanker is een relatief immunogene tumor en de aanwezigheid van tumor infiltrerende lymfocyten bevattende T-cellen en NK-cellen correleert met betere overleving van eierstok kankerpatiënten. Autologe NK-cellen van de patiënt zijn echter vaak in kleine aantallen aanwezig en worden sterk onderdrukt door de afweer remmende tumoromgeving, die deels bestaat uit eerdergenoemde ascites. Naast

het versterken van natuurlijk voorkomende NK-cellen, is aanvullende NK-cel immunotherapie een veelbelovende strategie.

Hoewel verschillende bronnen van NK-cellen worden onderzocht voor dit doel, richten we ons in **dit proefschrift** voornamelijk op natuurlijk voorkomende perifere bloed (PB) NK-cellen en NK-cellen die we in een 35-daags kweekprotocol kunnen genereren vanuit CD34+ hematopoëtische progenitor cellen (HPC) van een donor in het laboratorium. Deze donor HPC-NK-cellen zijn direct bruikbaar als een 'kant-en-klaar' immunotherapieproduct en hebben het bijkomende voordeel dat ze effectievere killers zijn dan NK-cellen die afkomstig zijn uit perifeer bloed. Adoptieve NK-celtherapie kan verder worden versterkt door cytokinestimulatie, het blokkeren van remmende mechanismen en genetische modificatie van specifieke mechanismen om tumor-reactiviteit te verbeteren.

In **Hoofdstuk 2** hebben we gekeken naar de rol van NK-cellen bij hooggradige sereus papillaire eierstokkanker (wat de meest voorkomende vorm is) en hebben we aangetoond dat de frequentie van NK-cellen in ascites een positief verband toont met een langere ziektevrije en algehele overleving. Daarnaast bleken de expressieniveaus van activatiemarkers op NK-cellen bij eierstokkanker patiënten significant lager te zijn dan op NK-cellen in buikvocht van patiënten met niet-maligne aandoeningen. DNAM-1, NKp30, NKp46, maar niet NKG2D en 2B4, zijn significant lager in NK-cellen van eierstokkanker patiënten waardoor deze minder actief zijn. Met behulp van een *in-vitro* activatie-proef hebben we aangetoond dat stimulatie met IL-15 of de IL-15-superagonist N-803 de degranulatie en IFN-γ-productie van NK-cellen tegen eierstok-tumorcellen kan verhogen. Superagonist N-803 is een gemodificeerde vorm van IL-15 met verbeterde bindings- en activerende eigenschappen en een toegevoegd IgG Fc-staart om de halfwaardetijd *in vivo* aanzienlijk te verlengen in vergelijking met recombinant humaan (rh)IL-15. Door het verband te leggen tussen het percentage NK-cellen en de klinische parameters van eierstokkanker-patiënten – en dat de functionaliteit kan worden versterkt door extra stimulatie met IL-15 – zijn we tot nieuwe inzichten gekomen voor toekomstige immunotherapieën op basis van NK-cellen.

In **Hoofdstuk 3** hebben we het therapeutische potentieel van N-803 verder onderzocht om de functionaliteit van HPC-NK-cellen tegen eierstokkanker en acute myeloïde leukemie (AML) te verbeteren. We hebben aangetoond dat N-803 stimulatie de productie van IFN-γ en proliferatie van HPC-NK-cellen verhoogt. In AML-modellen nam ook de frequentie van "serial killers" (NK-cellen die twee of meer kankercellen direct na elkaar aanvallen en doden) toe en was de expressie van intercellulair adhesiemolecuul 1 (ICAM-1) op de AML-cellen verhoogd. Hierdoor zijn ze een makkelijker doelwit voor NK-celgemedieerde doding. In eierstokkanker modellen was

er echter geen toename in de frequentie “serial killers” na toevoeging van N-803. Desondanks was de expressie van CXCL10 door de eierstok tumorcellen aanzienlijk verhoogd, wat op zijn beurt NK-cel infiltratie en aantrekking via CXCR3 kan verbeteren. Bij muizen met humane eierstokkanker die werden behandeld met HPC-NK-cellen plus N-803 of rhIL-15, bleek dat beide vormen van IL-15 de HPC-NK-cellen effectief ondersteunen. Dit resulteerde in aanzienlijk verminderde tumorgroei in vergelijking met de controlegroep die geen rhIL-15 of N-803 ontving. Al met al bieden deze gegevens een rationale voor N-803-gebaseerde cytokinesteun in zowel de eierstokkanker als AML setting om de overleving van NK-cellen te ondersteunen en de anti-tumoractiviteit van NK-cellen te verbeteren.

Voor **Hoofdstuk 4** hebben we uitgebreide flowcytometrie panels gebruikt om NK-celsubsets in detail te karakteriseren aan de hand van activatie, differentiatie en immuuncheckpoint markers. Hiervoor hebben we NK-cellen uit ascitesvocht van 26 patiënten met hooggradige sereus eierstokkanker met die van 11 goedaardige cystadenoom (controles) vergeleken. We hebben vervolgens de clustering methode FlowSOM gebruikt om de molecuul expressie van individuele cellen gemeten met flowcytometrie te analyseren en unieke subsets en co-expressie profielen te identificeren. Deze methode groepeert cellen met vergelijkbare eigenschappen in meerdere verschillende clusters. Daarbij hebben we twee interessante groepen van clusters geïdentificeerd: één groep clusters was verhoogd in ascites van eierstokkanker patiënten en was geassocieerd met verlies van de activatiereceptoren DNAM-1 en CD16, en met verhoogde expressie van inhibitie-checkpointmoleculen TIGIT, TIM-3 en PD-1. De tweede groep clusters was juist verlaagd bij patiënten met eierstokkanker en kwam overeen met een fenotype dat we normaliter zien op gezonde perifeer bloed NK-cellen. Opvallend was dat deze laatste groep clusters een negatief verband toonde met NK-cel remmende eiwitten die we gemeten hadden in ascites van eierstokkanker patiënten. Daarnaast was het opmerkelijk dat de groep clusters die verhoogd was bij eierstokkanker patiënten significant en sterk gecorreleerd was met de meerderheid van de NK-cel remmende eiwitten gemeten in ascitesvocht van de eierstokkanker patiënten. Alles tezamen hebben we NK-cel clusters en receptoren geïdentificeerd die geassocieerd zijn met de NK cel remmende omgeving in ascitesvocht. De remmende receptoren die we gevonden hebben kunnen als aanknopingspunten gebruikt worden voor toekomstige studies naar immuuncheckpoint blokkade die zich richten op relevante receptorroutes voor eierstokkanker.

Bij **Hoofdstuk 5** is het belang van tumorligandexpressie voor activerende receptoren verder onderzocht, omdat dit voor NK-cellen nodig is voor het herkennen en elimineren van tumorcellen. We hebben ons hier met name gericht op de interactie tussen tumor en NK-cellen van de receptor familie DNAM-1-, TIGIT- en CD96, omdat we DNAM-1 hadden geïdentificeerd als een van de belangrijkste activerende

receptoren die verminderd tot expressie komt op NK-cellen van eierstokkanker patiënten (Hoofdstuk 2). Ondanks lagere DNAM-1 expressie, waren TIGIT en CD96 respectievelijk gelijk aan of hoger dan die van gezonde perifeer bloed NK-cellen. We hebben de vermindering van DNAM-1 kunnen bevestigen met gezonde PB-NK-cellen door middel van co-cultuur van eierstokkanker tumorcellen in een monolaag, in een multi-cellulaire 3D structuur en bij eierstokkanker tumor dragende muizen. Expressie van andere NK-cel receptoren zoals PD-1, NKG2a en OX40 werd niet beïnvloed door de interactie tussen tumor en NK-cellen. Het activeren van NK-cellen met IL-15 resulteerde in verhoogde expressie van DNAM-1, maar verhoogde ook de expressie van TIGIT en CD96. Door TIGIT-blokkade met behulp van een anti-TIGIT antistof werd de degranulatie en IFNγ-productie van gezonde perifeer bloed NK-cellen en, belangrijker nog, NK-cellen afkomstig van eierstokkanker patiënten verhoogd in reactie op eierstok tumorcellen. Bij muizen met eierstok kanker resulteerde behandelding met IL-15, gezonde perifeer bloed NK-cellen en TIGIT-blokkade in verminderde tumor groei in vergelijking met onbehandelde muizen. Dit laat het belang zien van signalering via DNAM-1/TIGIT/CD96 op NK cellen en het klinische potentieel van (TIGIT) checkpointblokkade bij eierstokkanker.

Naast interacties tussen tumorliganden en NK-cel receptoren hebben we in **hoofdstuk 6** de remmende rol van de cellen en eiwitten in de tumoromgeving (ascites) van eierstokkanker verder in kaart te gebracht. Ascites staat bekend om het bevorderen van de groei en invasie van tumorcellen en bevat allerlei verschillende immuuncellen en signaalstoffen. Daarom hebben we uitgebreide signaalstof analyse uitgevoerd op ascites van eierstokkanker patiënten en op goedaardige buikvocht. Van deze ascites hebben we ook de remmende eigenschappen op de functie van NK-cellen bepaald, het verband met de eiwitten uit de ascites en klinische uitkomstparameters zoals overleving en CA-125, een eierstokkanker tumor marker. We ontdekten dat HPC-NK-cellen beter bestand waren tegen de remmende effecten van ascites in vergelijking met perifeer bloed NK-cellen. TGF-β1 bleek het eiwit te zijn dat het sterkst correleerde met door ascites veroorzaakte disfunctie van NK-cellen en verminderde overleving van eierstok kanker patiënten. Blokkering van TGF-β1-signalering met galunisertib herstelde de functionaliteit van NK-cellen gedeeltelijk in functionele *in vitro* proeven. Hoge TGF-β1 concentraties in ascites waren verder geassocieerd met een verminderde functie van NK-cellen, een slechte (ziekte vrije) overleving en met de aanwezigheid van M2-achtige macrofagen, B-celpopulaties en regulatoire T-cellen. Deze bevindingen laten de rol zien van het TGF-β1 cytokine bij het dempen van NK-cel immuniteit in gevorderd eierstokkanker. Op basis hier van zouden op NK-cel gebaseerde immunotherapieën voor eierstokkanker mogelijk baat kunnen hebben bij interferentie met TGF-β1 signalering in de tumor omgeving.

Hoofdstuk 7 vat het proefschrift samen en belicht de relevantie van het onderzoek voor patiënten met eierstokkanker. Daarnaast bespreekt het de stappen die in de toekomst nog gezet kunnen worden en hoe dit onderzoek zich verhoudt tot bestaande literatuur. Toekomstige patiënten kunnen baat hebben bij een therapeutisch product dat is afgestemd op de individuele patiënt. Denk hierbij aan combinatiestrategieën waarbij verschillende remmende moleculen die sterk tot expressie komen op de NK-cellen in een patiënt worden uitgeschakeld door middel van blokkade met antistoffen of genetische aanpassing van het NK-cel product voorafgaand aan infusie. Belangrijk hierbij is een doeltreffende ondersteunende cytokine, zoals N-803, of door genetische manipulatie waarbij de NK-cel het IL-15 molecuul zelf kan produceren. Dergelijke strategieën worden reeds met succes toegepast in (pre-)klinisch onderzoek in andere kankersoorten en zijn potentieel ook toepasbaar bij eierstokkanker.

Kortom, in dit proefschrift hebben we laten zien dat op NK-cellen gebaseerde immunotherapie een aantrekkelijke adjuvante behandelingsoptie is voor eierstokkanker-patiënten. Zij hebben momenteel beperkte behandelingsmogelijkheden, vooral na terugkeer van de ziekte. Bovendien kunnen tumorcellen, onderdrukkende immuun-cellen en remmende eiwitten in ascites de expressie van activerende receptoren op NK-cellen verlagen. Tegelijkertijd kunnen tumorcellen de expressie van remmende checkpoint receptoren verhogen. We hebben ook aangetoond dat IL-15 stimulatie essentieel is voor het ondersteunen en (re)activeren van NK-cellen voor langdurige persistentie en werkzaamheid na infusie. Verder hebben we ons vooral gericht op het identificeren van de dominante checkpoint moleculen op NK-cellen en hoe deze bijdragen aan NK-cel uitputting en remming in ascites. TIGIT bleek een belangrijk remmend checkpointmolecuul op NK-cellen in de context van eierstokkanker. Vervolgens hebben we aangetoond dat TGF-β1 een van de belangrijkste NK-cel remmende cytokines is die aanwezig is in ascitesvocht. Daarom bieden IL-15-gebaseerde stimulatie en blokkade van de TIGIT en TGF-β1 mogelijkheden om de remming van NK-cellen door eierstokkanker te voorkomen en NK-cel-gebaseerde immunotherapie te verbeteren. Alles tezamen bieden de resultaten van dit proefschrift nieuwe inzichten voor de verbetering van NK-celtherapie voor de behandeling van patiënten met eierstokkanker.

Curriculum Vitae

Ralph Johan Anton Maas was born on April 18, 1992, in Groesbeek and grew up in Wanroij. He completed his high school at Elzendaal collega in Boxmeer in 2010 and started a bachelor in Biomedical Sciences at Radboud University in Nijmegen. Graduating in 2013, he specialized in Human Pathobiology and minored in Infectious Diseases during his masters, reflecting his passion for Immunology.

During his master's, Ralph undertook internships that significantly and positively contributed to his enthusiasm to pursue an academic career. At the Internal Medicine Department of RadboudUMC, he investigated IL-38 under supervision of Dr. Mark Gresnigt and Prof. Dr. Frank van de Veerdonk. He continued his IL-38 research at the University of Colorado Denver School of Medicine, supervised by Prof. Dr. Charles A. Dinarello. He extended his work on IL-38 for an additional six months at both institutions while writing his internship reports.

In 2017, Ralph started his PhD journey at Radboud University Medical Center, under supervision of Dr. Willemijn Hobo, Prof. Dr. Harry Dolstra, and Prof. Dr. Joop Jansen. That same year, he relocated to Nijmegen. His research focused on exploring checkpoint molecules on NK cells as potential targets for ovarian cancer immunotherapy, a field that aligned with his immunology interests.

By 2021, Ralph began working for BioLegend, a role he undertook while completing the final experiments for his PhD and finalizing his thesis.

List of publications

Ralph J. A. Maas, Janneke S. Hoogstad-van Evert, Iris M. Hagemans, Jolanda Brummelman, Diede van Ens, Paul K. J. D. de Jonge, Laura Hooijmaijers, Shweta Mahajan, Anniek B. van der Waart, Charlotte K. J. C. Hermans, Janne de Klein, Rob Woestenenk, Antonius E. van Herwaarden, Nicolaas P. M. Schaap, Somayeh Rezaeifard, Daniele V. F. Tauriello, Petra L. M. Zusterzeel, Nelleke Ottevanger, Joop H. Jansen, Willemijn Hobo1* and Harry Dolstra* **Increased peritoneal TGF-β1 is associated with ascites-induced NK-cell dysfunction and reduced survival in high-grade epithelial ovarian cancer** Front Immunol. 2024 Sep 23:15:1448041.

Martin Jaeger, Axel Dietschmann, Sophie Austermeier, Sude Dinçer, Pauline Porschitz, Larsen Vornholz, **Ralph J.A. Maas**, Evelien G.G. Sprenkeler, Jürgen Ruland, Stefan Wirtz, Tania Azam, Leo A.B. Joosten, Bernhard Hube, Mihai G. Netea, Charles A. Dinarello, Mark S. Gresnigt **Alpha1-antitrypsin impacts innate host-pathogen interactions with Candida albicans by stimulating fungal filamentation** Virulence. 2024 Mar 22:2333367.

Jolien M.R. Van der Meer, Paul K.J.D. de Jonge, Anniek B. van der Waart, Alexander C. Geerlings, Jurgen P. Moonen, Jolanda Brummelman, Janne de Klein, Malou C. Vermeulen, **Ralph J.A. Maas**, Nicolaas P.M. Schaap, Janneke S. Hoogstad-van Evert, Petronella B. Ottevanger, Joop H. Jansen, Willemijn Hobo, Harry Dolstra **CD34+ progenitor-derived NK cell and gemcitabine combination therapy increases killing of ovarian cancer cells in NOD/SCID/IL2Rgnull mice** Oncoimmunology. 2021 Oct 1;10(1):1981049.

Jolien M.R. van der Meer, **Ralph J.A. Maas***, Karolin Guldevall*, Kim Klarenaar, Paul K.J.D. De Jonge, Janneke S. Hoogstad-van Evert, Anniek B. van der Waart, Jeanette Cany, Jeffrey T. Safrit, John H. Lee, Esther Wagena, Peter Friedl, Björn Önfelt, Leon F. Massuger, Nicolaas P.M. Schaap, Joop H. Jansen, Willemijn Hobo, Harry Dolstra **IL-15 superagonist N-803 improves IFNγ production and killing of leukemia and ovarian cancer cells by CD34+ progenitor-derived NK cells** Cancer Immunol Immunother. 2021;70(5):1305-1321.

Dennis M. de Graaf, **Ralph J.A. Maas**, Sanne P. Smeekens, Elan Eisenmesser, Jasmina S. Redzic, Monique M. Helsen, Nicholas E. Powers, Suzhao Li, Vassili Kalabokis, Mark S. Gresnigt , Leo A.B. Joosten, Charles A. Dinarello, Frank L. van de Veerdonk **Human recombinant interleukin-38 suppresses inflammation in mouse models of local and systemic disease** Cytokine. 2021 Jan:137:155334.

Ralph J.A. Maas, Janneke S. Hoogstad-van Evert, Jolien M.R. Van der Meer, Vera Mekers, Somayeh Rezaeifard, Alan J. Korman, Paul K.J.D. de Jonge, Jeannette Cany, Rob Woestenenk, Nicolaas P.M. Schaap, Leon F. Massuger, Joop H. Jansen, Willemijn Hobo, Harry Dolstra **TIGIT blockade enhances functionality of peritoneal NK cells with altered expression of DNAM-1/TIGIT/CD96 checkpoint molecules in ovarian cancer** Oncoimmunology. 2020 Nov 8;9(1):1843247.

Marina Krause,* Feng Wei Yang,* Mariska te Lindert, Philipp Isermann, Jan Schepens, **Ralph J.A. Maas**, Chandrasekhar Venkataraman, Jan Lammerding, Anotida Madzvamuse, Wiljan Hendriks, Joost te Riet, and Katarina Wolf **Cell migration through three-dimensional confining pores: speed accelerations by deformation and recoil of the nucleus** Philos Trans R Soc Lond B Biol Sci. 2019 Aug 19; 374(1779): 20180225.

Janneke S. Hoogstad-van Evert, **Ralph J.A. Maas***, Jolien M.R. van der Meer*, Jeannette Cany, Sophieke van der Steen, Joop H. Jansen, Jeffrey S. Miller, Ruud Bekkers, Willemijn Hobo, Leon F. Massuger*, Harry Dolstra* **Peritoneal NK cells are responsive to IL-15 and percentages are correlated with outcome in advanced ovarian cancer patients** Oncotarget. 2018 Oct 5;9(78):34810-34820.

*these authors contributed equally

PhD portfolio

PhD portfolio of Ralph Maas

Department: Laboratory Medicine (LH)
PhD period: 01/01/2017 – 11/12/2025
PhD Supervisor(s): Prof. Harry Dolstra and Prof. Joop Jansen
PhD Co-supervisor(s): Dr. Willemijn Hobo

Training activities	Years	ECTS
Courses	2017	0.5
Radboudumc Introduction Day Course: RIMLS	2017	0.75
Introductory course	2017	2.0
Course: RIMLS Introductory course	2017	2.25
Course: 'Management voor promovendi'	2017	1.0
12th ENII EFIS EJI Summer School on	2017	0.2
Advanced Immunology*	2018	1.0
Course: Scientific Integrity course	2018	3.0
Course: Flow Cytometry course by BD Bioscience	2019	0.25
Course: Within sight of my PhD		
Course: Scientific writing		
BCR career event		
Seminars	2017-2021	0.8
Radboud Research Rounds	2017-2021	4.8
Hematology meetings	2017-2021	0.4
Cancer Immunology & Immunotherapy meeting		
Conferences	2017-2020	3.0
4x RIMLS PhD retreat###*	2017-2019	3.0
3x Radboud Frontiers	2017-2019	2.0
Dutch Hematology Congress*	2017-2020	3.0
Dutch Tumor Immunology Meeting*	2017-2020	3.0
NVVI conference	2018	1.25
NK2018: meeting of the Society for Natural	2019	1.25
Immunity (US)#	2017-2020	1.5
NK2019: meeting of the Society for Natural		
Immunity (EU)		
3x Laboratory Hematology retreat***		
Other	2017-2021	2.2
Journal clubs		
Teaching activities		
Lecturing	-	-
Supervision of internships / other	2017-2021	8
Total		**45.15**

* Oral presentation, # poster

Data management

The research data presented in this thesis were obtained during my PhD at the Laboratory of Hematology – Department of Laboratory Medicine, Radboud university medical center (Radboudumc), the Netherlands. All primary (raw) and secondary (processed) data was captured and stored and backed-up daily on the Q and H-drive of the Laboratory of Hematology – Department of Laboratory Medicine. Data was stored according to the FAIR principles: Findable, Accessible, Interpretable and Reusable, on H:\22 LABGK LH\15 CTI research\Ralph Maas. In addition, data was stored in Labguru^{TM}, a digital lab book client which is centrally stored and backed-up daily on a local Radboudumc server. All data archives are stored on Labguru^{TM} and accessible by the associated senior staff members. Mouse studies described in **Chapters 3** and **5** were approved by the Central Animal Laboratory and the Animal Ethics Board of the Radboudumc. Human samples used in **Chapter 2-6** were collected in a biobank in accordance with the principles of the Declaration of Helsinki and institutional guidelines and regulations. The medical and ethical review board Committee on Research Involving Human Subjects Region Arnhem Nijmegen, Nijmegen, the Netherlands has given approval to conduct these studies. All raw and processed flow cytometry data described in Chapter **2-6** is available through

- Q:\FCM_Users\CHL\GVL\Project4\LMD and
- Q:\FCM_Users\CHL\GVL\Project12\LMD

To ensure interpretability of the data, all filenames, primary and secondary data, metadata, and descriptive files used to provide the final results are documented along with the data. Published data generated or analyzed in this thesis or part of published articles and its additional files are available from the associated corresponding authors on request.

Dankwoord

Het heeft even mogen duren, maar ook voor mij komt er een einde aan dit avontuur dat een PhD heet. Onderzoek doe je niet alleen en zonder de hulp en inzet van iedereen uit dit dankwoord – en nog veel collega's, patiënten, vrienden en anderen die niet bij naam genoemd zijn – was dit niet gelukt. Dit dankwoord is in chronologische volgorde geschreven. Het is namelijk voor mij onmogelijk is om op basis van bijdrage aan dit proefschrift iedereen op volgorde te bedanken.

Dan mag ik beginnen met **mijn ouders.** Zonder jullie was ik nooit zo ver gekomen. Het doet me pijn om te zien hoe ons gezin er nu voor staat. Desondanks zijn jullie het grootste deel van mijn leven mijn steun en toeverlaat geweest. Dat betekent nog steeds heel veel voor me. Ik heb ongelofelijk veel van jullie kunnen leren, zoals scheikunde van ons pap. En ons mam stond altijd voor me klaar om me te overhoren, zodat ik klaar was voor de volgende toets. Dit zal ik nooit vergeten en jullie beide eeuwig dankbaar voor zijn. Bedankt voor alle mooie herinneringen en ik hoop dat we betere tijden tegemoet gaan.

De volgende persoon die in mijn leven kwam: **Cecile**. Mijn lieve zus en paranimf tijdens de verdediging van mijn proefschrift. Ondanks dat we verschillende carrièrepaden bewandelen, vermijden we beiden niet de moeilijke route en schrikken we niet terug voor uitdagingen. De flauwe humor die we delen (ook met ons pap) doet me altijd goed. Misschien hebben we stiekem toch meer gemeen dan we altijd dachten. Het doet me deugd om te zien dat we vaak afspreken en onder het genot van een alcoholische versnapering super gezellige spelletjes avonden tot diep in de nacht hebben. Je bent een echte doorzetter en het woord klagen staat niet in je woordenboek. Ik kijk uit naar de ongetwijfeld vele mooie momenten die we samen nog gaan meemaken.

Tom, Cazzo. Er is niemand in mijn vriendenkring die zo betrokken was bij mijn PhD als jij. Niet zozeer vanwege het project zelf, maar omdat je niet kon wachten tot het eindelijk voorbij zou zijn – bij deze, het is gelukt. Hopelijk hebben we nu meer tijd om samen rummetjes te drinken en slechte actiefilms te kijken. Bedankt voor je eeuwige steun maat! De gedachte dat jij er altijd voor me bent en echt iemand bent waar je op kunt rekenen is me heel veel waard.

Zonder de ontspanning, sport en steun van de 'boefjes' was mijn PhD waarschijnlijk een stuk sneller klaar geweest. Toch bedankt voor alle gezelligheid **Guus**, **Jan**, **Kevin**, **Martijn**, **Remco en Seep**. Mijn game/hardloop/klus-maten **Teun**, **Tim en**

Yorick, wil ik speciaal benoemen vanwege hun interesse en steun. Bedankt voor jullie vriendschap.

Rinus en Marieke (Muis), op jonge leeftijd heb ik veel van jullie kunnen leren als knecht en met plezier op de boerderij meegeholpen. Op latere leeftijd is onze werkrelatie veranderd in een vriendschap. Ontspanning en vrienden waar je op kunt rekenen zijn belangrijke pijlers die je nodig hebt om door een PhD heen te komen. Bedankt voor alle gefrituurde eitjes, een klusruimte voor m'n mustang(s), de lekkere (liefst dikke, zo eentje waar de lepel rechtop in blijft staan, met spekjes) soep, alle onzin (vooral van Rinus natuurlijk) en alle gezelligheid!

We nemen nu een grote stap in de tijd en komen aan bij mijn BMW studie. De meesten hebben Nijmegen ondertussen verlaten, maar we hebben een geweldige tijd gehad samen. Het doet me goed om hier halfjaarlijks samen op terug te kijken. Bedankt voor het initiatief, **Tonke**. Zonder jou was het waarschijnlijk "wanneer iemand een verdediging heeft" geworden. Bedankt ook **Valerie en Sjoerd**, we zochten elkaar op voor het maken van opdrachten en met jullie samenwerken was een genot. Uiteraard ook bedankt voor de gezelligheid, **Amy, Corina, Jolien, Lineke, Max, Roos en Evelien.**

In dezelfde BMW periode mag ik **Thom, Rens, Maarten en Nick** bedanken. Met **Thom** deel ik een andere titel die je niet zomaar krijgt: we zijn namelijk beide trotste LASO masters. Dat zal ons voor het leven tekenen en verbinden. Er zijn weinig avonden zo ontspannen dan onze game-avonden. Bedankt hiervoor. **Rens,** jij was mijn #1 BMW bachelor collega. Met geen ander heb ik zoveel projecten samen gedaan. Met variërend succes. Na ons OMB project is statistiek nooit meer mijn sterkste punt geworden. Tevens is ook niemand met wie ik zoveel tequila heb gedronken. Aan het eerste heb ik mooie herinneringen. Aan het tweede vooral mooie foto's. **Maarten**, jouw flauwe droge humor word ik nog vaak aan herinnerd. Er lag hier tot voor kort nog steeds een bierdopje op ons bierdopje… **Nick**, ik ken niemand die zoveel leven in de brouwerij weet te krijgen als jij. Een avond uit met Nick is altijd een avontuur. Het was altijd erg vermakelijk om je door je studie heen te zien gaan met je topsportstatus en je vele dutjes tijdens colleges. Wie had toen gedacht dat jij de eerste van de groep zou zijn die zou gaan trouwen en een kind zou krijgen. Lekker bezig vriend.

Rond deze periode kwam ook **Wilbert** in beeld. Jij bedankt voor de goede zorgen voor ons mam. Je staat niet alleen altijd voor haar, maar ook voor Cecile en mijzelf. Tijdens de verbouwing maakte jouw hulp de meest uitdagende projecten (WC/ Badkamer) haalbaar. Dat waarderen we!

Ook tijdens mijn stages heb ik veel mogen leren. Met name aan mijn stages bij algemene interne en mijn stage in Colorado heb ik hele mooie herinneringen. **Frank** en **Mark,** bedankt voor het vertrouwen in mij bij het IL-38-project. **Mark**, ik had me geen betere stagebegeleider kunnen wensen. Je enthousiasme voor wetenschap in het algemeen en schimmels in het speciaal was aanstekelijk. Je hebt je kennis over labtechnieken met me gedeeld en hier heb ik tot de dag van vandaag veel aan. Zelfs veel later - tijdens mijn PhD - hebben we nog een kort schimmel project samen opgepakt. Buiten al het nuttige hebben we ook een geweldige periode samen gehad in Colorado samen met Martin, Duby, Charles en alle collega's uit Charles' lab. Ik zal ook niet snel vergeten hoe gemakkelijk je Mount Flagstaff op fietste. Ik dacht redelijk fit te zijn op de fiets, maar die wedstrijd heb ik geen enkele keer ook maar bijna kunnen winnen. Op Mount Evans was het **Martin** met de struggles, maar kudos aan hem want we hebben het wel gered! **Martin**, mijn tijd samen jou in Denver en daarna in Nijmegen zit vol goede herinneringen. Nog sorry van de muis, en dank aan jullie beide voor het co-auteurschap ten gevolge daarvan. Waar ik dat aan verdiend heb, weet ik tot de dag van vandaag niet ;) 'A' for effort I guess.

Charles, the discussion we had together with Frank about the IL-38 project was the first time in my life I felt like I really couldn't keep up. Your vast amount of knowledge, your ideas, and thoughts were always flooding, especially when Frank was around. If I was ever in doubt whether research was for me, it was you who convinced me and showed me that academia was a good path to be on. Especially in your Denver lab it was rewarding and fun. You have truly been an inspiration during my early career and I cannot fully express my gratitude for the opportunities and hospitality you showed me in Denver. To this day I always stock up on home-made limoncello with the recipe you gave me.

Dinarello's minions, thanks for the awesome time: **Duby** as a mentor, **Ben**, for showing me around, **Giulio**, for entertaining us and being my gymbuddy (and for borrowing your car), **Niki** as a great roommate, **Carlo** for his hospitality and **Tania** for keeping it all in check.

Lieve **Daniëlla**, of beter, **Daan**. Je wilde hier niet eens staan, zo bescheiden ben je. Maar zonder jouw steun was dit nooit gelukt. Bedankt voor al je geduld tijdens de zware momenten en je hulp om het tot een goed einde te brengen. Een PhD is een levenservaring en er komt veel bij kijken. Ondanks mijn voorbeeld heb je zelf toch besloten ook dit pad te bewandelen. Jij bent eeuwig op zoek naar uitdagingen en die zul je in je PhD wel vinden. We zijn samen al het een en ander tegen gekomen op ons pad, maar ik ben blij dat we het samen bewandelen. Ik kijk uit naar de volgende uitdaging: ons huisje verder uitbouwen en er samen iets bijzonders van maken. PS: het hele PhD proces duurde (nog) langer dan gedacht, dus bij deze ook nog heel erg

bedankt voor het regelen van zowat alles en nog wat in de laatste fase. Zonder jou was het een treurig feest geworden.

Mijn promotieteam is natuurlijk het meest betrokken geweest bij mijn PhD traject. Zonder hen was dit proefschrift nooit tot stand gekomen. We gaan chronologisch, dus eerst **Willemijn**. Oorspronkelijk ben ik aangenomen op jouw project en onder jouw begeleiding begonnen. Je stond altijd open voor een discussie en je bent altijd erg betrokken en enthousiast over data, experimenten en nieuwe plannen. Dat heeft een positief effect heeft gehad op mijn moraal, motivatie en plezier in het lab. Je geeft snelle feedback - in groot detail - waar ik veel en dankbaar gebruik van heb gemaakt. Je scherpe inzichten en steun hebben mij door de beginfase van dit traject geholpen. Dat was een periode waarin ik ongelofelijk veel van je heb kunnen leren. Mijn project over checkpoint en NK cellen bleek uiteindelijk echter toch beter bij het NK onderzoek van **Harry** te passen. Uiteraard zijn jullie beide continu nauw betrokken geweest bij mijn PhD. Via Frans hadden wij elkaar al wel eens eerder gezien, maar het was pas toen ik solliciteerde op een PhD positie bij het hematologie lab dat onze samenwerking van start ging. Ik ken weinig mensen die zo sterk gemotiveerd zijn een doel te bereiken, het NK cel product te ontwikkelen en gebruiken om kankerpatiënten te behandelen en genezen. Een nobel doel waar ik geprobeerd heb een steentje aan bij te dragen. Toen mijn motivatie richting het einde van het traject langzaam minder werd, heb jij me keer op keer gemotiveerd met je aanmoediging en je onvoorwaardelijke vertrouwen in mijn vermogen om dit PhD project tot een goed einde te brengen. Jouw steun heeft me geholpen de moeilijke momenten te overbruggen en weer verder te gaan, zelfs als ik het zelf even niet meer zag. Dank je wel dat je er altijd voor mij was en dat je me hebt geholpen om het beste uit mezelf te halen. **Joop**, jouw scherpe geest waren altijd in staat om de zwakke punten van een studie, die ik zelf over het hoofd had gezien, op te merken. Dat heeft ons werk naar een hoger niveau weten te tillen. Ook hield je altijd de haalbaarheid en de hoofdlijnen van mijn project goed in de gaten en zette je me aan om na te denken over het grotere geheel. Soms raak je als PhD student verzeild in experimenten, maar jij was er altijd om die sleur even te doorbreken. Bedankt voor alle input en discussies over mijn onderzoek.

Jolien, wij zijn ongeveer tegelijk begonnen en werkte allebei aan NK cellen. Daarom hebben we nogal veel experimenten samen gedaan. Zelfs tot midden in de nacht . En natuurlijk de vele congressen zoals NK2018 en de Summer school in Sardinië aan het begin van onze PhD. Je vrolijke, optimistische, sportieve en competitieve aanwezigheid was leuk om bij de groep te hebben. Ook buiten werk om! Mijn vaardigheden op het gebied van planning en initiatief zijn wat minder ontwikkeld dan die van jou. Gelukkig heb jij deze eigenschappen in overvloed. Hartstikke bedankt voor de fijne samenwerking!

Janneke, het was een plezier om met jou samen te werken en ik heb onze samenwerking altijd gewaardeerd. Je inzet voor onderzoek en onze NK cellen is, ondanks je drukke agenda, bewonderingswaardig. Bedankt ook voor het opzetten van de Biobank. Daar heb ik veel mooie experimenten mee kunnen doen. Alle ascites opwerkers, **Christina**, **Judith**, **Janneke**, **Jolien** en iedereen die hier betrokken bij was vanuit de kliniek, bedankt.

Anniek, bij jou kon ik altijd terecht met vragen. Als ik dacht 'Hmmm, wie zou dit weten?' was het antwoord meestal "Anniek". Bedankt voor alle hulp, feedback en het beantwoorden van mijn eindeloze vragen over muisexperimenten of statistiek. **Tim**, wij waren slechts korte tijd buren maar ik heb toch nog wat op je expertise en ervaring als senior PhD mee kunnen liften. Jammer dat we weinig kansen hebben gehad samen hardloopwedstrijden te doen met Rob. Hardlopen was immers ook jouw grote passie. Leuk om je zo af en toe nog eens tegen het lijf te lopen. **Lotte**, de manier waarop jij je PhD afgemaakt hebt zou ik van geleerd kunnen hebben. Helaas heb ik jouw goede voorbeeld niet gevolgd en er wat langer over gedaan. Bedankt voor je vrolijke en opgewekte aanwezigheid. Dit maakte een werkdag op kantoor een stuk gezelliger en leuker. **Jeannette**, you taught Jolien and myself many things including mouse work and the NK cell assays that we used throughout our PhD. Your guidance provided us with the tools and knowledge to begin our PhD journey. **Paul**, motormaat, met jou had ik van begin af aan al meteen een goede klik. De feestjes van de afdeling werden direct een stuk leuker vanaf het moment dat jij bij het lab kwam. Het hoogtepunt hier van moet de PhD retreat zijn geweest waar we na een pilsje of 3-4 teveel zijn gaan darten en armpje drukken. Maar ook nuchter hadden we een goede tijd. Onze trip met de convertible mustang in Texas heb ik geweldige herinneringen aan. Iedere keer dat ik in de buurt ben van Texas ga ik weer op zoek naar brisket, maar hij zal nooit zo lekker zijn als die ene random tent in de middle of nowhere. Bedankt voor alle gezelligheid! **Jesper**, paranimf, jij kwam me al vroeg tijdens mijn PhD steunen met wat mannelijk tegengas in het kantoor. Eindelijk had ik weer hoop na het vertrek van Tim om de verwarming weer wat omlaag te krijgen. Bedankt voor alle pizza's met extra korting. Daar heb ik veel en dankbaar gebruik van gemaakt. Ik heb bewondering voor je gevoel voor stijl en smaak. Dat is iets wat ik compleet mis. Bedankt ook voor je inzet tijdens mijn niet-meer-vrije zaterdag / zondag experiment. In dezelfde adem kan ik **Diede**, **Jolanda** en **Paul** (nog een keer) bedanken voor hen inzet. Dit was mijn meest ambitieuze experiment en zonder jullie hulp had ik dat laatste paper nooit kunnen schrijven. **Diede**, jou ga ik allereerst bedanken voor de vele keren dat je me geholpen hebt met mijn 'R' problemen. Dat was voor mij een hele struggle en zonder jouw hulp was dit nooit gelukt. De laatste twee hoofdstukken heb jij sowieso een belangrijke rol gespeeld om deze over de streep te trekken. Ook al bij het opzetten van de panels waren we samen de harde

kern Flow PhD'ers. Ik heb onze samenwerking als heel fijn en natuurlijk ervaren. De vloer bij Saioa is daar een mooi voorbeeld van. Sicke vloeg-leg-skills heb jij. Dat zal ik nooit vergeten!

Jolanda, jij bedankt voor alle hulp met Flow. Ik heb op dit gebied veel van je kunnen leren en die kennis gebruik ik tot de dag van vandaag nog steeds. Gaintration en spread matrix zijn termen die ik bij jou voor het eerst hoorde. Vooral deze laatste is veel werk, maar al vaak nuttig geweest. Jouw R-script heeft daarnaast het ascites hoofdstuk mogelijk gemaakt. Heel fijn dat je altijd voor me klaar stond om samen de data in te duiken en er het meeste uit te halen.

Paulien, NK buddy, bedankt voor het regelen van alle cords die we gebruikt hebben voor het NK onderzoek. Vooral bedankt voor het vaak opzoeken of de patiënt al op de afdeling was, zodat ik daar niet uren stond te wachten! Je vrolijke en spontane persoonlijkheid was super om bij de groep te hebben.

Ayla, volgens mij kwam de quote "zo hoop ik niet dat mijn PhD verloopt" van jou. Ik hoop het ook voor je, Ayla! Moge de afronding van jouw PhD wat vlekkelozer en sneller gaan! Jouw uitbundige persoonlijkheid met humor en je avontuurlijke zijn was geweldig om erbij te hebben. Ook heel vet dat je motor bent gaan rijden. Ik waardeer je mij in vertrouwen nam om je met dat avontuur te helpen!

Mijn studenten: **Pauline, Vera, Heleen, en Shweta**. Bedankt voor alle inzet. Het was me een waar genoegen met jullie samen te werken. Hopelijk hebben jullie iets van mij geleerd. Ik heb in ieder geval veel geleerd van jullie. **Vera**, je bent een harde werker en erg slim. Geen verrassing dus dat je een PhD bent gaan doen en al bijna klaar bent. **Heleen**, met jou in het lab was het altijd feest. Ik ken weinig mensen die gezelligheid zo 'uitstralen' als jij.

Somayeh, you came to the Netherlands with your daughter and joined our NK cell team. Your skills in the lab are only matched by your skills in the kitchen. You made some really tasty food for us. Highly appreciated! You are a bright and kind person. It was a pleasure working with you.

Menno, discussiëren met jou heb ik vele mooie herinneringen aan. Zeker omdat het vaak nergens over ging. Heerlijk. Je gevoel voor humor en sarcasme maakte het PhD leven een stuk draaglijker. Hoewel we relatief weinig samengewerkt hebben, zochten we elkaar vaak op in de Flow kamer bij Rob maar ook buiten werk. Vooruit, het was niet allemaal sarcastische humor en biertjes drinken. We hebben ook nog wat gesport. Ons befaamde padel groepje met Jesper en Jolien (en soms Paul als z'n knie t aan kon) was ook altijd mooi. Mooi om te zien hoe fanatiek je hier was!

Denise, hoewel ik meerdere mensen in dit dankwoord als gezellig beschrijf, zal ik dat bij jou niet doen, geen zorgen. We hebben ondertussen al een aantal inside jokes en tradities. Uiteraard onthoudt jij deze met je olifantengeheugen een stuk beter dan ik! In het lab hield je alles altijd super opgeruimd en schoon door iedereen op hun taken te wijzen. Dank je daarvoor! De BBQ's, broodjes hete kip en je enthousiasme/energie/praatvolume/vele verhalen koester ik.

Rob, wij delen onze passie voor Flow en jij bent al vanaf mijn bachelor mijn Flow mentor geweest. Bedankt voor het delen van je kennis (en de hardloopschoenen). Ik waardeerde je initiatief om hardloop evenementen te organiseren en ons daarvoor te motiveren! Mocht je weer een keer gaan lopen met het lab, dan doe ik mee.

Nelleke, ik kon natuurlijk niet door de gang lopen zonder even gezellig gedag te zeggen, zeker in de latere jaren van mijn PhD. Ik heb genoten van alle pubquizzen. Hopelijk volgen er nog meer! De befaamde stamppot avond laat zien wat voor persoon jij bent: sociaal, gezellig en gul.

Saskia, Ruth en Thessa, bij jullie kon ik altijd terecht met een vraag over een assay of techniek waar ik nog geen ervaring mee had. Jullie aanwezigheid in het lab maakte ons als PhD student een stuk makkelijk, bedankt! Thanks as well to **Mylène, Rinske, Maaike, Charlotte, Francesca** and **Saioa** for all the fun and entertainment during various side-activities and work. Ook **Bert** bedankt voor je input op mijn onderzoek.

Ook de analisten **Lisanne**, **Marij**, **Maud**, **Lisa**, **Janne**, **Greis**, **Aafke** en **Malou**, hartstikke bedankt voor alle inzet om de afdeling te laten draaien. Ik heb veelvuldig gebruik gemaakt van cellen die door jullie gekweekt zijn en zonder die cellen was dit boekje er niet gekomen. **Hanny,** in het verre verleden dat ik startte, was jij nog research analist. In die tijd heb je vele PhD studenten geholpen met je kennis, waaronder ik. Dank daarvoor! Er gaat veel kennis verloren met het vertrek van collega's, maar gelukkig ben jij gebleven.

Laura and Marcos, although we never formally worked during the same period it definitely feels like we did. Thanks for always welcoming me in the PhD room and for the many nice chats (and drinks) we had. I hope I didn't leave too much of a mess for you guys to continue working on our awesome projects!

9 789465 151670 >

Radboudumc
university medical center

IN DEI NOMINE FELICITER

Radboud University